INCREMENTAL AREA METHOD APPROACH FOR THE DETERMINATION OF AQUIFER PARAMETERS AND AQUIFER SYSTEMS IDENTIFICATION

by

A. Ufuk Şahin

B.S., Civil Enginering, Boğaziçi University, 2005

M.S., Civil Enginering, Boğaziçi University, 2008

Submitted to the Institute for Graduate Studies in
Science and Engineering in partial fulfillment of
the requirements for the degree of
Doctor of Philosophy

Graduate Program in Civil Engineering

Boğaziçi University

2012

ACKNOWLEDGEMENTS

First, I would like to express my sincere gratitude to my thesis supervisor, Prof. Cem B. Avcı for his guidance and support throughout the preparation of this thesis. Without his sympathy, patience and guidance, the accomplishment would be impossible.

I would also like to thank Assoc.Prof. Osman Börekçi and Prof. Nadim Copty for their kind and supportive attitude to me. I wish to express my appreciation to Prof. Erol Güler and Prof. Yalçın Yüksel for their final comments and contributions to my thesis.

I can not find the proper words to thank my dear friend, Emin Çiftçi, for his endless support and tea service. I owe my special thanks to Anıl Yıldız for spending his valuable time with me for the proof readings. I am deeply grateful to my colleagues in the Department of Civil Engineering, Boğaziçi University. It is hard to list them all but I promise that I will never forget their generous help.

My heartfelt gratitude goes to my family for their encouragement and lifelong supports: to my mother Nuray Şahin, my father Mithat Şahin, my sister Süzgün and my brother Ali. Last, I want to thank my family again, greatest thanks for all. This thesis is dedicated to my family.

ABSTRACT

INCREMENTAL AREA METHOD APPROACH FOR THE DETERMINATION OF AQUIFER PARAMETERS AND AQUIFER SYSTEMS IDENTIFICATION

Groundwater is one of the main freshwater resources for the demand of potable water, agriculture and industry. The protection and remediation of groundwater sources have become an important issue in order to provide sustainable development for the societies. To construct a proper remediation scheme for the contaminated groundwater resources, the mathematical and physical models require parameters which can be obtained from aquifer pump tests. The accurate and reliable determination of aquifer parameters is called as an inverse problem in the groundwater engineering literature. The performance of the conventional estimation methods developed and commonly used for the ideal aquifer conditions is insufficient when the aquifer media have a heterogeneous character. In this thesis, a new estimation approach, as simple as the traditional techniques, referred as Incremental Area Method (IAM) has been introduced to analyze transient pumping response of an aquifer under heterogenic circumstances. The potential uses and limitations of the proposed method have also been investigated for various aquifers pump test data. Furthermore, the spatial dependency of aquifer heterogeneity has been analyzed using Inverse Solution Algorithm (ISA) which was first established for the petroleum engineering reservoir cases. As a conclusion, the outcome of this research indicate that utilizing both the suggested IAM and adapted ISA to groundwater bearing flow problems leads to a realistic and robust interpretation of aquifer heterogeneity obtained from drawdown tests.

ÖZET

AKİFER SİSTEMLERİNİN TANIMLASINDA VE AKİFER PARAMETRELERİNİN BELİRLEMESİNDE ARTIK ALAN METODU YAKLAŞIMI

Yeraltı suları; içme suyu ihtiyacı, tarımsal ve sanayi faaliyetleri için ana temiz su kaynaklarından birisidir. Yeraltı su kaynaklarının korunması ve iyileştirilmesi toplumların sürdürülebilir kalkınmalarını sağlayan önemli bir konudur. Kirlenmiş yeraltı su kaynakları için uygun iyileştirme tasarılarının kurulması amacıyla geliştirilen matematiksel ve fiziksel tabanlı modeller akifer pompa testlerinden elde edilebilen model parametrelerini gerektirirler. Akifer parametrelerinin doğru ve güvenilir şekilde belirlenmesi yeraltı su mühendisliği literatüründe ters problem olarak adlandırılır. İdeal akifer durumları için geliştirilen ve yaygınca kullanılan geleneksel tahmin metotlarının performansı akifer heterojen bir karaktere sahip olduğunda yetersiz kalmaktadır. Bu araştırmada, geleneksel metotların basitliğine benzer Artık Alan Metodu (AAM) olarak nitelendirilen yeni bir tahmin etme yaklaşımı tanıtılmıştır. Önerilen metodun potensiyel kullanım alanları ve sınırları çeşitli pompa testi verileri için inlecenmiştir. Ek olarak, akifer heterojenliğinin uzaysal bağımlılığı ilk önce petrol mühendisliği rezervuar örnekleri için geliştirilmiş Ters Çözme Algorithması (TÇA) kullanılarak analiz edilmiştir. Sonuç olarak, bu araştırmada ortaya çıkan bulgular, önerilen AAM ile akifer problemlerine adapte edilen TÇA'nın birlikte kullanılmasının yeraltı suyu düşüm testi verilerinden elde edilen akifer heterojenliğinin daha gerçekçi ve sağlıklı bir şekilde yorumlanmasını sağlamaktadır.

TABLE OF CONTENTS

LIST OF FIGURES

LIST OF TABLES

LIST OF SYMBOLS

B	Volume Fraction Factor
b	Aquifer Thickness
b'	Thickness of Leaky Layer
C	Investigation Radius Coefficient
$C\forall$	Control Volume
CS	Control Surface
c_t	Total System Compressibility
E_i	i^{th} order Exponential Integral
g	Gravitational Acceleration
h	Hydraulic Head
h_0	Pre-pumping Head
I_0	Zero Order Modified Bessel Function of First Kind
J_0	Zero Order Bessel Function of First Kind
$\mathbf{K}$	Hydraulic Conductivity Tensor
K	Hydraulic Conductivity
K_0	Zero Order Modified Bessel Function of Second Kind
K'	Vertical Hydraulic Conductivity
K^*	Kernel Function
k	Permeability
k_D	Dimensionless Permeability
k_{in}	Instantaneous Permeability
k_{ref}	Reference Permeability
$\hat{n}$	Unit Normal Vector
P	Pore Pressure
p_D	Dimensionless Pressure
Q	Flow Rate
$\mathbf{q}$	Darcy Velocity Tensor
q	Darcy Velocity
R^2	Coefficient of Determination

r	Radial Distance
r_D	Dimensionless Radial Distance
r_w	Well Radius
S	Storativity
S_c	Storage Coefficient
S_s	Specific Storage
s	Drawdown
$\bar{s}$	Drawdown in Laplace Domain
$\hat{s}$	Estimated Drawdown
$\Delta s'$	Drawdown Derivative
$\mathbf{T}$	Transmissivity Tensor
T	Transmissivity
t	Time
t_D	Dimensionless Time
$\hat{t}_D$	Dimensionless Pseudo-time
u	Dimensionless Well Parameter
$\mathbf{v}$	Flow Velocity
$W_{1/2,1/2}$	Whittaker Function

β	The Compressibility of Fluid
β_b	The Compressibility of Bulk Volume
γ	Euler Constant
Δ	Log Cycle
δ_{ij}	Kronecker Delta
λ	Leakage Factor
μ	Viscosity
ξ	Saturated Thickness
ρ	Density of Fluid
ρ_w	Density of Water
ϕ	Porosity

LIST OF ACRONYMS/ABBREVIATIONS

ANN	Artificial Neural Network
ASTM	American Society for Testing and Materials
DIP	Double Inflection Point
FD	Finite Difference
FEM	Finite Element Method
HIP	Hantush Inflection Point
IAM	Incremental Area Method
ISA	Inverse Solution Algorithm
MAE	Mean Absolute Error
MW	Monitoring Well
PCA	Principal Component Analysis
PW	Pumping Well
RBFCM	Radial Basis Function Collocation Method
RMSE	Root Mean Squared Error
SMP	Slope Matching Process
SSE	Sum Squared Error
WCM	Walton Curve Matching

1. INTRODUCTION

There is no doubt that water is the essential substance for the existence of all kinds of living organism. Although 75% of the planet earth is composed of water, freshwater is ironically only 2.5% of this extensive amount of water. Furthermore, some freshwater resources which are contributing to global water budget such as polar ice, glaciers, biological systems and the atmosphere are not readily available for human use. Considering these interesting facts about the amount of water present on the earth, groundwater becomes a more important freshwater resource since groundwater approximately comprises 30% of attainable freshwater (Leap, 1999).

Groundwater is used to supply potable water demand, irrigation and industrial facilities. Access to freshwater resources, therefore, has a critical role on the rise and fall of the civilizations throughout the history. Hence the uncontrolled growth in world's population influences the potential freshwater sources negatively in line with the effects of the global warming; today's world turns out to be a place where the amount of available groundwater is insufficient to meet the increasing demand.

Recalling the awful truths about the stresses on the available water resources created by many directions such as the careless disposal of biological wastes, haphazard disposal of industrial facilities like mining and oil operations; the protection of water resources is inevitably emerged as a challenging task. From the very early studies dating back to Darcy's pioneering work on the groundwater flow, the tremendous amount of scientific researches have been focused on the protection of water resource, remediation of the contaminated aquifers and sustainable water management.

Mathematical and physical models have been established to analyze complex behavior of groundwater systems for various scenarios. For instance, a contaminant transport model employed to evaluate the propagation of the plume over the years requires a priori information about the medium in which groundwater flows. The success of this model, however, is directly related with the model parameters which can

be obtained from the field pump tests. Hence, the determination of aquifer parameters plays a key role for constructing a proper remediation scheme.

The ability to accurately determine aquifer parameters such as transmissivity and storativity from pumping test data has been one of the main focuses of this thesis. The estimation of these parameters based on the transient response of aquifer systems being stressed was first analyzed by Theis (1935) and then simplified by Cooper and Jacob (1946). Besides these traditional inversion techniques, the logarithmic derivative methods in well-test interpretation were later on studied by Chow (1952), Papadopulos and Cooper(1967), Neuman (1972), Sen (1986) and more recently Copty (2011). However, derivative calculations of drawdown data are prone to numerical oscillations unless the data obtained from the field are very smooth (Renard, 2005b). Renard *et al.* (2009) showed that slight anomalies in the drawdown data lead to large variations in the estimation of aquifer parameters due to the derivative calculation amplification and represented a shortcoming of the logarithmic derivative approach.

A new estimation technique called as Incremental Area Method (IAM) has been introduced to overcome the difficulties associated with derivative amplification process and to smooth the potential random errors during utilizing the conventional procedures. The IAM is a flexible method to detect the changes in aquifer heterogeneity character. The proposed method also enables to track the time variation of aquifer parameters which implies an alternative tool for aquifer system identification.

The spatial dependency of heterogenic behavior of an aquifer is investigated as a second objective of this thesis. Inverse Solution Algorithm (ISA) used in the petroleum engineering field for estimating the radial heterogeneity of oil and gas reservoirs has been modified to be applied to the groundwater bearing aquifer system. Butler (1988) derived the analytical formula solution for two concentric circles which have different transmissivity values to understand the effects of heterogeneity on the interpretation of estimation methods; the same analysis has been extended to three and four concentric rings system to evaluate the importance of effective mean transmissivity inside the cone of depression and the results were compared to the spatial transmissivity variation

obtained from ISA.

Thesis document is organized in eight chapters. The objectives of this study are elaborated in Chapter 1. A brief literature review of groundwater flow equation, definitions of forward and inverse problem in groundwater modeling are presented in Chapter 2. The methodology of Incremental Area Method for confined and leaky aquifer system is explained in Chapter 3. As an important outcome of this dissertation, the IAM for confined aquifer system has been introduced to groundwater literature as a research paper entitled "Aquifer Parameter Estimation using an Incremental Integration Method" which was published in Hydrological Processes, Avci *et al.* (2011). The mathematical background of ISA is given in Chapter 4. The applications of the IAM to determine confined and leaky aquifer parameters for various scenarios are shown in Chapter 5. Aquifer system identification by IAM is discussed in Chapter 6. The spatial dependency of transmissivity in heterogeneous medium is demonstrated by various numerical experiments in Chapter 7. The conclusions of thesis are drawn in Chapter 8.

2. LITERATURE REVIEW

2.1. Groundwater Flow in Porous Medium

Darcy (1856) conducted first physical experiment to elaborate groundwater flow mechanism in the porous medium in terms of soil and fluid properties such as hydraulic conductivity and piezometric head variation as following

$$\mathbf{q} = -\mathbf{K}\nabla h \tag{2.1}$$

where $\mathbf{q}$ is the Darcian velocity tensor, h is the hydraulic head, $\mathbf{K}$ denotes the hydraulic conductivity tensor given as

$$\mathbf{K} = \begin{bmatrix} K_{xx} & K_{xy} & K_{xz} \\ K_{yx} & K_{yy} & K_{yz} \\ K_{zx} & K_{zy} & K_{zz} \end{bmatrix} \tag{2.2}$$

Mass conservation principle requires that influx and outflux mass rates coming through the control surface are balanced with the change in accumulated mass storage in the control volume with time (Lee, 1999)

$$\iiint\limits_{C\forall} \frac{\partial(\rho\phi)}{\partial t} d\forall + \iint\limits_{CS} \rho\mathbf{v} \cdot \hat{n} dA = 0 \tag{2.3}$$

where ρ is mass density, t is time, ϕ is system porosity, $d\forall$ is the differential volume element in the control volume $C\forall$, $\mathbf{v}$ is the flow velocity, $\hat{n}$ stands for the outward unit normal vector, and dA is the differential area element on the control surface CS. Applying the divergence theorem, the surface integral can be expressed in terms of volume integral as follows (Arfken, 1985)

$$\iint\limits_{CS} \rho\mathbf{v} \cdot \hat{n} dA = \iiint\limits_{C\forall} \nabla \cdot (\rho\mathbf{v}) d\forall \tag{2.4}$$

The mass balance equation in Equation 2.3, then, yields to continuity equation in the differential form given as

$$\frac{\partial(\rho\phi)}{\partial t} + \nabla \cdot (\rho \mathbf{v}) = 0 \tag{2.5}$$

where ∇ denotes the gradient operator.

Before combining the continuity equation and Darcy's Law, the left hand side (LHS) of Equation 2.5 can be expanded as

$$\frac{\partial(\rho\phi)}{\partial t} = \phi\frac{\partial\rho}{\partial t} + \rho\frac{\partial\phi}{\partial t} \tag{2.6}$$

The first term in the right hand side (RHS) of Equation 2.6 indicates the compressibility of fluid whereas the second term in the RHS indicates the rate of porosity change (Lee, 1999). The compressibility of fluid β can be defined as

$$\beta = \frac{\partial\rho}{\rho\partial P} \tag{2.7}$$

where P is the pore pressure. The change in the porosity can be expressed in terms of the compressibility of bulk volume β_b as follows (Bear, 1979)

$$\beta_b = \frac{1}{1-\phi}\frac{\partial\phi}{\partial P} \tag{2.8}$$

Equation 2.6 can be shown as the pressure change in time by applying chain rule given as

$$\begin{aligned} \phi\frac{\partial\rho}{\partial t} &= \phi\frac{\partial\rho}{\partial P}\frac{\partial P}{\partial t} = \phi\beta\rho\frac{\partial P}{\partial t} \\ \rho\frac{\partial\phi}{\partial t} &= \rho\frac{\partial\phi}{\partial P}\frac{\partial P}{\partial t} = \rho(1-\phi)\beta_b\frac{\partial P}{\partial t} \end{aligned} \tag{2.9}$$

The rate of pore pressure change can also be written in terms of hydraulic head change

as follows

$$\frac{\partial P}{\partial t} = \rho g \frac{\partial h}{\partial t} \tag{2.10}$$

Substituting Darcy velocity shown in Equation 2.1 into Equation 2.5 and combining Equation 2.9 and Equation 2.10, governing groundwater flow equation in porous medium can be expressed as

$$\nabla \cdot (\mathbf{K} \nabla h) = S_s \frac{\partial h}{\partial t} \tag{2.11}$$

where S_s is the specific storage defined as the volume of water released from storage in a unit volume of elastic aquifer per unit change in head as follows

$$S_s = \rho g \left[\phi\beta + (1 - \phi)\,\beta_b\right] \tag{2.12}$$

Freeze and Cherry (1979) suggested a different specific storage formulation as

$$S_s = \rho g \left[\phi\beta + \beta_b\right] \tag{2.13}$$

In practice, there is no difference in the usage of Equation 2.12 or Equation 2.13.

The groundwater flow equation is also written in terms of transmissivity and storativity values with the uniform aquifer thickness b given as

$$\nabla \cdot (\mathbf{T} \nabla h) = S \frac{\partial h}{\partial t} \tag{2.14}$$

where $\mathbf{T}$ indicates the transmissivity vector and S represents the storavity. Transmissivity is defined as the ease with which water can move through an aquifer and storativity is defined as the volume of water released from storage per unit surface area of the aquifer per unit change in head (Schwartz and Zwang, 2003). Transmissivity

and storativity are given as follows

$$\begin{aligned} \mathbf{T} &= \mathbf{K}b \\ S &= S_s b \end{aligned} \tag{2.15}$$

2.2. Forward Problem in Groundwater Modeling

The solution of groundwater flow equation described in Equation 2.14 is considered as the forward formulation for the groundwater modeling based on the predefined values of aquifer parameters. The reliability and robustness of the mathematical models given in the set of governing equations depend on the model assumptions. Hence the reality, in general, is too complex to be simulated exactly; the assumptions behind the mathematical models are fairly restrictive (Wang and Andersen, 1982). The inherent complexity of groundwater flow equation can be overcome by imposing proper boundary conditions to aquifer system and making necessary assumptions for the analytical solution of some special cases. For instance, if the principal directions of anisotropy coincide with the axial directions of the chosen coordinate frame, the transmissivity tensor is then reduced to more simple form as (Batu, 1998)

$$\mathbf{T} = T_{ij}\delta_{ij} \tag{2.16}$$

where T is transmissivity, and δ_{ij} is Kronecker delta.

If Equation 2.14 is expanded for three dimensional Cartesian coordinate system, groundwater flow equation turns out to be (Schwartz and Zwang, 2003);

$$\frac{\partial}{\partial x}\left(T_x\frac{\partial h}{\partial x}\right) + \frac{\partial}{\partial y}\left(T_y\frac{\partial h}{\partial y}\right) + \frac{\partial}{\partial z}\left(T_z\frac{\partial h}{\partial z}\right) = S\frac{\partial h}{\partial t} \tag{2.17}$$

Under steady-state conditions, Equation 2.17 simplifies to the well-known Laplace equation if the aquifer is homogeneous and isotropic. Transient solution of Equation 2.17 is also obtained with the same assumptions about homogeneity and isotropicity.

If the vertical head change is negligible compared to the change in other directions, Equation 2.17 can be expressed in two dimensional form (Schwartz and Zwang, 2003).

Mathematical models for groundwater flow in a confined aquifer have been developed to simulate the reality in a simplified form since the last century. One of the earliest quantitative study on the solution groundwater flow in a confined aquifer dated back to work of Thiem in 1906. The necessary assumptions behind Thiem (1906) solution are listed as (Fetter, 2001)

- Aquifer is infinite in extent.
- Aquifer is homogeneous and isotropic.
- All flow is radial toward the well and steady.
- Groundwater flow is horizontal and Darcy's law is valid.
- Aquifer is stressed by a fully penetrating pumping well with a constant discharge rate.

Based on the listed assumptions, Thiem (1906) solution is then given as

$$h = h_0 + \frac{Q}{2\pi T} \ln\left(\frac{r}{R}\right) \tag{2.18}$$

where h is hydraulic head at the distance r from the pumping well, h_0 is the prepumping hydraulic head, Q is the pumping rate and R is the influence radius for the pumped aquifer. Theis (1935) suggested the first mathematical analysis of transient response of the confined aquifer systems being stressed. Figure 2.1 represents the schematic illustration of a fully confined aquifer.

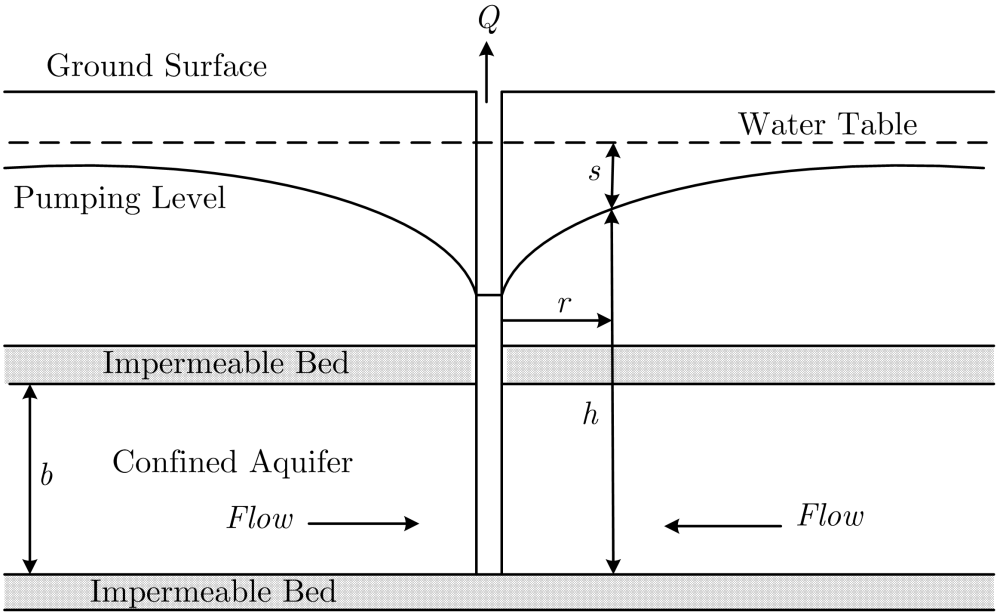

Figure 2.1. Schematic Illustration of a Fully Confined Aquifer.

The one dimensional groundwater flow equation describing hydraulic head in a homogenous, isotropic confined aquifer can be expressed in polar coordinates as;

$$\frac{\partial^2 h}{\partial r^2} + \frac{1}{r}\frac{\partial h}{\partial r} = \frac{S}{T}\frac{\partial h}{\partial t} \tag{2.19}$$

and the following initial and two boundary conditions respectively are necessary to find the analytical solution;

$$\begin{aligned} \text{Initial Value} \qquad & h(r,0) = h_0 \\ 1^{\text{st}}\,\text{Boundary Condition} \qquad & h(\infty,t) = h_0 \\ 2^{\text{nd}}\,\text{Boundary Condition} \qquad & \lim_{r\to 0}\left(r\frac{\partial h}{\partial r}\right) = \frac{Q}{2\pi T} \end{aligned} \tag{2.20}$$

Solution to Equation 2.19 can be achieved with the following assumptions (Fetter, 2001):

- All geologic formations are horizontal and have infinite horizontal extent.
- The potentiometric surface of the aquifer is horizontal before the pumping test.

- All changes in the position of the potentiometric surface are due to the effect of the pumping well alone.
- Aquifer is homogeneous and isotropic, all flow is radial toward the well.
- Groundwater flow is horizontal and Darcy's law is valid.
- The pumping well has an infinitesimal diameter and fully penetrating, pumping rate is constant and there is no recharge source to the aquifer.

Theis (1935) solution was then formulated as;

$$h_0 - h = s = \frac{Q}{4\pi T} W(u) \tag{2.21}$$

where s is the drawdown and $W(u)$ is the Theis well function. Well function is represented as

$$W(u) = \int_u^\infty \frac{e^{-x}}{x} dx \tag{2.22}$$

where u is the dimensionless parameter given as

$$u = \frac{r^2 S}{4Tt} \tag{2.23}$$

The exponential integration in Equation 2.22 can be expanded by the infinite series as (Domenico and Schwartz, 1998)

$$W(u) = -\gamma - \ln u + \sum_{i=1}^{\infty} \frac{(-1)^{i+1} u^i}{i \times i!} \tag{2.24}$$

where γ is Euler's constant and approximately 0.577216. Figure 2.2 represents the value of well function $W(u)$.

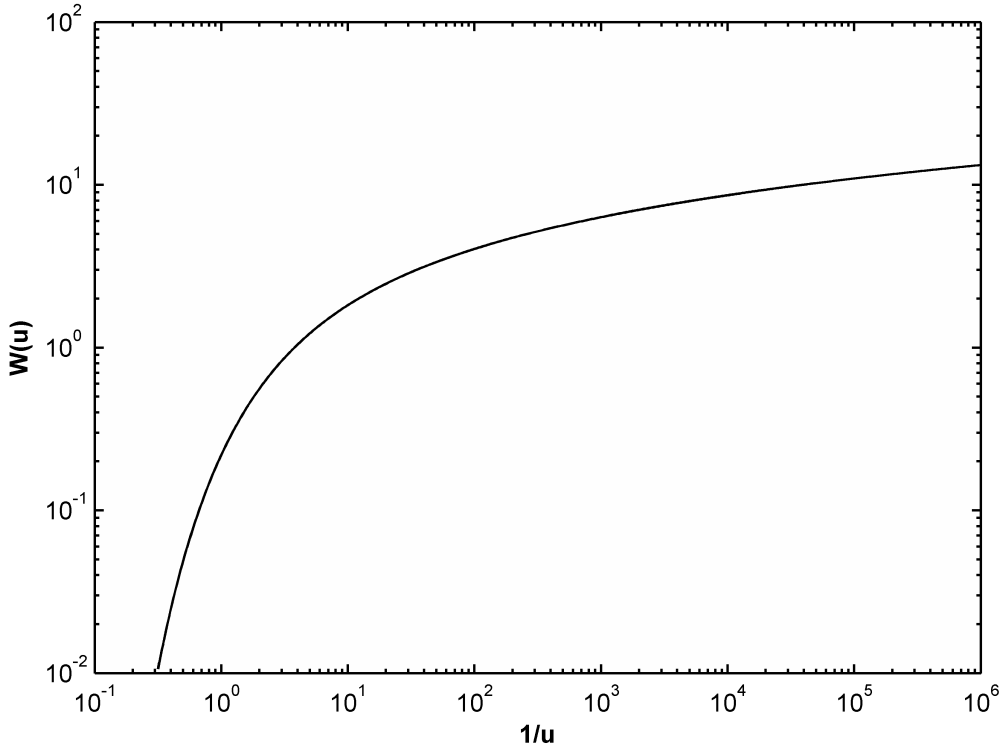

Figure 2.2. Theis Well Function $W(u)$.

The governing groundwater flow equation can be modified to simulate the flow character in the leaky aquifer systems by taking into account the storage effects of the underlain and/or overlain confining layers (Batu, 1998). Since aquitards can leak water to aquifer, the net effect of this leakage causes to a reduction of the drawdown in the confined aquifer. The vertical recharge rate due to aquitard leakage can be written as

$$q = K' \frac{s}{b'} \tag{2.25}$$

where K' is the hydraulic conductivity of aquitard and b' is the thickness of leaky layer. Substituting Equation 2.25 into the Equation 2.19, the governing equation of homogeneous, isotropic leaky aquifer model can be expressed in terms of drawdown and vertical leakage as follows:

$$\frac{\partial^2 s}{\partial r^2} + \frac{1}{r}\frac{\partial s}{\partial r} - \frac{K's}{Tb'} = \frac{S}{T}\frac{\partial s}{\partial t} \tag{2.26}$$

Hantush and Jacob (1955) first derived an analytical solution by taking into account the following assumptions (Fetter, 2001; Schwartz and Zhang, 2003):

- The pumping well fully penetrates the aquifer and has a constant pumping rate.
- Groundwater flow in the aquitard (leaky confining layer) is vertical and that layer has a uniform hydraulic conductivity (K') and thickness (b').
- Storage in the aquitard is negligible.
- Leakage across the aquitard comes from an aquifer whose head is assumed to be not affected by pumping.

Schematic view of a leaky confined aquifer model defined by Hantush and Jacob (1955) is illustrated on Figure 2.3.

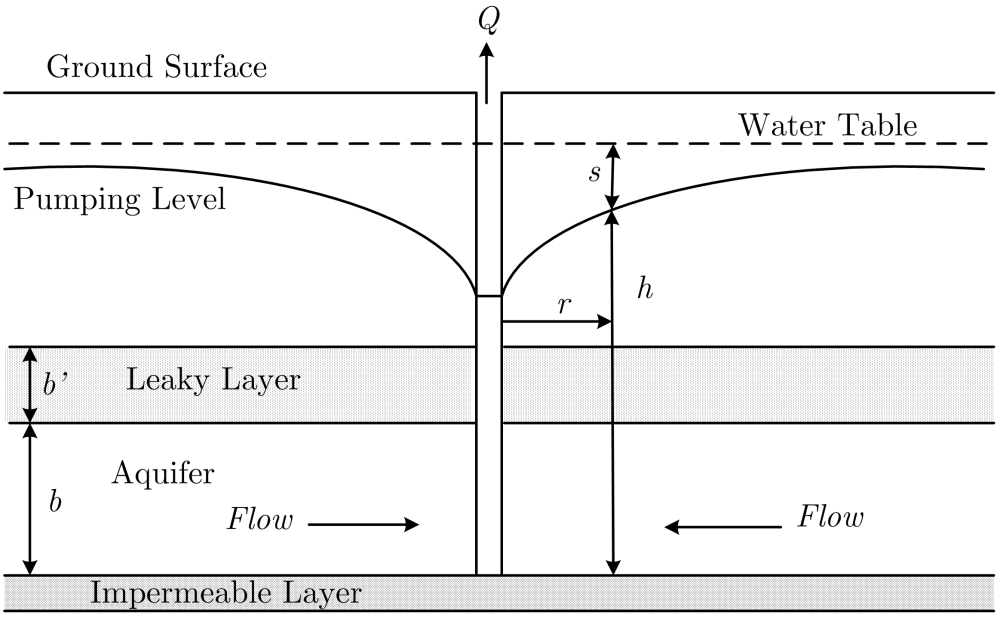

Figure 2.3. Schematic Illustration of a Leaky Confined Aquifer.

Based on these assumptions, the solution of Equation 2.26 can be given as

$$s = \frac{Q}{4\pi T} W\left(u, r/B\right) \tag{2.27}$$

where $B = \sqrt{\frac{Tb'}{K'}}$ and $W\left(u, r/B\right)$ denotes the leaky well function. The Hantush and

Jacob (1955) well function $W(u, r/B)$ is expressed as

$$W(u, r/B) = \int_{u}^{\infty} \frac{1}{x} \exp\left(-x - \frac{r^2}{4B^2 x}\right) dx \tag{2.28}$$

Equation 2.28 can be approximated the following formula as (Prodanoff *et al.*, 2006)

$$\begin{aligned} W(u, r/B) \cong\ & 2K_0(r/B) - I_0(r/B) \times \left[-E_i\left(\tfrac{r^2}{4B^2 u}\right)\right] \\ & + \left[\exp\left(-\tfrac{r^2}{4B^2 u}\right)\right] \times \left\{\gamma + \ln u + \left[-E_i(-u)\right] - u + u\left[\tfrac{I_0(r/B)-1}{r^2/4B^2}\right]\right. \\ & \left. -u^2 \sum_{n=1}^{\infty} \sum_{m=1}^{n} \tfrac{(-1)^{n+m}(n-m+1)!}{(n+2)!^2} \left(\tfrac{r^2}{4B^2}\right)^m u^{n-m}\right\} \end{aligned} \tag{2.29}$$

where K_0 is the modified zero order Bessel function of second kind, I_0 is the modified zero order Bessel function of first kind, $-E_i$ term is the exponential integral defined as

$$W(u) = E_1(u) = -E_i(-u) = \int_{u}^{\infty} \frac{1}{x} \exp(-x)\, dx, \quad u > 0 \tag{2.30}$$

The transient response of leaky aquifer being stressed is shown as

$$s = \frac{Q}{4\pi T} W(u, r/B) \tag{2.31}$$

Equation 2.29 reduces to some special cases according to the well function variables u and r/B values. If the r/B value approaches to zero, the Hantush and Jacob (1955) solution yields to the Theis (1935) solution since the aquitard becomes impermeable as $K' = 0$ (Freeze and Cherry, 1979). If the steady-state condition is satisfied, well function then depends on the function of r/B value. When u value approaches to infinity, the Hantush and Jacob (1955) well function vanishes (Prodanoff *et al.*, 2006). The following equation summarizes these conditions as

$$\begin{aligned} W(u, 0) &= W(u) \\ W(0, r/B) &= 2K_0(r/B) \\ W(\infty, r/B) &= 0 \end{aligned} \tag{2.32}$$

Unconfined aquifer has a different physical mechanism compared to the confined aquifer model because delayed yield stage of pumping period is responsible for the decrease in the recording drawdown data which are not observed in the typical confined aquifer. First mathematical models for analyzing pumping response of unconfined aquifer were suggested by Boulton (1954; 1963). More realistic approach to analyze unconfined aquifer character was later on studied by Neuman (1972, 1974, 1975 and 1979) and Streltsova (1972a,b, and 1973). According to Neuman (1972) model, unconfined aquifer model has the following assumptions which enable to find an analytical solution (Batu, 1998):

- Aquifer is homogeneous but anisotropic.
- Aquifer is pumped by constant discharge rate, pumping well is fully penetrated to impermeable horizontal layer, skin and seepage effects of well is neglected.
- Darcy's law is valid, aquifer remains saturated at all times.
- Water is released from storage by compaction of the aquifer, expansion water and gravity drainage at the free surface.

The governing equation of Neuman (1972) unconfined aquifer model shown in Figure 2.4 is given as;

$$K_r \frac{\partial^2 s}{\partial r^2} + \frac{K_r}{r}\frac{\partial s}{\partial r} + K_z \frac{\partial^2 s}{\partial z^2} = S_s \frac{\partial s}{\partial t} \qquad 0 < z < \xi \tag{2.33}$$

where K_r and K_z indicate the radial and vertical hydraulic conductivities, respectively. The initial conditions for drawdown s and the saturated thickness ξ, respectively, are

$$\begin{aligned} s\,(r, z, 0) &= 0 \\ \xi\,(r, 0) &= b \end{aligned} \tag{2.34}$$

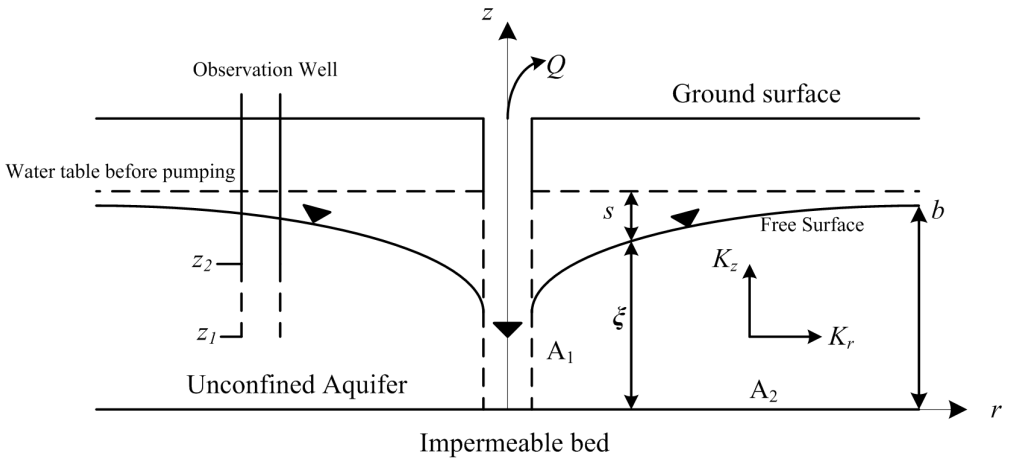

Figure 2.4. Schematic Illustration of Unconfined Confined Aquifer.

The boundary condition at infinity, impervious boundary A_2, and the well, respectively, are given as followings

$$\begin{aligned} s(\infty, z, 0) &= 0 \\ \frac{\partial s(r, 0, t)}{\partial z} &= 0 \\ \lim_{r\to\infty} \int_0^{\xi} r \frac{\partial s}{\partial r} dz &= -\frac{Q}{2\pi K_r} \end{aligned} \tag{2.35}$$

Neuman (1972) utilized a perturbation technique to linearize the governing equation in Equation 2.33 and the boundary and initial conditions given in Equation 2.34 and 2.35 as following:

$$\frac{\partial^2 s}{\partial r^2} + \frac{1}{r}\frac{\partial s}{\partial r} + K_D \frac{\partial^2 s}{\partial z^2} = \frac{1}{\alpha_s}\frac{\partial s}{\partial t} \qquad 0 < z < b \tag{2.36}$$

and

$$\lim_{r\to 0}\int_0^b r\frac{\partial s}{\partial r}dz = -\frac{Q}{2\pi K_r}$$
$$\frac{\partial s\left(r,b,t\right)}{\partial z} = -\frac{1}{\alpha_y}\frac{\partial s\left(r,b,t\right)}{\partial t} \tag{2.37}$$

where

$$K_D = \frac{K_z}{K_r}, \quad \alpha_s = \frac{K_r}{S_s}, \quad \alpha_y = \frac{K_z}{S_y} \tag{2.38}$$

Solution of Equation 2.36 was provided by Neuman (1973) as

$$s = \frac{Q}{4\pi T}\int_0^\infty 4yJ_0\left(y\beta^{1/2}\right)\left[\omega_0\left(y\right)+\sum_{n=1}^{\infty}\omega_n\left(y\right)\right]dy \tag{2.39}$$

where

$$\omega_0\left(y\right) = \frac{\left\{1-\exp\left[-t_s\beta\left(y^2-\gamma_0^2\right)\right]\right\}\cosh\left(\gamma_0 z_D\right)}{\left\{y^2+\left(1+\sigma\right)\gamma_0^2-\left[\frac{\left(y^2-\gamma_0^2\right)^2}{\sigma}\right]\right\}\cosh\left(\gamma_0\right)} \tag{2.40}$$

and

$$\omega_n\left(y\right) = \frac{\left\{1-\exp\left[-t_s\beta\left(y^2+\gamma_n^2\right)\right]\right\}\cosh\left(\gamma_n z_D\right)}{\left\{y^2-\left(1+\sigma\right)\gamma_n^2-\left[\frac{\left(y^2+\gamma_n^2\right)^2}{\sigma}\right]\right\}\cosh\left(\gamma_n\right)} \tag{2.41}$$

where

$$t_s = \frac{Tt}{Sr^2},\ t_y = \frac{Tt}{S_y r^2},\ b_D = \frac{b}{r},\ z_D = \frac{z}{b},\ \sigma = \frac{t_y}{t_s},\ \beta = \left(\frac{K_D}{b_D}\right)^2,\ y = xb_D \tag{2.42}$$

The terms γ_0 and γ_n are formulated as

$$\gamma_0 = \beta_0\frac{b}{r} \quad \text{and} \quad \gamma_n = \beta_n\frac{b}{r} \tag{2.43}$$

The roots of the following equation provide the values of γ_0 and γ_n as

$$\begin{aligned} &\sigma\gamma_0 \sinh(\gamma_0) - (y^2 - \gamma_0^2)\cosh(\gamma_0) = 0 \qquad \gamma_0^2 < y^2 \\ &\sigma\gamma_n \sinh(\gamma_n) + (y^2 + \gamma_n^2)\cosh(\gamma_n) = 0 \end{aligned} \tag{2.44}$$

where

$$(2n-1)\frac{\pi}{2} < \gamma_n < n\pi, \qquad n \geq 1 \tag{2.45}$$

Numerical techniques are widely used to deal with the more realistic situations which have no analytical solutions (Wang and Andersen, 1982). By the advent of modern computers, a large variety of numerical techniques such as finite difference, finite element and boundary element methods become more applicable to solve the groundwater flow equation for various scenarios. More comprehensive basis of the usage of finite difference method in groundwater modeling can be found in the works of Remson *et al.* (1971), Peaceman (1977), Wang and Andersen (1982). Narasimhan and Witherspoon (1976) provided an integrated finite difference method for analyzing fluid flow in porous media. Finite Difference based computer program MODFLOW (McDonald and Harbough, 1983) has been advanced over the last a few decades to solve the groundwater flow equation as well as the contaminant transport problems in heterogeneous, anisotropic aquifers system.

Finite element method (FEM), another classical numerical technique, is widely used in groundwater modeling. Zienkiewicz (1971), Huebner (1975), Wang and Andersen (1982), Voss (1984), Huyarkorn *et al.* (1986), Cooley (1992) and Torak (1993) provided the refinements and improvements on the solution algorithms used in modeling as well as the detailed explanations of the method. FEM based computer programs such as SUTRA (Voss, 1984) and MODFE (Cooley, 1992; Torak, 1993) are used to approximate groundwater flow solutions and contaminant transport problems encountered in groundwater practice.

2.3. Inverse Problem in Groundwater Modeling

The determination of aquifer parameters, namely, transmissivity and storativity which control the movement of groundwater in a porous medium, is considered as inverse problem in the hydrogeology literature. Aquifer pumping tests are one of the most commonly used in-situ testing methods to provide information on the hydraulic characteristics of the groundwater bearing zones. The success of the mathematical model depends on the accuracy of the aquifer parameters. In groundwater inverse problems, however, the sought after parameters are usually hydrogeologic properties and the available information are the measured dependent variables such as water level elevations or solute concentration. The inverse methods adapt a parameterization process and subsequently use a forward equation to relate these parameters to field measurements; the process then uses performance criteria to define acceptable parameter estimate (Avci *et al.*, 2011).

The simplest inverse methodology that can be considered is the graphical curve matching techniques which are at the core of the use of the analytical methods developed for characterizing aquifer and pumping test conditions. The ideal curve and the drawdown data are plotted with the same log-log scale and then superimposed to select an arbitrary matching reference point located anywhere on the type curve (Schwartz and Zhang, 2003). The matched coordinate points are then utilized to calculate aquifer parameters by the formulations given in Equation 2.21.

Walton (1962) devised the graphical curve matching method for leaky confined aquifer. In a similar manner to the Theis curve matching procedure, the field time drawdown curve and theoretical family of type curves are plotted and superimposed. The following steps are applied with the modifications to leaky aquifer as follows (Sahin, 2008)

- The field data curve should be matched to one of the type curves for r/B, if it is not, an imaginary type curve is drawn by interpolating between two r/B curves to satisfy matching.

- Coordinates of the matching point and r/B value are recorded, aquifer parameters are then computed as

$$\begin{aligned} T &= \frac{Q}{4\pi s} W\left(u, r/B\right) \\ S &= \frac{4uTt}{r^2} \\ K' &= \frac{Tb'\left(r/B\right)^2}{r^2} \end{aligned} \tag{2.46}$$

The classical curve matching procedures provide aquifer parameters without much computation efforts as discussed above. These methods, however, have some shortcomings if the perfect match is not satisfied. The basic assumptions behind the traditional curve matching techniques are violated by inherent complexity of pumping mechanism, uncertainty effects and heterogenic character of the aquifer material which cause the difficulties in curve matching. Mathematical models have been developed to find analytical formulation of parameters estimation for an aquifer where the heterogenic uncertainty exists. Papadopulos (1965) proposed an analytical model to investigate the drawdown distribution around the pumping well with a constant discharge rate in anisotropic and homogenous aquifer. Hanush (1996a,b) develop methods to analyze drawdown data in an anisotropic aquifer for different cases. Neuman *et al.* (1984) conducted studies on anisotropic confined aquifer based on Papadopulos model. Butler (1988) utilized a mathematical model to estimate aquifer parameters for the constant rate pumping test in non-uniform radially symmetric cases, the author then developed his model for variable rate pumping tests (Butler and McElwee, 1990). Butler and Liu (1993) presented an analytical solution for the case of transient, pumping induced drawdown in non-uniform aquifer for radially asymmetric case. Several researchers suggested new methods to improve the estimation of aquifer parameters for confined and leaky aquifers. Karasaki *et al.* (1988), Spane (1993) and Spane and Wurstner (1992) proposed the time derivative analysis of drawdown curve. Parks *et al.* (1996) pointed that characteristic time-drawdown and derivative curves are integrated with geology to identify the nature of heterogeneities and assess their impact on long term

aquifer response to pumping. Sen and Wagdani (2008) suggested the slope matching procedure (SMP) and its application for short duration field tests in arid region. Relatively few studies on determination of leaky aquifer parameters have been suggested. Amin (2005) developed the techniques for the estimation of rate of leakage based on the time derivate analysis. Copty *et al.* (2006) constructed an analytic relation to define equivalent transmissivity for steady flow toward a well. More recently, Trinchero *et al.* (2008) proposed the double inflection point method (DIP) based on the derivative of time-drawdown curve to determine leaky aquifer parameters.

As geostatistical approach, Kriging and Co-kriging method are suggested to analyze spatial correlation between observed heads and unknown hydraulic conductivities (Yeh *et al.*, 1996; Zhang and Yeh, 1997). Mayer and Huang (1999) proposed the maximum likelihood method to estimate aquifer parameters with stated variables and parameter residual. A large number of researchers (Woodbury and Ulrych, 2000; Copty and Findikakis, 2004a,b; Neuman *et al.*, 2004, 2007; Jiang *et al.*, 2004; Jiang and Woodbury, 2006; Firmani *et al.*, 2006; Riva *et al.*, 2009; Murakami *et al.*, 2010) have shown that the physical characters of the aquifer parameters can be properly described by utilizing stochastic techniques. Hydraulic parameters can be established using drawdown data and available field information for the assessment of the site data as an inverse problem. Field parameters are obtained from water level drawdown observed at various locations in the aquifer have been presented in the literature as the studies of (Kitidanis, 1986; Carrera and Neuman, 1986a,b; McLaughlin and Townley, 1996; de Marsily *et al.*, 1999; Jiang and Woodbury, 2006; and Sun and Yeh, 2007).

Yeh and Liu (2000) introduced the hydraulic tomography as a new test method to improve the inverse problem approach which has led to the requirement of more detailed and elaborate pumping test methods. The approach uses the data collection from the field in order to provide tomographic estimates for the hydraulic properties. The researchers also studied the effects of pumping and observation wells configuration on the optimal pumping scheme and investigated the applicability and robustness of this iterative inverse method for hypothetical heterogeneous aquifer medium. Liu *et al.* (2007) conducted a laboratory sandbox experiment to investigate the validity of

transient hydraulic tomography method and reported that the estimation performance of algorithm provide a good agreement to local and large scale hydraulic parameter set which are independently collected. Illman *et al.* (2007) reviewed the multi-method and multi scale validation of hydraulic conductivity tomograms conducting a sandbox experiment for deterministic heterogeneity which is previously studied by Yeh and Liu (2000). The authors indicated that steady-state estimation performance is highly sensitive to errors and biases appeared in conductivity tomograms which have not been examined in the previous studies (Gottlieb and Dietrich, 1995; Bohling *et al.*, 2002; and McDermott *et al.*, 2003) in detail. Zhue and Yeh (2006) proposed the hydraulic tomography method to analyze the aquifer heterogeneity using temporal moments of drawdown recovery data.

Some researchers have suggested that statistical approaches should be used to analyze the inherent complexity of heterogeneity on the aquifer systems being stressed. Three-dimensional random stationary function based hydraulic conductivity model has been presented by Indelman (2003) to show the axisymmetric anisotropy and Gaussian correlations under the transient well flow conditions of the heterogeneous aquifer. The author reported that estimated transmissivity values from pumping period where the Cooper and Jacob (1946) assumption govern which means non-linear term disappear is close to the effective conductivity of uniform horizontal flow. A first order correlation analysis has been suggested by Wu *et al.* (2005) to show that the effective transmissivity values obtaining as an average of hydraulic parameters over the cone of depression region converges to geometric mean of the area between pumping and monitoring well for only late time of pumping period whereas storativity values were noted to converge to the arithmetic mean in this zone. Wu *et al.* (2005) also concluded that effective transmissivity is influenced by degree of heterogeneity appeared inside the cone of depression, loacation, size as well as the average value over the cone of depression region. Tumlinson *et al.* (2006) indicated that the Cooper and Jacob (1946) based transmissivty values obtaining from single well aquifer tests for arbitrary block heterogeneity distribution, in general, may lead to representative volumetric, a weighted average of transmissivity values of all heterogeneity which propagation of the cone of depression involve at the particular time. According to their research findings, the authors claimed

that a rapid change in the weighted average of transmissivity values occurs in the initial pumping period near the pumping well while stabilized conditions and spatial average of transmissivity may be observed for the distances which are considerable far away pumping well during the late pumping period. Similar arguments were also supported by Rhode *et al.* (2007); the researchers analyzed the volumetric evaluation of the influence zone for the lognormal transmissivity distribution to reflect block heterogeneity for the two aquifer systems which had both spatially random and spatially correlated data sets. They also illustrated that the heterogeneity in the well vicinity is the main mechanism impacting the drawdown data in the early time pumping and that volumetric weighted mean transmissivity values at late pumping period do not converge over time to an asymptotic line during the late time pumping period if the steady-shape conditions are not satisfied.

Heuristic algorithms namely genetic algorithms, simulated annealing, tabu search method, and artificial neural network become recently more popular to understand the uncertainty effects caused by aquifer heterogeneity in estimation of aquifer parameters (Glover, 1993; McKinney and Lin, 1994; Pan and Wu, 1998; Zheng and Wang, 1999). Cheng and Yeh (1992) suggested a quasi-Newton algorithm by use of the Adjoint State method to solve inverse problems of parameter estimation. Balkhair (2002) developed an artificial neural network (ANN) model to estimate confined aquifer parameter values using by pumping test data for large diameter wells. Lin and Chen (2006) introduced a new ANN model to estimate aquifer parameter values. The authors criticized the Balkhair (2002) model and demonstrated the superior aspects of their model over the classical curve matching procedures (Sahin, 2008). Samani *et al.* (2007) modified the Lin and Chen (2006) ANN model by introducing the principle component analysis (PCA) which reduces the input vector dimension. Sahin (2008) suggested an iterative ANN model to estimate leaky aquifer parameters.

The important contribution for understanding of pumping response in nonhomogeneous aquifer came from petroleum engineering. Oliver (1990) derived semi-analytical formula to a weight function for the spatial transmissivity variation of an aquifer in his distinguished paper. Feitosa *et al.* (1994) suggested an inverse solution

algorithm to determine the reservoir permeability distribution from well test pressure data and pressure buildup data using Oliver's (1990) weight function.

As a summary, several inverse solution approaches have been suggested to estimate aquifer parameters. These approaches can be classified under two major groups. First group includes the statistical and stochastical process whereas the second group seeks to formulate deterministic solutions which may or may not be cooperated with optimization algorithms.

3. INCREMENTAL AREA METHOD

Theoretical well functions have been derived over the years to predict ground water level behavior in aquifer systems being stressed by groundwater extraction. The drawdown data collected during pump tests are typically analyzed using graphical curve matching procedures to estimate aquifer parameters based on these well functions. Difficulty in identification of aquifer characteristics and estimation of parameters may arise when the field data do not perfectly match the drawdown curves obtained from the well functions. The present study provides a new method for the interpretation of aquifer pump tests which supplements the existing curve matching procedures in case ideal conditions do not exist; the proposed method provides a greater degree of flexibility in the data analysis for diagnostic tool purposes. The method, referred as the Incremental Area Method (IAM) is based on integrating the logarithmic based drawdown curves within a discrete time period and matching the results with a corresponding time integral of well function which governs ideal confined aquifers. The application of the proposed method to synthetically generated data and field data showed that IAM represents a viable method which yields information on potential non-idealness of the aquifer and provides aquifer parameter estimation thus potentially overcoming drawdown data curve matching difficulties.

3.1. Confined Aquifer Methodology [1]

Aquifer pump test results are typically analyzed using graphical curve matching procedures to estimate aquifer parameters. In conventional curve matching procedure, an arbitrary matching point is chosen to serve as a reference point that can be located anywhere on the graph which is drawn for the same log-log scale of time-drawdown curve and the theoretical type curve. For visual practice both curves are plotted on the transparent graph and then superimposed. These procedures have inherent shortcomings when a perfect match is not realized for the complete drawdown data or

[1]The organization of this section mostly depends on our research paper which was published in Hydrological Process, Avci *et al.* (2011).

when the heterogeneity conditions are reflected in the field data and matching becomes difficult with idealized type curves as illustrated in Figure 3.1.

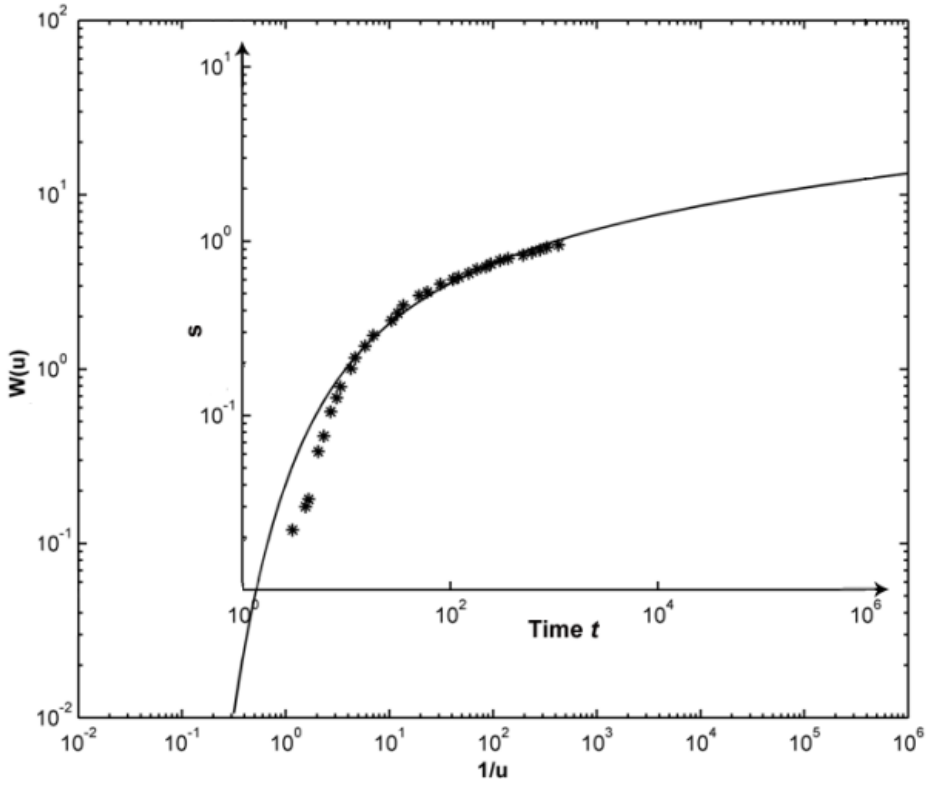

Figure 3.1. Theis Curve Fit (Drawdown data taken from Batu, 1998).

The curve matching process is basically based on the similarity solution between the analytical type curve and the field data drawdown curve. According to the curve matching technique, the perfect match is conceptually achieved if the noise-free field data scaled in both directions (drawdown vs. time) by the scale factors $Q/4\pi T$ and dimensionless parameter u. The unknown transmissivity value controls the drawdown scale whereas both of storativity and transmissivity are responsible of time shifting. A new methodology is suggested for the interpretation of aquifer pump tests which provides a greater degree of flexibility in the data analysis. The method, referred as the Incremental Area Method (IAM) is based on integrating the incremental drawdown portion within a time integral and matching the results with a similar time integral of

the governing aquifer function. Thus, the match point yields the aquifer parameters since a unique integration value was identified in the drawdown data and the aquifer function. The calculation of incremental area underneath the drawdown curve avoids the scale factors in the field data and this area then shares the same properties of confined aquifer type curve as shown in Figure 3.2. The integration can be done by starting at any point of the pumping test and the window of integration can be chosen arbitrarily which allows the analysis to be done at various times during the test and establish potential heterogeneities within the developing radius of influence.

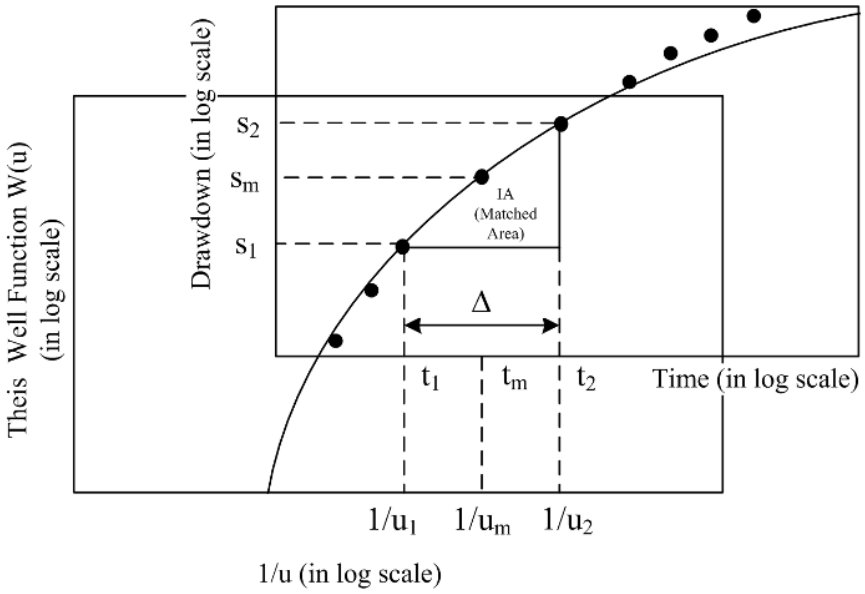

Figure 3.2. Schematic Representation of Incremental Area (IA) for integration increment Δ.

The theoretical formulation of the incremental area IA for the Theis type curve is as follows:

$$IA\left(\Delta, u_1, u_2\right) = \phi - \psi \tag{3.1}$$

where

$$\phi = \int_{\log_{10} 1/u_1}^{\log_{10} 1/u_2} \log_{10} \left(\int_u^\infty \frac{e^{-t}}{t} dt \right) d\left(\log_{10} 1/u\right) \text{ and } \psi = \int_0^\Delta \log_{10} \left(\int_{u_1}^\infty \frac{e^{-t}}{t} dt \right) d\Delta \quad (3.2)$$

The incremental area IA underneath the real field drawdown data can be approximated using Simpson's Integration Rule as follows:

$$IA = \Delta \times \left[\frac{2}{3} \log_{10} \left(\frac{s_2}{s_1} \right) + \frac{1}{6} \log_{10} \left(\frac{s_3}{s_1} \right) \right] + O\left(\Delta^2\right) \quad (3.3)$$

The values of the incremental area function can be obtained from Equation 3.1 using numerical integration techniques including dividing the integration time increment period into subintervals and then applying Composite Simpson's rule. It should be noted that for $log1/u > 2$ (e.g. $u < 0.01$) where the Cooper-Jacob (1946) approximation is valid, Equation 3.1 can be evaluated analytically. For $u < 0.01$ letting $x = log1/u$, ψ in Equation 3.3 can then written in terms of natural logarithm as

$$\phi = \int_{x_1}^{x_2} \log\left(-\gamma + x\right) dx \quad (3.4)$$

Equation 3.4 can be evaluated by denoting $z = -\gamma + x$ and integration will yield:

$$\phi = \int_{z_1}^{z_2} \log\left(z\right) dz \Rightarrow \phi = z\left(\log\left(z\right) - 1\right)\Big|_{z_1}^{z_2} \quad (3.5)$$

The well function term can be taken outside of the integration in ψ due to that $\log 1/u$ is independent of time increment Δ which is considered as the log-cycle value in logarithm base 10. Figure 3.3 indicates the error between numerical and analytical integration of Theis (1935) well function for the increment rate $\Delta = 1$.

The integration distance Δ has an impact on the transmissivity estimation which is averaged inside the cone of depression. For the small values of Δ, variation of transmissivity with time is more sensitive than that for the large values of Δ. Incremental

area values can easily be linked to the dimensionless u values by constructing a fit equation for the practical uses as following:

$$\log_{10}(1/u) = \frac{p_1 A^3 + p_2 A^2 + p_3 A + p_4}{A + q_1} \tag{3.6}$$

where A represents the incremental area, p_1, p_2, p_3,p_4, and q_1 are the coefficients of suggested fit curve. Table 3.1 indicates the coefficients of fit equation described in Equation 3.6 within 95% confidence level and summarized the statistical performance of the fit equation for various Δ values for $log_{10}(1/u)$ in the range of -0.5 to 8.

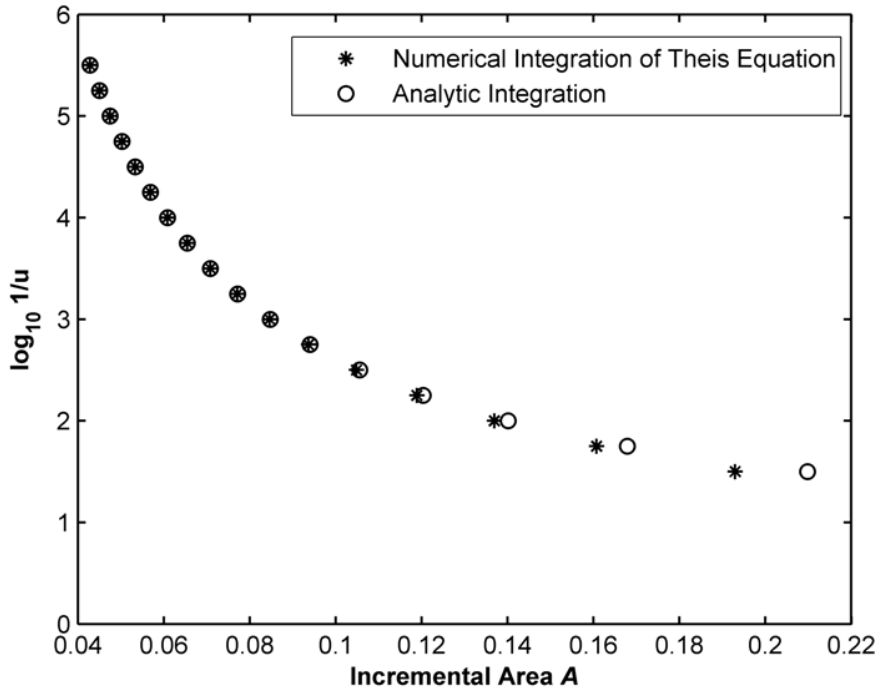

Figure 3.3. Error Comparison of Numerical and Analytical Integration for $\Delta = 1$.

Table 3.1. Statistical Performance of the Fit Equation.

Δ	p_1	p_2	p_3	p_4	q_1	SSE	R^2	RMSE
0.25	71.98	-15.91	0.4210	0.01325	-1.83E-05	0.4646	1	0.005307
0.5	5.103	-4.159	0.4839	0.05263	-1.04E-04	0.259	1	0.004024
1	0.3778	-1.096	0.6155	0.20730	-6.74E-04	0.08886	1	0.002434
2	0.02598	-0.2759	0.9071	0.79790	-5.28E-03	0.04419	1	0.001844

The incremental area IA values for various integration increment Δ are shown in a more general form in Figure 3.4.

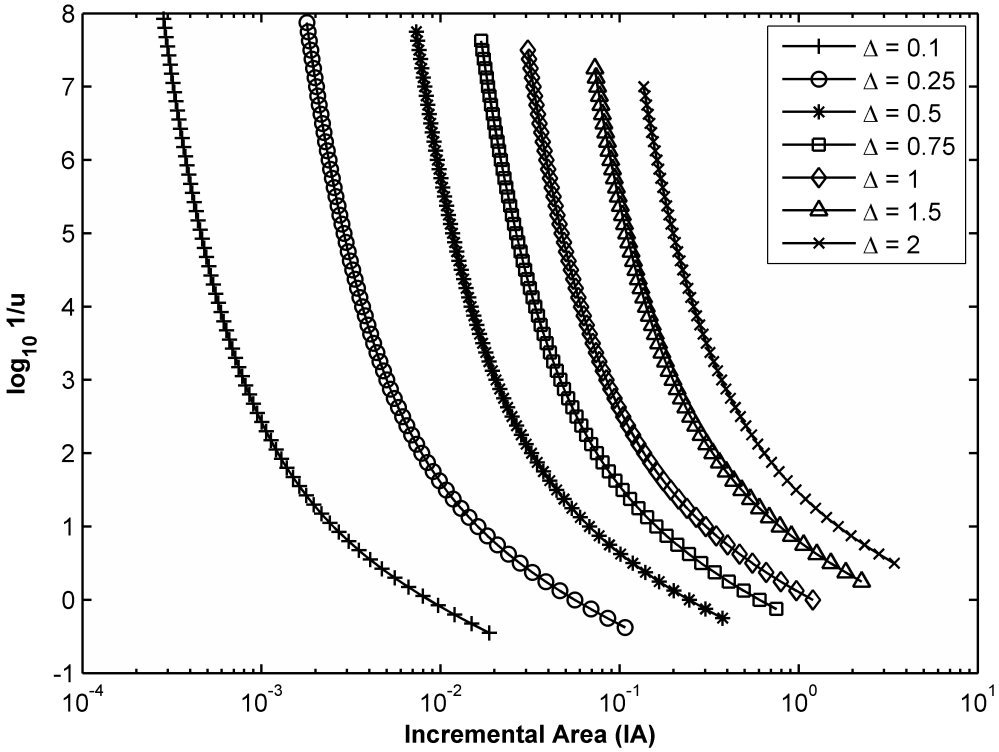

Figure 3.4. The Effect of Integration Time Interval Δ on Incremental Area (IA) values (Avci *et al.*, 2011).

Having established the theory behind incremental area matching between the real field data and the Theis (1935) well function curves and the means by which

the incremental area values can be calculated, the methodology to investigate actual drawdown data is proposed as follows (Avci *et al.*, 2011):

(i) Plot the field time-drawdown data in log-log scale.

(ii) Select any two points on the time-drawdown curve that are apart with an integration time increment (any increment value can be selected based on Figure 3.4). Use these two points and corresponding drawdown measurements between them to calculate the incremental area.

(iii) The incremental area underneath the field data can be estimated using Simpson's rule as given in Equation 3.3 (Interpolation of drawdown data may be required if there is no drawdown data at midpoint of the integration time increment).

(iv) Use Figure 2.2 to calculate the matching value for u and the corresponding value of $W(u)$ for a corresponding equivalent ideal aquifer incremental area.

(v) Use Equation 2.21 and Equation 2.23 to calculate the transmissivity and storativity values, respectively.

(vi) Plot the variation of the transmissivity and storativity versus the corresponding starting time of the integration time increment as a visual tool for the identification of potential changes in the aquifer system and aquifer parameters as the cone of depression expands from the pumping well. This method will, therefore, allow analysis of the drawdown curve in discrete sections and will be able to detect variations from ideal confined aquifer conditions as the aquifer parameters will be dependent on the location at which the incremental area is being matched.

(vii) Perform sensitivity analysis of the transmissivity and storativity values with respect to the integration time increment.

The illustrative summary of the proposed methodology is given in Figure 3.5.

Under ideal conditions the value of the aquifer parameters should be independent of the integration time increment as well as the starting point of the integration time increment. However, the drawdown curve obtained as the cone of depression expands outward from the pumping well may deviate from ideal drawdown curve conditions. Any heterogeneity or non ideal conditions that would be present within the cone of

depression would result in the variation of transmissivity and storativity values as the cone of depression expands (Avci *et al.*, 2011).

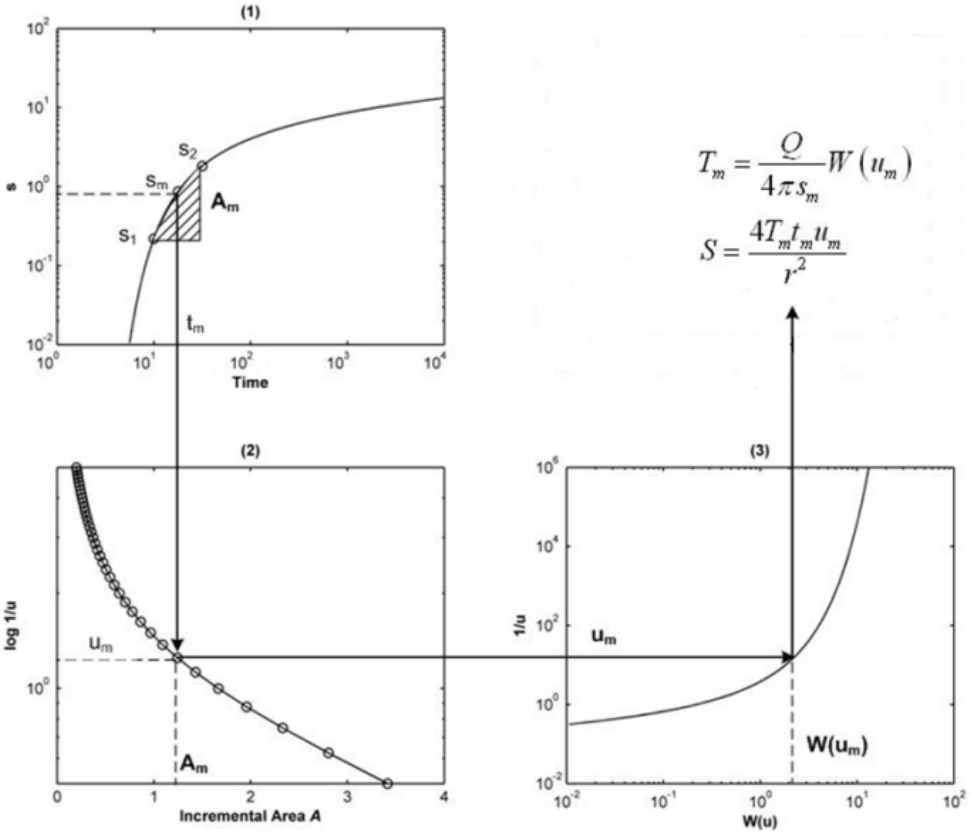

Figure 3.5. Schematic View of Application of IAM (Avci *et al.*, 2011).

These variations would be noted from the results of the steps vi and vii. The use of the proposed methodology will therefore allow tracking the variation of the aquifer using drawdown data within an observation well as equivalent ideal confined aquifer parameters which are illustrated in Figure 3.5. This feature of the analysis will provide the following key results (Avci *et al.*, 2011):

- Estimation of aquifer parameters variation with time.
- Obtaining equivalent transmissivity and storativity values within different parts of the drawdown data if the cone of depression has extended enough.
- Identification of deviations from ideal confined aquifer conditions.
- Identification of characteristics of the aquifer behavior within the cone of depres-

sion (start of leakage, presence of boundary conditions).

3.2. Leaky Aquifer Methodology

The same logic behind the incremental area methodology can be extended to determine leaky aquifer parameters estimation. The groundwater movement in leaky aquifer has a different manner due to leakage from aquitard overlain the confining layer. Since the vertical leakage feeds the aquifer, drawdown values of leaky aquifer can not drop as much as in the confined aquifer case. This situation can be simply observed in the well function which produces the constant drawdown values after a certain period of time. The additional aquifer parameter called as leakage factor, therefore, appears in the parameter estimations. The IAM, however, has been established to elaborate transmissivity and storativity for a single type curve. If the leakage factor is known, IAM then can be safely applied to estimate aquifer. Therefore, IAM for leaky aquifer can be first utilized to estimate leakage factor, the given methodology in the previous section or the suggested procedure will be used to elaborate aquifer parameters as well. The deeper analysis of leaky well is needed for this purpose.

Transient drawdown of a leaky confined aquifer was given in Equation 2.27. For a homogenous leaky aquifer, the steady-state drawdown was given by de Glee (1930) as

$$s_{\max} = \frac{Q}{2\pi T} K_0(\lambda) \tag{3.7}$$

where K_0 is the zero order modified Bessel function of second kind and λ is leakage factor. The leaky well function can be normalized dividing by steady state value of each λ given as

$$\frac{s}{s_{\max}} = \frac{W(u,\lambda)}{2K_0(\lambda)} \Rightarrow 2\left(\frac{s}{s_{\max}}\right) K_0(\lambda) = W(u,\lambda) \tag{3.8}$$

Figure 3.6 indicates the relation between normalized drawdown and leakage factor for $0.001 \leq \lambda \leq 2$ and $0.5 \leq 1/u \leq 10^6$.

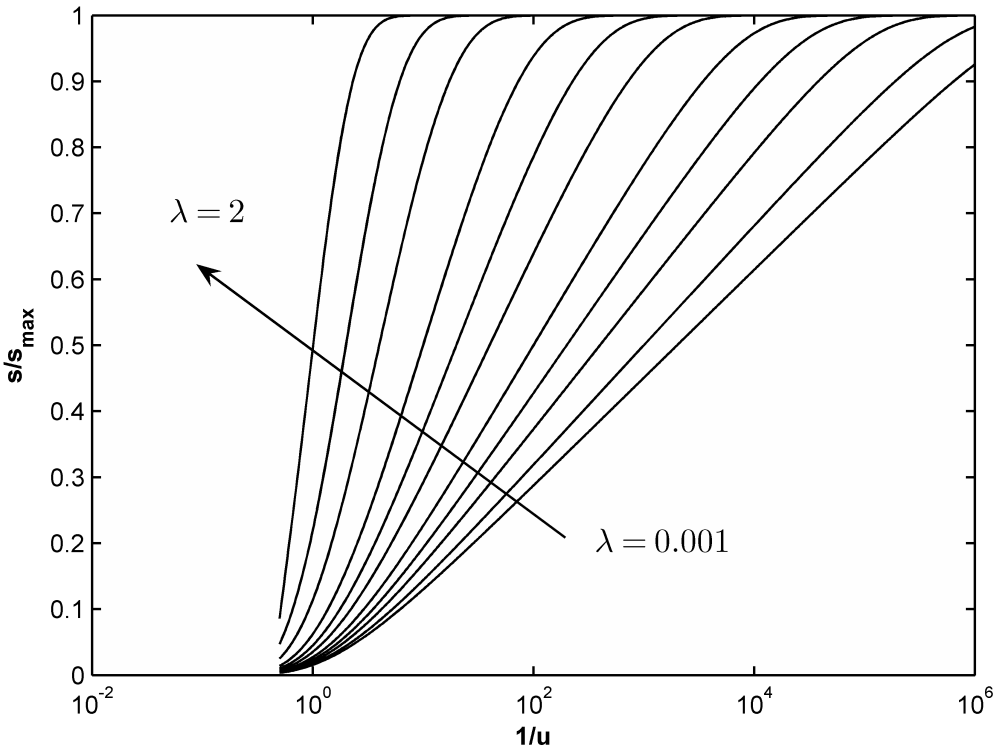

Figure 3.6. Normalized Leaky Well Function.

The leaky well function ranges over a semi-infitine domain. The well function described in Equation 2.27 can be approximated properly by finite serial expansion. Considering the Maclaurian series of exponential function, the leaky well function can be written as following form

$$\begin{aligned} W(u,\lambda) &= \int_u^\infty \frac{\exp(-y-\lambda^2/4y)}{y} dy \\ &\Rightarrow \int_u^\infty \frac{\exp(-y)}{y} \exp\left(-\lambda^2/4y\right) dy \\ &= \int_u^\infty \frac{\exp(-y)}{y} \sum_{n=0}^\infty \frac{(-1)^n}{n!} \left(\frac{\lambda^2}{4y}\right)^n dy + \int_u^\infty \frac{\exp(-y)}{y} R_n dy \end{aligned} \tag{3.9}$$

where R_n is the remainder term. The infinite series in Equation 3.9 was obtained by performing term by term integration of the series. In the range of $0 \leq \lambda^2/4u < \infty$, rearrangement of the integral in Equation 3.9 eventually leads to the following form

(Gautcshi and Cahill, 1972)

$$W(u,\lambda) \cong \sum_{n=0}^{\infty} \frac{(-1)^n}{n!} \left(\frac{\lambda^2}{4u}\right)^n E_{n+1}(u) \tag{3.10}$$

where

$$E_{n+1}(u) \cong \frac{1}{n}\left[\exp(-u) - uE_n(u)\right] \tag{3.11}$$

Gautcshi and Cahill (1972) also indicated that the recurrence relation can be used safely in the forward direction (increasing n) for arguments less than five. Stability of recurrence relation fails when Equation 3.11 is used to evaluate Equation 3.10 for $u > 5$. These instability limits, fortunately, lie in a small region $10 < \lambda < 100$ and $5 < u < 50$ which is a region not likely to be encountered in groundwater practice (Kluitenberg and Warrick, 2001). The E_n terms are expressed in terms of E_1, the leaky well function can be written in a general form as follows

$$W(u,\lambda) = E_1(u)\left(1 + \sum_{n=1}^{\infty} \frac{(\lambda/2)^{2n}}{n \times n!}\right) + \sum_{m=1}^{\infty}\sum_{n=m}^{\infty}\left(-\frac{1}{u}\right)^m \exp(-u)\frac{(\lambda/2)^{2n}}{n \times n!} \tag{3.12}$$

The modified zero order Bessel function of second kind appeared in the left hand side of Equation 3.8 can be approximated by serial expansion as

$$K_0(\lambda) = -\left[\left(\ln\frac{\lambda}{2} + \gamma\right) I_0(\lambda) - \sum_{n=1}^{\infty}\frac{2}{n} I_{2n}(\lambda)\right] \tag{3.13}$$

where I_0 is the modified zero order Bessel function of first kind which can be written as

$$I_0(\lambda) = \sum_{n=0}^{\infty}\frac{1}{n!^2}\left(\frac{\lambda}{2}\right)^{2n} \tag{3.14}$$

For $\lambda \leq 2$, $I_0(\lambda)$ term can be approximated by the following formulation with an

average error of 0.15%.

$$I_0(\lambda) \approx 1 + \sum_{n=1}^{\infty} \frac{(\lambda/2)^{2n}}{n \times n!} \tag{3.15}$$

Substituting Equation 3.12 and Equation 3.13 into the Equation 3.8 yields to

$$\begin{aligned} E_1(u) = -2\left(\frac{s}{s_{\max}}\right)\left[(\ln \lambda/2 + \gamma) - \frac{1}{I_0(\lambda)} \sum_{n=1}^{\infty} \frac{2}{n} I_{2n}(\lambda)\right] \\ - \frac{1}{I_0(\lambda)} \sum_{m=1}^{\infty} \sum_{n=m}^{\infty} \left(-\frac{1}{u}\right)^m \exp(-u) \frac{(\lambda/2)^{2n}}{n \times n!} \end{aligned} \tag{3.16}$$

The difficulty arisen in Equation 3.16 is to determine how many terms which provide a good approximation within an acceptable error bound. For the smaller leakage factor values (i.e. for $\lambda \leq 0.01$), the leaky well function reduces to Theis well function. Therefore, there is no need to extra E_n terms in the recursion equation, Equation 3.16 eventually leads to

$$\begin{aligned} -2\left(\frac{s}{s_{\max}}\right)(\ln \lambda/2 + \gamma) = E_1(u) \\ \Rightarrow -2\left(\frac{s}{s_{\max}}\right)(\ln \lambda - \ln 2 + \gamma) = -\ln u - \gamma \\ = -2\left(\frac{s}{s_{\max}}\right)(\ln \lambda - \ln 2 + \gamma) + \gamma = \ln 1/u \end{aligned} \tag{3.17}$$

For practical range of leakage factor (i.e. $0.01 \leq \lambda \leq 2$), the exponential integral term, appeared in the right hand side of Equation 3.16, is truncated first two terms for $u \leq 1$ under Cooper-Jacob assumption. Rearrangement of Equation 3.16 yields to

$$-(\ln \lambda/2 + \gamma) = \frac{-\gamma - \ln u}{2(s/s_{\max})} + M \tag{3.18}$$

where M is the reminder term. Thus, Equation 3.16 can be expressed in the following form

$$\alpha \ln \lambda + \beta = \ln(1/u) \tag{3.19}$$

where α and β are the coefficients of the linear equation and are given as

$$\begin{aligned} \alpha &= -1.5942\,(s/s_{\max}) - 0.2021 \\ \beta &= 2.4786\,(s/s_{\max}) - 0.5326 \end{aligned} \tag{3.20}$$

The values of α and β are tabulated in Table 3.2 and also shown in Figure 3.7. When the dimensionless type curves are plotted for $0.001 \leq \lambda \leq 2$ and $0.5 \leq 1/u \leq 10^6$, type curves are almost linear for $0.2 \leq s/s_{\max} \leq 0.8$ as illustrated in Figure 3.8.

Table 3.2. α and β Values.

s/s_{max}	α	β	R^2
0.2	-0.5200	-0.0313	0.9946
0.25	-0.6005	0.1076	0.9967
0.3	-0.6804	0.2355	0.9982
0.35	-0.7604	0.3558	0.9992
0.4	-0.8404	0.4709	0.9997
0.45	-0.9201	0.5834	0.9999
0.5	-0.9996	0.6948	1
0.55	-1.0794	0.806	0.9999
0.6	-1.1591	0.919	0.9998
0.65	-1.2386	1.0355	0.9996
0.7	-1.3179	1.1578	0.9995
0.75	-1.397	1.2889	0.9993
0.8	-1.4763	1.4333	0.9992
0.85	-1.5565	1.5989	0.9991
0.9	-1.6383	1.8033	0.9992

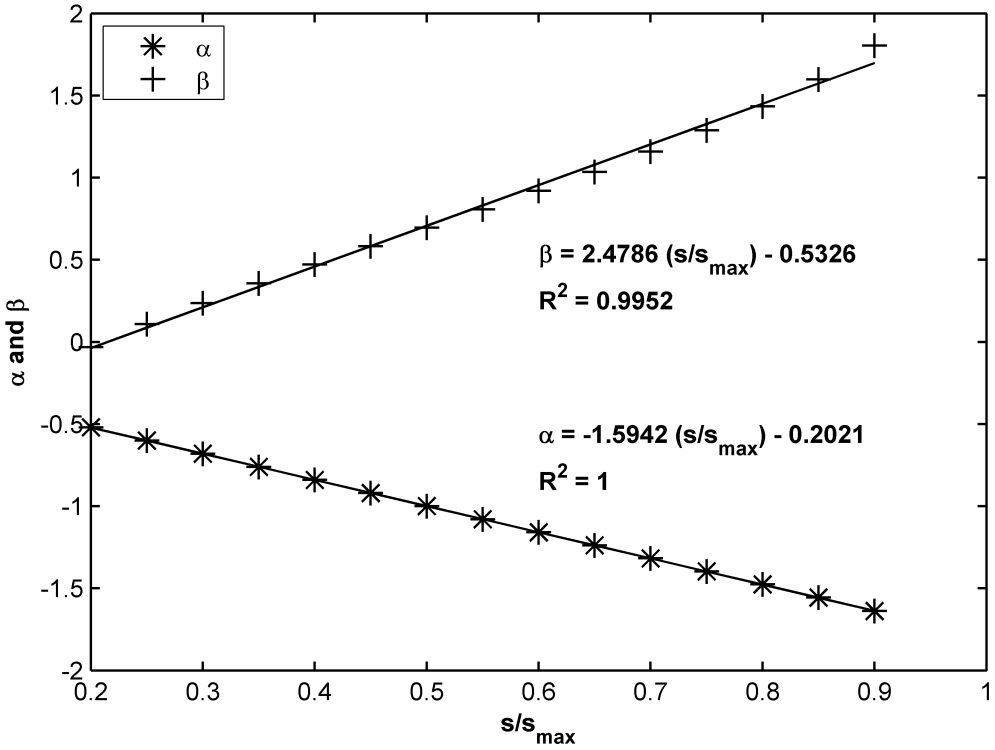

Figure 3.7. α and β Variation with s/s_{max}.

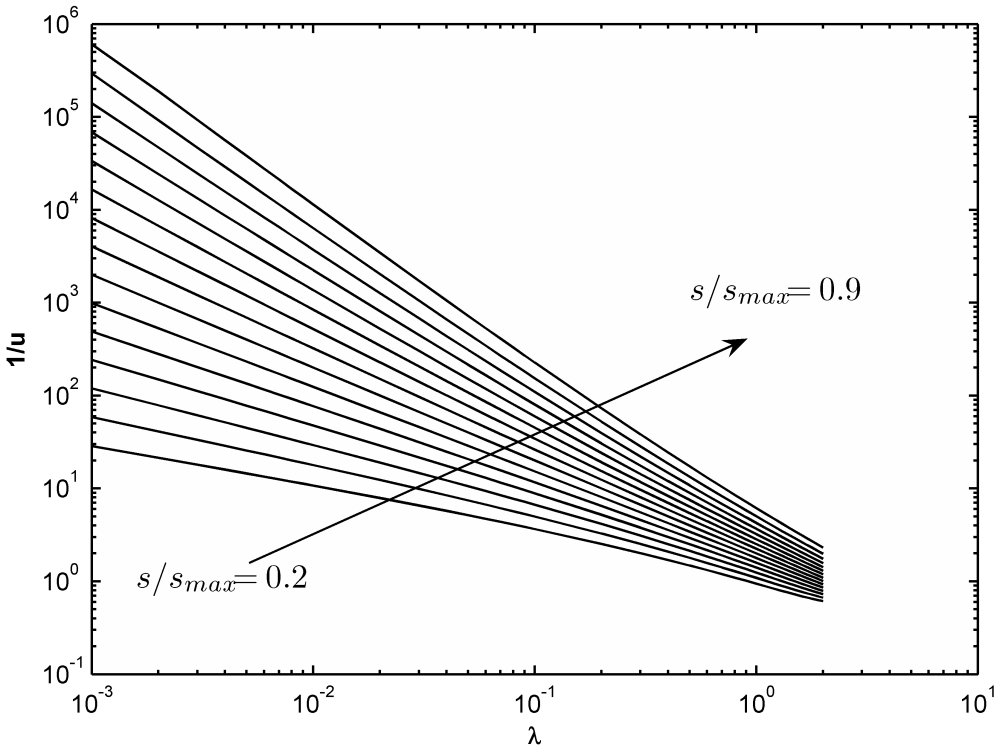

Figure 3.8. Linearization of Dimensionless Time and Leakage Factor for Various s/s_{max}.

In the standard curve matching procedure, leakage factor is first determined by superimposing curves; aquifer parameters, namely transmissivity and storativity, are then calculated. Following the same logic, incremental area first provides the leakage factor, and then Equation 3.19 can be used to determine dimensionless time $1/u$. The incremental area or the trapezoidal area under the leaky type curves is different for each leakage factor values as illustrated in Figure 3.9 which is generated for the areas between $s/s_{max} = 0.25$ and $s/s_{max} = 0.75$.

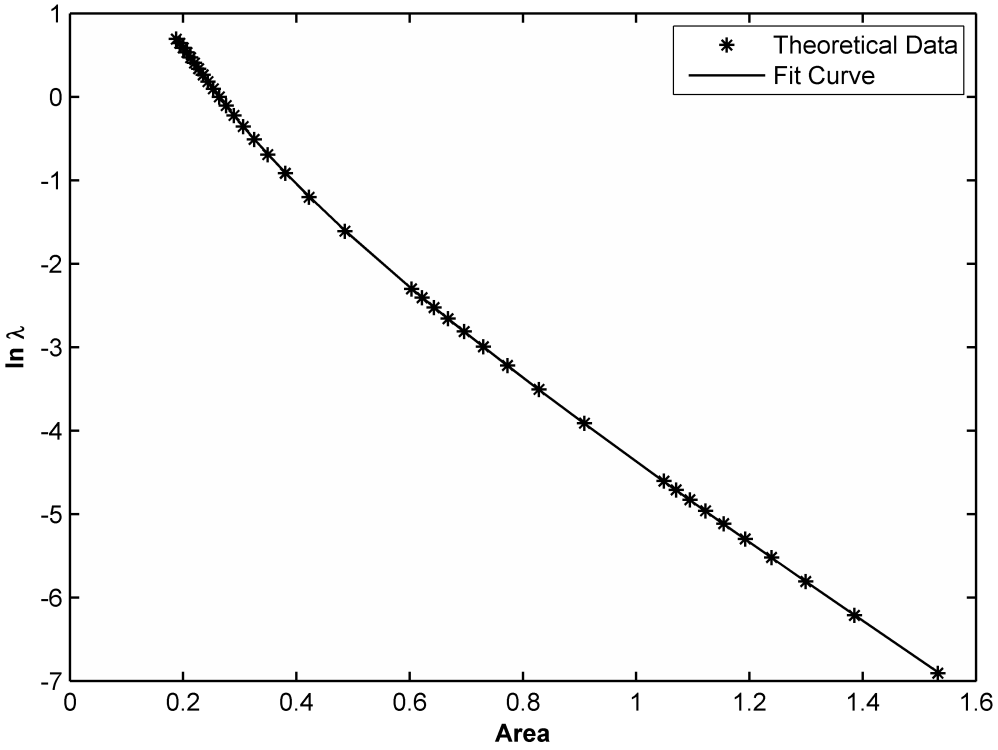

Figure 3.9. The Relation between $1/u$ and Area.

A rational fit curve also shown in Figure 3.9 can be used to estimate leakage factor for the normalized drawdowns in between $s/s_{max} = 0.25$ and $s/s_{max} = 0.75$ with the statistical properties of SSE and R^2 as 0.002787 and 1, respectively as

$$\ln(\lambda) = \frac{-4.329A^2 - 1.46A + 0.6843}{A + 0.168} \tag{3.21}$$

The suggested methodology to determine confined aquifer parameters are listed as:

(i) Examine the field drawdown data. If the trend of drawdown data in late time approaches a constant value, normalize the field drawdown data dividing by that value and plot the time-normalized drawdown data in semilog scale.

(ii) Fit the normalized drawdown-time curve if possible.

(iii) Select s/s_{max} values for 0.25, 0.5, and 0.75. Read the corresponding $log_{10}t$ values to calculate the trapezoidal area or incremental area underneath the time-normalized drawdown data.

(iv) Use Figure 3.9 or Equation 3.21 to estimate the leakage factor.

(v) Use Equation 3.7 to estimate transmissivity.

(vi) Use Equation 2.23 to calculate storativity. For $s/s_{max} = 0.5$, $u = \lambda/2$, storativity can be calculated as

$$S = \frac{2Tt_{0.5}(\lambda)}{r^2} \tag{3.22}$$

(vii) The vertical conductivity can be calculated as

$$K' = \frac{Tb'\lambda^2}{r^2} \tag{3.23}$$

The items (i) to (iv) can be used to estimate leakage factor. After estimation of leakage factor, IAM procedure explained in the previous section can be followed to track the time variation of aquifer parameters such as transmissivity and storativity.

4. INVERSE SOLUTION ALGORITHM

The analytical and numerical studies explained in the previous sections have investigated the large scale average hydraulic parameters conditions with the types of potentially suitable areal averaging methods, as well as early and late time behavior of time drawdown curves. Tóth (1966) studied the late time pumping response of heterogeneous aquifer and showed that the type curve behavior plotted in log-log and semi-log scales yield a unique value consistent with the average of aquifer parameters inside the influence zone. Similar researches addressed this theory and concluded that transmissivity values (termed as an equivalent transmissivity) obtained from pumping response converge to some mean of large scale aquifer condition within the cone of depression. Meier *et al.* (1998) and Sanchez-Vila *et al.* (1999) claimed that transmissivity value estimation of the aquifer results in two different aspects of the pumping period: first, transmissivity values are close to geometric mean of material within the well vicinity during the initial pumping period and late time pumping response represents the equivalent transmissivity of the entirety of the influenced aquifer domain. Desbarats (1992), however, suggested that transmissivity values between monitoring wells could be interpreted as transmissivities averaged as harmonic mean across the circular areas centered at each observation point. Streltsova (1988) showed that geometrical configuration of the heterogeneity would impact the transmissivities and storativity values obtained from pumping tests. Butler (1988) indicated that the Theis (1935) method will provide weighted averages of near-well and far-field transmissivity and storativity values in radially symmetric heterogeneous aquifers. This approach has also been supported in Streltsova (1988) which stated that the soil matrix material near to well vicinity has a significant impact on the pumping response rather than the far end material of aquifer during pumping period. Butler (1986, 1988, and 1990) and Butler and McElwee (1990) reviewed the transient pumping response obtained in an aquifer with a circular heterogeneity distribution; transmisivity values were estimated using analytical techniques for the interpretation of drawdown data. Osiensky *et al.* (2000) used numerical simulations of aquifer pumping test conditions to show that representative transmissivity values of the heterogeneity could be derived by the Theis (1935) method

for multiple well aquifer tests under specific drawdown versus time plots.

Despite the tremendous amount of research conducted for understanding the heterogeneous field structure, the literature review suggests that there is still a need for methods that can be applied to pumping test data in order to predict the variation of the transmissivity field. The recent works of Avci *et al.* (2011) and Copty *et al.* (2011) have provided insight into the radial variability of the transmissivity field from single well pumping tests. Avci *et al.* (2011) has used an integration technique for the discrete portion of the drawdown data to assess changes in the hydraulic properties as the cone of depression expands during the pumping test. Copty *et al.* (2011) has presented a derivative based approach which again allows for the detection of the transmissivity variation during the pumping test as a similar approach presented by Sen (1986). Both of these methods, however, represent an averaged concept of the transmissivity field over the entire cone of depression as it expands with time rather than an assessment of the transmissivity field variation with distance.

A large number of well test analysis techniques have been developed both in the groundwater and petroleum engineering fields that have been an excellent source of knowledge transfer from one field to the other. The methods derived in the oil and gas sector for assessing heterogeneous formations were reviewed to establish their potential use for aquifer setting conditions. A literature survey showed that Oliver (1990) derived an analytical expression for the problem of a well bore pressure response in an infinite reservoir with a small arbitrary spatial variation in permeability. The subsequent work of Feitosa *et al.* (1994) studied the application of Oliver (1990) formulation to elaborate the radial permeability variation as an inverse solution algorithm (ISA) for the petroleum engineering.

4.1. Mathematical Background of ISA

Oliver (1990) developed an analytic approach for predicting the variation of the transmissivity field in the radial direction for heterogeneous petroleum reservoirs. The solution was derived for assessing the wellbore-pressure response for a well located in

an infinite petroleum reservoir with a small arbitrary spatial variation in permeability for petroleum engineering cases. The governing equation for a slightly compressible fluid, single phase flow under the assumptions of negligible reservoir wellbore storage and skin effects was given in a dimensionless form as

$$\nabla \cdot \left(k_D\left(r_D,\theta\right)\nabla p_D\right) = \frac{\partial p_D}{\partial t_D} \tag{4.1}$$

The boundary conditions for the constant formation fluid withdrawal rate were taken as

$$\begin{aligned} \frac{1}{2\pi}\int_{-\pi}^{\pi} k_D\left(r_D,\theta\right) r_D \frac{\partial p_D}{\partial r_D} d\theta = -1 \quad \text{at} \quad r_D = 1 \\ \frac{\partial p_D}{\partial \theta} = 0 \qquad \text{at} \quad r_D = 1 \end{aligned} \tag{4.2}$$

where k_D is dimensionless permeability, p_D is dimensionless pressure, is dimensionless distance and t_D denotes the dimensionless time. Oliver (1990) assumed that the arbitrary heterogeneous permeability distribution function had small variation with respect to the average permeability where the permeability function was formulated as:

$$k_D\left(r_D,\theta\right) = \frac{1}{1- \in f\left(r_D,\theta\right)} \tag{4.3}$$

where $f\left(r_D,\theta\right)$ has and $O\left(1\right)$ is small. The solution of Equation 4.1 was obtained by taking Laplace transforms and a perturbation expansion in power of $\in$. The dimensionless pressure term in the wellbore of the extraction well pumping at constant discharge rate was formulated as:

$$p_D = -\frac{1}{2}\ln\left(t_D\right) - 0.4045 - \frac{\in}{2\pi}\int_{1}^{\infty} G\left(\xi, t_D\right)\int_{-\pi}^{\pi} f\left(\xi,\theta\right) d\theta d\xi \tag{4.4}$$

where $G(\xi, t_D)$ is expressed as:

$$G(r_D, t_D) = \frac{\sqrt{\pi}}{2} \int_0^{t_D} \frac{r_D}{t^2} \exp\left(-\frac{r_D^2}{2t}\right) W_{1/2,1/2}\left(\frac{r_D^2}{t}\right) dt \tag{4.5}$$

The slope of the dimensionless pressure term is given as:

$$t_D \frac{\partial p_D}{\partial t_D} = -\frac{1}{2} - \frac{\in}{2\pi} \int_1^{\infty} K(\xi, t_D) \int_{-\pi}^{\pi} f(\xi, \theta) d\theta d\xi \tag{4.6}$$

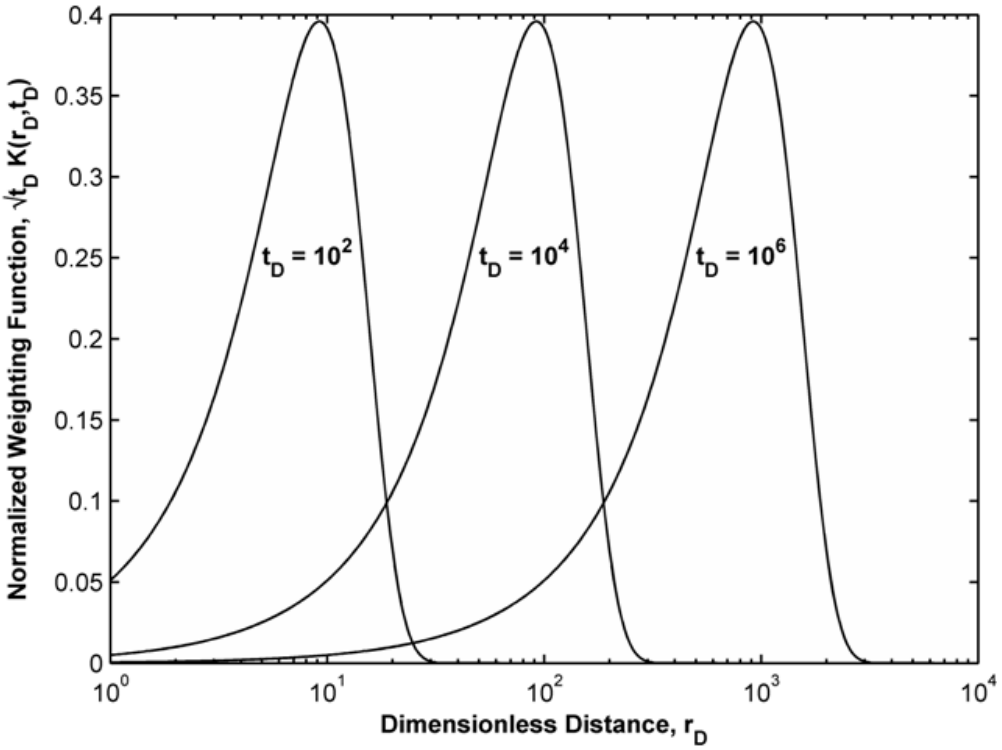

Figure 4.1. Weighting Function for t_D values of 10^2, 10^4, and 10^6.

The function depicted in Equation 4.6 can be simplified for small values of the multiplication with the pressure derivative approaching to the value of -1/2 and a kernel function $K(r_D, t_D)$ for >100 as follows:

$$\sqrt{t_D} K(r_D, t_D) = 0.5 \sqrt{\frac{\pi r_D^2}{t_D}} \exp\left(-\frac{r_D^2}{2t_D}\right) W_{1/2,1/2}\left(\frac{r_D^2}{t_D}\right) \tag{4.7}$$

where $W_{1/2,1/2}(z)$ is the confluent hypergeometric function referred as Whittaker's function. Figure 4.1 illustrates the weighting function given in Equation 4.7 for various dimensionless time values.

Feitosa *et al.* (1994) developed the Inverse Solution Algorithm (ISA) method based on the solution of Oliver (1990) to estimate the permeability variation in a petroleum reservoir using the extraction well pressure response data. The authors first assumed that the permeability variation of distance $k(r)$ was a harmonic mean of $k(r,\theta)$ in the direction of radial distance r as follows:

$$\frac{1}{k(r)} = \frac{1}{2\pi}\int_0^{2\pi} \frac{1}{k(r,\theta)} d\theta \tag{4.8}$$

Oliver (1990)'s solution was rearranged with the dimensionless variables as follows:

$$\Delta p'_D = \frac{1}{2} - \frac{1}{2}\int_1^{\infty} K^*(r_D, t_D)\left(1 - \frac{k_{ref}}{k(r_D)}\right) dr_D \tag{4.9}$$

where the kernel function K^* is twice the value of the weighting function which is defined in Equation 4.7, k_{ref} is the reference permeability, and $\Delta p'_D$ represents the dimensionless pressure derivative. For the homogeneous reservoir case where $k(r_D)$ is equal to k_{ref} for all values of r, the integral on the right hand side of Equation 4.9 vanishes; otherwise when the permeability is constant with $k(r) = k_1$, the pressure derivative reduces to the following form

$$\Delta p'_D = \frac{1}{2}\frac{k_{ref}}{k_1} \tag{4.10}$$

This leads to the following condition:

$$\int_1^{\infty} K^*(r_D, t_D) dr_D = 1 \tag{4.11}$$

Combining these equations and dimensionless variables, Feitosa *et al.* (1994) demon-

strated that the permeability variation was a function of distance given as follows:

$$\frac{1}{k_{in}} = \frac{h\Delta p'}{70.6qB\mu} = \int_1^\infty K^* \left(r_D, \hat{t}_D\right) \left(\frac{1}{k\left(r_D\right)}\right) dr_D \tag{4.12}$$

where k_{in} represents the instantaneous permeability in units of milidarcy (mD), $\hat{t}_D$ is the dimensionless pseudo-time, and r_D is the dimensionless distance, h is the reservoir thickness in units of ft, $\Delta p'$ represents the pressure change in the well in units of psi, q is the constant discharge rate in units of standard barrel per day, B is the volume fraction factor and μ is the viscosity in units of centipoise (cp). The model parameters used in the algorithm should be expressed in their dimensionless form and definitions. The time dependent pressure derivative is written as

$$\Delta p' = \frac{dp}{d\left(\ln t\right)} \tag{4.13}$$

Based on the Darcy's law, Feitosa *et al.* (1994) defined the instantaneous permeability as:

$$k_{in} = \frac{70.6qB\mu}{h\Delta p'} \tag{4.14}$$

The dimensionless pseudo-time was defined by Feitosa *et al.* (1994) as

$$\hat{t}_D = \frac{0.00634k_{in}t}{\phi c_t \mu r_w^2} \tag{4.15}$$

where ϕ denotes porosity, c_t stands for total system compressibility in units of psi^{-1}, r_w is wellbore radius in units of ft, and t is time in units of days. The dimensionless radius can be written as following

$$r_D = r/r_w \tag{4.16}$$

It should be noted that instantaneous permeability and pseudo-time values are time dependent variables. Inserting these variables into the ISA, Feitosa *et al.* (1994)

demonstrated the instantaneous permeability variation with distance to be as:

$$\frac{1}{k_{in}\left(t_n\right)} = \sum_{i=1}^{n-1} \int_{r_{i-1,D}}^{r_{iD}} K^*\left(r_D, \hat{t}_D\right)\left(\frac{1}{k\left(r_D\right)}\right) dr_D + \int_{r_{n-1,D}}^{\infty} K^*\left(r_D, \hat{t}_D\right)\left(\frac{1}{k\left(r_D\right)}\right) dr_D \tag{4.17}$$

The integrals of Equation 4.17 can be integrated numerically including the trapezoidal rule.

In order to estimate the radial permeability variation in aquifer pumping setting, the first drawdown derivative needs to be computed; the instantaneous permeability and pseudotime values can then be calculated using Equation 4.14 and Equation 4.15, respectively. The permeability values can be determined using Equation 4.17 where the integrals are evaluated using numerical integration techniques and the investigation radius concept can be inserted to determine integral limits as given by Feitosa *et al.* (1994):

$$r_i = Cr_w\sqrt{\hat{t}_D} \tag{4.18}$$

where C is multiplication factor and is reported to vary between 1.5-2 (van Poolen, 1964; Peaceman, 1978; Lee, 1982; Oliver, 1990 and Feitosa *et al.*, 1994). A backward substitution can be performed to understand the effect of the radius investigation coefficient C on the estimation procedure. For each C value, ISA provides estimates of the different radial distances and transmissivity values. Butler (1988) showed that the drawdown at any point in a radially symmetric two ring transmissivity field could be considered to have dependent and independent near well properties respectively; the semi-log distance drawdown approach was shown to yield an expression that was equivalent to the Thiem (1906) equation. This approach was used to establish the means for approximating a C multiplication factor; the distance drawdown formula

was taken be approximated within a non-uniform aquifer as:

$$\hat{s}_i = \hat{s}_{i-1} + \frac{Q}{2\pi\hat{T}_i} \log\left(\frac{r_i}{r_{i-1}}\right) \tag{4.19}$$

Estimated drawdown values can be compared with the observed drawdown values for each C value, and the most efficient C value can be obtained. If $r_D > 3\sqrt{\hat{t}_D}$, the weighting function depicted in Figure 4.1 approaches zero and the using integral mean value theorem, the second part of integral in Equation 4.17 can be approximated by

$$\int_{r_{n-1,D}}^{\infty} K^*\left(r_D, \hat{t}_D\right)\left(\frac{1}{k\left(r_D\right)}\right) dr_D = \frac{1}{k_{ave,n}} \int_{r_{n-1,D}}^{3\sqrt{\hat{t}_D}} K^*\left(r_D, \hat{t}_D\right) dr_D \tag{4.20}$$

where $1/k_{ave,n}$ indicates the weighted average of $1/k\left(r\right)$ on the interval of $r_{n-1,D} \leq r_D \leq 3\sqrt{\hat{t}_D}$. Simply setting $k\left(r\right) = k_{ave,n}$, the inverse solution algorithm can be completed.

Ryou (1995) modified Feitosa *et al.* (1994) solution to apply ISA for monitoring wells located at a distance from the petroleum reservoir pumping well using the kernel function K provided by Oliver (1990). The author suggested a new instantaneous permeability formulation including the dimensionless radial distance to the pumping well term enabling the estimations of permeability variation of an aquifer by using monitoring well data. This new definition was derived to be:

$$k_{in} = \frac{70.6qB\mu}{h\Delta p'} \exp\left(-\frac{r_D^2}{4\hat{t}_D}\right) \quad \text{for} \quad \hat{t}_D \geq 25r_D^2 \tag{4.21}$$

Equation 4.21 relates to the pseudo-time implicitly as given Equation 4.15. An iterative scheme is needed to obtain instantaneous permeability to apply ISA as described in this text. A Newton-Raphson iteration scheme was used to calculate the instantaneous permeability based monitoring well data throughout the examples given in this thesis.

Ryou (1995) showed the radial permeability variation as following:

$$\frac{1}{2k_{in}}\exp\left(-\frac{r_D^2}{4\hat{t}_D}\right)=\frac{1}{k_{in}}\left[\frac{1}{2}\exp\left(-\frac{r_D^2}{4\hat{t}_D}\right)-\int_{r_D}^{\infty}K\left(\xi,\hat{t}_D\right)d\xi\right]+\int_{r_D}^{\infty}K\left(\xi,\hat{t}_D\right)\frac{1}{k\left(\xi\right)}d\xi \tag{4.22}$$

Rearrangement of Equation 4.22 yields

$$\frac{1}{k_{in}}=\frac{\int_{r_D}^{\infty}K\left(\xi,\hat{t}_D\right)\frac{1}{k(\xi)}d\xi}{\int_{r_D}^{\infty}K\left(\xi,\hat{t}_D\right)d\xi} \tag{4.23}$$

The numerator term of Equation 4.22 can be expanded inserting the following variables:

$$u\left(r_D-a\right)=\begin{cases}0 & r_D<a\\ 1 & r_D\geq a\end{cases} \tag{4.24}$$

$$\Delta\left(\frac{1}{k_i}\right)=\begin{cases}\frac{1}{k_1} & i=1\\ \frac{1}{k_i}-\frac{1}{k_{i-1}} & i=2,3,...,n\end{cases} \tag{4.25}$$

The numerator term of Equation 4.22 can be rewritten regarding the Equation 4.24 and Equation 4.25 at $t=t_n$ as

$$\int_{r_D}^{\infty}K\left(\xi,\hat{t}_{nD}\right)\frac{1}{k\left(\xi\right)}d\xi=\int_{r_D}^{\infty}K\left(\xi,\hat{t}_{nD}\right)\left[\begin{array}{r}\frac{1}{k_1}+\Delta\left(k_2\right)u\left(\xi-\xi_2\right)+...\\ +\Delta\left(k_n\right)u\left(\xi-\xi_{n-1}\right)\end{array}\right]d\xi \tag{4.26}$$

Equation 4.26 yields to

$$\int_{r_D}^{\infty} K\left(\xi,\hat{t}_{nD}\right)\frac{1}{k\left(\xi\right)}d\xi = \frac{1}{k_1}\int_{r_{1D}}^{\infty} K\left(\xi,\hat{t}_{D}\right)d\xi + \Delta\left(\frac{1}{k_2}\right)\int_{r_{2D}}^{\infty} K\left(\xi,\hat{t}_{nD}\right)d\xi + \left(\frac{1}{k_n}\right)\int_{r_{n-1D}}^{\infty} K\left(\xi,\hat{t}_{nD}\right)d\xi \tag{4.27}$$

Rearranging Equation 4.27 yields to the following form by changing integral limits:

$$\begin{aligned}\int_{r_D}^{\infty} K\left(\xi,\hat{t}_{nD}\right)\frac{1}{k\left(\xi\right)}d\xi = \frac{1}{k_1}\int_{r_{1D}}^{\infty} K\left(\xi,\hat{t}_{D}\right)d\xi \\ + \Delta\left(\frac{1}{k_2}\right)\left[\int_{r_D}^{\infty} K\left(\xi,\hat{t}_{nD}\right)d\xi - \int_{r_D}^{r_{2D}} K\left(\xi,\hat{t}_{nD}\right)d\xi\right] + ... \\ + \Delta\left(\frac{1}{k_n}\right)\left[\int_{r_D}^{\infty} K\left(\xi,\hat{t}_{nD}\right)d\xi - \int_{r_D}^{r_{n-1D}} K\left(\xi,\hat{t}_{nD}\right)d\xi\right]\end{aligned} \tag{4.28}$$

Substituting Equation 4.39 into Equation 4.23, the instantaneous permeability at $t = t_n$ then given as

$$\frac{1}{k_{in}} = \frac{\frac{1}{k_{n-1}}\int_{r_D}^{\infty} K\left(\xi,\hat{t}_{nD}\right)d\xi + \sum_{i=2}^{n-1}\Delta\left(\frac{1}{k_i}\right)\int_{r_D}^{r_{n-1D}} K\left(\xi,\hat{t}_{nD}\right)d\xi}{\int_{r_D}^{\infty} K\left(\xi,\hat{t}_{nD}\right)d\xi} + \frac{\Delta\left(\frac{1}{k_n}\right)\left[\int_{r_D}^{\infty} K\left(\xi,\hat{t}_{nD}\right)d\xi - \int_{r_D}^{r_{n-1D}} K\left(\xi,\hat{t}_{nD}\right)d\xi\right]}{\int_{r_D}^{\infty} K\left(\xi,\hat{t}_{nD}\right)d\xi} \tag{4.29}$$

Equation 4.29 shows that the sequence $1/k_n$ can be computed recursively. To start the inversion algorithm, the permeability value at the time point in the pressure derivative data is calculated simply setting by $1/k_{in} = 1/k_1$. For the next time steps, rearrangement of Equation 4.29 will give the permeability average difference between the

investigated radial distances as following:

$$\Delta\left(\frac{1}{k_n}\right) = \frac{\frac{1}{k_{in}}\int_{r_D}^{\infty} K\left(\xi,\hat{t}_{nD}\right)d\xi - \frac{1}{k_{n-1}}\int_{r_D}^{\infty} K\left(\xi,\hat{t}_{nD}\right)d\xi}{\int_{r_D}^{\infty} K\left(\xi,\hat{t}_{nD}\right)d\xi - \int_{r_D}^{r_{n-1D}} K\left(\xi,\hat{t}_{nD}\right)d\xi} + \frac{\sum_{i=2}^{n-1}\Delta\left(\frac{1}{k_i}\right)\int_{r_D}^{r_{n-1D}} K\left(\xi,\hat{t}_{nD}\right)d\xi}{\int_{r_D}^{\infty} K\left(\xi,\hat{t}_{nD}\right)d\xi - \int_{r_D}^{r_{n-1D}} K\left(\xi,\hat{t}_{nD}\right)d\xi} \tag{4.30}$$

After computing $\Delta(1/k_n)$, the unknown permeability value k_n can be computed as

$$k_n = \frac{1}{\frac{1}{k_{n-1}} + \Delta\left(\frac{1}{k_n}\right)} \tag{4.31}$$

4.2. Application of ISA on Groundwater Aquifer Model

The ISA methodology given in the previous section has been developed to establish the radial permeability variation for petroleum reservoir model. Although model parameters utilized in the ISA are similar to the groundwater bearing aquifer model parameters, a proper unit conversions and matching among the input parameters, which may appear in one model type and does not exist in the other, should be conducted. For the application of the ISA methodology on a typical groundwater bearing aquifer model, Equation 4.14 can be expressed as:

$$k_{in} = \frac{70.6qB\mu}{h\rho_w g\Delta s'} \tag{4.32}$$

where ρ_w is the density of water, g is the gravitational constant and $\Delta s'$ is the drawdown derivative with respect to natural logarithm of time. Substituting the density of water (1000 kg/m^3 at 20°C), gravity g (9.81 m^2/s), viscosity of water μ (1.12 cp), volume fraction factor B (1), and then making necessary unit conversions, the instantaneous

permeability in units of mD can be formulated as:

$$k_{in} = 106.5412 \frac{q}{h\Delta s'} \tag{4.33}$$

where q is the pumping rate in units of m^3/day and h is the aquifer thickness in units of m. The dimensionless pseudo-time described in Equation 4.15 can be written for groundwater bearing aquifer conditions as:

$$\hat{t}_D = \frac{0.00634 k_{in} \rho_w g t}{S_c \mu r_w^2} \tag{4.34}$$

where S_c is the storage coefficient. Substituting the constant values and making unit conversions, the dimensionless pseudo-time can be expressed as:

$$\hat{t}_D = \frac{7.4827 \times 10^{-4} k_{in} t}{S_c r_w^2} \tag{4.35}$$

where k_{in} is the instantaneous permeability in units of mD calculated in Equation 4.33, S_c is the storage coefficient in units of m^{-1} and r_w is the pumping well radius in units of m, and t is time in units of days.

According to the modification of Ryou (1995), the instantaneous permeability variation for the monitoring wells are given in terms of groundwater bearing aquifer model parameters as:

$$k_{in} = 106.5412 \frac{q}{h\Delta s'} \exp\left(-\frac{r_D^2}{4\hat{t}_D}\right) \tag{4.36}$$

Once the variation in permeability is calculated, the results can be converted to the transmissivity field based on the Darcy's law given in Schwartz and Zhang (2003) as follows:

$$T = k_{in} h \frac{\rho_w g}{\mu} \tag{4.37}$$

Inserting constant values to be found within an aquifer setting and making the necessary unit conversions, the transmissivity in units of m^2/day can be written as

$$T = 7.5677 \times 10^{-4} k_{in} h \tag{4.38}$$

Thus, application of ISA can be summarized as following:

- Conduct a pumping test
- Take the derivative of drawdown data to be used in time dependent pressure variation shown in Equation 4.13.
- Compute the instantaneous permeability and dimensionless pseudo- time, respectively. If the pumping test data obtained from monitoring wells, an iterative scheme is needed as shown in Equation 4.21. Newton-Raphson iteration is recommended.
- Apply ISA as explained in the previous section.
- Obtain permeability variation in terms of dimensionless distances.
- Convert the calculated permeability to the transmissivity, and the dimensionless distances to radial distances as given in Equation 4.37 and Equation 4.16, respectively.

4.3. Illustrative Examples of ISA

For the demonstration of ISA, the test case of Feitosa *et al.* (1994) was repeated in this section. The authors studied the variation in permeability of an hypothetical reservoir using extraction well data. Reservoir model is assumed to be a five-zone-multi-composite reservoir with the following permeability distribution:

$$\begin{aligned}
k_1 &= 20 \text{ mD}, \ r_w \leq r < r_1 = 32 \quad \text{ft} \\
k_2 &= 30 \text{ mD}, \ r_1 \leq r < r_2 = 151 \quad \text{ft} \\
k_3 &= 10 \text{ mD}, \ r_2 \leq r < r_3 = 534 \quad \text{ft} \\
k_4 &= 18 \text{ mD}, \ r_3 \leq r < r_4 = 1055 \text{ ft} \\
k_5 &= 40 \text{ mD}, \ r_4 \leq r < r_5 = 5000 \text{ ft}
\end{aligned} \tag{4.39}$$

The extraction well operated with the flow rate of 300 RB/D. Reservoir porosity ϕ is 0.20, total system compressibility c_t is 10^{-5} psi^{-1}, fluid viscosity μ is 1 cp, wellbore radius r_w is 0.30 ft, and reservoir thickness h is 20 ft were taken for 30 days extraction. Initial pressure is assumed to be as 6000 psi.

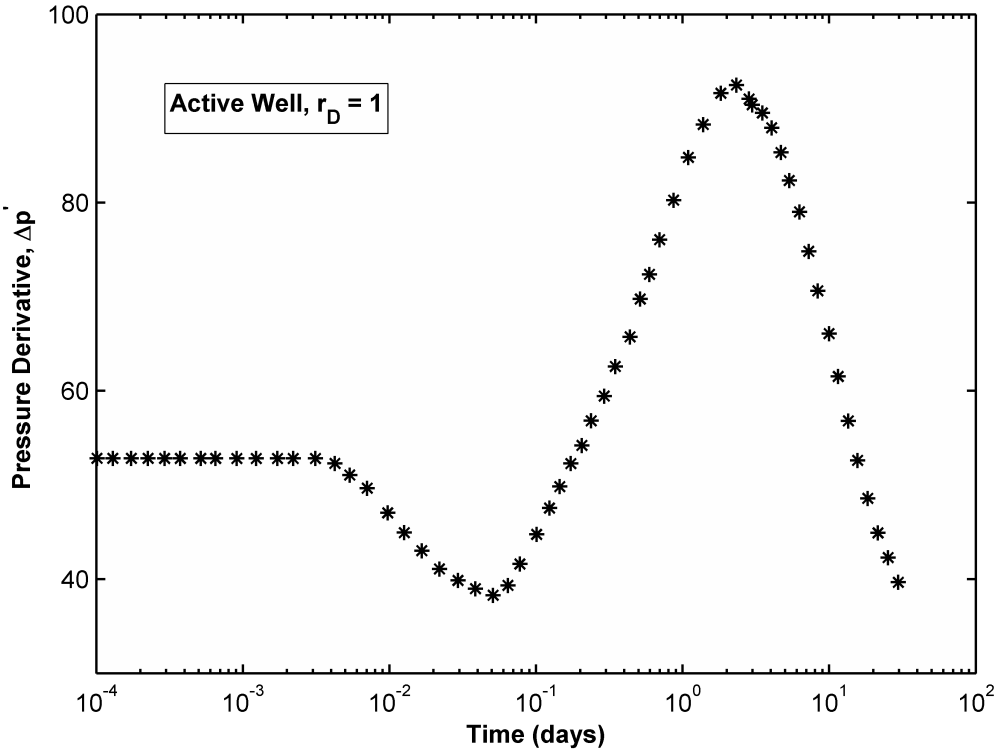

Figure 4.2. Pressure Derivative of Sample Problem.

Figure 4.2 illustrates the pressure derivative of sample problem. Figure 4.3 represents the effect of C coefficient on the ISA solution. The same problem was also reviewed by Ryou (1995) to show the applicability of ISA for monitoring well data. The same model simulation parameters and reservoir zoning in ISA analysis for pumping well drawdown data were utilized to compare ISA performance using monitoring well data. It is clearly observed that ISA solution with $C = 1.5$ for monitoring wells perform a good estimation until the particular value of distances as provided by Ryou (1995) throughout the examples which indicate the permeability variations of the monitoring wells located at the relative distances of r_D =10, 50 and 100 with respect to the extraction wellbore radius, respectively. Figures 4.4 to 4.6 demonstrate this situation.

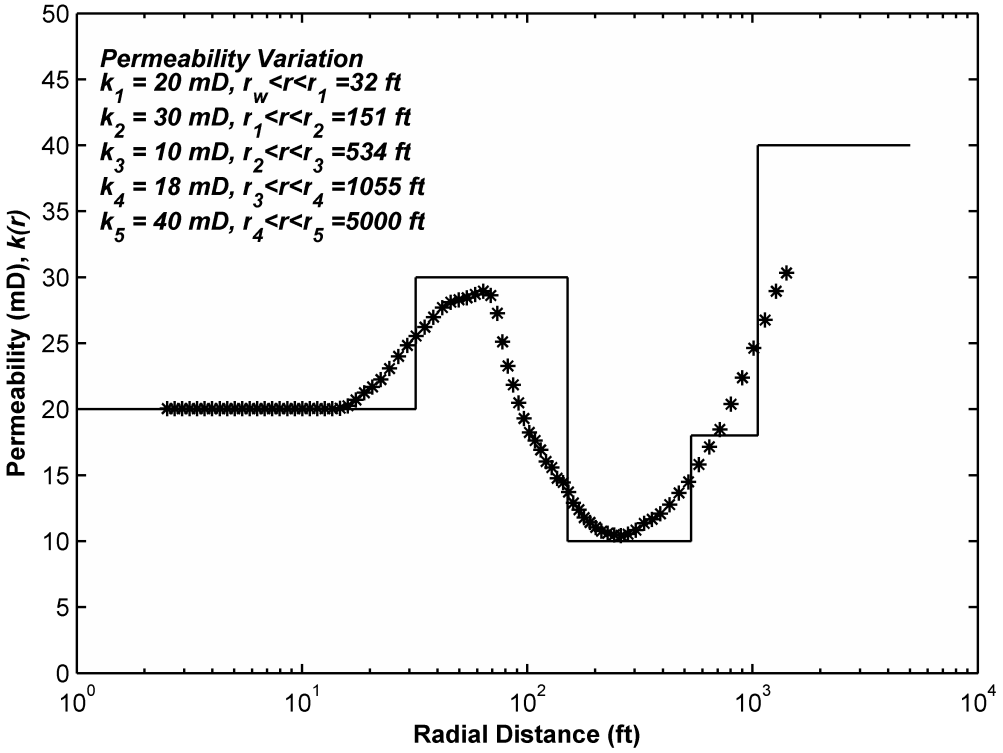

(a)

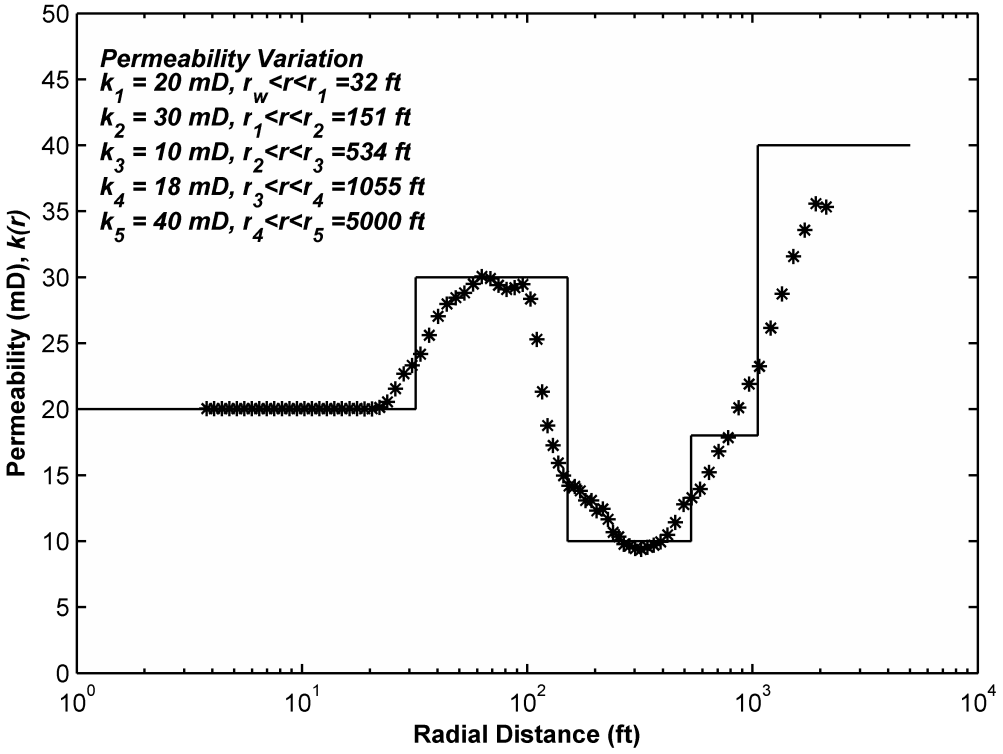

(b)

Figure 4.3. ISA Solution for (a) $C = 1$ (b) $C = 1.5$.

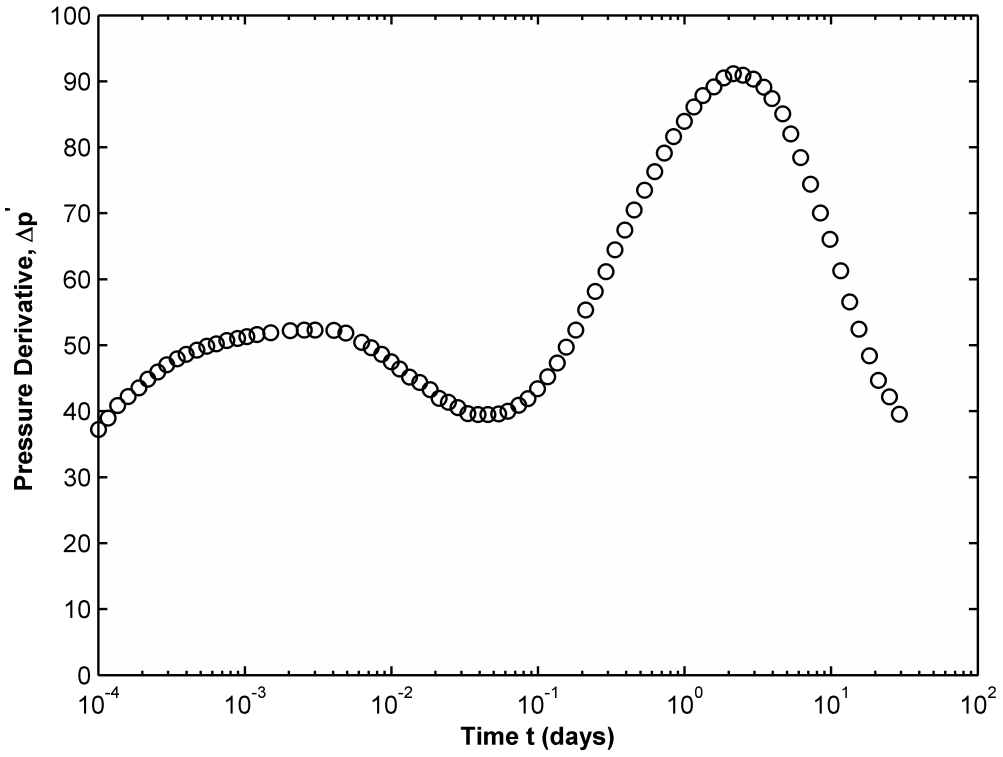

(a)

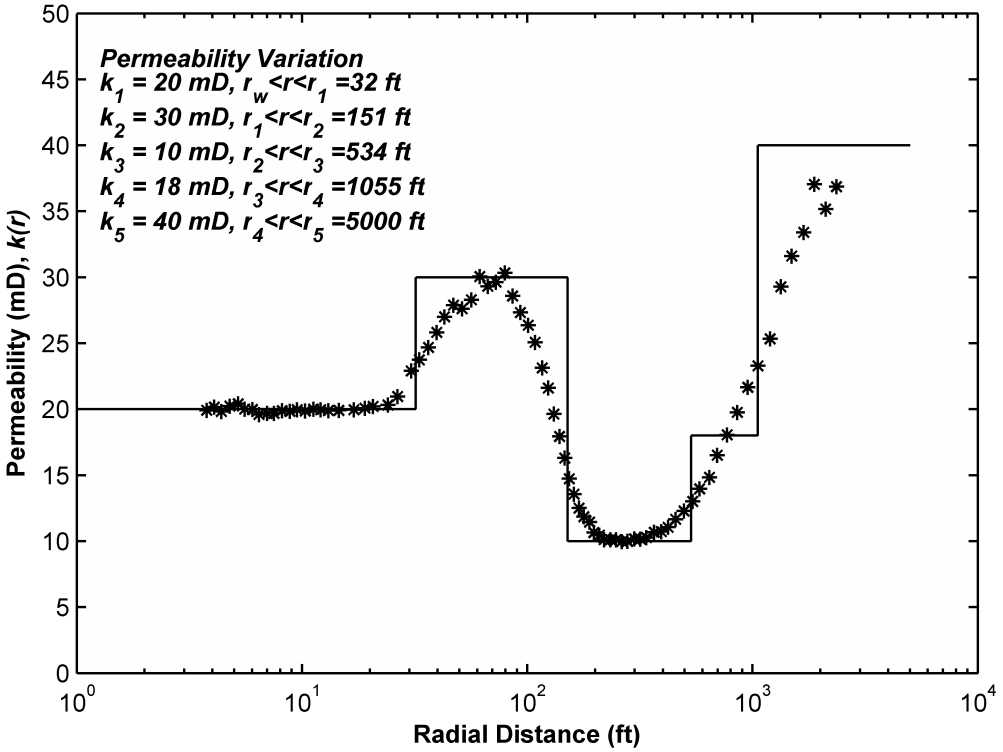

(b)

Figure 4.4. Monitoring Well @$r_D = 10$ (a) Pressure Derivative Data (b) ISA Solution ($C = 1.5$).

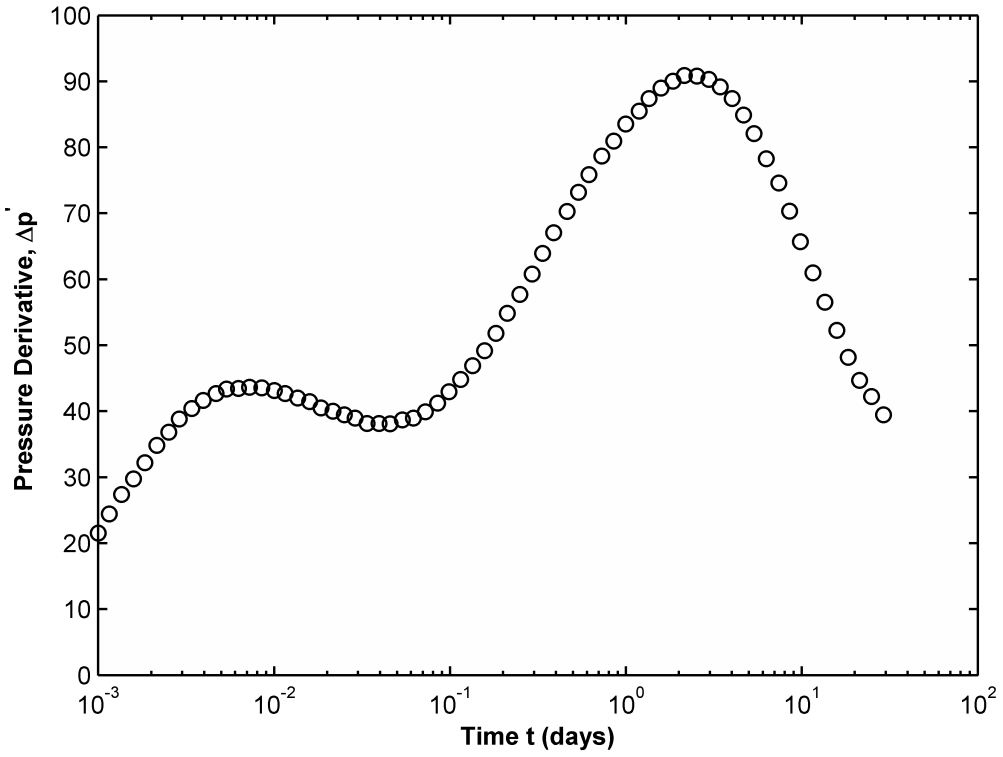

(a)

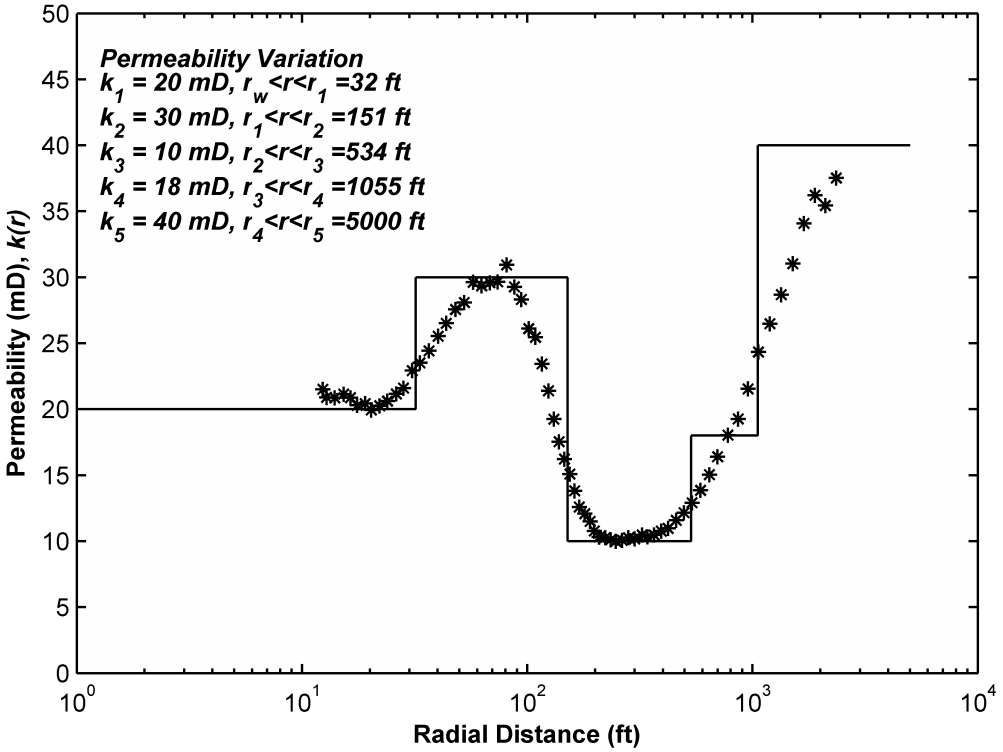

(b)

Figure 4.5. Monitoring Well @$r_D = 50$ (a) Pressure Derivative Data (b) ISA Solution ($C = 1.5$).

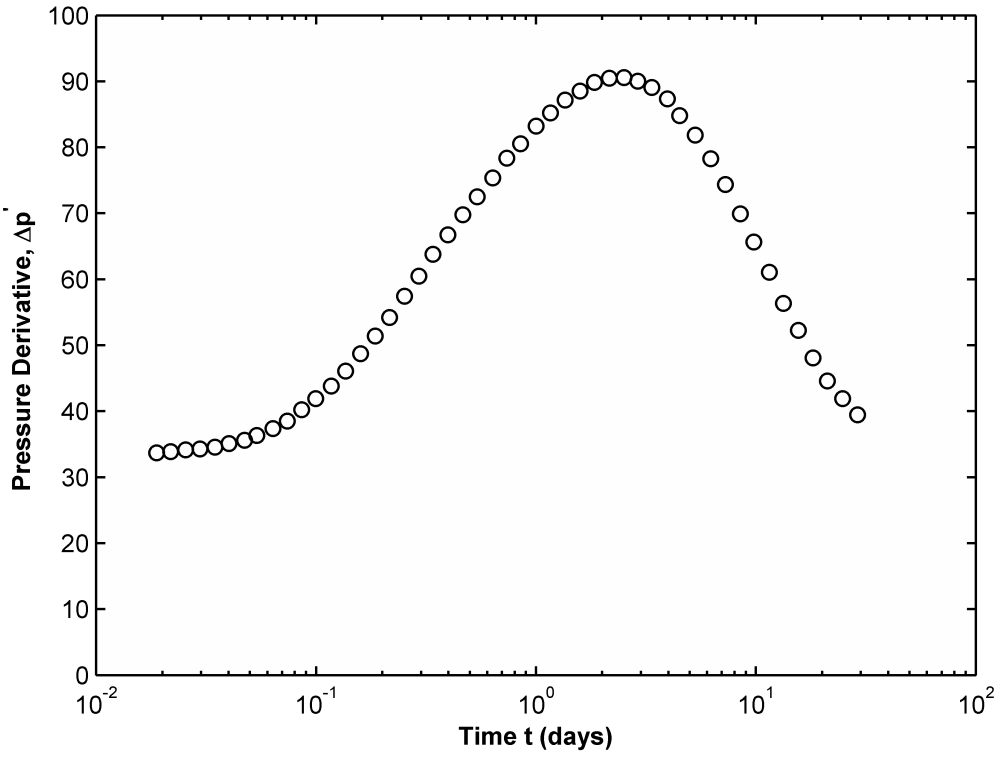

(a)

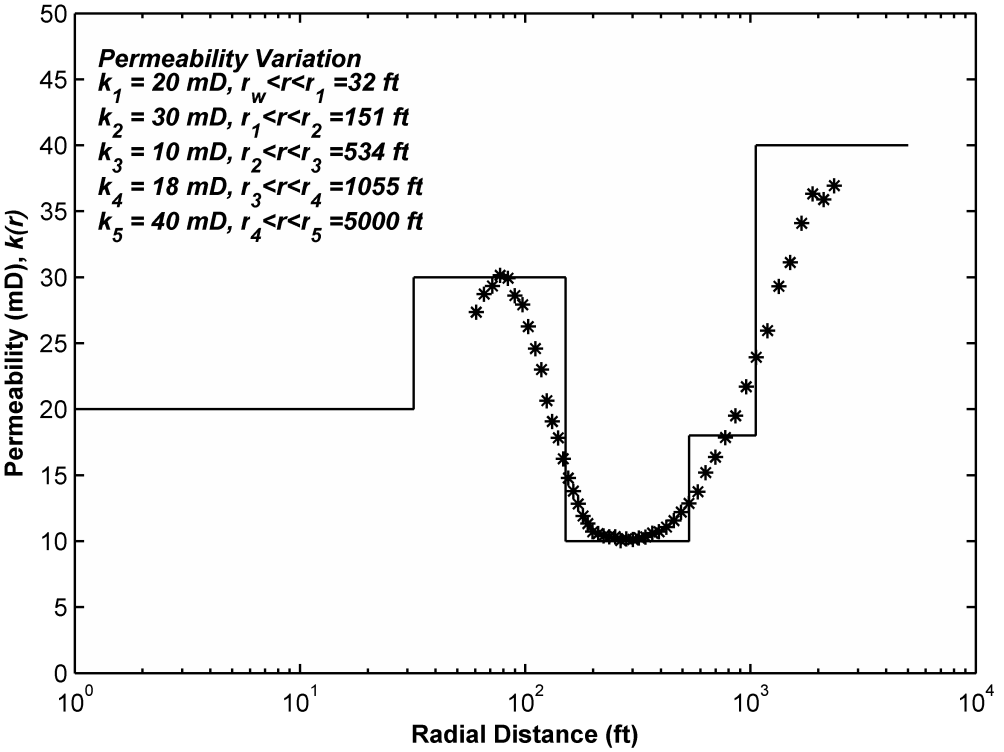

(b)

Figure 4.6. Monitoring Well @$r_D = 100$ (a) Pressure Derivative Data (b) ISA Solution ($C = 1.5$).

5. APPLICATIONS OF INCREMENTAL AREA METHOD

5.1. IAM Based Aquifer Parameters Estimation for Confined Aquifer

The validity and the use of the proposed approach were assessed with synthetically generated drawdown data as well as data collected during an actual pumping test. The synthetic data were generated for ideal confined aquifer (with measurement errors), heterogeneous aquifer (log normal transmissivity distribution) and a bounded ideal confined aquifer conditions. The pumping test data obtained in the "Oude Korendijk" South of Rotterdam, The Netherlands (Kruseman and de Ridder, 1992) was selected because the aquifer that was stressed showed that the characteristics of the aquifer changed with the expansion of the cone of depression; the drawdown data obtained from the three monitoring wells during the pumping test behaved differently and showed a strong heterogeneity in the field; therefore the assessment of the data was not straightforward and the features of the proposed method could be clearly demonstrated.

5.1.1. Ideal Confined Aquifer Drawdown with Measurement Errors

The proposed IAM was first implemented on the drawdown data set generated from a hypothetical homogeneous confined aquifer which was modified to incorporate random variations up to 2% of the measurement value. This exercise was conducted to review the IAM sensitivity to random noise for the prediction of aquifer parameters. The confined aquifer data was generated using the Theis (1935) equation. The serial approximation of the Theis well function depicted in Equation 2.24 was calculated via using the first 1000 terms of the series expansion for the first-order exponential integral (Abramowitz and Stegun, 1965). Hypothetical homogeneous, infinite extent confined aquifer pumping test is conducted with the discharge rate of 1.0 m^3/min. The drawdown data were generated for the monitoring well placed at a distance 25 m from the pumping well. Aquifer transmissivity and storativity were taken as 0.5 m^2/min and 0.0001, respectively.

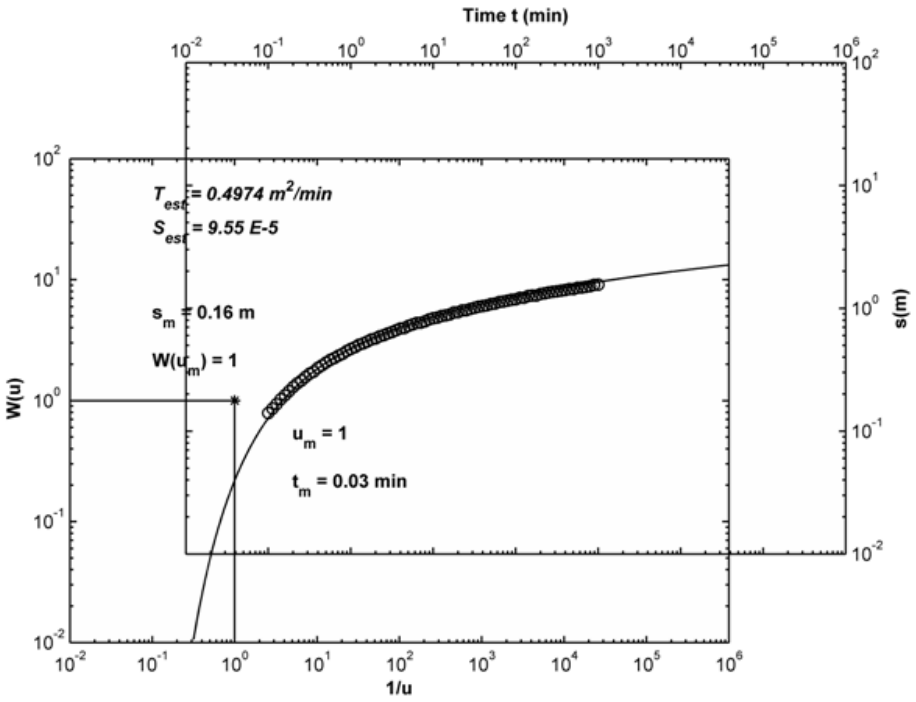

Figure 5.1. Pumping Response of the Hypothetical Aquifer with Random Noise.

Random noise was added to the ideal drawdown data resulting in the imperfect drawdown data generated at the observation point is given in Figure 5.1. Transmissivity and storativity values of the synthetically generated aquifer were estimated as 0.4974 m^2/min and 9.95E-5, respectively by graphical matching method shown in Figure 5.1. The prediction performance of IAM with and without random noise is given in Figure 5.2.

The results show that the IAM method can overcome random errors potentially present in the drawdown data in establishing the aquifer parameters for ideal confined aquifer conditions.

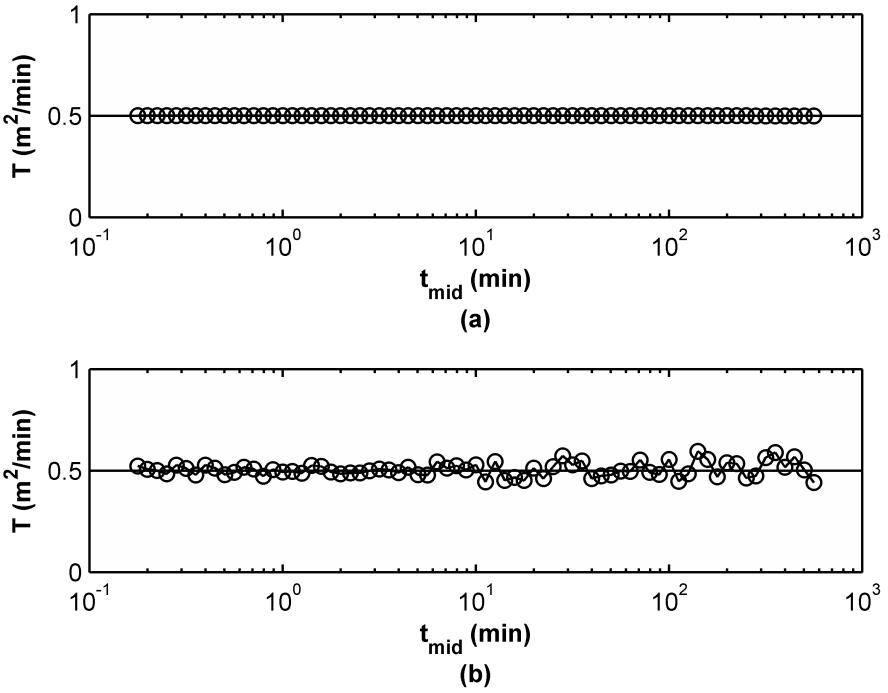

Figure 5.2. IAM Transmissivity Estimation (a) Noise-free Drawdown Data (b) Drawdown Data with Random Noise.

5.1.2. Heterogeneous Confined Aquifer

A pumping test in a hypothetical heterogeneous confined aquifer was simulated by using the PMWIN-MODFLOW (Chiang and Kinzelbach, 2001) numerical model. The heterogeneity of the aquifer was assumed to be a log-transmissivity field throughout the aquifer in the light of the previous investigations (Freeze, 1975; Delhomme, 1979; Clifton and Neuman, 1982; Hoeksema and Kitanidis, 1985; and Dagan, 1986, 1989). The transmissivity field was generated by PMWIN-MODFOW that had a mean transmissivity value of 1 m^2/day, a variance value of 2 m^2/day, and a correlation length of 10 m. The storativity was taken to be homogeneous with a unique value (0.0002) throughout the aquifer domain. Aquifer thickness was assumed to be 10 m. A 2 m^3/day of discharge rate at a well centered in a 499 m by 499 m aquifer domain size was simulated. The hypothetical transmissivity distribution and the locations of monitoring wells are illustrated in Figure 5.3 and Figure 5.4 respectively. In Figure 5.5, log-normal distri-

bution of the generated transmissivity field is shown. Simulation model parameters are summarized in Table 5.1.

Table 5.1. Confined Aquifer Simulation Parameters.

Field Generation Parameters	Value	Simulation Parameters	Value
Domain Size (m x m)	499 x 499	Cell Size (m x m)	1 x 1
Number of Cells	499 x 499	Pumping Rate (m^3/day)	2
Integral Scale (m)	10	Duration (day)	1
Mean (m^2/day)	1	Time Step	200
Variance(m^2/day)	2	Time Multiplier	1.01

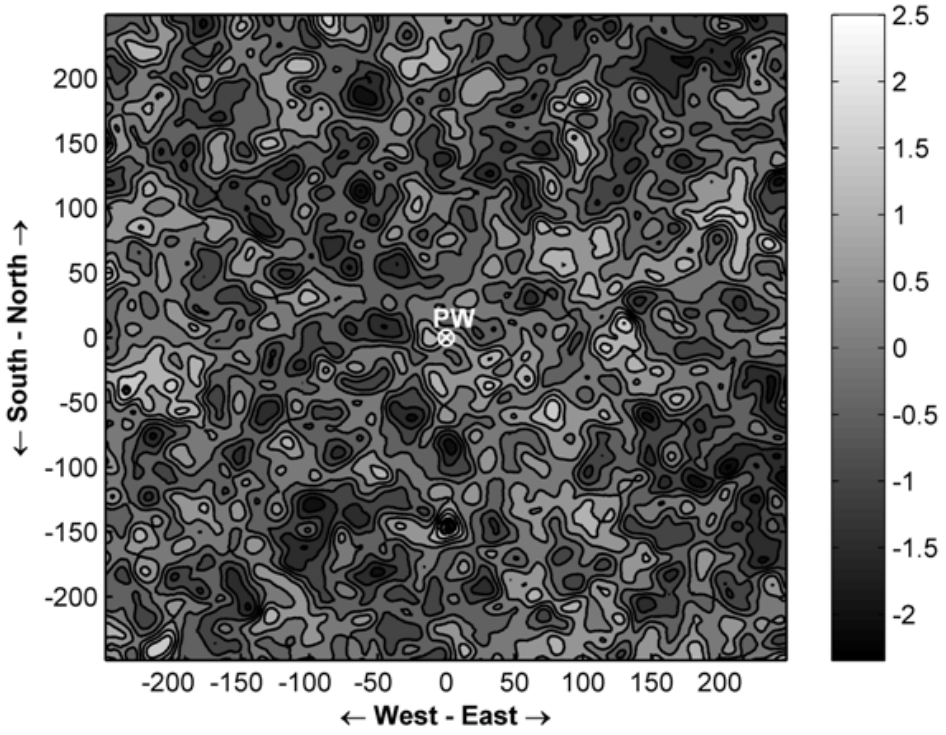

Figure 5.3. Transmissivity Map of Hypothetical Heterogeneous Aquifer.

The semi-log plot of drawdown data versus t/r^2 for the observation wells are shown in Figure 5.6. It is noted that they do not fall on the same straight line as expected due to the presence of heterogeneity in the aquifer. The drawdown data were

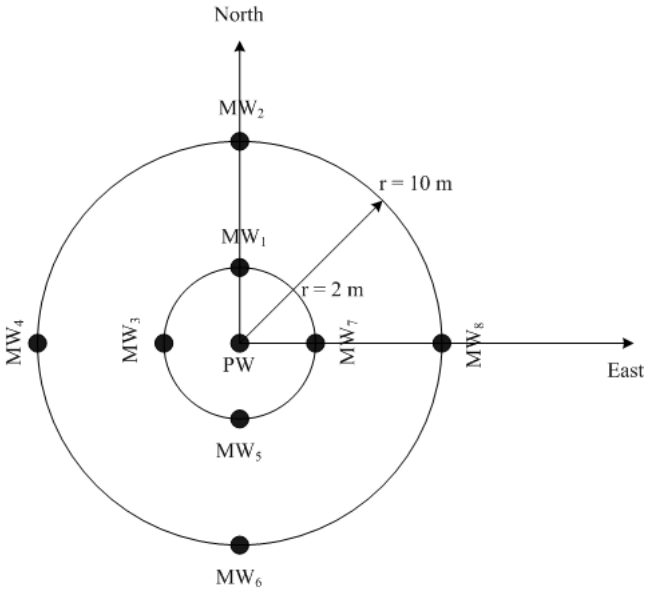

Figure 5.4. Monitoring Wells Configuration.

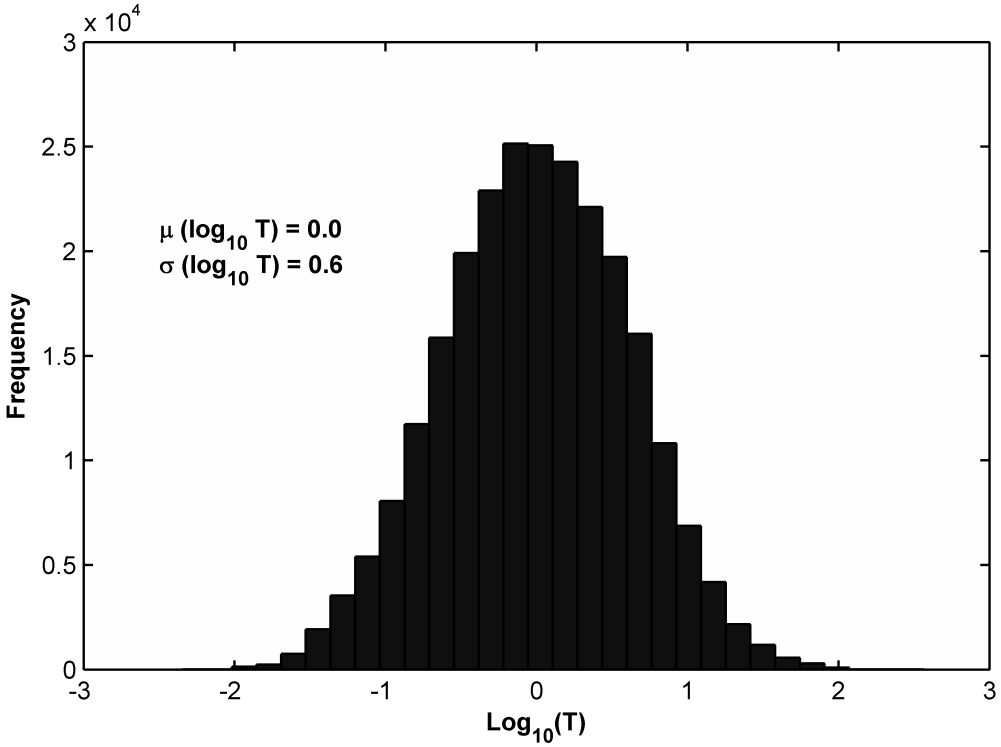

Figure 5.5. Log-normal Hydraulic Conductivity Distribution.

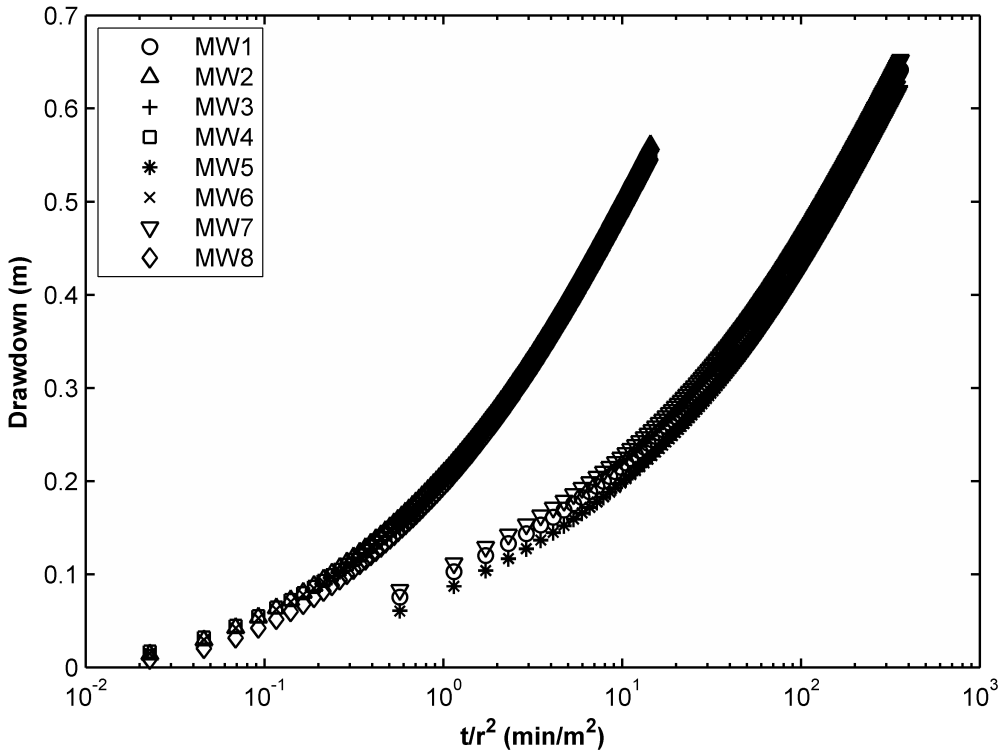

Figure 5.6. Drawdown Data of Hypothetical Heterogeneous Aquifer Model.

assessed with the IAM procedure and the transmissivity calculations variation with time is given in Figure 5.7. The following conclusions can be drawn:

- The transmissivity values vary with the expansion of the zone of influence indicating that the aquifer has heterogeneous features and that the Theis curve matching would not be an adequate assessment tool.
- The transmissivity values show a converging pattern toward the value of 1 log m^2/day as the cone of depression increases with time. This is an indication the drawdown variation at the later stages of the pumping test is being influenced by an "averaged" transmissivity field towards the latter part of the pumping test; the individual local variations in the aquifer properties tend to lose their influence on the drawdown response as time increases.
- The local transmissivity distribution near the monitoring wells are greater than the overall average of the transmissivity field that influences the drawdown .

The temporal and spatial scaling of the transmissivity can be explained for the general

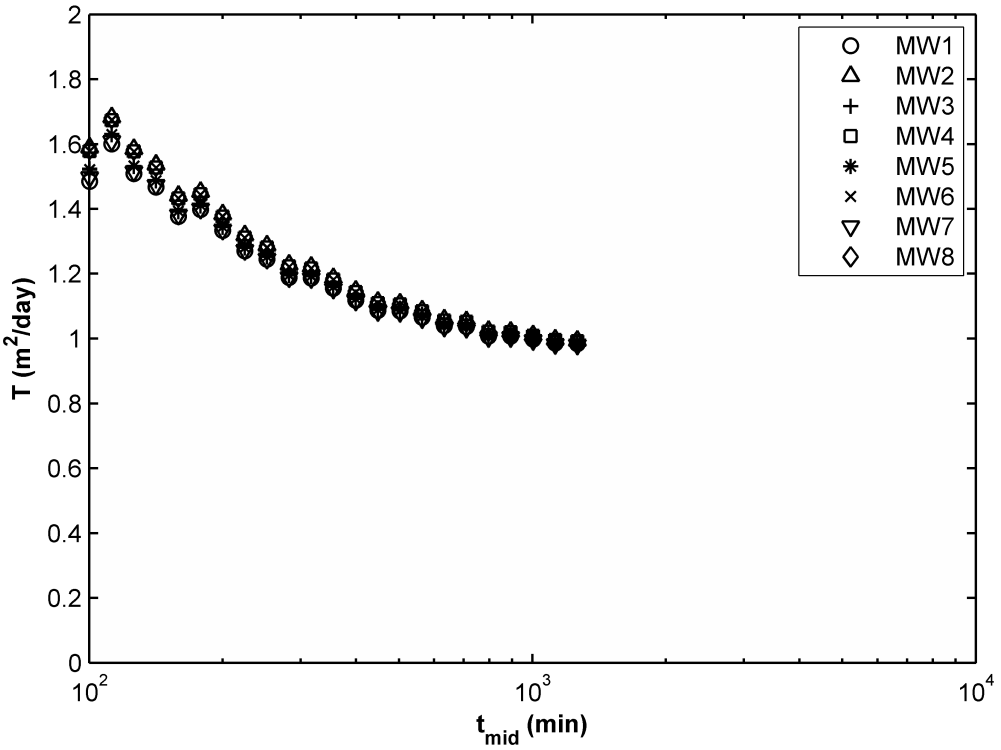

Figure 5.7. Transmissivity Variation.

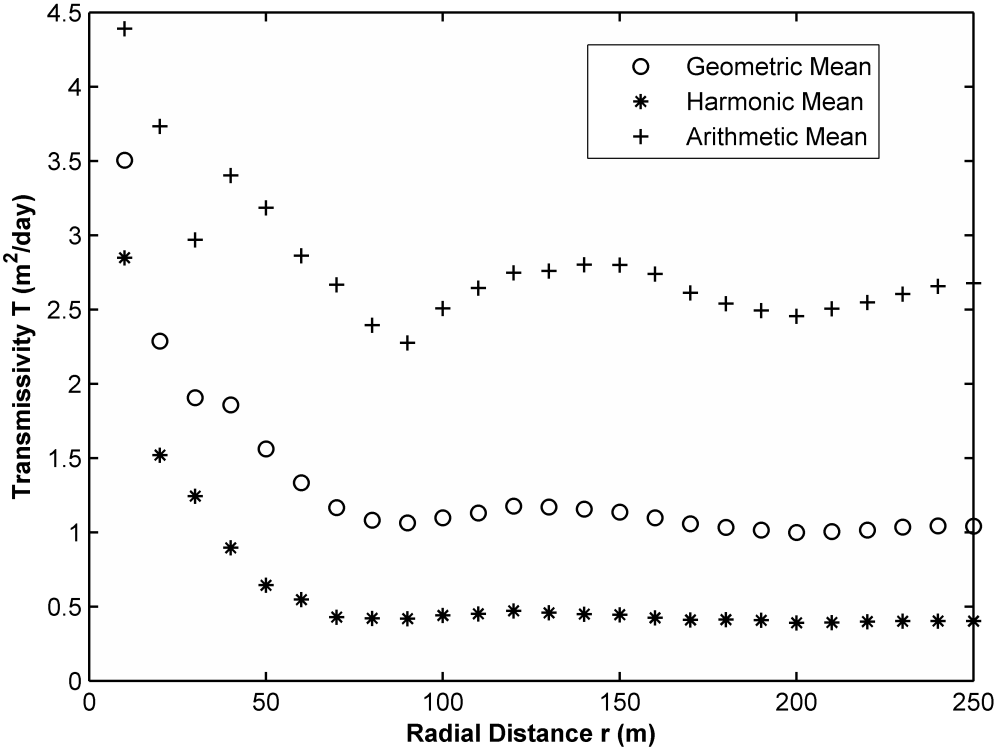

Figure 5.8. Radial Variation of Transmissivity Values.

cases by referring to the work of Oliver (1990) and for this specific example (lognormal distribution) to the work of Wu *et al.* (2005). Oliver (1990) reviews the problem for the pressure response in an infinite aquifer with an arbitrary spatial variability in permeability. A formulation is derived for the slope of the drawdown response in the extraction well which related to the integral of the transmissivity field within the cone of depression and a Fredholm Weighting function. The transmissivity field is obtained by knowing the slope of drawdown data from the field and relating it to the integral equation. Ultimately an equivalent transmissivity value is obtained based on a harmonic integration of the spatially heterogeneous transmissivity field. Wu *et al.* (2005) investigated through numerical experiments the effective transmissivity and storativity value for an equivalent homogeneous aquifer of Gaussian random parameter fields. Their results looked at the change of these parameters with time as well as the principal directions of the effective transmissivity. The authors indicated that the effective aquifer parameters tend to the geometric mean at large times. The early time calculations of the transmissivity from a single observation well show variance with time whereas at a late time the estimated transmissivity value converge to a single value representing an average value over the cone of depression. In summary, variability of the transmissivity values are expected to be present within the sampling point as the cone of depression develops however the transmissivity value obtained from the analysis of the measuring point will ultimately converge to an equivalent value. The timing for which the equivalent transmissivity values will converge will be influenced by the location, size, and degree of heterogeneity as the cone of depression evolves.

It should be noted that there are a number of approaches related to the averaging procedure for heterogeneous aquifers as the cone of depression expands with time from the pumping well. There are basically three approaches used: weighted arithmetic, harmonic, and geometric means for the long-term transmissivity values (Bibby, 1979; Oliver, 1990, 1993; Wu *et al.* 2005; Meier *et al.* 1998, 1999). The arithmetic mean, harmonic and geometric mean transmissivity values were therefore calculated with respect to distance as plotted in Figure 5.8 to be in line with the available methods of averaging in the literature. The formulas used for the transmissivity mean calculations

in Figure 5.8 given as:

$$\begin{aligned} Aritmetic\,Mean &= \tfrac{1}{N_i}\sum_{i=1}^{r_i} T_i \\ Geometric\,Mean &= \sqrt[N_i]{\prod_{i=1}^{r_i} T_i} \qquad\qquad r_i = 10, 20, ..., 250 \\ Harmonic\,Mean &= \frac{N_i}{\sum_{i=1}^{r_i} \frac{1}{T_i}} \end{aligned} \tag{5.1}$$

where r_i denotes the radius of circle drawn from the center of transmissivity field, N_i represents the number of data inside the circle, and T_i is the transmissivity values in the circle. A 10 m increment value was preferred to calculate the arithmetic, geometric and harmonic mean values of hypothetical field within that radius. The geometric mean tends to unity as is expected because of the log-normal distribution that was used in the generation of the transmissivity field with increasing radial distance from the pumping well location. The correlation between long term pumping test aquifer parameter estimations and geometric mean transmissivity value has been indicated in the work of Warren and Price (1961), Lachassagne *et al.* (1989), Butler and Liu (1991), Meier *et al.* (1998) and Sanchez-Vila *et al.* (1999). The present analysis indicates that IAM correctly identifies the trend of the transmissivity field distribution near the monitoring wells in the initial pumping test period as well as the long term pumping test period where the behavior of the drawdown is based on the mean of the transmissivity within the cone of depression. Estimated transmissivities for the different observation points tend to converge to a single value, which in a multi-log-Gaussian field corresponds to the geometric mean of the transmissivity values. As expected the initial transmissivity calculations show large variations during the initial expansion phases of the cone of depression.

5.1.3. Hypothetical Bounded Aquifer

Drawdown data from a monitoring well located 20 m away the pumping well in a bounded ideal confined aquifer shown in Figure 5.9 was generated using superposition of the Theis Well Function; this was again calculated using the first 1000 terms of the series expansion for the first-order exponential integral (Abramowitz and Stegun,

1972). The hypothetical homogeneous, confined aquifer with aquifer transmissivity and storativity values taken as 0.05 m^2/min and 0.0001, respectively was stressed by the pumping at a discharge rate of 0.5 m^3/min.

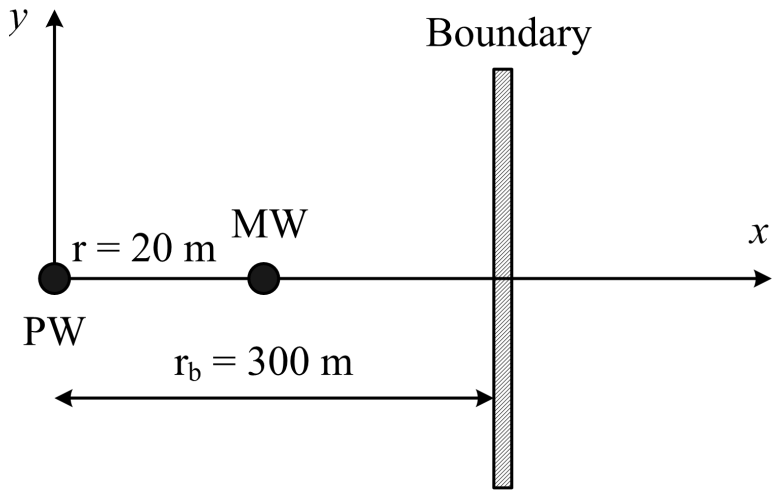

Figure 5.9. Schematic View of Bounded Ideal Confined Aquifer.

The log-log and semi-log drawdown data for a monitoring well located at distance 20 m from the pumping well is given in Figure 5.10. Semi-log plot of the drawdown data indicated in Figure 5.10b shows that two distinct slopes in the drawdown curve develop due to boundary effect. The drawdown change at early times is caused by the pumping well alone. The slope of later times corresponds to the drawdown change is due to both the real and the imaginary well simulating the presence of the boundary. The combination of the pumping and imaginary wells lead to drawdown change in one log cycle of time to be twice that of pumping well alone (Schwartz and Zhang, 2003). The values of the drawdown in Figure 5.10a were analyzed to establish the variation of the transmissivity and storativity with time. The results are shown in Figure 5.11 for three different integration time increments ($\Delta = 0.1, 0.5$ and 1). These increments provide the correct pre-boundary and post-boundary effects in the Cooper-Jacob approximation zones. However the transition period is shorter for the short term integration time increment which is expected.

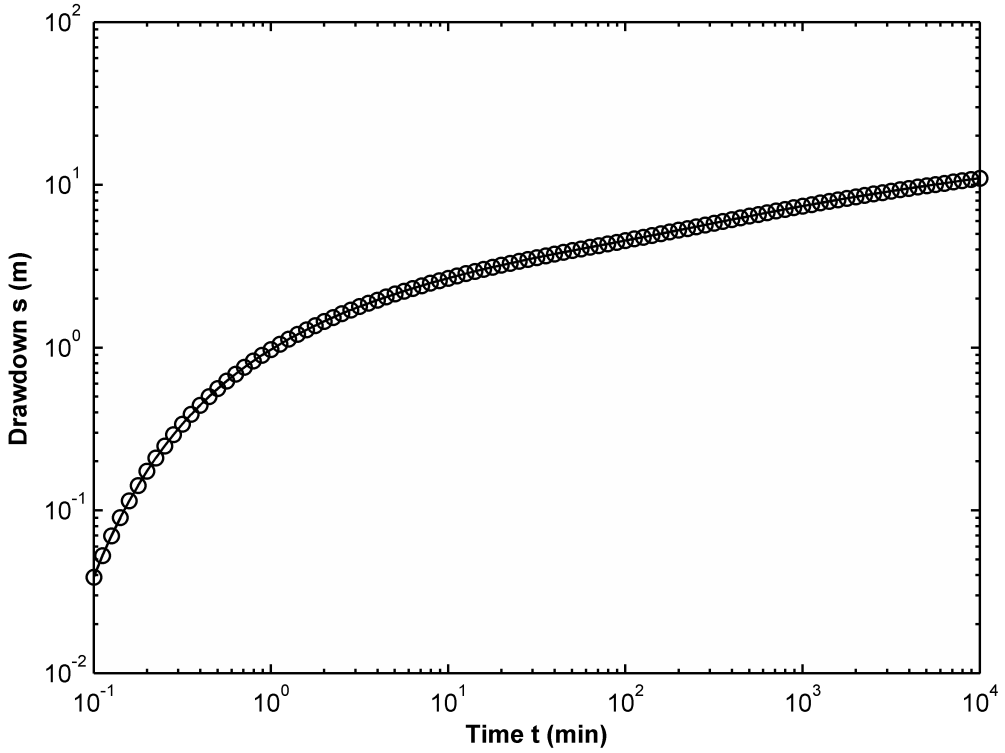

(a)

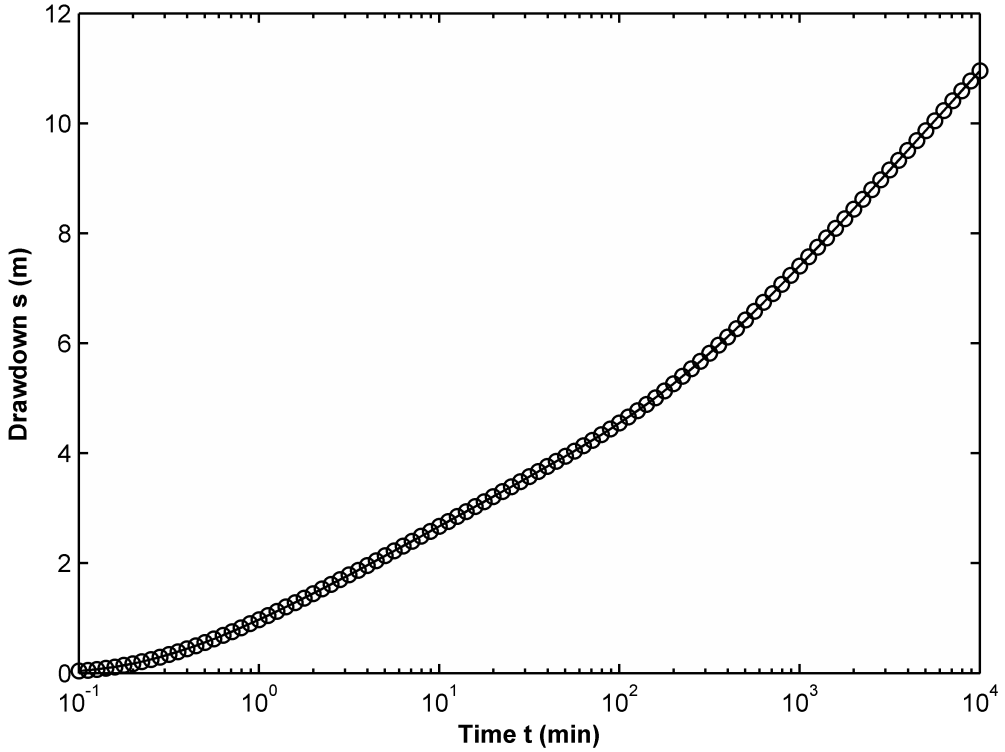

(b)

Figure 5.10. Time Drawdown Data of Bounded Aquifer (a) Log-log Scale (b) Semi-log Scale.

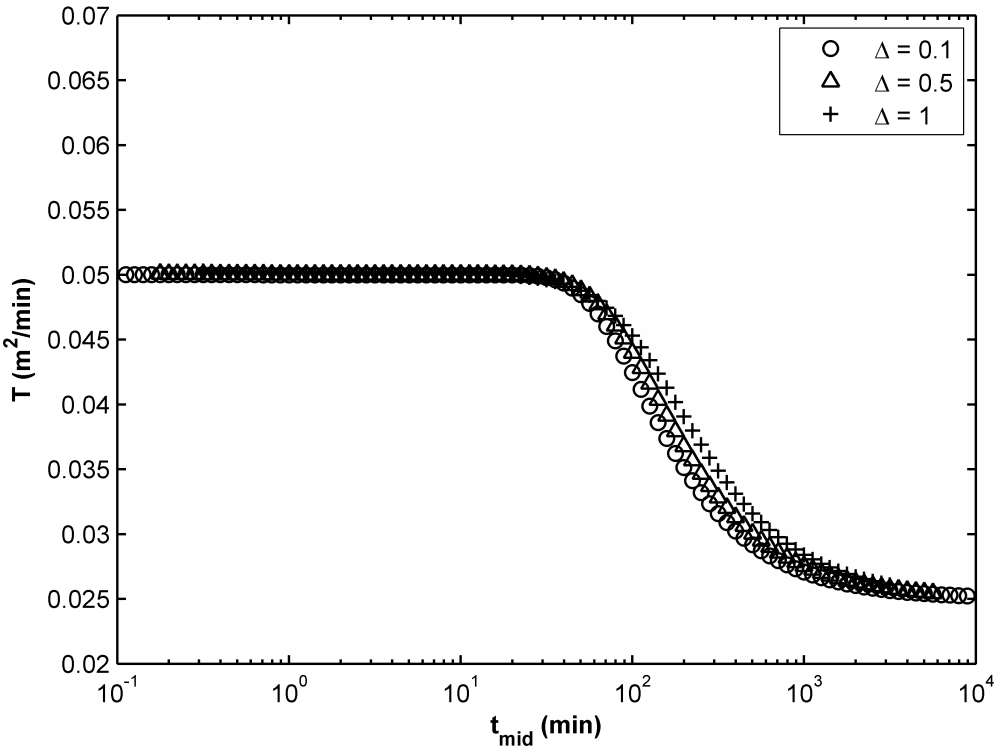

(a)

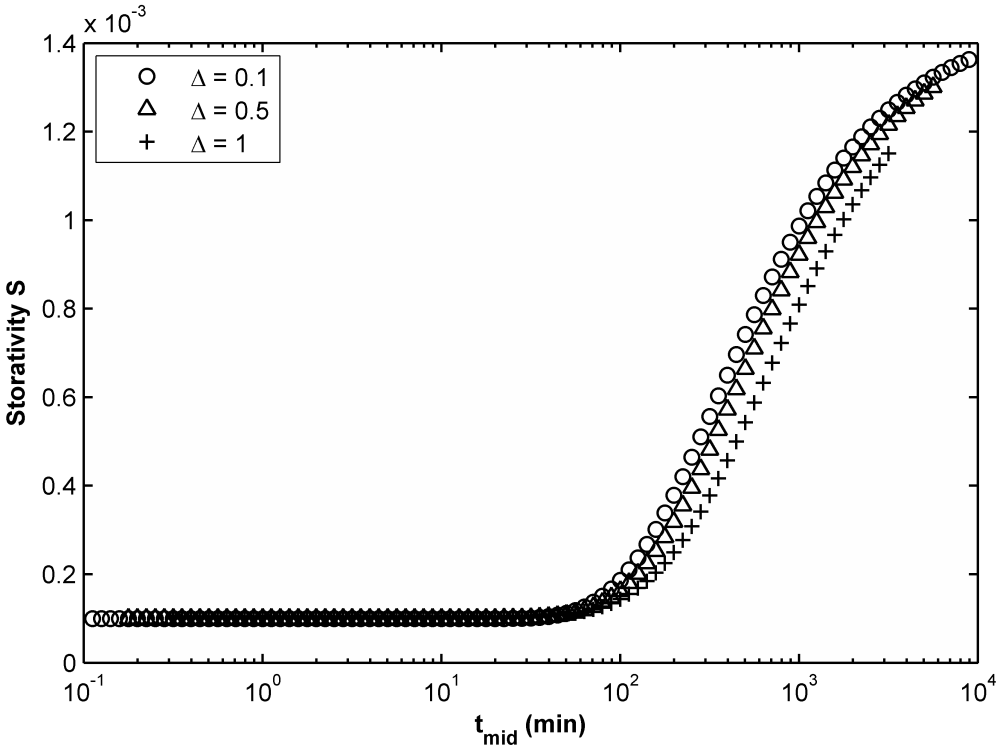

(b)

Figure 5.11. IAM Based Bounded Confined Aquifer Estimation (a) Transmissivity Variation (b) Storativity Variation.

In practical applications, the analysis of the pumping test would be conducted by examining and assessing the predicted aquifer parameters as in Figure 5.11. For this case, the figure indicates that the aquifer parameters change as the cone of depression moves outward from the extraction well. The fact that initially the transmissivity and storativity values remain constant until a certain point in time would be taken as the presence of real confined aquifer with homogeneous features within a certain distance from the well. The change of the aquifer parameters after a certain point would be indicative of non homogeneity being present within the expanding cone of depression. The stabilization of the aquifer parameters at a later stage shows that the aquifer behaves as a virtual ideal confined aquifer that is equivalent to the non-homogeneous real aquifer within the cone of depression. The virtual ideal confined aquifer parameters in Figure 5.11 should, therefore, not be part of the real aquifer parameter quantification; however the fact that the transmissivity of the virtual equivalent ideal aquifer being halve of the initial transmissivity value ought to be taken the presence of a boundary with zero transmissivity value at some distance from the pumping well.

5.1.4. Field Data

The proposed methodology was applied to the water drawdown data obtained during a pumping test conducted in the region of "Oude Korendijk" South of Rotterdam, The Netherlands (Kruseman and de Ridder, 1992). Apparently an impermeable confining layer exists in the first 18 m below the surface consisting of clay, peat, and clayey fine sand. The confined aquifer unit is present between 18 and 25 m below ground level consisting of coarse sand with some gravel. The base of the aquifer is made of fine sandy and clayey sediments. The pumping well was placed over the whole thickness of the aquifer; the drawdown was measured in monitoring wells located at distances of 30 m, 90 m, and 215 m from the pumping well, and at different depths as shown in Figure 5.12. The extraction rate was constant discharge at a rate 788 m^3/day for approximately 14 hours.

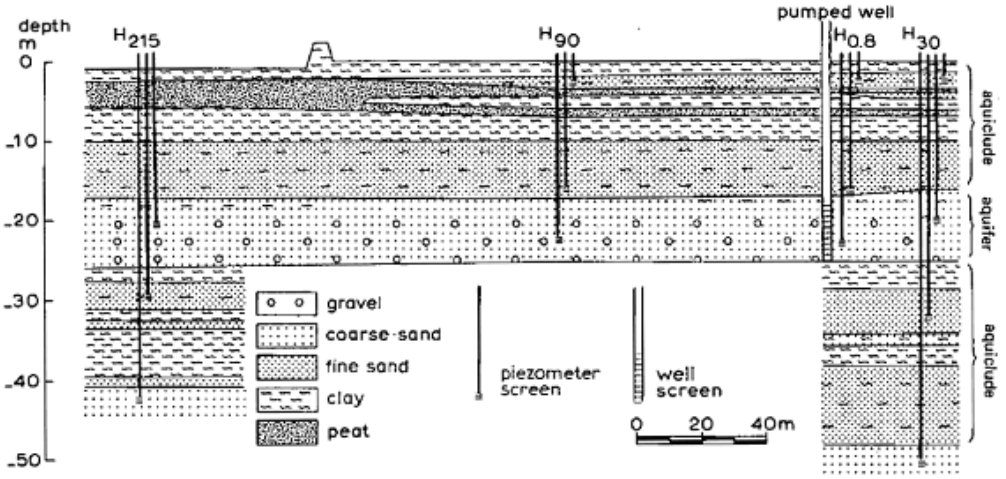

Figure 5.12. Lithological Cross-section of the Pumping Test Site "Oude Korendijk", The Netherlands, (Kruseman and de Ridder, 1992).

Figure 5.13 shows the drawdown observed at wells MW_{30}, MW_{90} and MW_{215} plotted on t/r^2 on semi-log curve. The following observations can be made from these plots:

- It is not possible to match the field data in Figure 5.13 with Theis Well Function type curve. Heterogeneity is apparently present in the aquifer as the drawdown curves do not fall on a unique curve. Drawdown collected from MW_{215} fall altogether below the other field data from the other two monitoring wells. This discrepancy indicates systematic heterogeneity in the aquifer material composition, (i.e. changes in hydraulic properties with distance from the well).
- Drawdown data plotted on semi-logarithmic scale shows that the radius of influence intercepts a seemingly higher transmissivity area for MW_{30} and MW_{90} data when the zone of influence expands. Kruseman and de Ridder (1992) indicated that the geological data collected in the test site showed the main aquifer to be overlain by rather thick fine-sand layer in areas further away from the pumping well that gives rise to leakage.

The IAM method requires data to be collected in regular logarithmic time intervals to be implemented. As Renard *et al.* (2009) indicates, however, the number of data

points is usually limited and irregularly spaced in time because of manual sampling. The author indicates that a resampling (with a spline interpolation) may be necessary to obtain a fixed number of time intervals regularly spaced in a logarithmic scale. For the present data shown in Figure 5.13, Radial Basis Function Collocation Method (RBFCM) was utilized as an interpolation technique to determine the drawdown values corresponding to the mid-time values which could not recorded in the field data. The IAM was applied to the monitoring wells existing drawdown and interpolated data with the results shown in Figure 5.14.

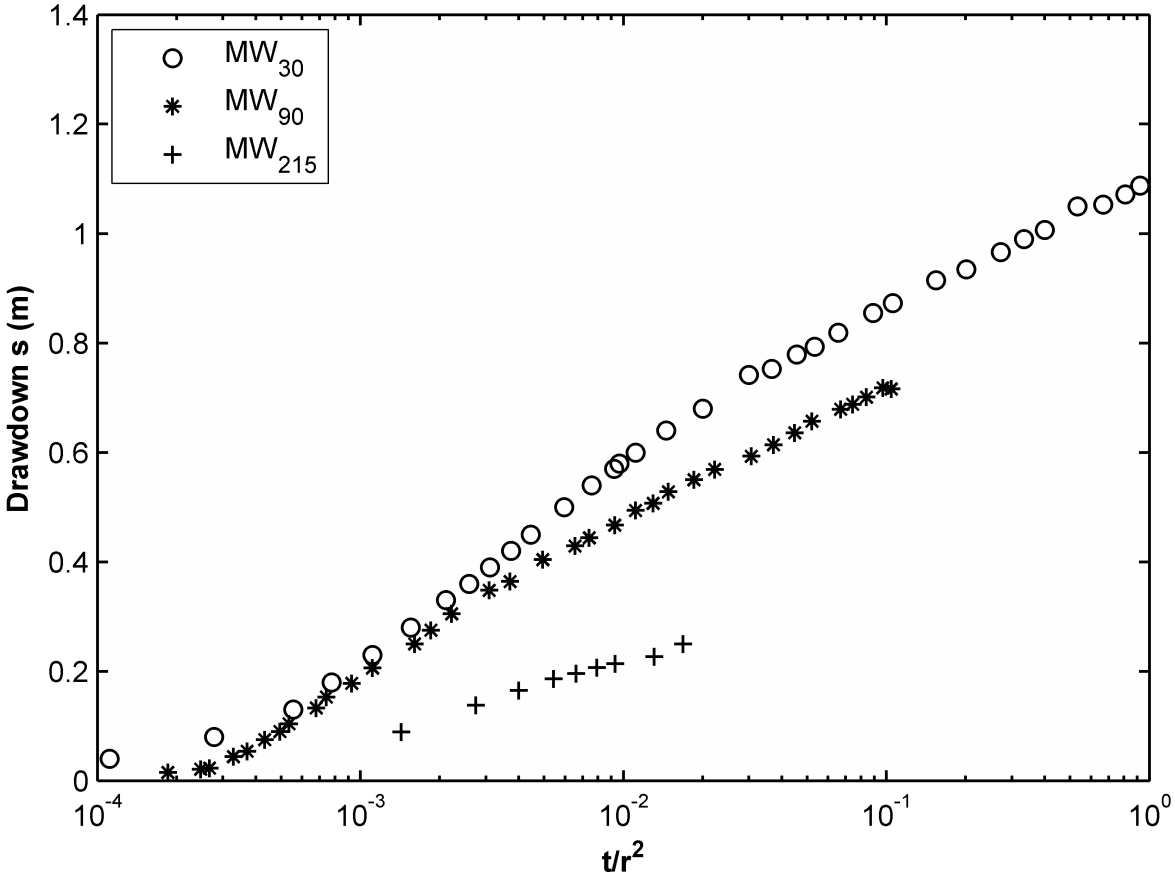

Figure 5.13. Drawdown Measurement at the Monitoring wells.

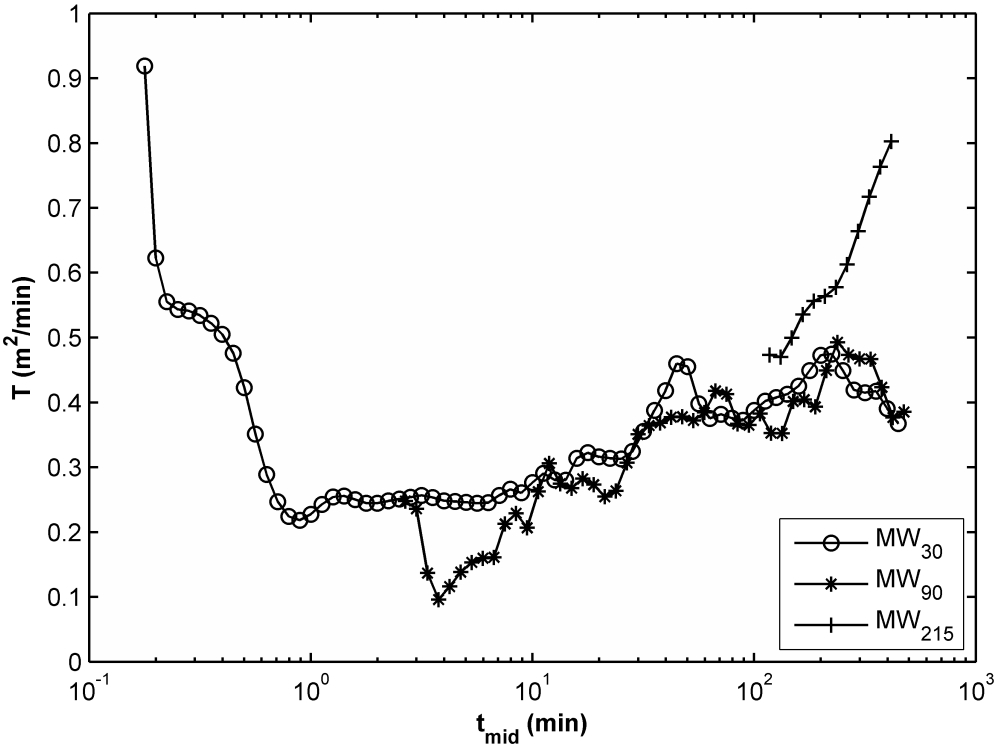

(a)

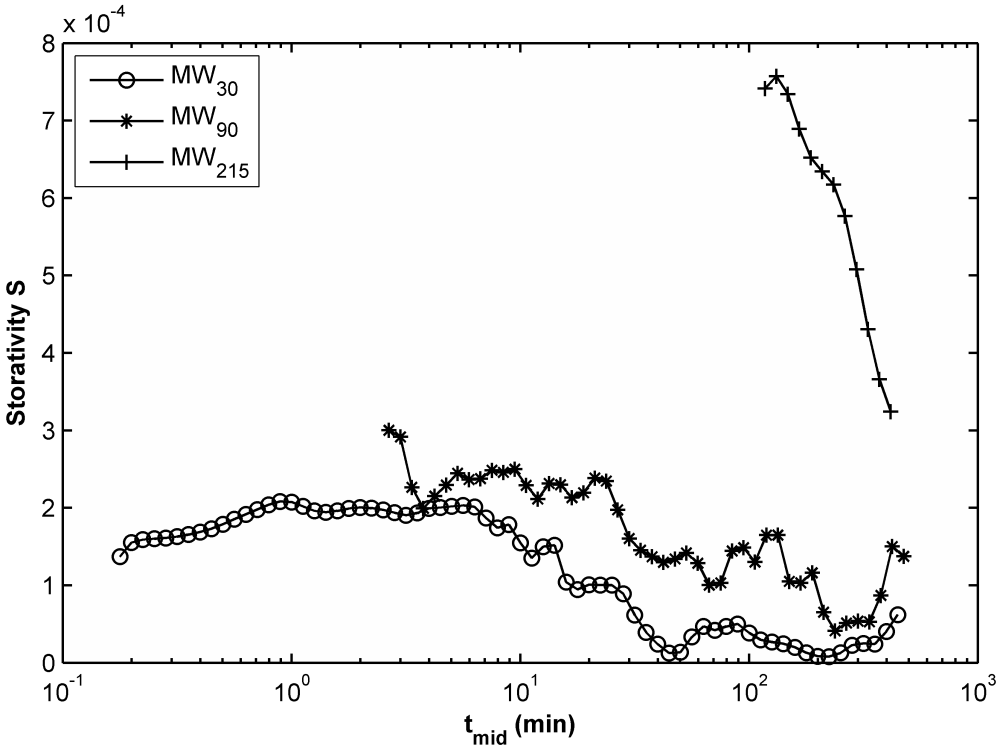

(b)

Figure 5.14. IAM Based Aquifer Estimation (a) Transmissivity Variation (b) Storativity Variation.

The analysis of the data in MW_{30} shows that:

- The transmissivity calculations based on the drawdown observed within the first minute of pumping vary starting from a value of 1 m^2/min (1440 m^2/day) and then decreasing sharply to 0.25 m^2/min (360 m^2/day). Sen (1994) indicates that the aquifer material around the well is likely to be composed of coarse grains hence resulting in ground water flow with almost without resistance; this leads to the initial high transmissivity estimates. The cone of depression expands until a more resistant aquifer material further away from the vicinity of the wells is encountered after the first minute of pumping.
- The material just beyond the coarse material around the well is seen to exhibit a confined aquifer behavior where the transmissivity value is calculated by the IAM as 0.25 m^2/min (360 m^2/day) in the period between the first minute of pumping and continuing until minutes. The aquifer material within the cone of depression can be taken to be homogeneous and confined aquifer. The storavitity is estimated to be in this time frame as shown in Figure 5.14. Kruseman and de Ridder (1992) used the Jacob straight line fit to field data from MW_{30} and estimated the value of transmissivity T =385 m^2/day (0.27 m^2/min) and storativity $S = 1.7 \times 10^{-4}$. The cone of depression by this time has reached MW_{90}.
- The transmissivity value show an increase starting from the t =10 minutes onward until t =40 minutes from 0.25 m^2/min (360 m^2/day) to 0.45 m^2/min (648 m^2/day), respectively. The cone of depression likely encounters a higher transmissivity zone beyond the initial homogeneous zone or a leaky zone which results in the increase in the calculated transmissivity values. The geological information collected near the pumping well would indicate that there is a zone where leakage from the upper confined layer occurs.
- The IAM results show that at times greater than t =40 minutes of pumping, the transmissivity fluctuates between 0.35 m^2/min (504 m^2/day) and 0.45 m^2/min (648 m^2/day), as the cone of depression further expands. This may mean that the impact of the leakage area within the cone of depression loses it influence.

The analysis of the data in MW_{90} shows that:

- The drawdown response noted in the monitoring well depicts a variable transmissivity calculation during the entire data collection period. The value of the estimated transmissivity varies between 0.1 m^2/min (144 m^2/day), and 0.45 m^2/min (648 m^2/day) between the t =30 minutes and t =200 minutes.
- There is a continual increase in the estimated transmissivity during this time period which indicates a leaky condition to be present within the cone of depression. This means that the drawdown data cannot be calculated using a confined aquifer approach but it needs to be considered as a leaky aquifer analysis.

The analysis of the data in MW_{215} shows that:

- The drawdown response noted in the monitoring well depicts a variable transmissivity calculation during the entire data collection period. The value of the estimated transmissivity varies between 0.48 m^2/min (691 m^2/day), and 0.8 m^2/min (1152 m^2/day) between t =100 minutes and t =500 minutes.
- There is a continual increase in the estimated transmissivity during this time period which indicates a leaky condition to be present within the cone of depression. This means that the drawdown data cannot be calculated using a confined aquifer approach but it needs to be considered as a leaky aquifer analysis.

5.2. IAM Based Aquifer Parameters Estimation for Leaky Aquifer

The validity and limitations of IAM procedure for leaky aquifer were tested for different situations which is often encountered in hydrology practice. Leaky aquifer parameters were first estimated for the hypothetical homogeneous aquifer to show the application of IAM approach. Moreover, IAM was applied for heterogenous aquifer which is simulated by MODFLOW to understand the limitation of the suggested methodology. Finally, the suggested method was used to estimate aquifer parameters using the real field data. The sensitivity analysis has been conducted to elaborate the performance of the suggested IAM for each scenario.

5.2.1. Hypothetical Homogeneous Leaky Aquifer

A hypothetical one day pumping test was conducted in homogeneous leaky, confined aquifer. A monitoring well was installed 50 m away the pumping well which operated a constant withdrawal rate of 500 m^3/day . The thickness of semi-confining layer is assumed as 20 m. The transmissivity and storativity of the leaky aquifer were assumed to be 142 m^2/day and 4×10^{-4}, respectively. The leakage factor r/B was 0.23 and the vertical hydraulic conductivity was chosen as 0.601 m/day to generate the drawdown response of the hypothetical homogeneous leaky aquifer which is summarized in Table 5.2.

Following the steps of the suggested methodology, the corresponding logarithmic time values of $s/s_{max} = 0.25$, $s/s_{max} = 0.5$ and $s/s_{max} = 0.75$ can be computed as 0.8798, 1.3434, and 1.8099, respectively, as shown in Figure 5.15. Based on the IAM theory, it can be seen the normalized drawdown values are almost linear, therefore, the incremental or trapezoidal area is easily calculated that leakage factor can be determined without curve matching effort. Trapezoidal area of sample drawdown data yields to 0.4659. Using fit equation given in Equation 3.21 or Figure 3.9, leakage factor was calculated as 0.2286.

IAM based leaky aquifer paramater estimation was compared to the classical estimation techniques such as Walton (1962) type curve matching and Hantush (1956) inflection point method which is an alternative method that does not require use of type curves.

Table 5.2. Drawdown Data of Leaky Aquifer Model.

$Q = 500\ m^3/day$	$T = 142\ m^2/day$	$S = 4 \times 10^{-4}$	$K_v = 0.0601\ m/day$
$r = 50\ m$	$b' = 20\ m$	$r/B = 0.23$	
Time (min)	Drawdown s (m)	Time (min)	Drawdown s (m)
1	0.0065	30	0.5223
1.5	0.021	40	0.5847
2	0.0396	50	0.6315
2.5	0.0595	60	0.6681
3	0.0795	120	0.7885
3.5	0.0989	180	0.8403
4	0.1175	210	0.8558
4.5	0.1353	240	0.8672
5	0.1521	480	0.9009
6	0.1834	720	0.9064
7	0.2116	960	0.9075
8	0.2373	1200	0.9077
9	0.2607	1320	0.9078
10	0.2822	1440	0.9078
20	0.4322		

The suggested IAM predicted the transmissivity and storativity of sample leaky aquifer as 142.51 m^2/day and 3.99×10^{-4}, respectively. The vertical hydraulic conductivity was computed as 0.0596 m/day. Using the predicted aquifer parameters, drawdown values of sample problem were regenerated to conduct sensitivity analysis which indicates the general performance of the suggested method as illustrated in Figure 5.16.

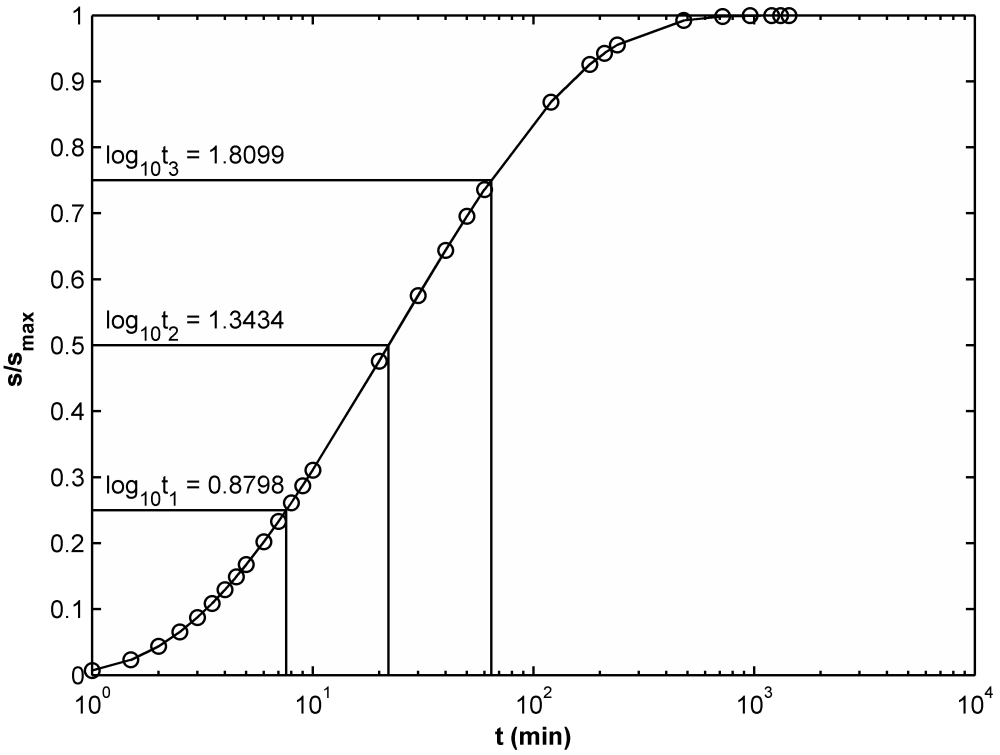

Figure 5.15. Normalized Drawdown Curve of Sample Problem.

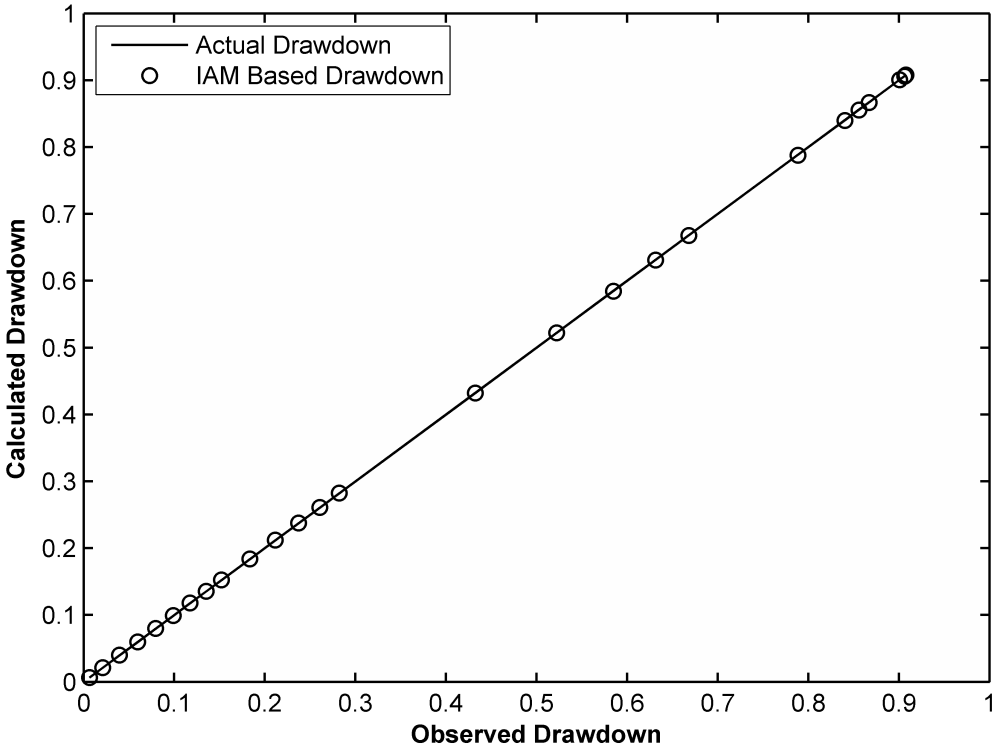

Figure 5.16. Comparison of IAM Based Drawdown Estimation and Actual Drawdown.

RMSE between the IAM based drawdown and actual drawdown was calculated as 0.0003 which is considerable a small value compared to the classical estimation methods. Walton (1962) curve matching method (WCM) estimates the transmissivity and storativity as 159.16 m^2/day and 3.54×10^{-4}, respectively, with the estimation in leakage factor of 0.2. Although Hantush (1956) inflection point (HIP) method predicts the leaky aquifer parameters close to traditional curve matching technique, the performance of this method is not as good as the suggested IAM procedure as summarized in Table 5.3.

Table 5.3. Comparison of IAM Estimation Performance.

Method	T (m^2/day)	S	r/B	K_v (m/day)	R^2	RMSE	R-RMSE (%)
IAM	142.51	3.99E-04	0.2286	0.0596	1	0.0003	0.47
WCM	159.16	3.54E-04	0.2	0.0509	0.9996	0.022	22.47
HIP	158.66	3.72E-04	0.1884	0.045	0.9977	0.0261	15.58

5.2.2. Hypothetical Heterogeneous Leaky Aquifer

A three layered aquifer model was modeled to simulate the pumping response of leaky aquifer. In this test case, a pumping well located at the center of aquifer domain withdraws the water with a constant discharge rate of 20 m^3/day. Transient drawdown behavior of the aquifer model at the hand was observed in a borehole installed at the north direction of pumping well with a distance of 15 m. The overlying layer and aquitard layer have the constant vertical hydraulic conductivity values as 0.1 m/day, 0.001 m/day, respectively, and thickness of those are given as 5 m, 2 m, respectively. Storativity values of the layers are provided as 3.75×10^{-4}, 1.5×10^{-4}, and 7.5×10^{-4}, respectively. Although the overlying layer and aquitard have constant horizontal conductivity values as 1 m/day and 0.01 m/day, respectively, a 10 m thickness leaky aquifer layer has a heterogeneous conductivity distribution which has a log mean of 1 m/day with the variance of 1 m/day and was generated by Field Generation package of PMWIN-MODFLOW (Chiang and Kinzelbach, 2001). Layer properties of aquifer

model is listed in Table 5.4. Aquifer domain was divided into 499 by 499 meshgrid system to analyze drawdown response of 1 day pumping duration. The initial hydraulic head of aquifer model is 100 m everywhere. Model parameters used in the simulation are summarized in Table 5.5.

Table 5.4. Layer Properties of Leaky Aquifer Model.

	Layers		
Layer Properties	Overlying	Aquitard	Leaky
Horizontal Conductivity (m/day)	1	0.01	1*
Vertical Conductivity (m/day)	0.1	0.001	Variable
Thickness (m)	5	2	10
Storativity	3.75×10^{-4}	1.5×10^{-4}	7.5×10^{-4}
Effective Porosity	0.1	0.1	0.1

*Geometric mean of log-K distribution

Table 5.5. Leaky Aquifer Model Parameters.

Field Generation Parameters	Value	Field Generation Parameters	Value
Domain Size (m x m)	500 x 500	Duration (day)	1
Cell Size (m x m)	1 x 1	Time Step	100
Number of Cells	499 x 499	Correlation Length Ratio	0.1
Pumping Rate (m^3/day)	20	log-Mean	1
Monitoring Well Distance (m)	15	log-Variance	1

The conceptual view of leaky aquifer model explained above is also illustrated in Figure 5.17. The pumping response of hypothetical leaky aquifer model is given in Figure 5.18. Applying the IAM procedure shown in Figure 5.19 to estimate aquifer parameters, the mean transmissivity inside the cone of depression can be predicted as 1.4509 m^2/day whereas the conventional techniques, namely WCM and HIP, estimate

the transmissivity as 1.5158 m^2/day and 1.4667 m^2/day, respectively.

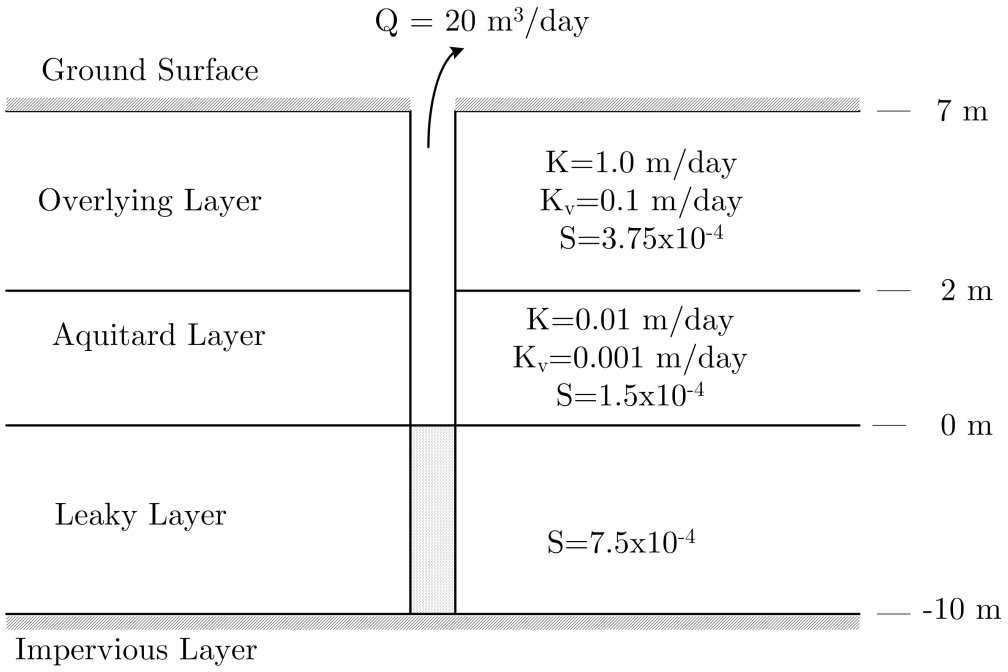

Figure 5.17. Conceptual View of Leaky Aquifer Model.

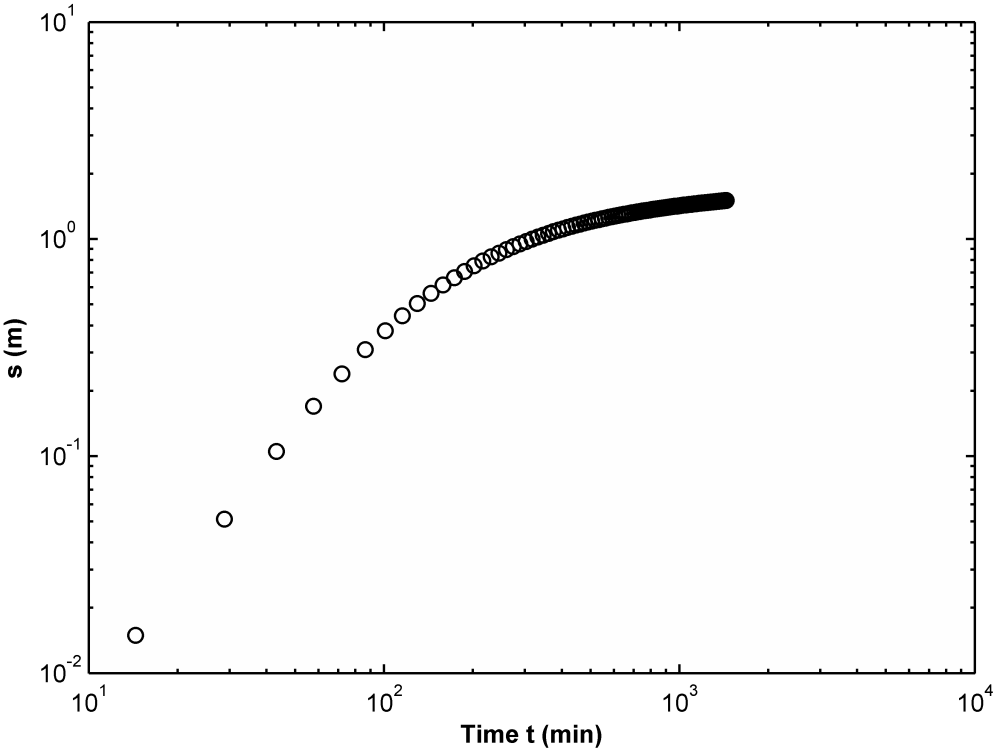

Figure 5.18. Drawdown Curve of Leaky Aquifer Model.

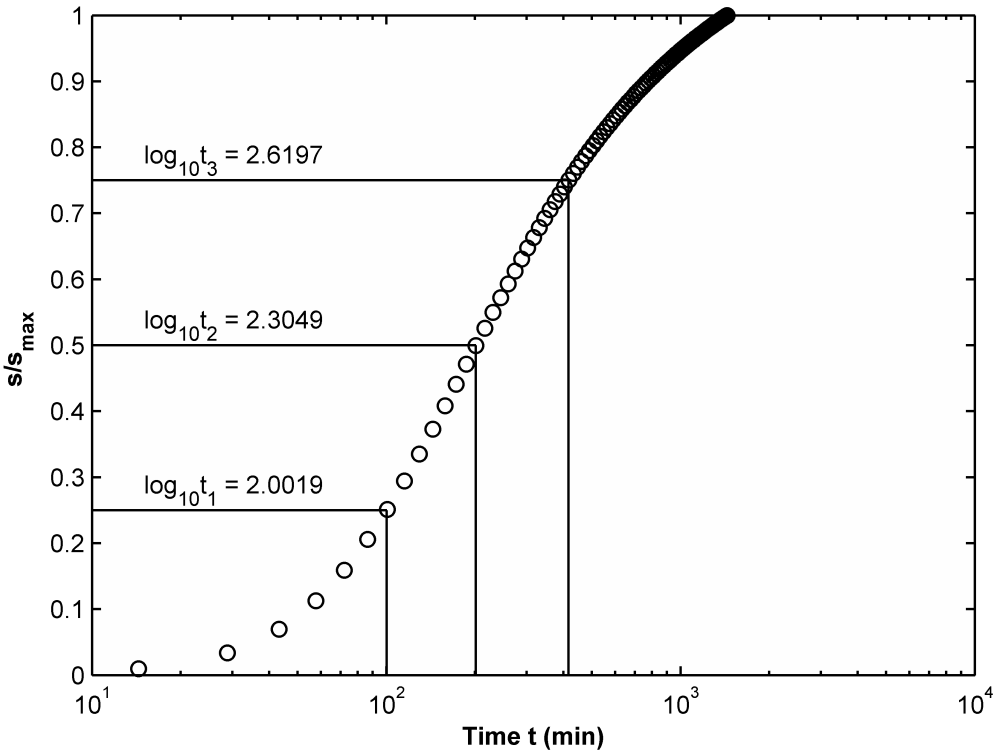

Figure 5.19. Normalized Drawdown Curve of Leaky Aquifer Model.

Using the predicted aquifer parameters obtaining from each estimation method, drawdown data were regenerated to compare the performance of each method as shown in Figure 5.20. Estimated aquifer parameters are also tabulated in Table 5.6. IAM and HIP show almost the same estimation performance considering the RMSE between actual and regenerated drawdown values. On the other hand, WCM approximately doubles the error between observed and calculated drawdown values comparing to the errors realized in the HIP and IAM. One of the main reasons caused the poor estimation performance of WCM is that the smaller r/B values in the leaky type curve family originate from nearly same value of dimensionless time $1/u$ for early times, and also the inflection points after which stabilize the type curve due to the leakage mechanism of leaky aquifer system are not clear enough to decide to the proper match. This difficulty may be overcome by the iterative curve matchings just as used in most commercial aquifer tests analysis software. IAM, however, estimates the aquifer parameters within a reliable and robustness accuracy as listed in Table 5.6 avoiding the need of curve matching method or utilizing of commercial softwares.

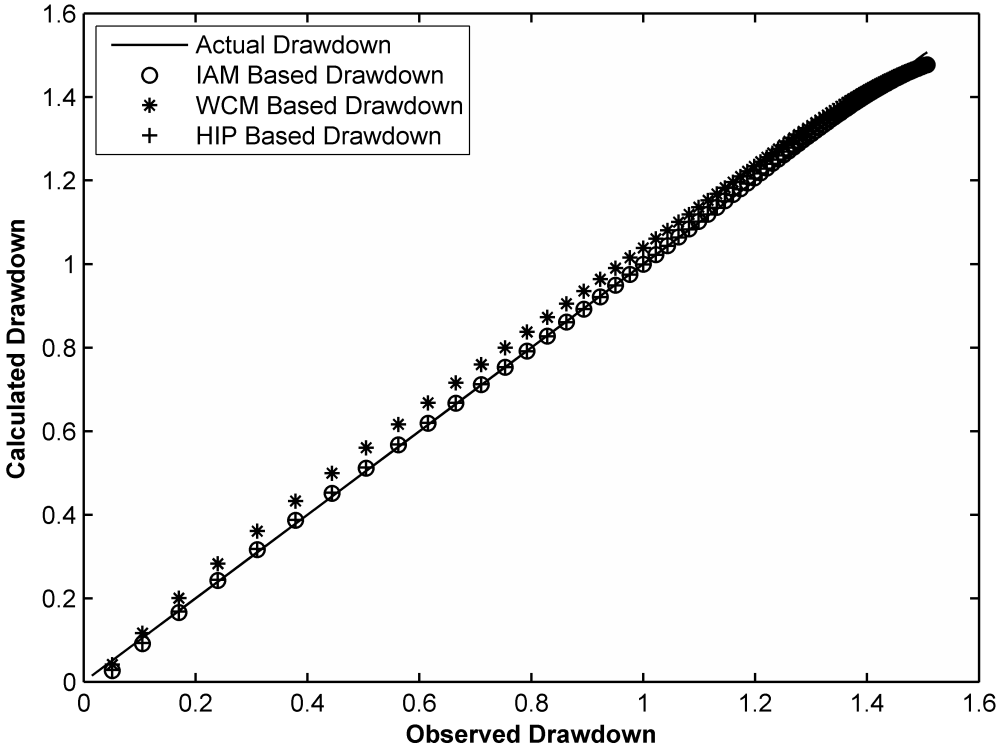

Figure 5.20. Drawdown Comparison for Estimation Methods.

Table 5.6. Comparison of Estimation Methods for Leaky Aquifer Model.

Method	T (m^2/day)	S	r/B	K_v (m/day)	R^2	RMSE
IAM	1.4509	0.0012	0.6755	0.0294	0.9990	0.0123
WCM	1.5158	0.0011	0.65	0.0285	0.9972	0.0297
HIP	1.4667	0.0012	0.6688	0.0292	0.9990	0.0122

5.2.3. Real Field Data

The field drawdown data was taken from a report prepared for Geological Survey Program South Dakota Department of Environment and Natural Resources (Rich, 2006). The well field located in southwestern Vermillion as shown in Figure 5.21. Pumping tests were conducted from June 2 through June 4, 2003 to assess and characterize the general hydraulic properties of the aquifer in the well field in order to

assist the city in determining any appropriate modifications to its wellhead protection area. Well # 3-Active is the pumping well whose discharge rate during the pumping phase of the test was kept steady at 520 gallons per minute and pumped water was discharged into the city's water storage facilities. Distance from the pumping well to the observation Well # 1-inactive is 434 ft. Aquifer thickness was reported as 76 ft.

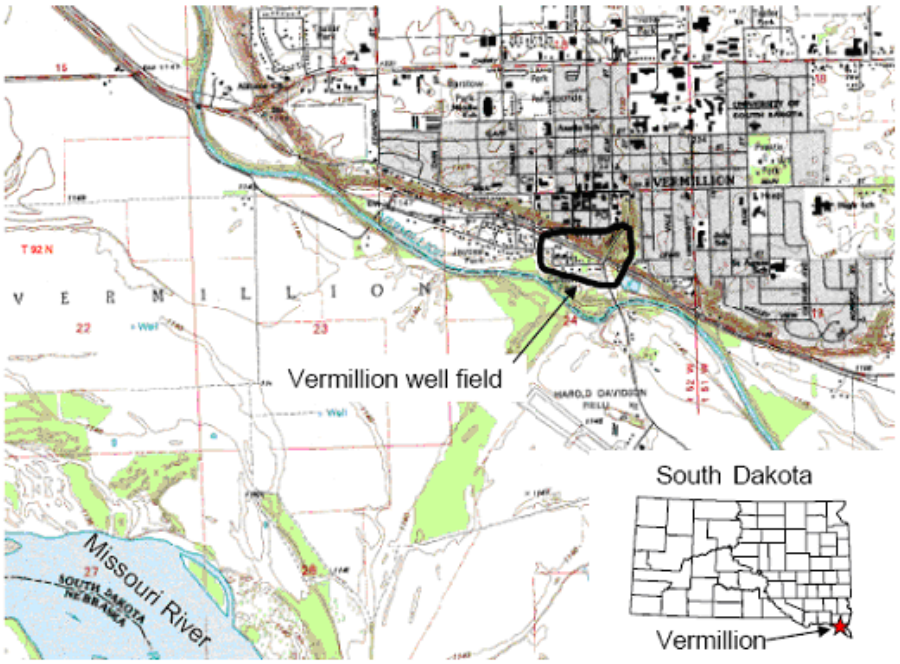

Figure 5.21. Map of Well Field Area (Rich, 2006).

The pumping response of aquifer shown in Figure 5.22 indicates the deviations from ideal type curve manner which can be as a result of heterogenetic character of aquifer, recording errors and uncertainty nature of pumping mechanism. Applying proposed IAM as shown in Figure 5.23 to the field data, aquifer parameters such as transmissivity, storativity and vertical hydraulic conductivity estimated as 40.84 ft^2/min, 4.1×10^{-4}, and 1.74×10^{-4} ft/min, respectively.

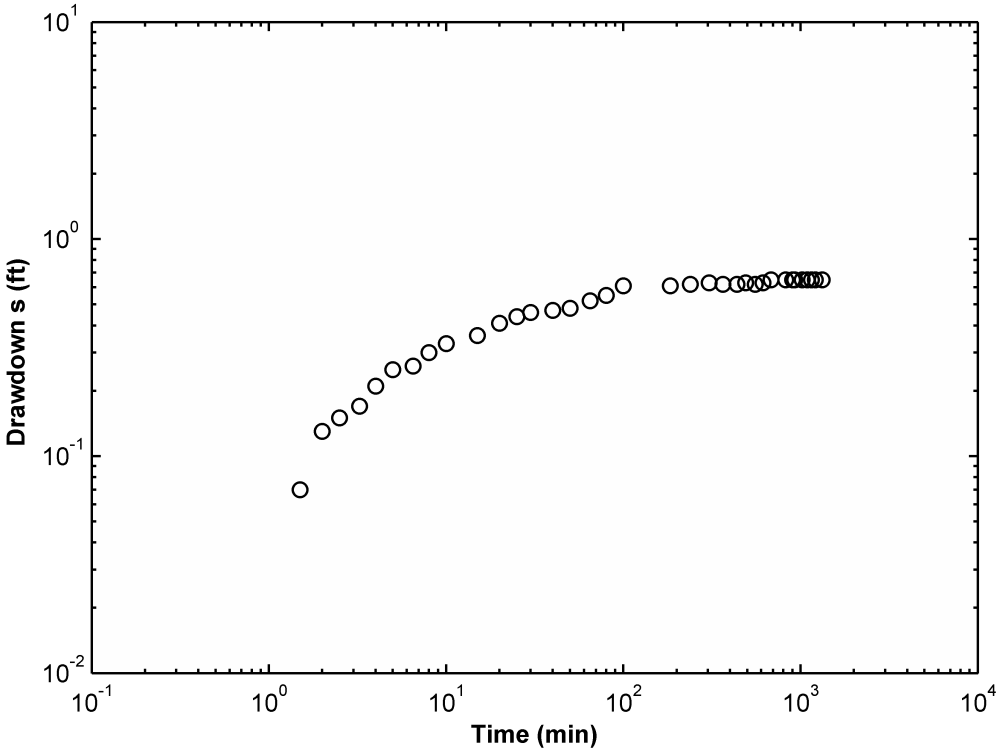

Figure 5.22. Drawdown Data of Real Field Test.

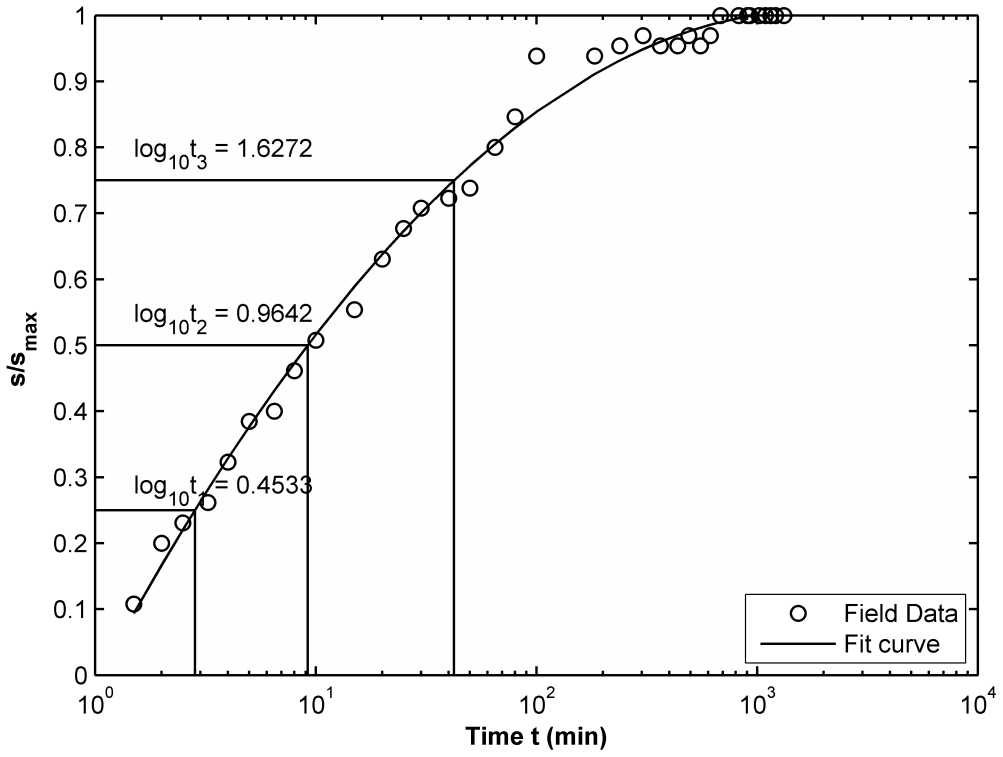

Figure 5.23. Normalized Drawdown Curve of Real Field Test.

For the sensitivity analysis, RMSE value of IAM shows that when the aquifer homogeneity is violated, the introduced prediction approach still estimates the aquifer parameters better than the conventional techniques as summarized in Table 5.7. Figure 5.24 indicates the drawdown comparison based on the each prediction method.

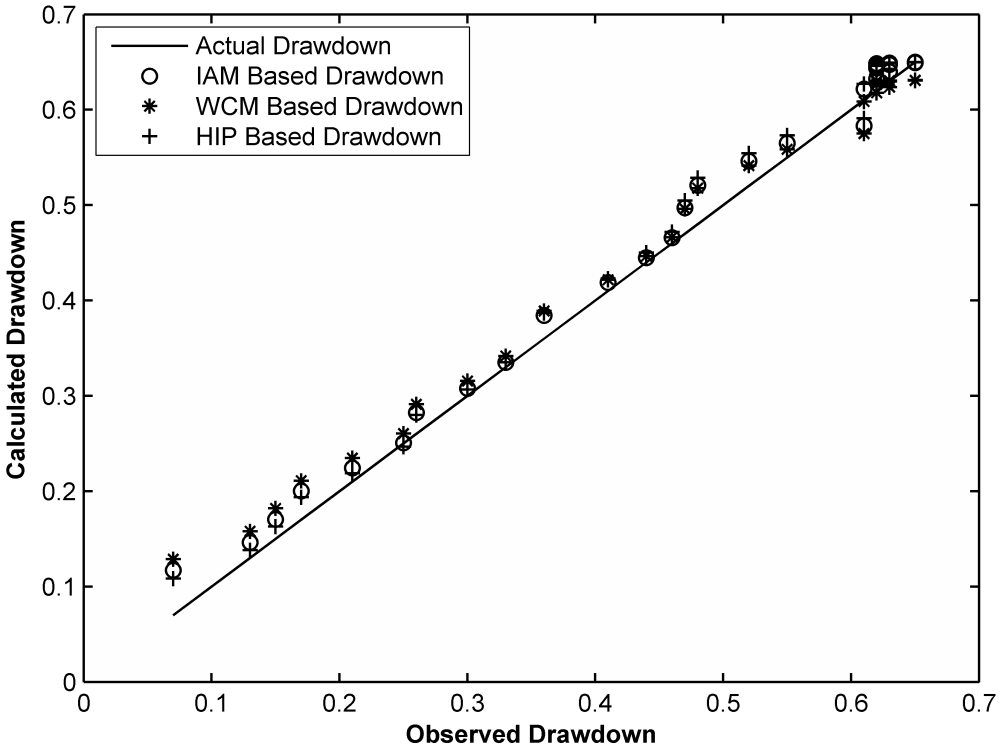

Figure 5.24. Drawdown Comparison for Field Data.

Table 5.7. Comparison of Estimation Methods for Field Data.

Method	T (ft^2/min)	S	r/B	K_v (ft/min)	R^2	RMSE
IAM	40.8385	4.1×10^{-4}	0.1029	1.74×10^{-4}	0.9947	0.0189
WCM	42.5519	3.62×10^{-4}	0.1	1.72×10^{-4}	0.9939	0.0223
HIP	38.1381	4.52×10^{-4}	0.1209	2.25×10^{-4}	0.9937	0.0195

6. AQUIFER IDENTIFICATION BY IAM

Aquifer parameters are typically estimated by comparing the theoretical response (based on the conceptual model) to the observed drawdown behavior during pump tests by graphical curve matching techniques (Renard, 2005a,b). ASTM D 4043-96 suggests a decision procedure to assist in selecting analytical models and methods applicable to specific hydrogeologic site characteristics and on the basis of the nature of the stress on the aquifer imposed by the pumping well. The analytical models derived for various aquifer types can be found in Barenblatt *et al.* (1960), Hantush (1961, 1964), Stallman (1965), Streltsova (1976, 1988), Dawson and Istok (1991), Kruseman and de Ridder (1992), Raghavan (1993), Batu (1998), and Fetter (2001). It should be noted that the Theis (1935) method is still widely used for non ideal aquifer conditions due to the simplicity of the analysis (Misstear, 2001).

The drawdown time derivative analysis represents a powerful tool for the characterization of aquifer in addition to the curve matching procedures. Chow (1952) was one of the first researchers to demonstrate the use of the time derivative of the drawdown curve for estimating the transmissivity of an ideal confined aquifer. Parks and Bentley (1996) used the derivative analysis to assess which sections of the drawdown data collected from short term aquifer tests in heterogeneous aquifers fall in the infinite acting radial flow. Pressure derivative type analysis was also used on slug tests within confined aquifers (e.g. Bourdet *et al.*, 1983; Ehlig-Economides, 1988; Karasaki *et al.*, 1988; Ostrowski and Kloska, 1989). Mejias *et al.* (2009) used derivative of pressure data measured during hydraulic testing of low-permeability formations through the use of packers. Straface *et al.* (2007) and Straface (2009) used the derivative approach to assess the confined aquifer hydraulic parameters from early time period of pumping. Avci *et al.* (2010) recently used the time derivative of drawdown data to establish aquifer parameters and system identification for step-drawdown testing.

The use of derivative plots generated from drawdown data has become a common practice in the analysis of aquifer parameters for all types of aquifer settings and pump-

ing test methodology. Walton (1987) explained that time-drawdown plot in semi-log scale and also distance-drawdown curve from the well can be categorized as specialized plots which can yield additional information on the type of aquifer systems. Diagnostic plots of the scaled first or second derivative of the pressure or flow-rate response for each type of hydraulic tests (constant rate, constant-pressure, or slug/pulse) were developed by Beauheim *et al.* (2004) for well testing in fractured media. Singh (2008) developed diagnostic plots for the confined aquifer parameters from early drawdown utilizing the derivative analysis for estimating aquifer parameters from early drawdown data of large diameter wells and extended the suggested approach to identify leaky aquifer parameters (Singh, 2010). In summary, diagnostic plots provide support in the system identification and parameter estimations on top of the site characterization effort and the pumping test analysis.

The logarithmic time-derivative procedure has shortcomings as the cone of depression expands outwardly from the pumping well, the aquifer features such as heterogeneity, bounded zones, leakage come into play and reflect their influence in the development of the drawdown curves observed in the monitoring wells. The numerical derivative values will be useful if good data (adequate number and accurate measurements) are available. The calculated derivative can be extremely variable if the time variation between two measurements is rather large and/or the drawdown measurements are affected by measurement uncertainties.

The logarithmic time derivative of the Theis (1935) well function is given as:

$$\frac{\partial s}{\partial \ln t} = \frac{Q}{4\pi T}\left[\frac{\partial W(u)}{\partial \ln t}\right] = \frac{Q}{4\pi T t}\exp(-u) \tag{6.1}$$

The Theis (1935) solution converges asymptotically toward the Cooper and Jacob (1946) solution when $u \leq 0.01$. The logarithmic time derivative of Cooper and Jacob (1946) approximation is expressed as

$$\frac{\partial s}{\partial \ln t} = \frac{Q}{4\pi T}\left[\frac{\partial \ln(2.25Tt/r^2S)}{\partial \ln t}\right] = \frac{Q}{4\pi T} \tag{6.2}$$

The logarithmic time derivative has to be evaluated numerically on field data using individual water levels measured at specific time values during the pumping test. An important aspect of performing the derivative analysis is the selection of an appropriate calculation method. Renard *et al.* (2009) suggested the following numerical derivation methodologies:

$$\frac{\partial s}{\partial \ln t_m} = \frac{s_i - s_{i-1}}{\ln t_i - \ln t_{i-1}} \tag{6.3}$$

where t_m is arithmetic or geometric mean of the time interval. The second approximation may be to evaluate the slope between two successive data points and multiply it by the time corresponding to the center of the interval:

$$\frac{\partial s}{\partial \ln t_m} = \left(\frac{s_i - s_{i-1}}{t_i - t_{i-1}}\right)\left(\frac{t_i + t_{i-1}}{2}\right) \tag{6.4}$$

Alternative differentiation schemes have been proposed by Bourdet *et al.* (1989) and Spane and Wurstner (1992) to overcome some of the difficulties when noise (oscillations) develops from poor data which makes interpretation of the diagnostic plot difficult. The Bourdet *et al.* (1989) derivative uses the following three-point formula to compute derivatives from drawdown data by numerical differentiation as

$$\begin{aligned}\left(\frac{\partial s}{\partial \ln t}\right)_i &= \frac{\left(\frac{\Delta s_1}{\Delta t_1}\Delta t_2 + \frac{\Delta s_2}{\Delta t_2}\Delta t_1\right)}{\Delta t_1 + \Delta t_2} \\ &= \frac{\left(\frac{s_i - s_{i-1}}{\ln t_i - \ln t_{i-1}}\right)(\ln t_{i+1} - \ln t_i) + \left(\frac{s_{i+1} - s_i}{\ln t_{i+1} - \ln t_i}\right)(\ln t_i - \ln t_{i-1})}{\ln t_{i+1} - \ln t_{i-1}}\end{aligned} \tag{6.5}$$

The derivative formula given in Equation 6.5 is a weighted average of slopes computed from data points on either side of center node i. These slopes ($\Delta s_1/\Delta t_1$ and $\Delta s_2/\Delta t_2$) are also known as the left and right derivatives, respectively. The Bourdet method uses data points separated by a fixed distance measured in logarithmic time to remove noise from the calculations. The Bourdet method was used to elaborate the derivative of the drawdown data for the examples which were analyzed in this chapter.

6.1. Conceptual Diagnostic Curves

The applicability and effectiveness of integration of the water level drawdown curve with respect to time as in the IAM case rather than taking the logarithmic derivatives with respect to time was investigated in this chapter as a potential tool for aquifer system identification and parameter assessment. Renard *et al.* (2009) indicated that the use of the drawdown and the logarithmic time derivative plotting on the same graphic can provide information on small changes on the drawdown curve, therefore, help to identify the aquifer system and sometimes provide information on the aquifer parameters. Figure 6.1 shows several specific diagnostic plots given by Gringarten *et al.* (1974).

The IAM diagnostic plots were given in Figure 6.2 together with the logarithmic based diagnostic plots for comparison purposes. Figure 6.2a shows the diagnostic plot for the Theis (1935) well function. It was indicated that the logarithmic based derivative values become stabilized at late time periods reflecting the infinite acting radial flow feature (constant derivative value) only after the Cooper and Jacob (1946) approximation becomes valid. The IAM based transmissivity estimate, on the other hand, shows that the diagnostic plot is a straight line for the entire duration of the pumping period including the pre-Cooper and Jacob approximation. This is an important aspect of the IAM assessment since it allows the use of early drawdown data to assess ideal confined aquifer behavior conditions.

Figure 6.2b shows the diagnostic plots for ideal aquifers bounded by a no-flow boundary at some distance from the extraction well. The drawdown function is obtained by the superposition of two Theis (1935) well functions placed some distance apart simulating constant rate extraction from an ideal aquifer. The drawdown function at early times is caused by a single Theis (1935) well function alone and is identified as a constant value of the transmissivity in the IAM diagnostic plot until the presence of the second well function starts being felt by the monitoring point and the transmissivity decreases to half of the initial value. The IAM method picks up the ideal behaviors of the confined aquifers earlier than the logarithmic time derivative plots.

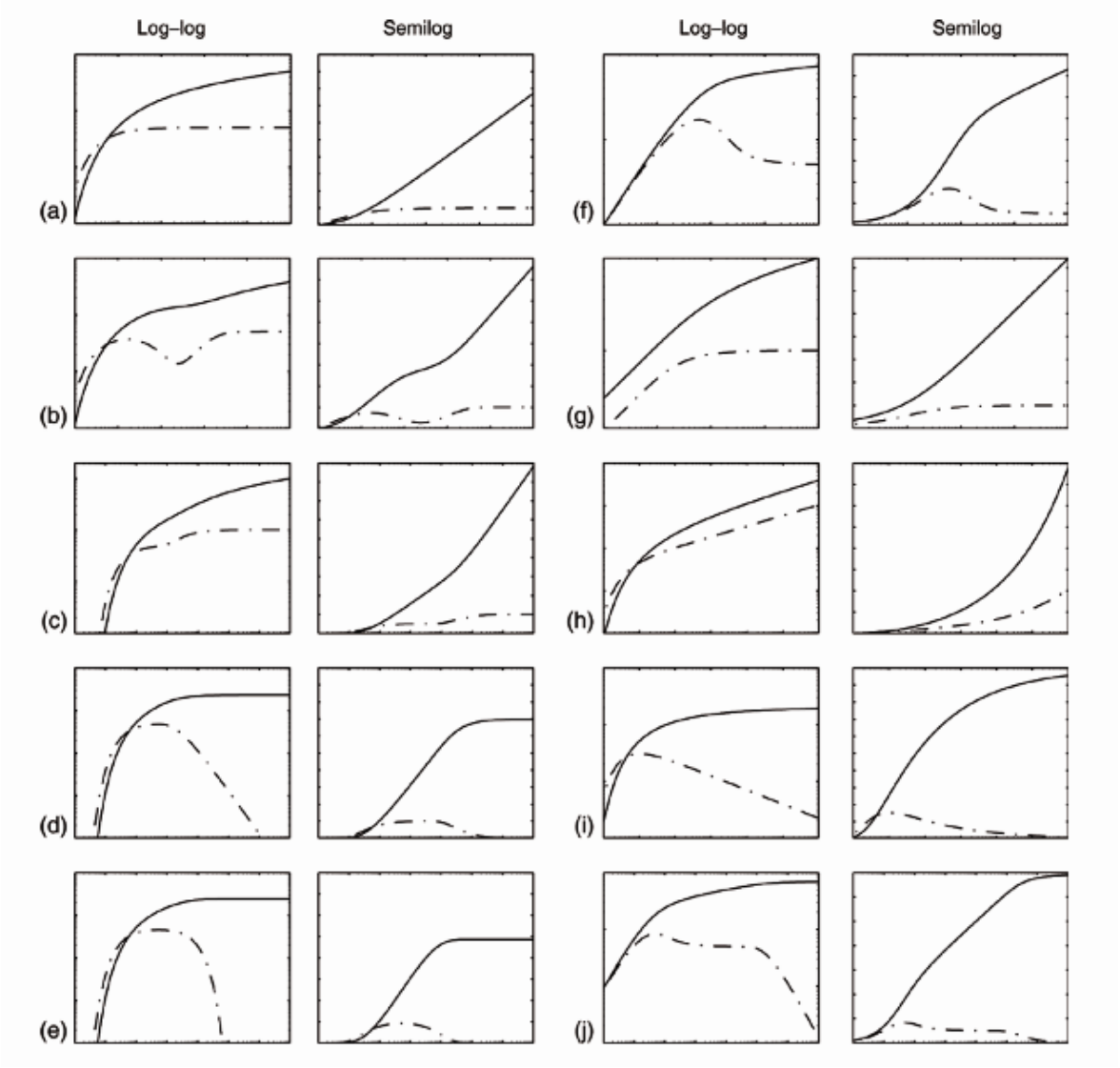

Figure 6.1. Drawdown (solid line) and Derivative (dashed line) Curves for Various Aquifer Types (a) Confined Ideal (b) Unconfined (c) Confined with a No-flow Boundary (d) Confined with a Constant Boundary (e) Leaky (f) Aquifer with Well-bore Storage (g) Single Vertical Fracture (h) General Radial-Flow with n $<$ 2 (i) General Radial-Flow with n $>$ 2 (j) Aquifer with Infinite Radial Flow.

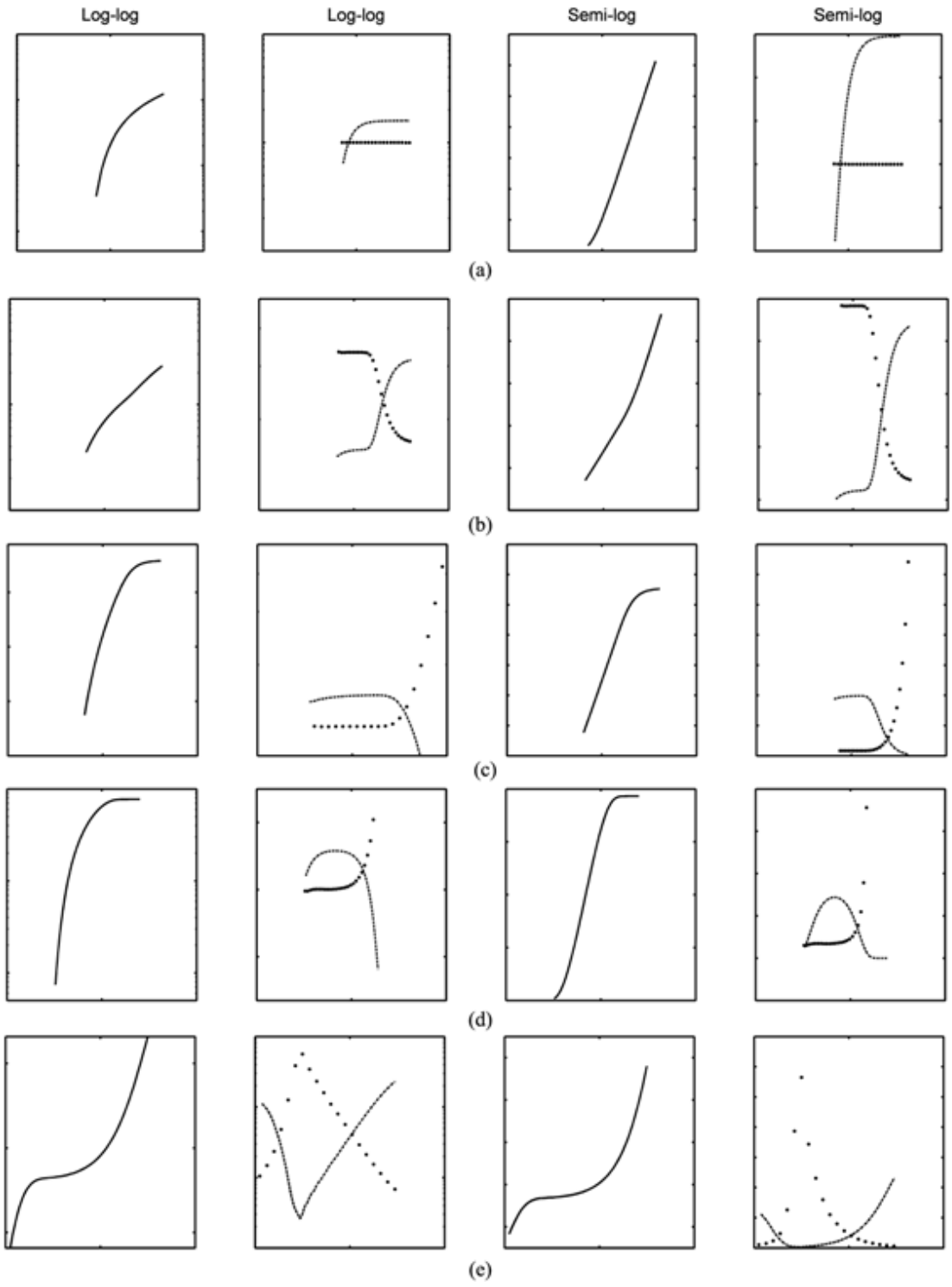

Figure 6.2. Drawdown Curves (solid line) and Log-time Derivative Curves (dashed line) and IAM Based Diagnostic Curves (circles) for Various Aquifer Settings. (a) Ideal Confined Aquifer (b) Confined Aquifer with a No-flow Boundary (c) Confined Aquifer with a Constant Head Boundary (d) Leaky Aquifer (e) Unconfined Aquifer.

Figure 6.2c shows the diagnostic plots for ideal aquifers bounded by a constant hydraulic head boundary at some distance from the extraction well. The drawdown function is again obtained by the superposition of two Theis (1935) well functions simulating constant rate extraction from an ideal aquifer and an injection from the second well placed some distance apart. As in the previous case, the drawdown data at early times allows the identification of the transmissivity value until the effects of the second well pumping is felt at the monitoring point. The transmissivity calculated with the IAM method starts increasing towards infinity as the water level drawdown stabilize from the constant head boundary effect.

Figure 6.2d shows the diagnostic plots for the case of a leaky aquifer simulated with the Hantush (1956) leaky well function. The IAM transmissivity estimations are constant values prior to the effect of leakage from the semi confining beds; once the leakage effects are felt as in the case of the constant head hydraulic boundary, the apparent transmissivity values start increasing toward infinity. The IAM diagnostic shapes will vary for leakage conditions which may provide additional information for hydraulic parameter estimation. It should also be noted that the rate of increase of the IAM transmissivity is higher for the leaky case conditions than it is for the constant head boundary case in the confined aquifer.

Figure 6.2e shows the diagnostic plots for unconfined aquifers generated by the Moench (1997) algorithm. The IAM based diagnostic plots shows three separate stages. The initial stage of the transmissivity variation with time is noted to be a constant value and represents the confined aquifer behavior when the pumping starts and the delayed yield is not yet felt by the aquifer system. The second stage of the diagnostic plot is the increase and subsequent decrease of the transmissivity value as the delayed yield begins to impact the water level drawdown and then fades as the drainage of the unconfined portion of the aquifer finalizes. The third stage is the stabilization of the transmissivity values once the delayed yield effects are not felt by the aquifer and the system starts behaving as an ideal aquifer once again.

Despite having identified unique features of the aquifer systems for the above

aquifer systems, it should be evident that the IAM diagnostic plots as in the case of logarithmic time derivative diagnostic plots will not provide unique and exactly identifiable signatures in all cases. This is due to the fact that different aquifer systems may result in similar water level variations; similarity in diagnostic plots will be present for unconfined, double porosity aquifer systems where delayed yield occurs from unsaturated zone drainage and matrix drainage, respectively. In addition the time increment which will be used to develop the IAM will influence the shape of the diagnostic plots; different time increments will yield diagnostic plot shapes that will be similar but not entirely unique. Lastly the aquifer conditions and the controlling parameters will influence the shape of the diagnostic plots generated from the drawdown data. Potential heterogeneities, however, will have slight impacts on the derived diagnostic shapes as will be evident in the next section when the IAM method is implemented on field data.

6.2. Field Data Assessment

The effectiveness of the IAM diagnostic plots was investigated by analyzing field data collected from leaky, unconfined, bounded and heterogeneous aquifer settings. As will be noted, the selected case studies were among those that did not provide ideal drawdown behavior that matched the aquifer system in which the pumping test was conducted. This was done specifically to review the usefulness of the IAM diagnostic plots when analyzing non-ideal drawdown behavior within an identified aquifer system setting.

6.2.1. Confined Heterogeneous Aquifer

The IAM was applied as a diagnostic tool to identify the heterogeneous character of the Horkheimer Insel site in the Neckar valley in southern Germany, based on the work of Schad and Teutsch (1994). The investigators described the aquifer as consisting of approximately 4 m of poorly sorted sand and gravel deposits of braided river environment of Holocene age. The aquifer at the hand is overlain by the 5-6 m of mostly clayey flood deposits and underlain by a hydraulically tight clay and limestone formation of middle Triassic age.

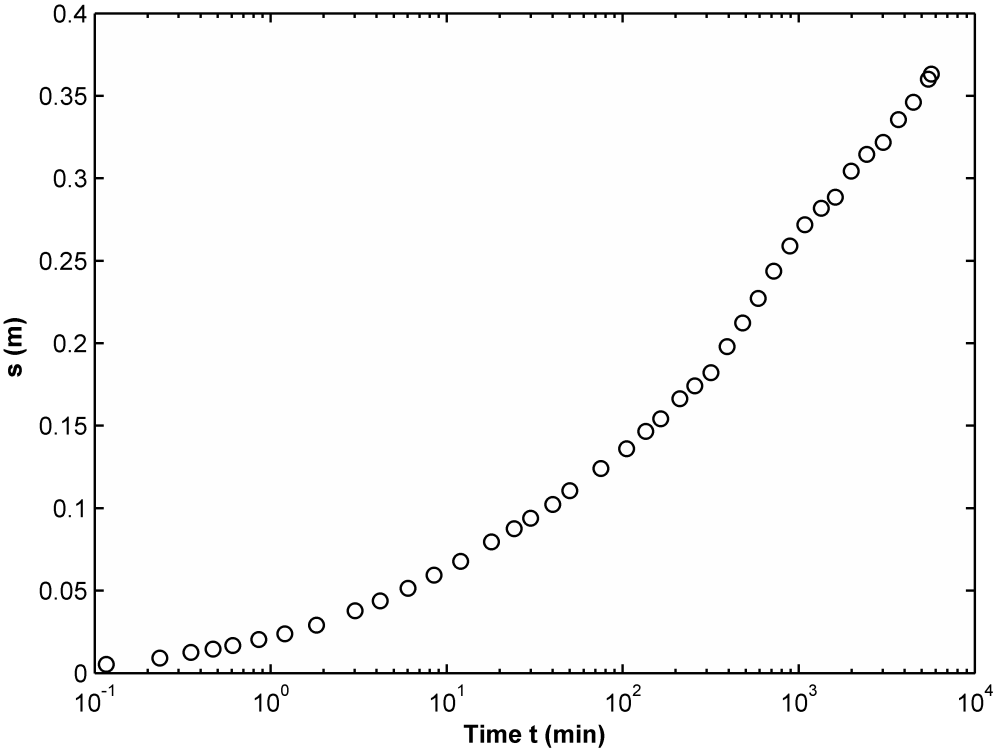

(a)

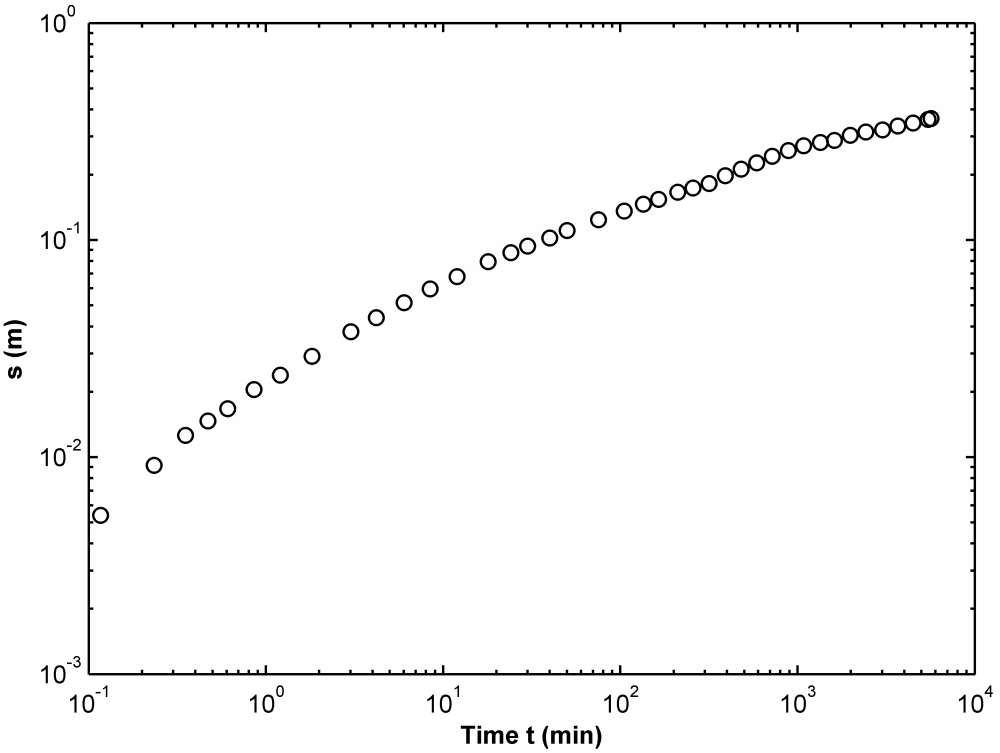

(b)

Figure 6.3. Drawdown Data for Heterogeneous Confined Aquifer (a) Semi-Log Scale (b) Log-Log Scale (Drawdown data are obtained from Schad and Teutsch, 1994).

Aquifer was stressed by a constant withdrawal rate of 13.6 l/s (1175.04 m^3/day) for 4 hours long duration. The IAM was applied to the drawdown data, as shown in Figure 6.3, obtained from monitoring well-10 located at a distance of 15.2 m to the pumping well with the log-cycle value Δ of 0.5. Although drawdown derivative approach follows the increasing trend of transmissivity values as depicted in Figure 6.4a, it does not provide a satisfactory assessment about the aquifer characteristic as well as the parameters estimation. The IAM based diagnostic plot for the monitoring well shown in Figure 6.4b, however, indicates the following features:

- The IAM identifies a trend in the predictions of the transmissivity field where the distribution of transmissivity near the monitoring wells in the initial pumping test period tends to converge to a particular transmissivity value in the later stages of the pumping test.
- For nearby monitoring wells, the transmissivity values in the early stages of the pumping period are greater than the long term transmissivity values. The transmissivity values yield a value of 1.19 m^2/min (1714 m^2/day).
- This type of behavior has been observed in the long term of pumping when the aquifers have a heterogeneous character with the distribution of log-normal transmissivity. Warren and Price (1961), Lachassagne *et al.* (1989), Butler and Liu (1991), Meier *et al.* (1998), and Sanchez-Vila *et al.* (1999) show that estimated aquifer parameters obtained from long term pumping tests are strongly correlated with geometric mean of the aquifer domain being stressed.

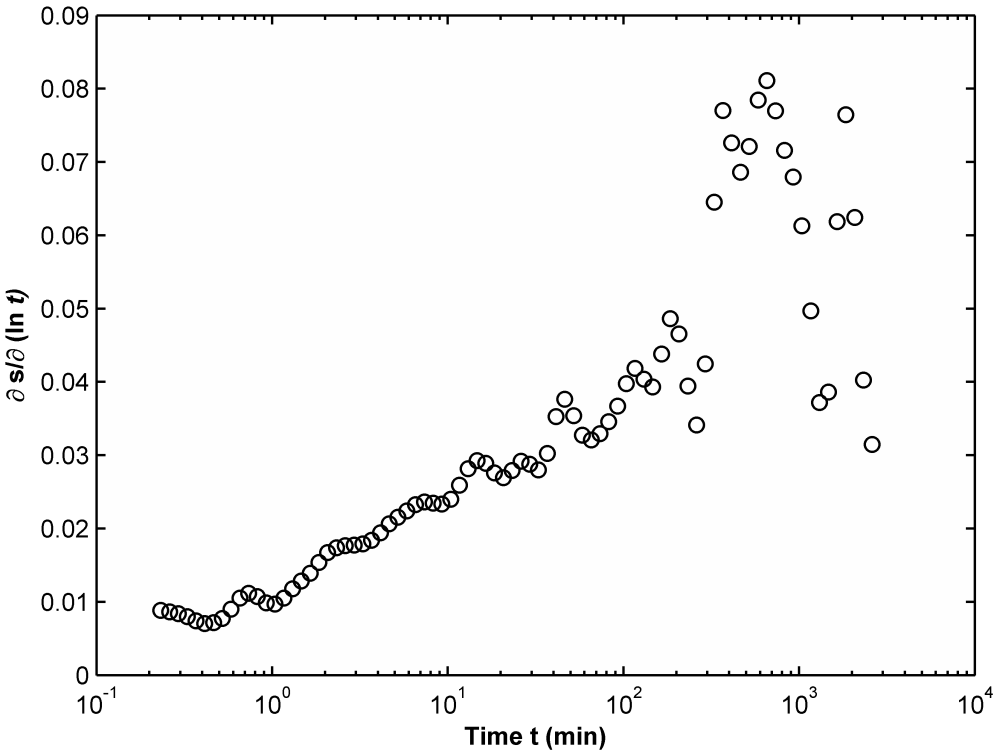

(a)

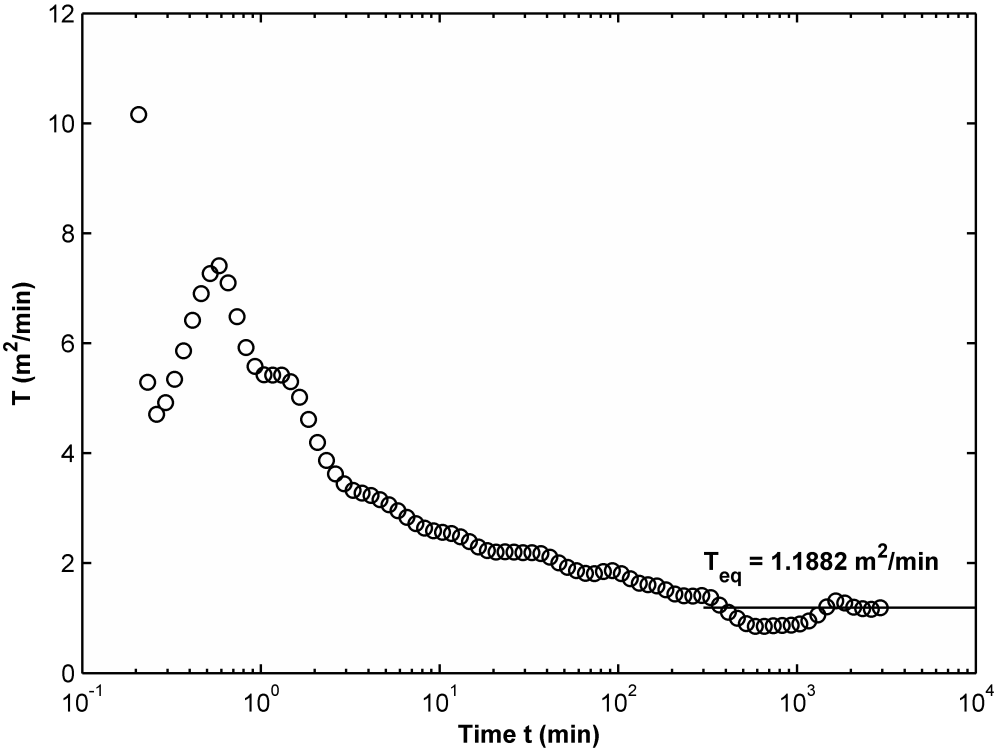

(b)

Figure 6.4. Diagnostic Plots for Heterogeneous Confined Aquifer (a) Derivative Based Diagnostic Plot (b) IAM Based Based Diagnostic Plot.

6.2.2. Confined Bounded Aquifer

Pumping test data was used to investigate the IAM performance on the analysis of bounded confined aquifer. A-57-hour-long pump test was conducted at a rate of 63.5 m^3/h (1524 m^3/day) at a site located on the borderline between the Paris and the Aquitaine sedimentary basins (Bourbiaux *et al.*, 2007). The hydrological site covered an area of 210 m by 210 m and showed large productivity/permeability differences, in a ratio exceeding 10, between the monitoring wells. The investigators noted the existence of a low-permeability region in the South-Eastern region of the site which was observed in the monitoring well M5 located at a distance of 160 m away from the pumping well. Drawdown data obtained from the site is illustrated in Figure 6.5. The IAM assessment of this data with the log-cycle $\Delta = 0.5$ is shown in Figure 6.6b; the results clearly indicate the bounds of the confined aquifer as implied in the work of Bourbiaux *et al.*, (2007).

The transmissivity value obtained from IAM analysis can be estimated to be close to 385 m^2/day between 10 and 200 minutes of testing; the estimated transmissivity values are nearly halved when the boundary effects become dominant following 2000 minutes of pumping period. Based on the superposition theory, if an aquifer is bounded with a no-flow boundary, transmissivity values near the boundary cause higher drawdown compared to the pumping tests which are conducted in the aquifers with infinite extend boundary. This situation is clearly demonstrated in Figure 6.6b.

In the light of the results, the characteristic of aquifer can be identified as bounded with a no flow barrier as shown in Figure 6.2b. The use of derivative based diagnostic plot as given in Figure 6.6a is not preferable due to that the available test data may cause larger deviations which complicate the identification of aquifer characteristic. Another advantage of the use of IAM is that equivalent transmissivity value of the aquifer can easily be estimated which provides information about the propagation of cone of depression with time.

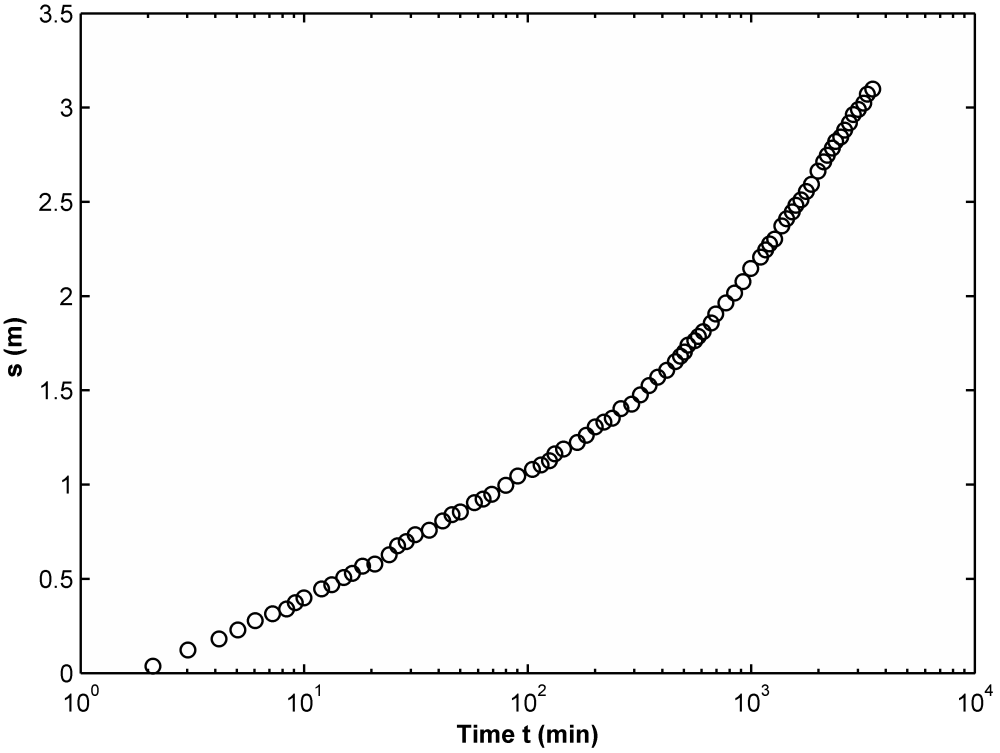

(a)

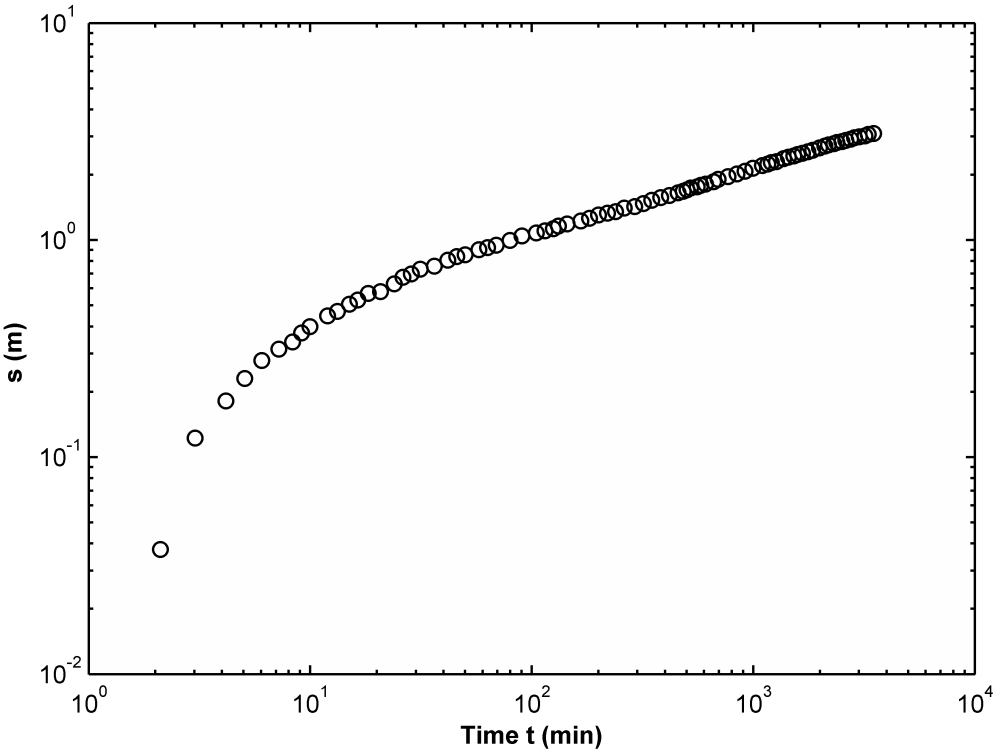

(b)

Figure 6.5. Drawdown Data for Confined Aquifer with No-Flow Barrier (a) Semi-Log Scale (b) Log-Log Scale (Drawdown data are obtained from Bourbiaux *et al.*, 2007).

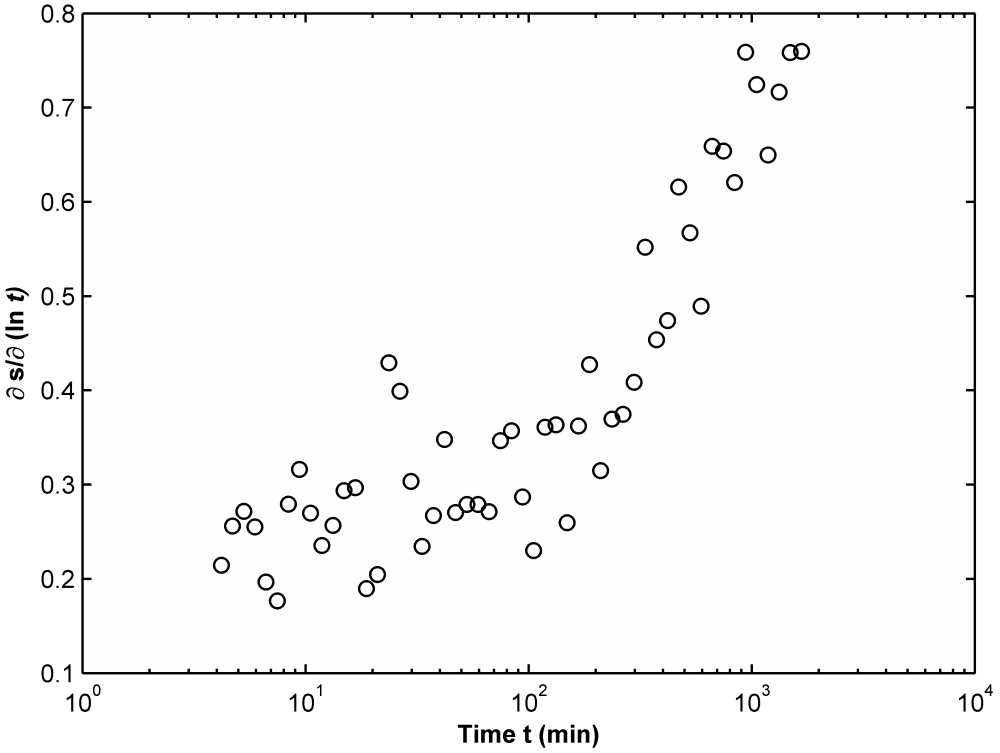

(a)

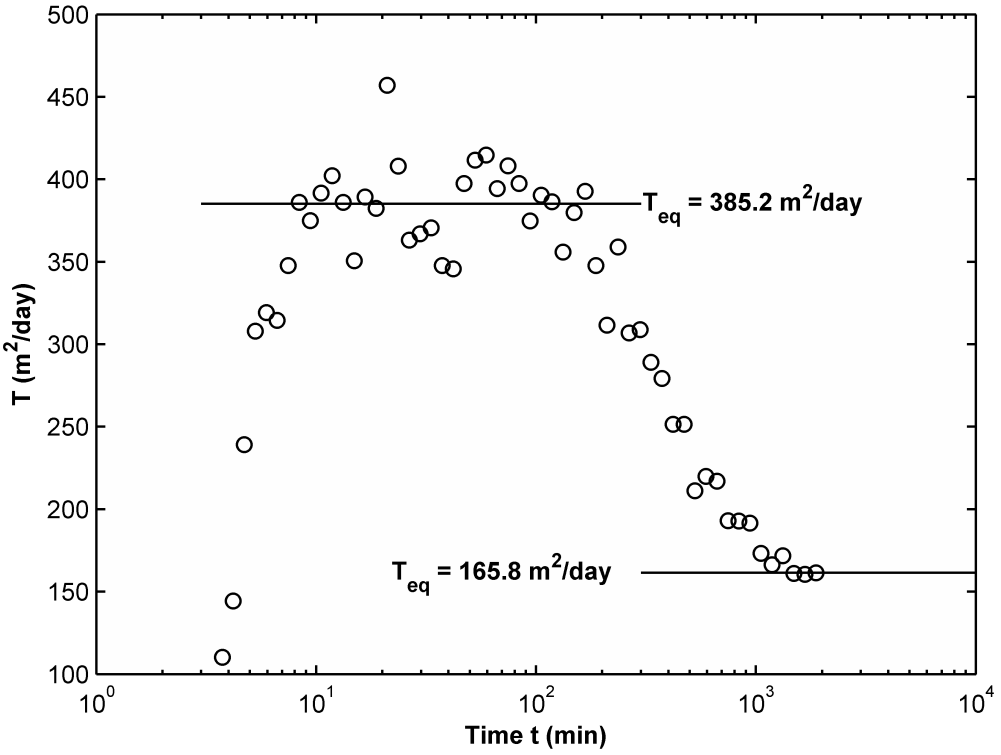

(b)

Figure 6.6. Diagnostic Plots for Confined Aquifer with No-Flow Barrier (a) Derivative Based Diagnostic Plot (b) IAM Based Based Diagnostic Plot.

6.2.3. Leaky Aquifer Test Analysis

In the report of Pratt (1993), a pumping test was conducted in a semi confining layer of the three-layered aquifer system in Escambia County, Florida. The hydrogeologic conceptual model was taken to be a water-table zone overlying a leaky semi-confining low permeability zone which itself overlies a main producing zone. Three monitoring wells (MW 01, MW 02 and MW 03) were installed into the main producing zone to monitor water levels during the pumping test at radial distances of 100, 102 and 606 ft, respectively. Pumping rate was kept constant at 2500 gallons per minute (gpm) for the duration of the test. Water level data obtained were analyzed using Hantush (1956) method by the researcher. Hydraulic properties were estimated by the researcher as shown in Table 6.1:

Table 6.1. Leaky Aquifer Hydraulic Properties (Pratt, 1993).

Hydraulic Property	MW 01	MW 02	MW 03
k_z/k_r	0.1	0.1	0.1
Br (ft)	1250	1280	1350
T (ft^2/day)	10640	9580	11270
S	7.10E-04	4.40E-04	4.80E-04
k' (ft/day)	0.26	0.22	0.23
k_z (ft/day)	5.9	5.3	6.2
k_r (ft/day)	59	53	62

Drawdown data of each monitoring well are shown in Figure 6.7, Figure 6.9 and Figure 6.11, respectively. IAM with the log-cycle (Δ) of 0.5 was applied for the drawdown data of each observation well.

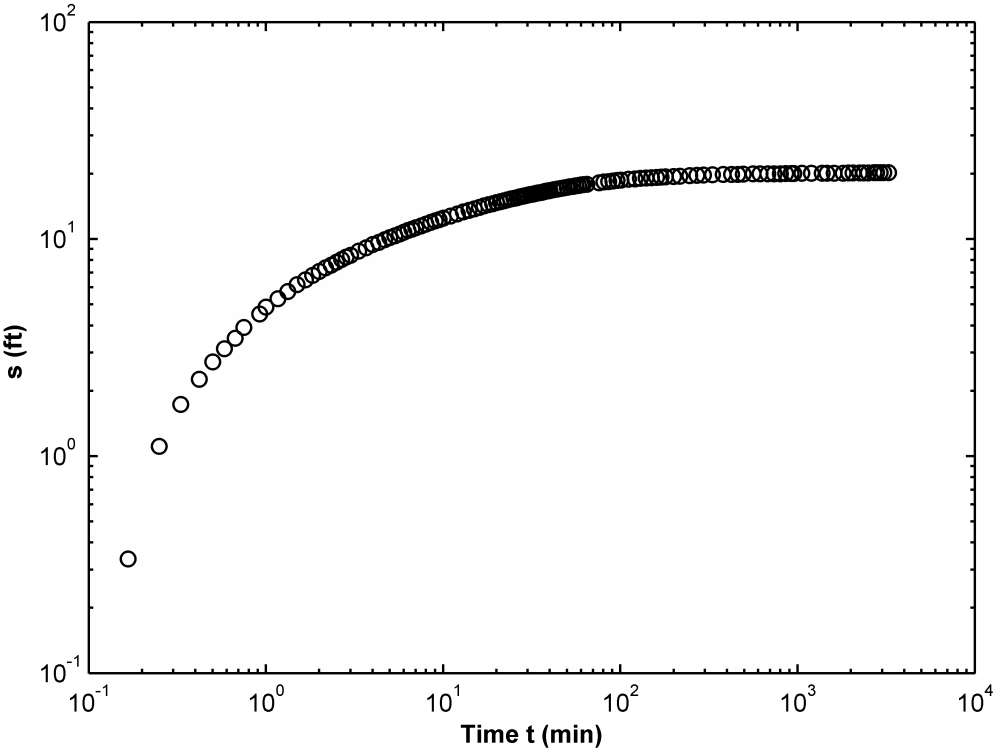

(a)

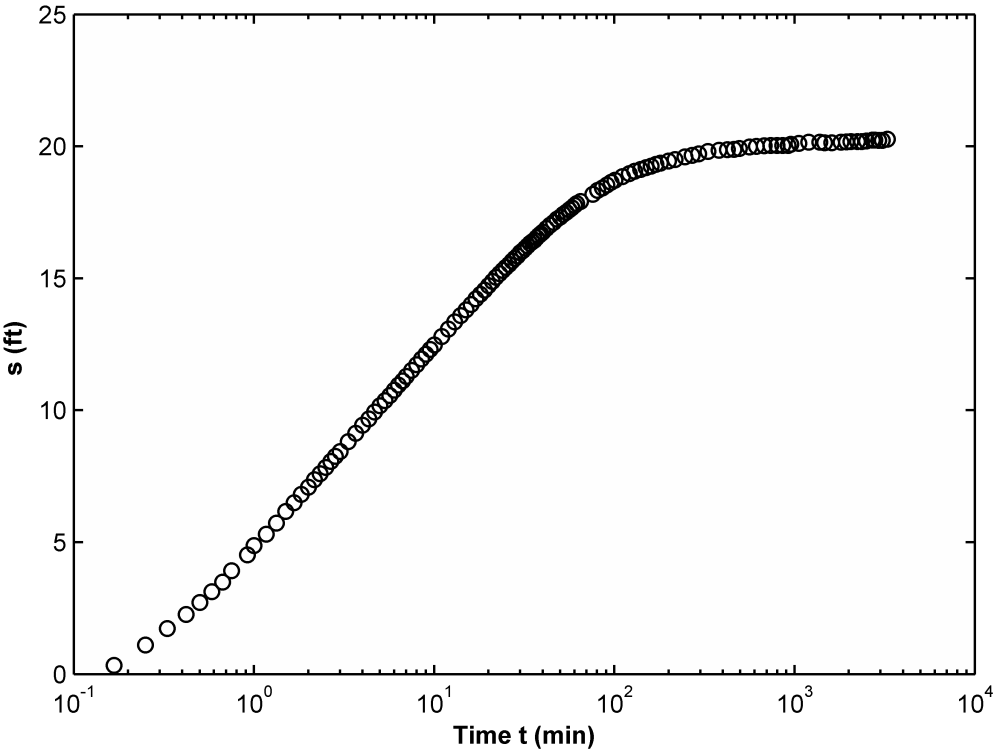

(b)

Figure 6.7. Drawdown Data at MW01 (a) Log-Log Scale (b) Semi-Log Scale (Drawdown data are obtained from Pratt, 1993).

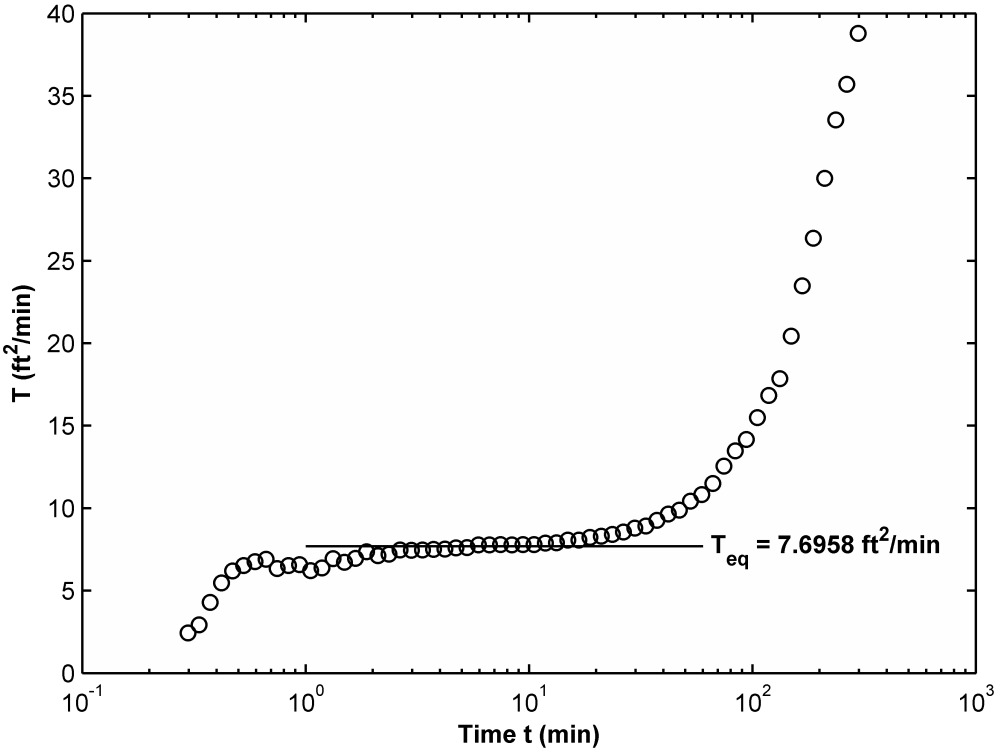

(a)

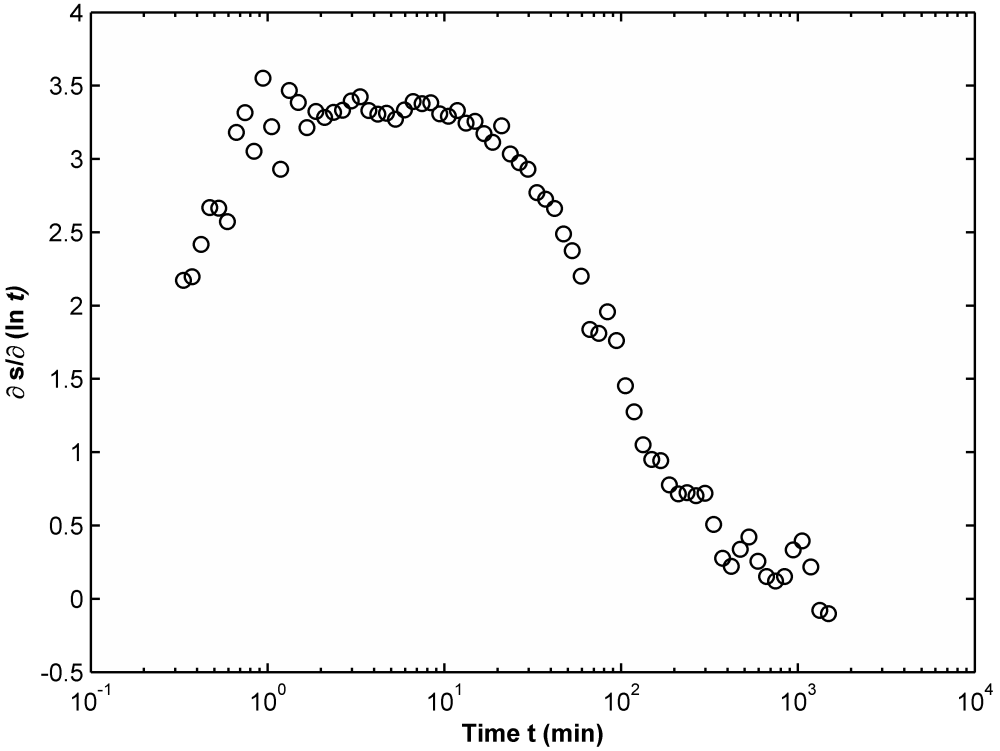

(b)

Figure 6.8. Test Analysis of MW01 (a) IAM Based Diagnostic Plot (b) Derivative Based Diagnostic Plot.

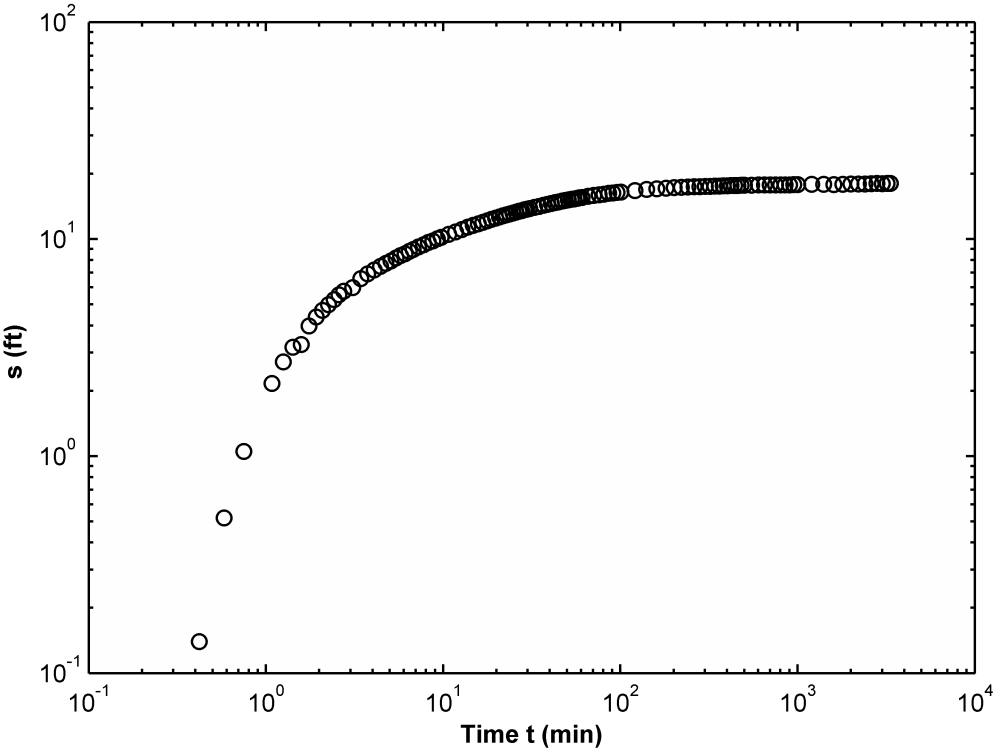

(a)

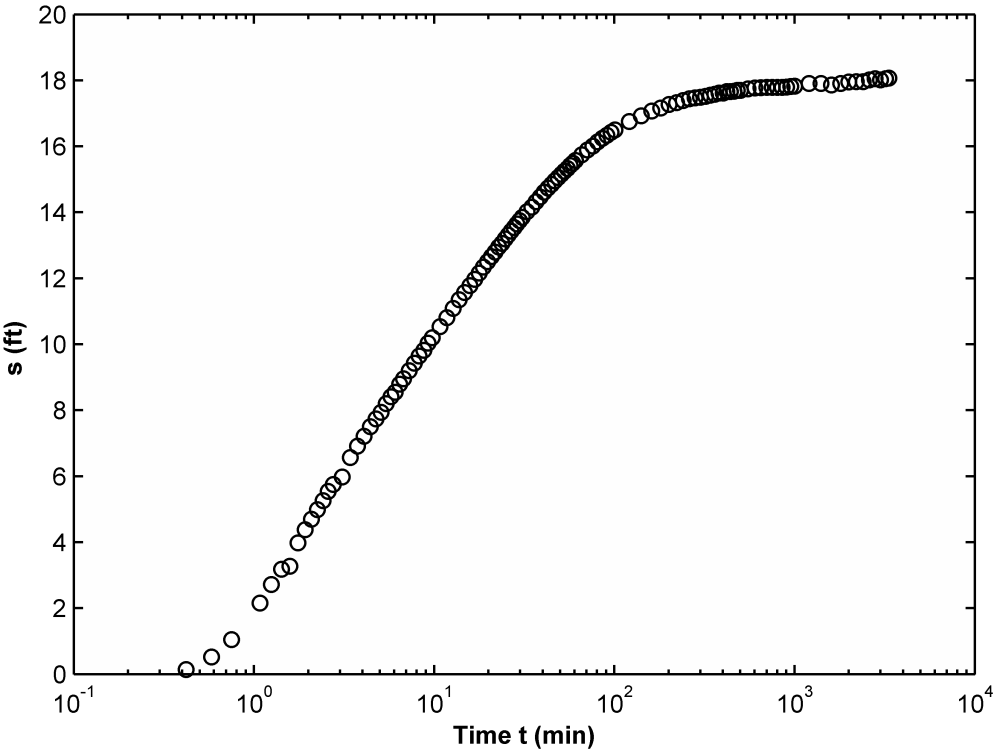

(b)

Figure 6.9. Drawdown Data at MW02 (a) Log-Log Scale (b) Semi-Log Scale (Drawdown data are obtained from Pratt, 1993).

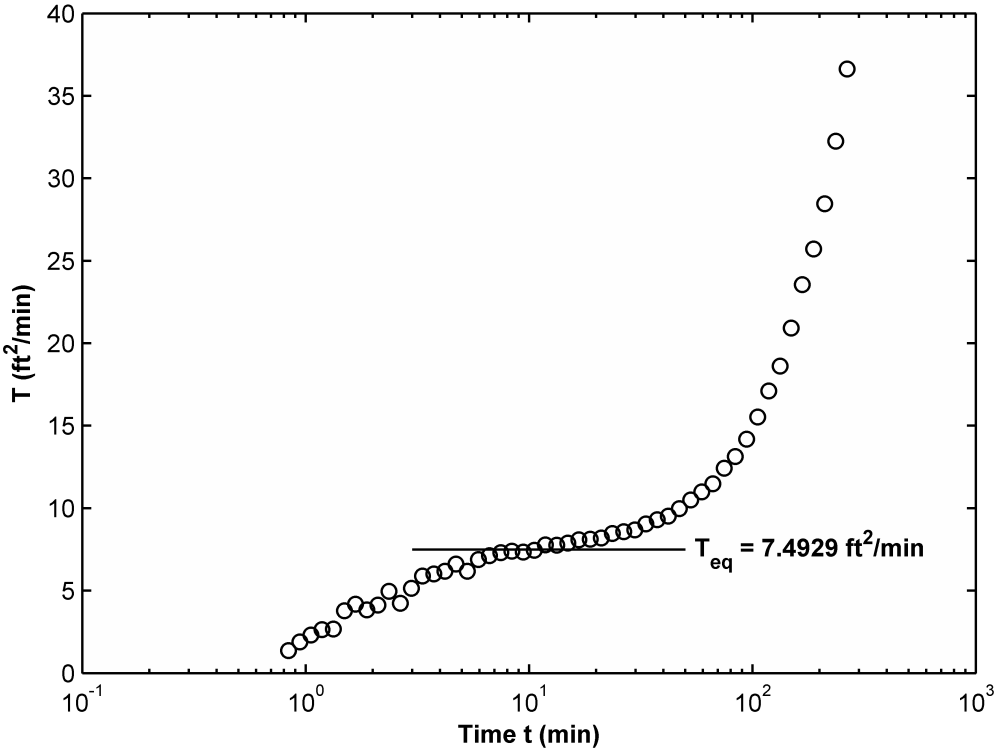

(a)

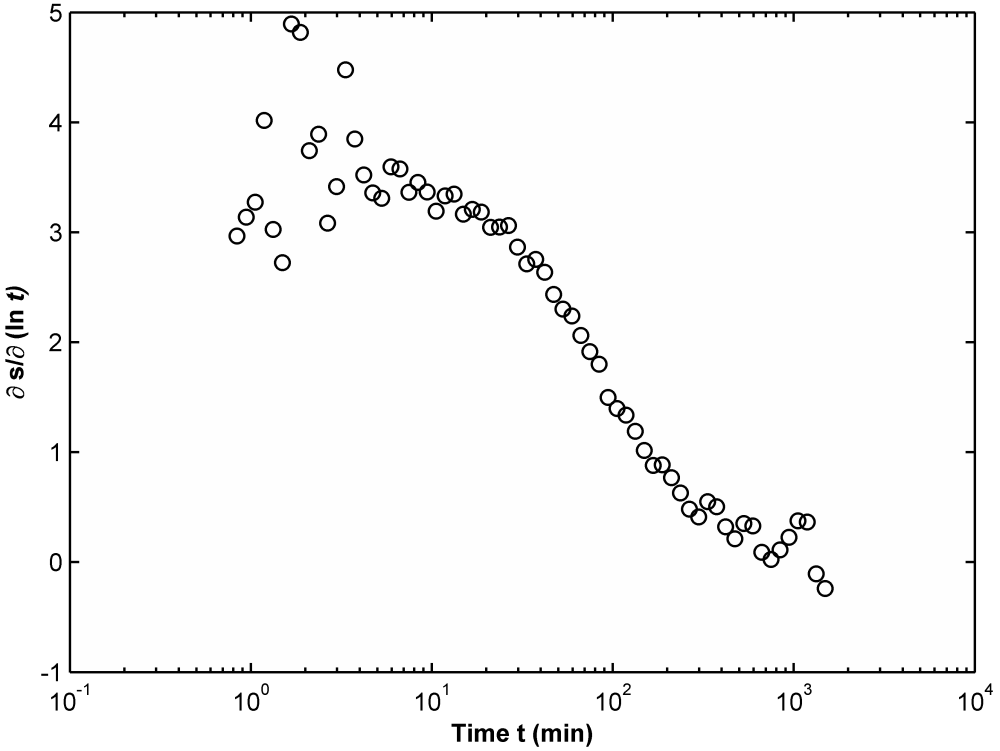

(b)

Figure 6.10. Test Analysis of MW02 (a) IAM Based Diagnostic Plot (b) Derivative Based Diagnostic Plot.

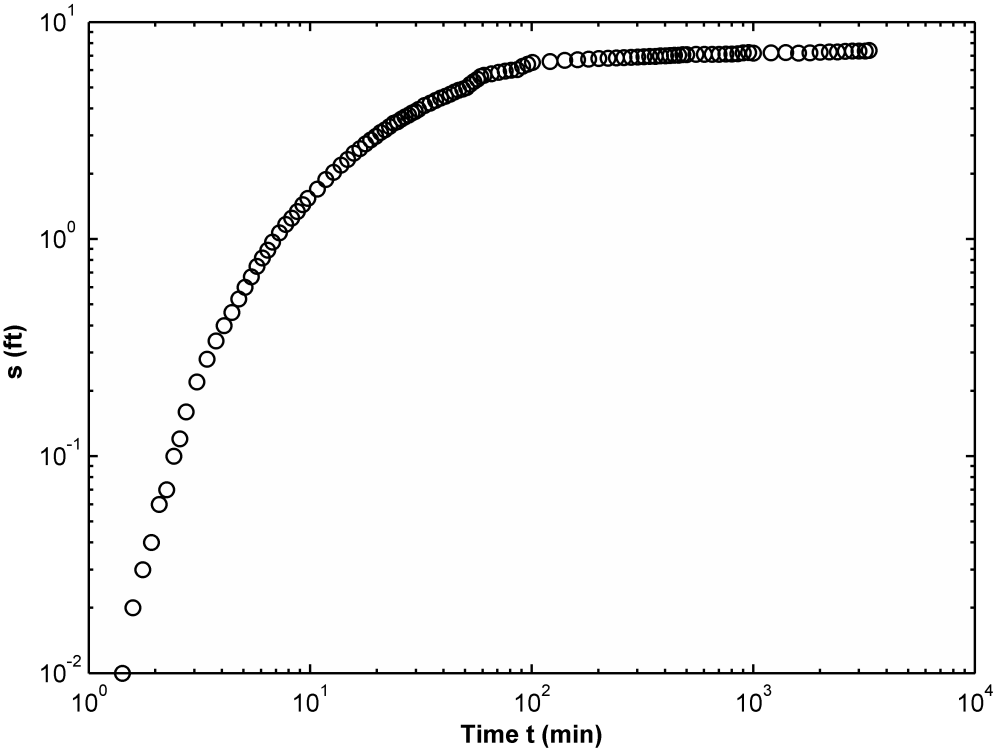

(a)

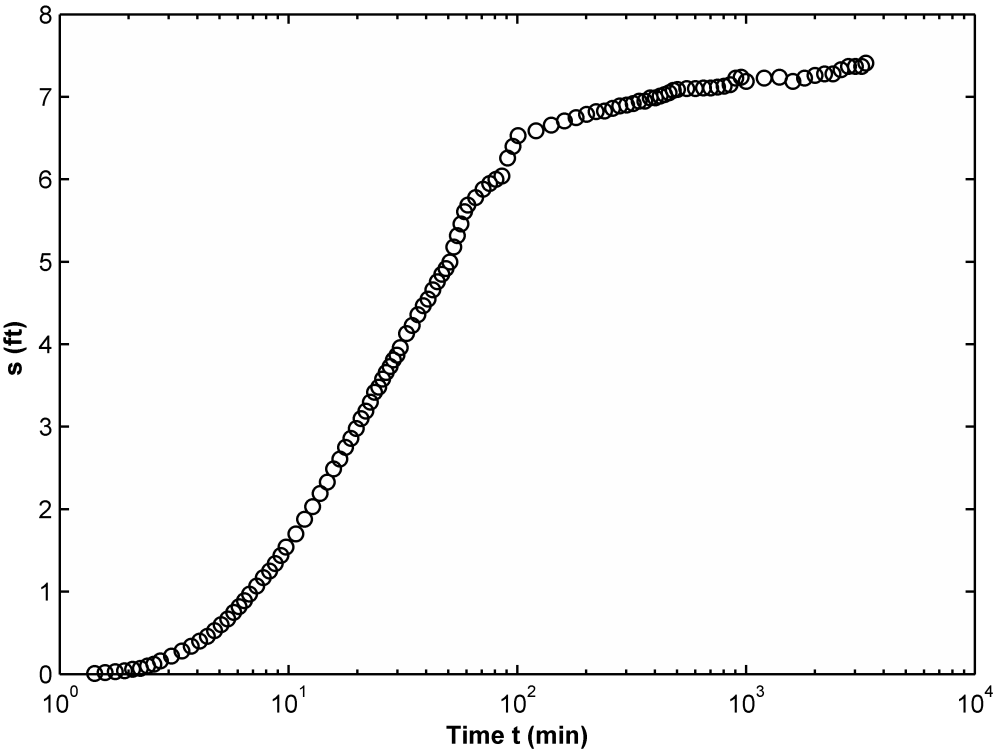

(b)

Figure 6.11. Drawdown Data at MW03 (a) Log-Log Scale (b) Semi-Log Scale (Drawdown data are obtained from Pratt, 1993).

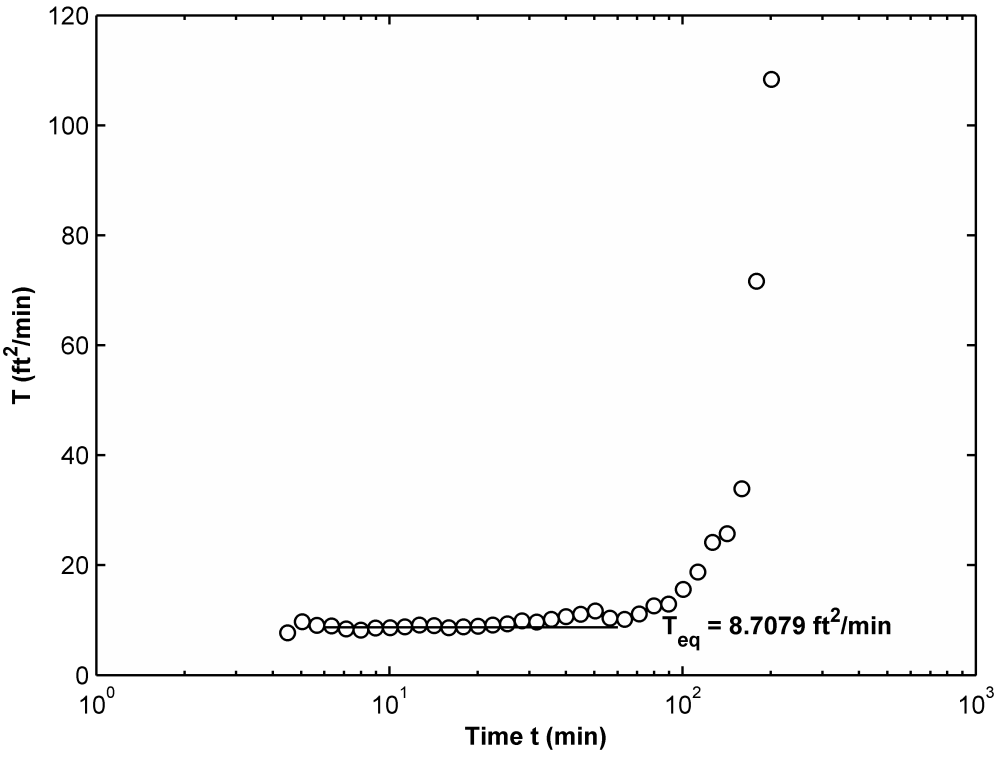

(a)

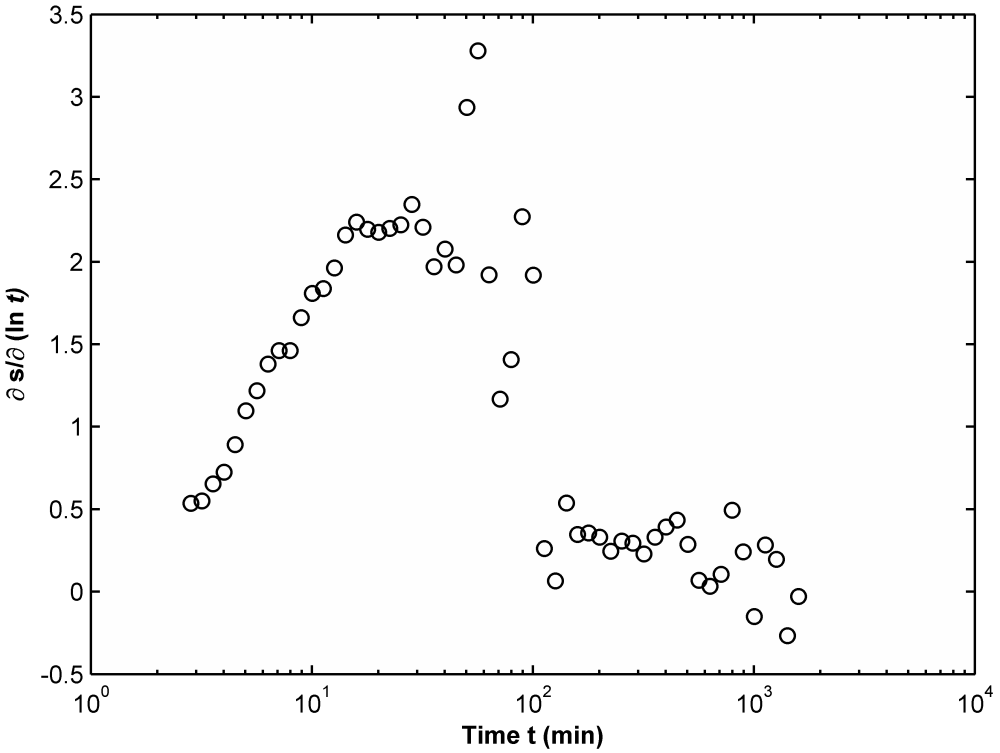

(b)

Figure 6.12. Test Analysis of MW03 (a) IAM Based Diagnostic Plot (b) Derivative Based Diagnostic Plot.

The IAM analysis of available pumping test data for each monitoring well provides the following information:

- All IAM based transmissivity values from the monitoring wells show an increasing trend following the initial steady value of the transmissivity in line with the previously identified diagnostic plot for leaky aquifers (Figure 6.2d). The sharply increasing apparent transmissivity values are indicative of the leakage occurrence and stabilization of the drawdown values.
- MW01 and MW03 show almost constant transmissivity value of 7.7 ft^2/min (11000 ft^2/day) and 8.7 ft^2/min (12500 ft^2/day), respectively prior to the leakage effects increasing the value of the transmissivity; these values are in line with the Hantush (1956) evaluation of the pumping test data. A constant time line, in which the transmissivity remains constant, is not evident for the IAM based diagnostic plot for MW02.

Again, the logarithmic time derivative curves of drawdown data for each monitoring well show the larger deviations from the ideal leaky aquifer diagnostic curve due to the imperfections of test data obtained from pumping tests. As stated earlier, the advantage of using IAM is clearly observed that IAM smoothes the potential imperfections of data which may be as a result of heterogeneity of the aquifer, misreading test data, or inherent complexity of pumping procedure by integrating drawdown data within a discrete time frame rather than taking time derivative of drawdown data.

6.2.4. Unconfined Aquifer Test Analysis

In the report of de Fosset and Pratt (2003), a multi-well aquifer test was conducted at a site located in coastal Franklin County, Florida, USA. The test/production well was penetrated to a depth of 30 ft below land surface with a screen extending from depths of 5 ft to 30 ft to the bottom of an unconfined aquifer. Three observation wells, namely SP-1, SP-2 and SP-3, were placed at radial distances of 90 ft, 137 ft and 49 ft from the extraction well, respectively. The drawdown test was conducted for a 72 hour duration with a constant discharge rate of 25 gpm. The Neuman (1972) analytical

solution was used by the investigators to analyze the test data for wells as shown in Table 6.2.

The transient pumping response of each monitoring well was plotted on Figure 6.13, Figure 6.15 and Figure 6.17, respectively. Although the hydrogeologic characterization of the aquifer system was taken to be an unconfined aquifer, only one of the monitoring wells showed typical features associated with delayed yield impact on the water level drawdown. SP-1 and SP-3 drawdown data in log-log scale did not show a significant decrease in the rate of drawdown level that would be present if a delayed yield effect was evident. Only SP-2 drawdown data showed evidence signaling the presence of a leakage source.

Table 6.2. Unconfined Aquifer Hydraulic Properties (de Fosset and Pratt, 2003).

Hydraulic Property	SP-1	SP-2	SP-3
r (ft)	90	137	49
b (ft)	25	25	25
r^2/b^2	13	30	3.8
T (ft^2/day)	1100	1200	1200
S	0.01	0.004	0.003
S_y	0.09	0.09	0.007
β	1.8	2.45	0.1
k_z/k_r	0.14	0.08	0.03

The IAM based diagnostic plots with $\Delta = 0.5$ for the three wells shown in Figure 6.14a, Figure 6.16a and Figure 6.18a, respectively, indicate the following features:

- All IAM based transmissivity values were stabilized toward the end of the pumping test period. This indicates that the aquifer is behaving as an ideal confined aquifer system toward the end of the pumping period which is to be expected once the delayed yield from the dewatered sections of the aquifer loses its influ-

ence. The stabilized transmissivity values are in line with the Neuman (1972) based transmissivity estimates obtained from the investigators. The transmissivity predictions for SP-1, SP-2 and SP-3 are 0.8 ft^2/min (1150 ft^2/day), 1.09 ft^2/min (1570 ft^2/day), and 0.69 ft^2/min (994 ft^2/day), respectively.

- The IAM diagnostic plot of SP-3 is the only diagnostic plot that shows similarities to the ideal diagnostic plot for unconfined aquifers shown in Figure 6.2e. A stabilized transmissivity value in the initial part of the drawdown data followed by an increase and subsequent decrease showing the start and end of the delayed yield impacts followed by a stabilization of the transmissivity values. The diagnostic plots of SP-1 and SP-2 do not exhibit the variation of the transmissivity associated with the delayed yield; however the drawdown data also do not have the necessary variations to exhibit the variation of the transmissivity values. The IAM diagnostic plots would, therefore, help in the aquifer system characterization with only the data from SP-3.

Drawdown derivative approach verifies the results of IAM analysis that the analyzed aquifer can be identified as an unconfined aquifer based on drawdown data at themonitoring well SP-3, hence derivative curve of SP-3 given in Figure 6.18b has a similar pattern of diagnostic plot shown in Figure 6.1b.

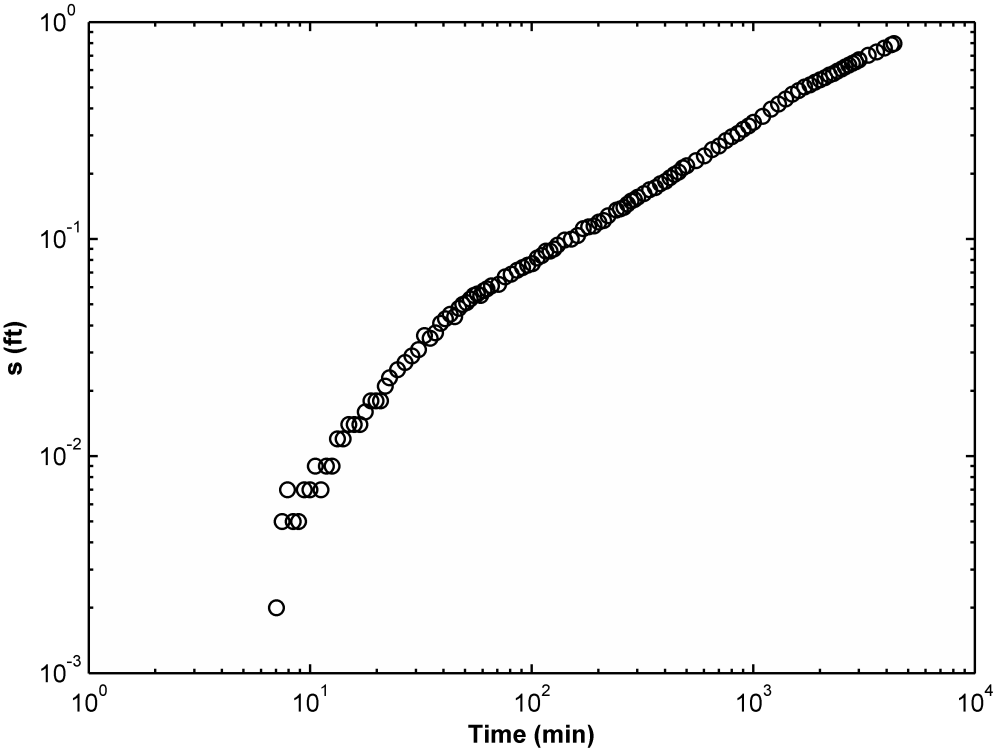

(a)

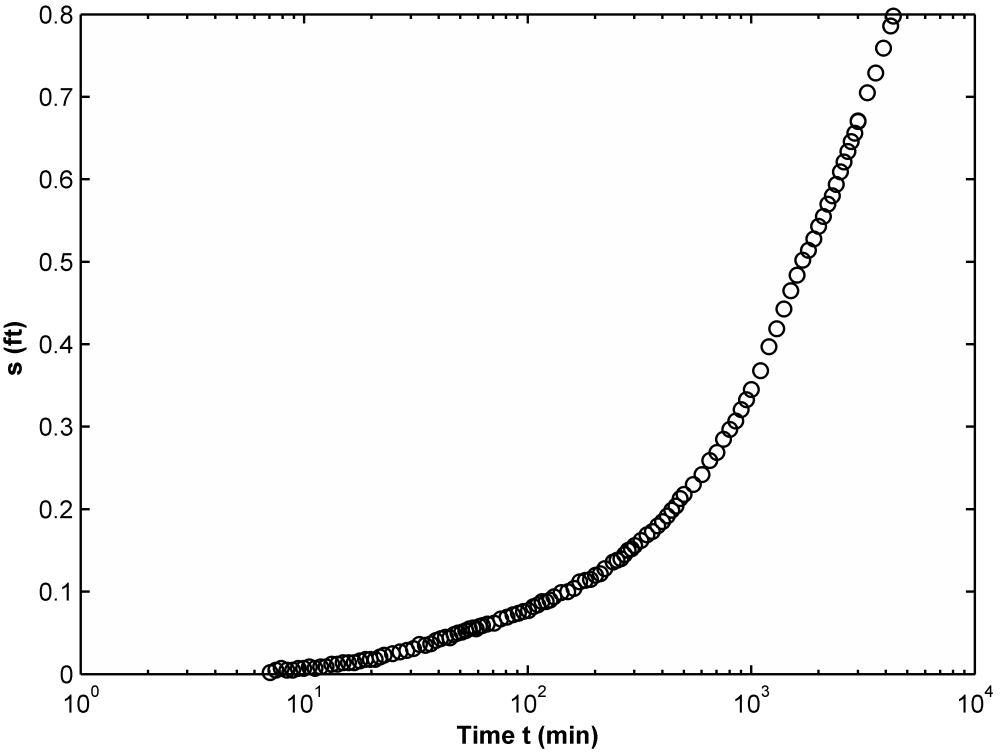

(b)

Figure 6.13. Drawdown Data for SP-1 (a) Log-Log Scale (b) Semi-Log Scale (Drawdown data are obtained from de Fosset and Pratt, 2003).

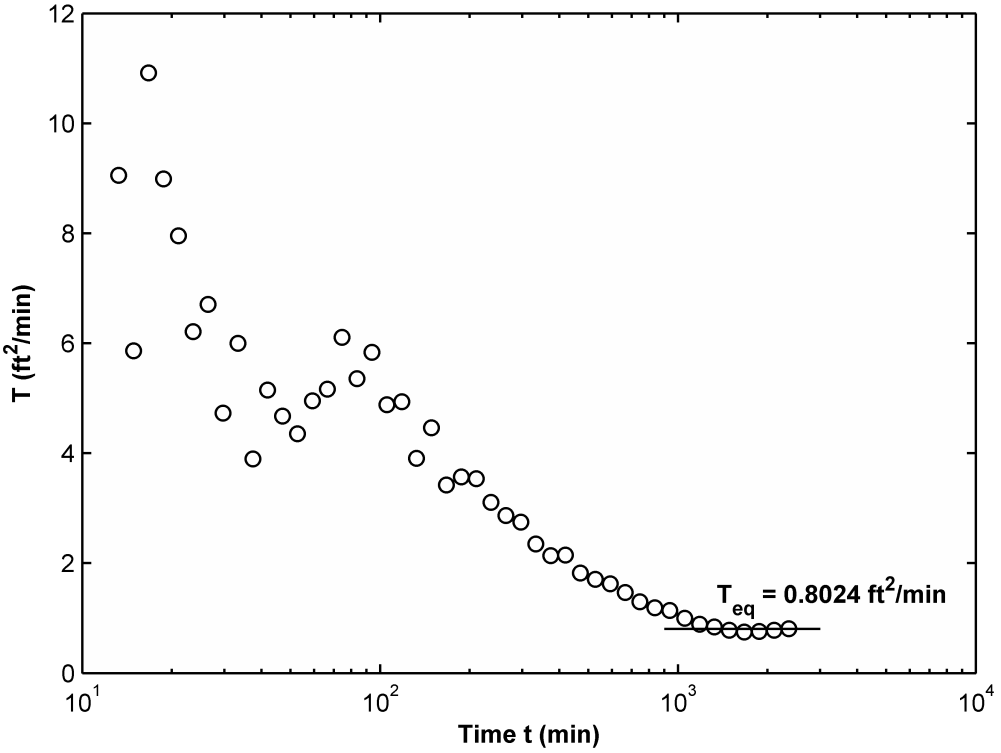

(a)

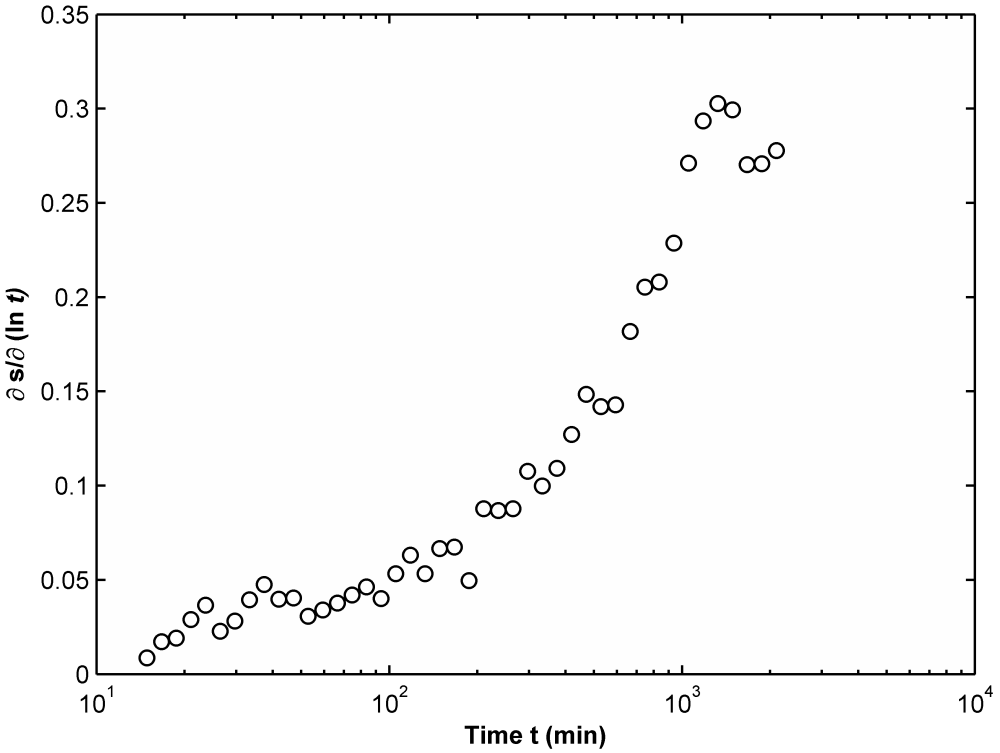

(b)

Figure 6.14. Test Analysis of SP-1 (a) IAM Based Diagnostic Plot (b) Derivative Based Diagnostic Plot.

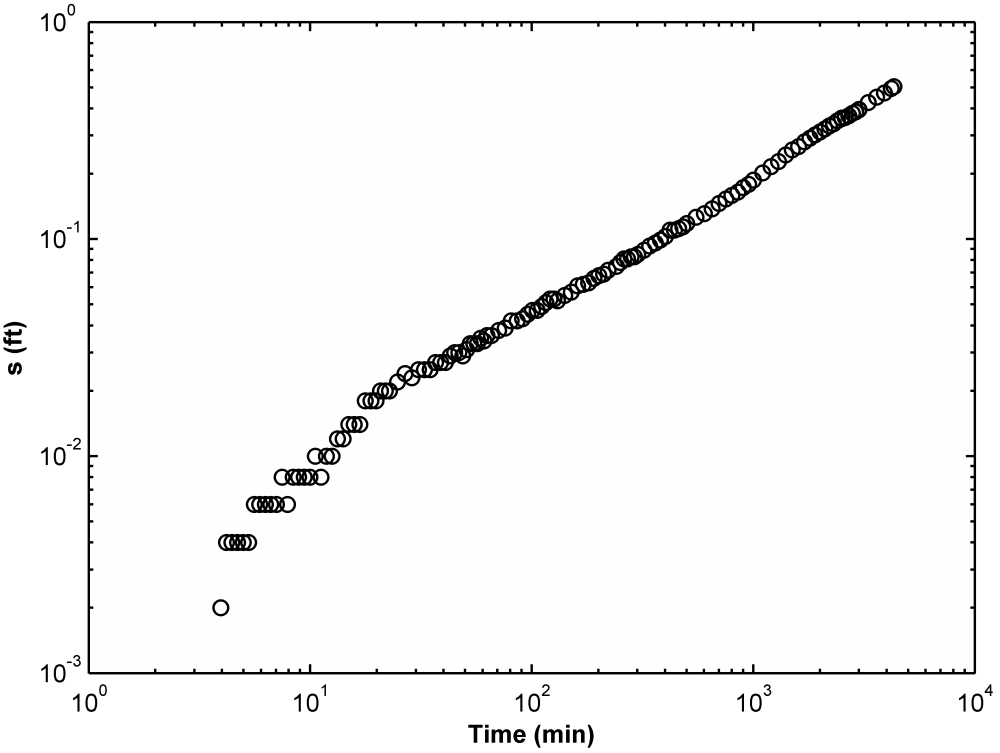

(a)

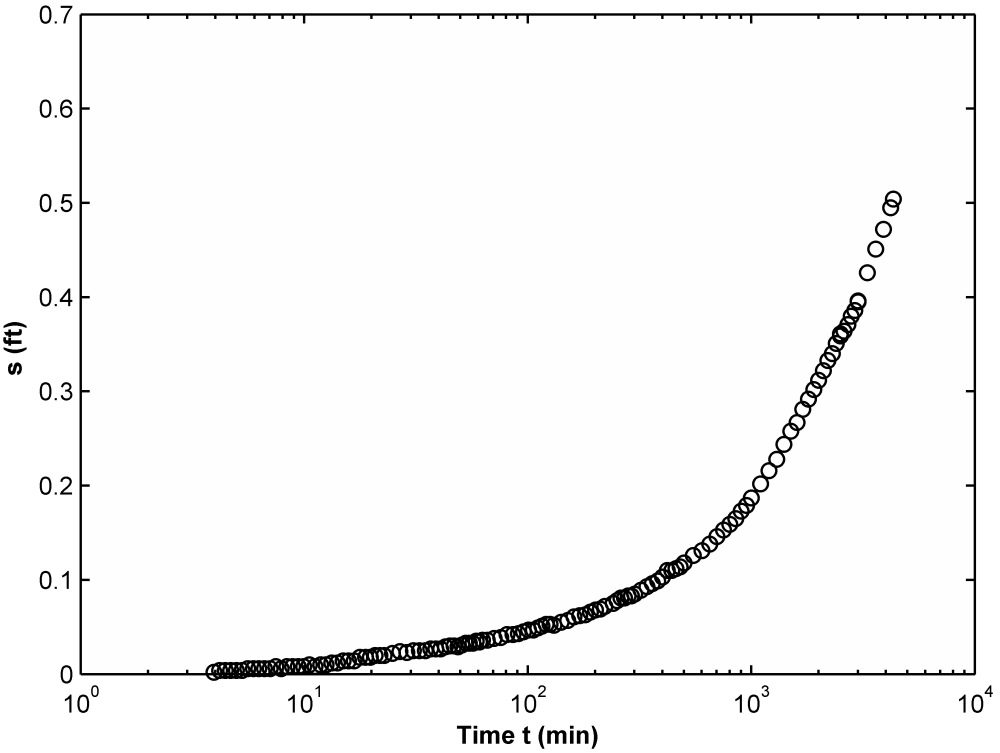

(b)

Figure 6.15. Drawdown Data for SP-2 (a) Log-Log Scale (b) Semi-Log Scale (Drawdown data are obtained from de Fosset and Pratt, 2003).

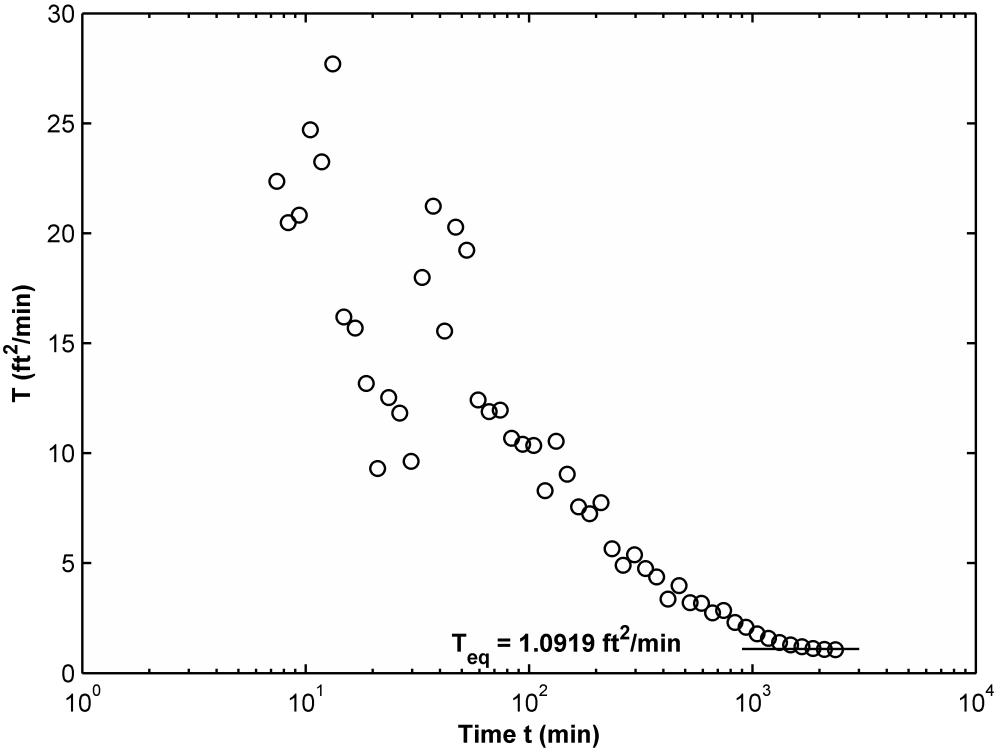

(a)

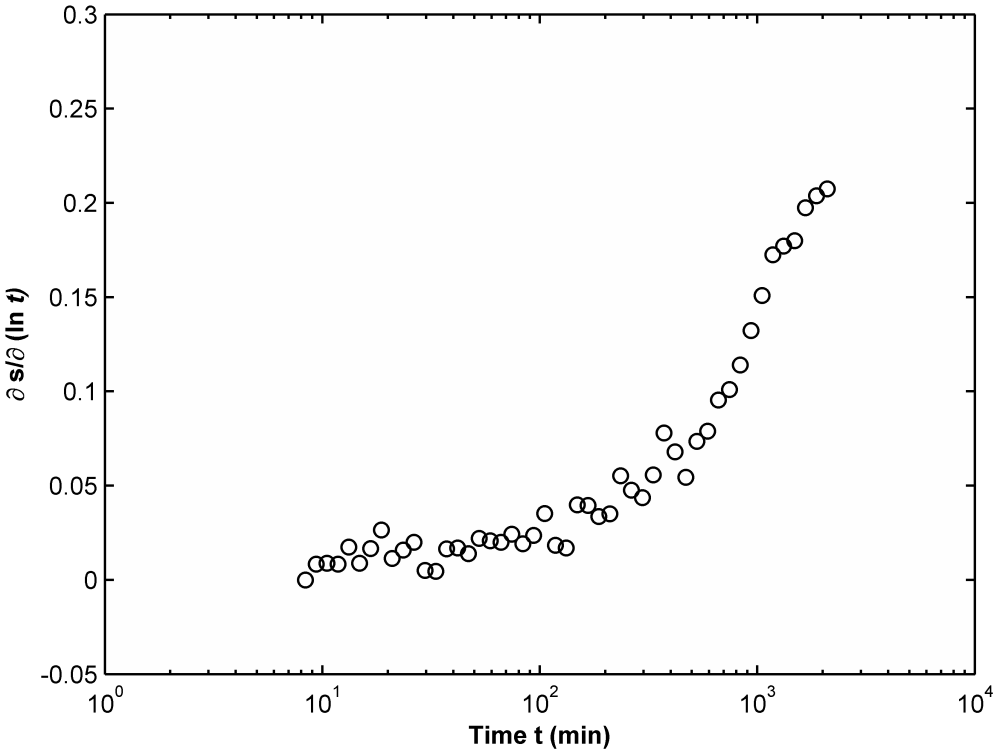

(b)

Figure 6.16. Test Analysis of SP-2 (a) IAM Based Diagnostic Plot (b) Derivative Based Diagnostic Plot.

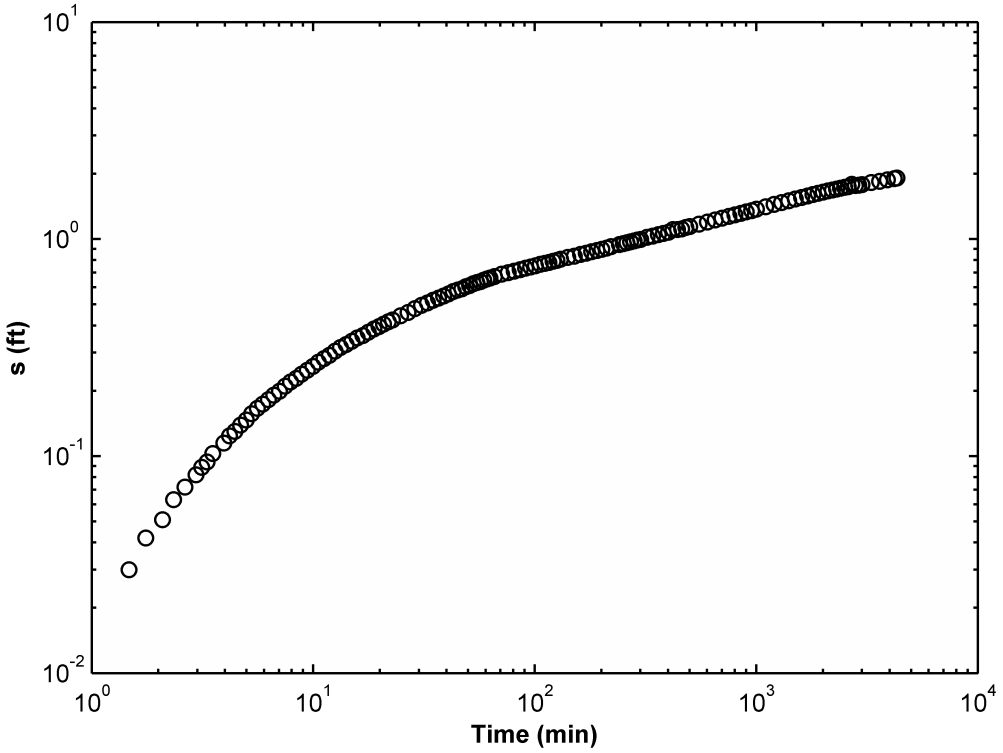

(a)

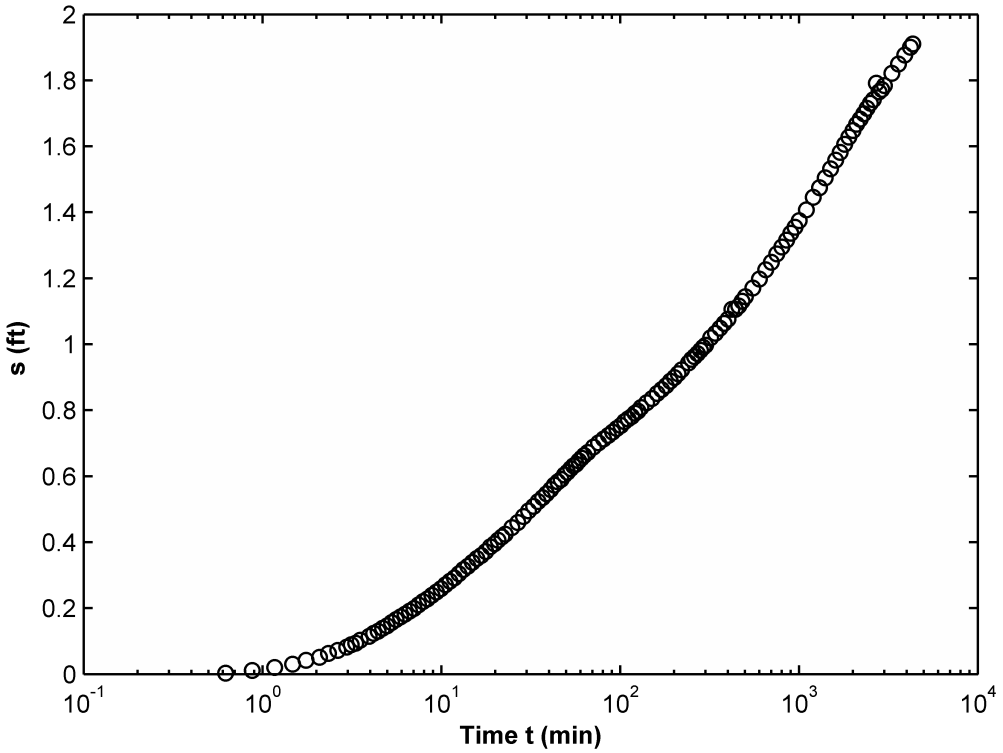

(b)

Figure 6.17. Drawdown Data for SP-3 (a) Log-Log Scale (b) Semi-Log Scale (Drawdown data are obtained from de Fosset and Pratt, 2003).

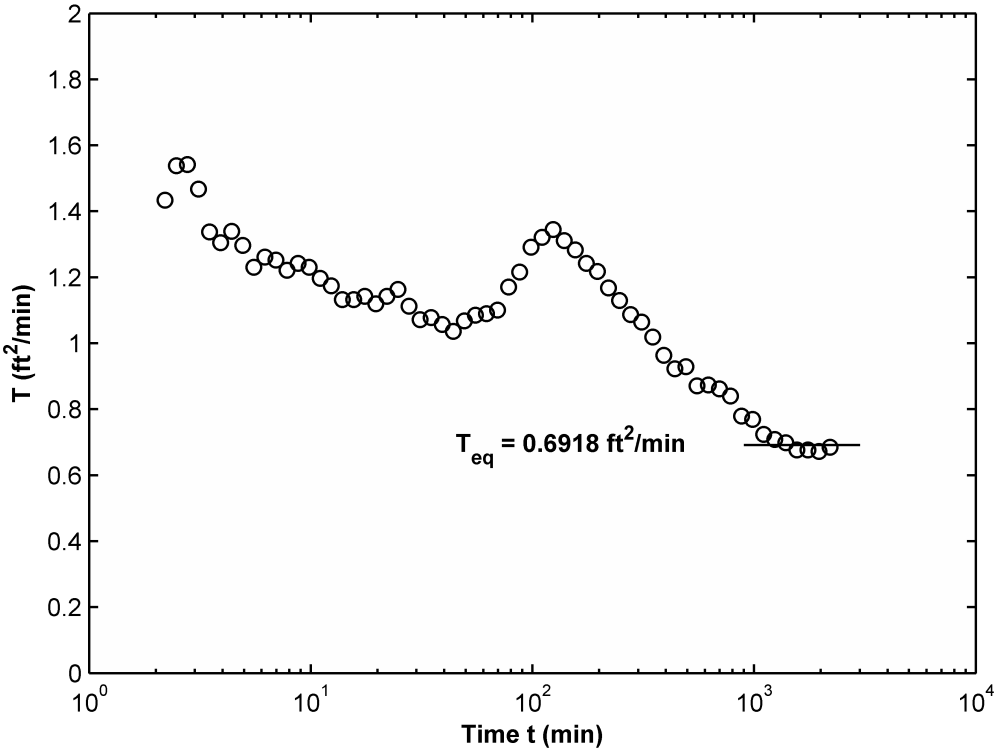

(a)

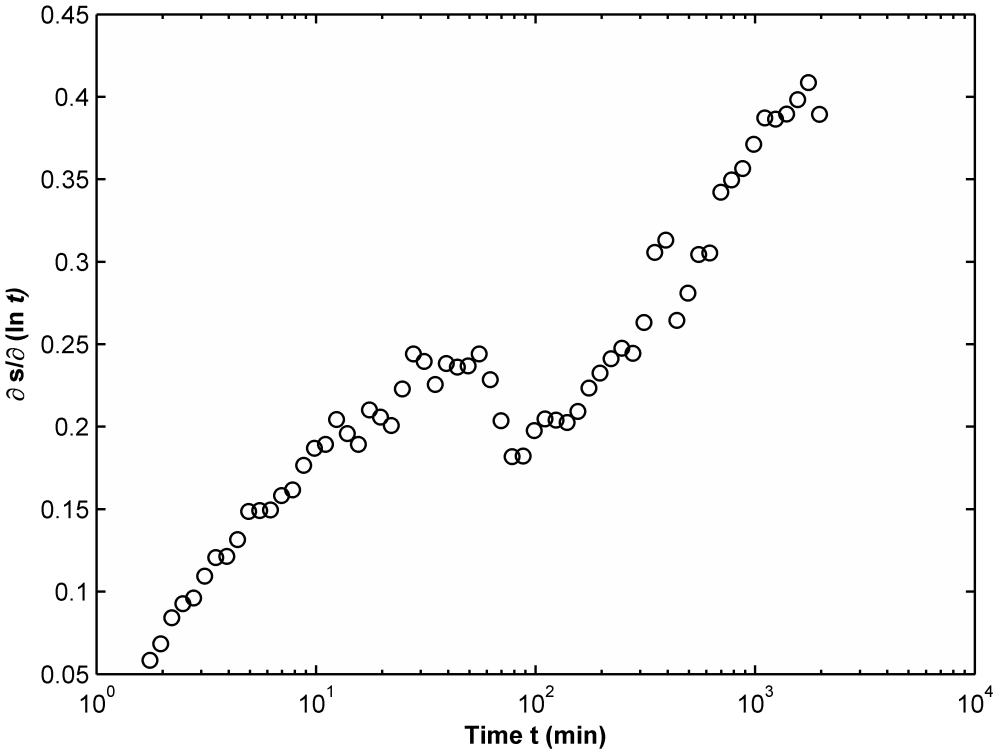

(b)

Figure 6.18. Test Analysis of SP-3 (a) IAM Based Diagnostic Plot (b) Derivative Based Diagnostic Plot.

7. ASSESSING RADIAL TRANSMISSIVITY VARIATION IN HETEROGENEOUS AQUIFERS BY ISA

Time variation of transmissivity can safely be obtained using IAM, however, the suggested IAM can not provide information about the spatial variation of transmissivity fields. Sen (1986) proposed a slope matching procedure (SMP) to elaborate the time dependent transmissivity variation as well as the parameter estimation scheme based on the drawdown derivative approach as follow:

$$\alpha = -\frac{e^{-u}}{W(u)} \tag{7.1}$$

where α is the slope of the type curve at any point. Calculating the slope between successive two points in drawdown data on log-log scale excluding first drawdown data, this method enables to find the corresponding u values, and therefore to estimate the variation of aquifer parameters with time (Sen, 1986). Copty *et al.* (2011) suggested a new technique similar to the SMP again based on the ratio of drawdown to the logarithmic derivative of drawdown as follow

$$\gamma = \frac{2.3s}{\Delta s'} = W(u)\, e^{u} \tag{7.2}$$

where γ is the dimensionless ratio and $\Delta s'$ is drawdown derivative with respect to logarithm (base 10) of time. For any particular value of γ, the value of well function can be uniquely find and aquifer parameters are then estimated (Copty *et al.*, 2011). However, these techniques have inherent shortcomings if the drawdown data reflect large variation as stated earlier. On the other hand, none of these methods does not show the spatial dependency of transmissivity variation. Bear (1979) showed the propagation of cone of depression with time to approximate the spatial variation of transmissivity based on the Cooper-Jacob (1946) approximation as

$$r = 1.5\sqrt{\frac{Tt}{S}} \tag{7.3}$$

More recently, Copty *et al.* (2011) investigated the radial transmissivity variation for different heterogeneity sets utilizing the monitoring well data very near to pumping well and compared the transmissivity values to the geometric mean of influence radius given as

$$r = 1.577\sqrt{\frac{Tt}{S}} \tag{7.4}$$

Inverse solution algorithm (ISA) developed by Feitosa *et al.* (1994) has an ability to reflect the spatial variability of aquifer heterogeneity. The effectiveness of the proposed analytical inversion technique explained in Chapter 4 was assessed against analytical and numerical based benchmark cases. The analytical benchmarks were developed for aquifer settings where the transmissivity was a radially symmetric non-uniform field. The numerical benchmarks were obtained using MODFLOW (Harbaugh *et al.*, 2000) for the aquifers which have heterogeneous transmissivity fields with log-normal Gaussian distribution.

7.1. Analytical Benchmarks

The governing ground water flow equation for N concentric circles around a fully penetrating pumping each having a constant hydraulic property well can be formulated as

$$\frac{\partial^2 s_i}{\partial r^2} + \frac{1}{r}\frac{\partial s_i}{\partial r} = \frac{S_i}{T_i}\frac{\partial s_i}{\partial t} \qquad i = 1, 2, ..., N \tag{7.5}$$

where s_i represents the drawdown in ring i, S_i denotes the storage coefficient of ring i and T_i is the transmissivity of ring i. The boundary and initial conditions are given as follows:

$$\begin{aligned} \lim_{r_w \to 0} 2\pi r_w T_1 \frac{\partial s_1}{\partial r} &= -Q \\ s_N(\infty, t) &= 0 \\ s_i(r, 0) &= 0 \end{aligned} \tag{7.6}$$

where r_w is the radius of pumping well. In order to satisfy the continuity of flow between the rings, interference boundary conditions in successive rings should meet the compatibility equations given as follows

$$\begin{aligned} s_i\left(r_i,t\right) &= s_{i+1}\left(r_i,t\right) \\ T_i\frac{\partial s_i\left(r_i,t\right)}{\partial r} &= T_{i+1}\frac{\partial s_{i+1}\left(r_i,t\right)}{\partial r} \qquad\qquad i=1,2,...,N-1 \end{aligned} \tag{7.7}$$

The above formulation represents the groundwater flow equation for a confined aquifer with a radially symmetric non-uniform transmissivity field. Utilizing the Laplace transform, the general solution of the system in the Laplace domain is as follows:

$$\bar{s}_i\left(p,r\right) = c_{2i-1}K_0\left(\phi_i r\right) + c_{2i}I_0\left(\phi_i r\right) \tag{7.8}$$

where I_0 and K_0 are the zero order modified Bessel functions of first and second kind, respectively, c is the constant coefficient, $\phi_i = \sqrt{S_i p/T_i}$, and p is the Laplace transform variable.

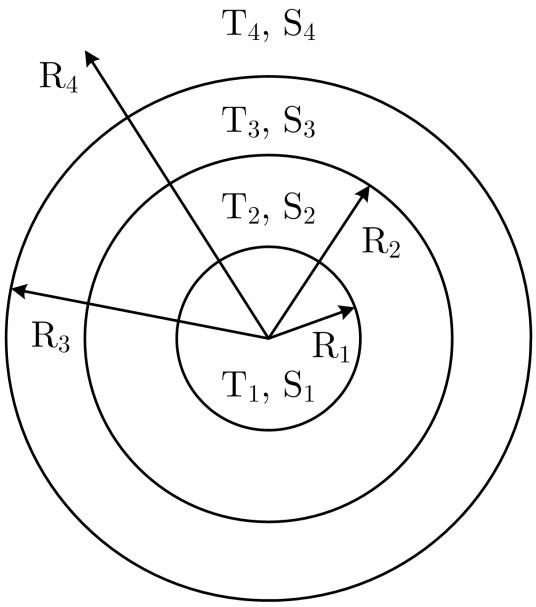

Figure 7.1. Schematic View of Radially Symmetric Non-uniform Aquifer Setting.

Butler (1988) derived the analytical formula solution for two concentric circles; the analytic benchmark case was extended to three and four ring systems in this re-

search. The settings are shown in Figure 7.1.

Butler (1988) solution in the Laplace domain for both governing equations and boundary and initial conditions are given in Equation 7.5 and Equation 7.6, respectively; the drawdown at a monitoring well located in a distance of r is then given in Laplace transform domain p as follows:

$$\bar{s}_1(p,r) = \frac{Q}{2\pi T_1}\left(\frac{K_0(\phi_1 r)}{p} + \frac{\left(K_1(\phi_1 R)K_0(\phi_2 R) - \frac{T_2}{T_1}\frac{\phi_2}{\phi_1}K_0(\phi_1 R)K_1(\phi_2 R)\right)I_0(\phi_1 r)}{p\left(\frac{T_2}{T_1}\frac{\phi_2}{\phi_1}I_0(\phi_1 R)K_1(\phi_2 R) + I_1(\phi_1 R)K_0(\phi_2 R)\right)}\right) \tag{7.9}$$

$$\bar{s}_2(p,r) = \frac{Q}{2\pi T_1}\left[\frac{K_0(\phi_1 R)I_1(\phi_1 R) + K_1(\phi_1 R)I_0(\phi_1 R)}{p\left(\frac{T_2}{T_1}\frac{\phi_2}{\phi_1}I_0(\phi_1 R)K_1(\phi_2 R) + I_1(\phi_1 R)K_0(\phi_2 R)\right)}\right]K_0(\phi_2 r) \tag{7.10}$$

where I_i and K_i are the modified Bessel functions of first and second kind of order i ($i = 0, 1$), respectively. The solution for three and four concentric rings (N =3 and N =4) were derived for the Laplace Domain drawdown formulation in order to extend Butler (1988)'s solution and to provide a more extensive benchmark setting.

Using Equation 7.7 and Equation 7.8, drawdown response in Laplace domain of a hypothetical aquifer system for $N = 4$ can be calculated analytically. Considering Equation 7.8, 8 unknown coefficients should be found. However, from the well and far end boundary conditions, the first coefficient c_1 and last coefficient c_8 are known as $Q/2\pi T_1 p$ and 0, respectively. Therefore, size of the system matrix reduces to 6 by 6 matrix. As a general statement, extracting first and final coefficients, $2 \times (N-1)$ square matrix can be written for N rings system. For $N = 4$ rings system, matrix equation can be shown as

$$\varsigma x = \eta \tag{7.11}$$

where x is unknown coefficient matrix including c_2 to c_7. ς and η are shown in Equation 7.12 and Equation 7.17, respectively.

$$\varsigma = \begin{bmatrix} I_0(\phi_1 R_1) & -K_0(\phi_2 R_1) & -I_0(\phi_2 R_1) & 0 & 0 & 0 \\ T_1\phi_1 I_1(\phi_1 R_1) & T_2\phi_2 K_1(\phi_2 R_1) & -T_2\phi_2 I_1(\phi_2 R_1) & 0 & 0 & 0 \\ 0 & K_0(\phi_2 R_2) & I_0(\phi_2 R_2) & -K_0(\phi_3 R_2) & -I_0(\phi_3 R_2) & 0 \\ 0 & -T_2\phi_2 K_1(\phi_2 R_2) & T_2\phi_2 I_1(\phi_2 R_2) & T_3\phi_3 K_1(\phi_3 R_2) & -T_3\phi_3 I_1(\phi_3 R_2) & 0 \\ 0 & 0 & 0 & K_0(\phi_3 R_3) & I_0(\phi_3 R_3) & -K_0(\phi_4 R_3) \\ 0 & 0 & 0 & -T_3\phi_3 K_1(\phi_3 R_3) & T_3\phi_3 I_1(\phi_3 R_3) & T_4\phi_4 I_1(\phi_4 R_3) \end{bmatrix} \tag{7.12}$$

$$\eta = \begin{bmatrix} -\frac{Q}{2\pi p T_1} K_0(\phi_1 R_1) \\ \frac{Q}{2\pi p}\phi_1 K_1(\phi_1 R_1) \\ 0 \\ 0 \\ 0 \\ 0 \end{bmatrix} \tag{7.13}$$

Using Matlab, Equation 7.11 can easily be solved, the full analytic expression of the Laplace domain solution was however found to be too cumbersome to explicitly write in this study and has therefore been omitted. The Stehfest (1970) algorithm is applied to convert the Laplace domain formulations to the time domain for the solutions obtained for $N = 3$ and 4 concentric circles.

The Stehfest (1970) algorithm is based on asymptotic expansion and extrapolation as following (Lee, 1999)

$$f[t] \approx \frac{\ln 2}{t} \sum_{n=1}^{M} K_n \bar{f}\left[\frac{n \ln 2}{t}\right] \tag{7.14}$$

where

$$K_n = (-1)^{n+M/2} \sum_{k=\left\lfloor \frac{n+1}{2} \right\rfloor}^{\min(n,M/2)} \frac{k^{M/2}(2k)!}{(M/2-k)!k!(k-1)!(n-k)!(2k-n)!} \tag{7.15}$$

with M being an even number and $\lfloor\rfloor$ being the integer part of $(n+1)/2$.

For the generation of drawdown response for N rings system, following items should be used:

- Write down the system equation as given in Equation 7.11 using Equation 7.7 and Equation 7.8.
- Solve Equation 7.11 to obtain the drawdown response of an aquifer in Laplace domain.
- Use Stehfest (1970) algorithm shown in Equation 7.14 to convert Laplace domain solution to the time domain solution numerically.

The benchmark problems used for this study, therefore, consist of an aquifer setting where concentric rings of transmissivity are present around the extraction well. Groundwater drawdown data were generated at various distances from the extraction well using the above formulations; these results were then used to estimate the concen-

tric ring transmissivity using ISA and compared with the actual transmissivity field within the concentric circles.

7.2. Numerical Benchmark Selection

The literature review shows that a large number of heterogeneous aquifer investigations were conducted using numerical simulations with a log-normal Gaussian randomly transmissivity fields. The random fields were generated with a mean transmissivity value together with a selected variance. The present numerical benchmarks were established using a similar field system to obtain simulation results for hypothetical heterogeneous confined aquifer models. Three hydraulic conductivity sets which included 100 fields for each setting were generated using the Turning Band Algorithm (TBM) (Mantoglou and Wilson, 1982). The sets were taken as small, medium and large heterogeneity character and then simulated with the MODFLOW (Harbaugh *et al.*, 2000) computer code. Drawdown data generated from the numerical simulations were used as input into the ISA and the radial characteristics of the transmissivity field were evaluated.

7.3. Transmissivty Field Predictions

The proposed ISA method was applied to analytical and numerical benchmark problems discussed in the previous section in order to assess the ability to predict the radial variation of the transmissivity field. In each case, the most suitable transmissivity field was obtained by comparing the actual drawdown curves computed from the benchmark conditions and the predicted cone of depression propagation based on the C coefficient in Equation 4.18.

7.3.1. Analytical Test Case 1: Butler Case ($N = 2$)

Considering the aquifer system for Butler (1988) case ($N = 2$), hypothetical drawdown values were generated in the Laplace domain. The inner ring boundary was located at $r = 10$ m from the extraction well. The outer ring extended to infinite. A

monitoring well was installed at a distance of 1 m away from the pumping well. A 3-day long pumping test was conducted at a discharge rate of 1 m^3/day. Storativity of the hypothetical aquifer was considered as a constant throughout the aquifer domain as 1×10^{-4}.

Figure 7.2 shows the drawdown generations at the monitoring well located 1 m away from pumping well for three different T_2 settings. Figure 7.3 shows the spatial variation of transmissivity field using the ISA. Figure 7.4 displays the predicted drawdown values using the estimated transmissivity field given in Figure 7.3 for various T_2/T_1 values. In this simulation, the coefficient $C = 1.5$ predicted the best drawdown match. As can be seen from Figure 7.4, there is a very good agreement between the generated and the predicted drawdown curves for a monitoring well located at $r = 1$ m.

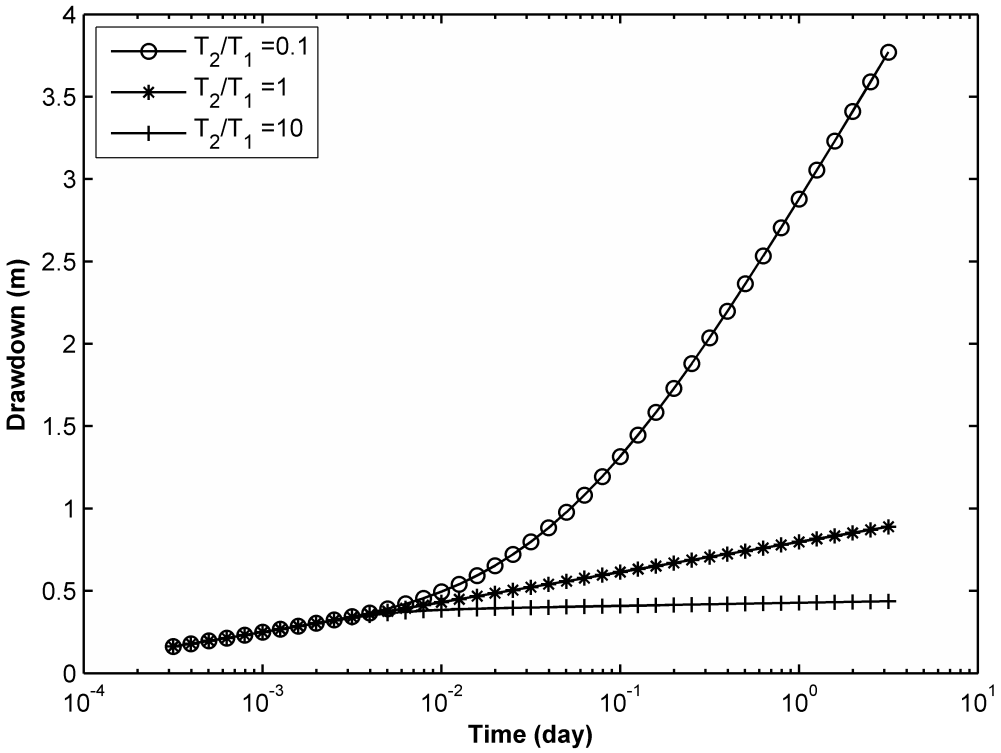

Figure 7.2. Generated Drawdown Values for $R/r = 10$, $S_2/S_1 = 1$.

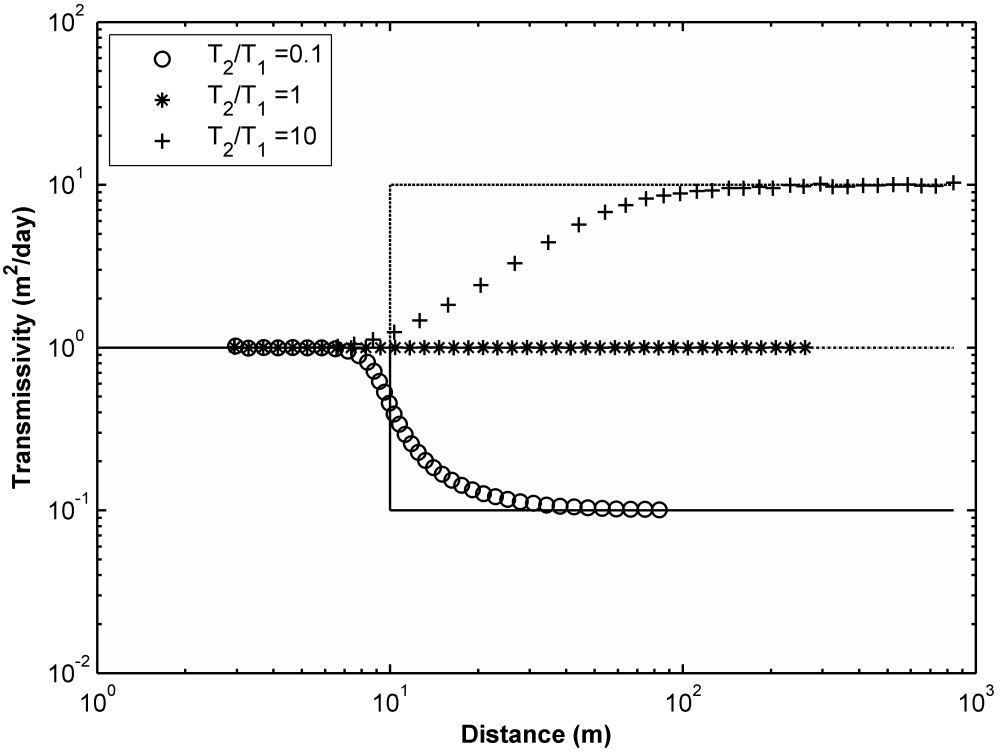

Figure 7.3. ISA Transmissivity Predictions for T_2/T_1 values (C = 1.5).

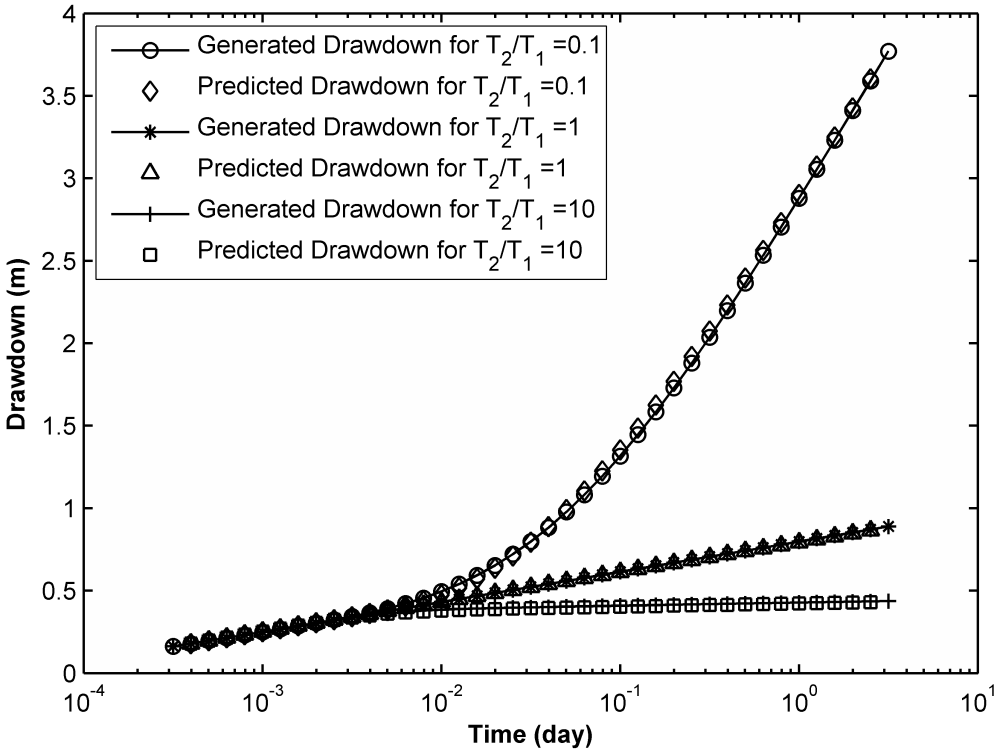

Figure 7.4. Predicted and Generated Drawdown Curves for Various T_2/T_1.

7.3.2. Analytical Test Case 2: Three Ring System ($N = 3$)

The problem considered in Test Case 1 was extended to the solution for a three ring system. A hypothetical aquifer having a 10 m thickness was stressed at a discharge rate of 1 m^3/day and drawdown data were simulated at a monitoring well located 1 m away pumping well for a 3-day pumping period. The storativity of each ring was assumed as a constant value (0.0001) throughout the aquifer domain. Transmissivity variation of the aquifer is given as:

$$\begin{aligned} T_1 &= 1 \ \mathrm{m^2/day}, \ r_w \leq r < R_1 = 10\,\mathrm{m} \\ T_2 &= 2 \ \mathrm{m^2/day}, \ R_1 \leq r < R_2 = 50\,\mathrm{m} \\ T_3 &= 0.5 \ \mathrm{m^2/day}, \ R_2 \leq r \end{aligned} \tag{7.16}$$

The analytical generation of the drawdown data and the aquifer transmissivity characterization using ISA are depicted in Figure 7.5 and Figure 7.6 respectively.

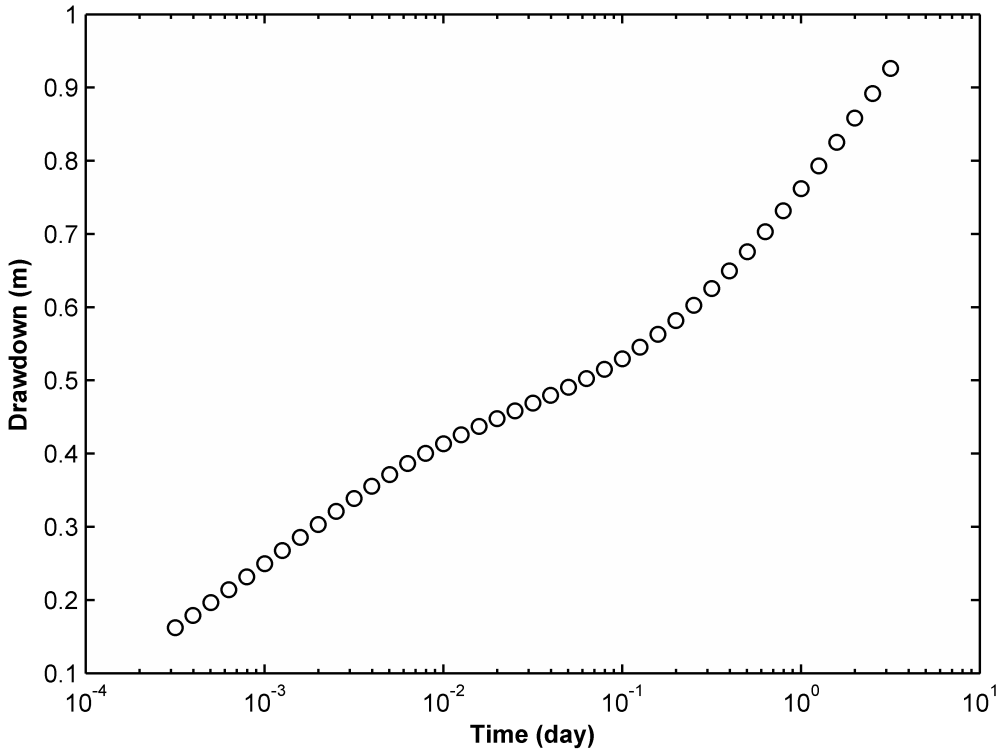

Figure 7.5. Drawdown - Time Curve for Monitoring Point Located at r =1 m.

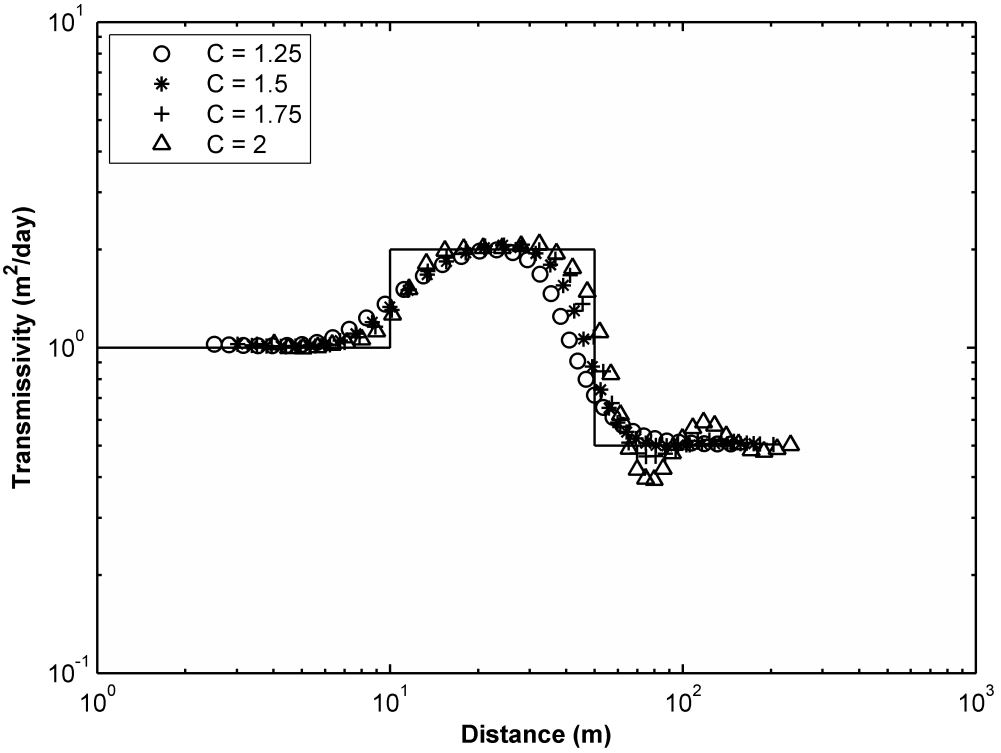

Figure 7.6. ISA Transmissivity Predictions for Three Ring System.

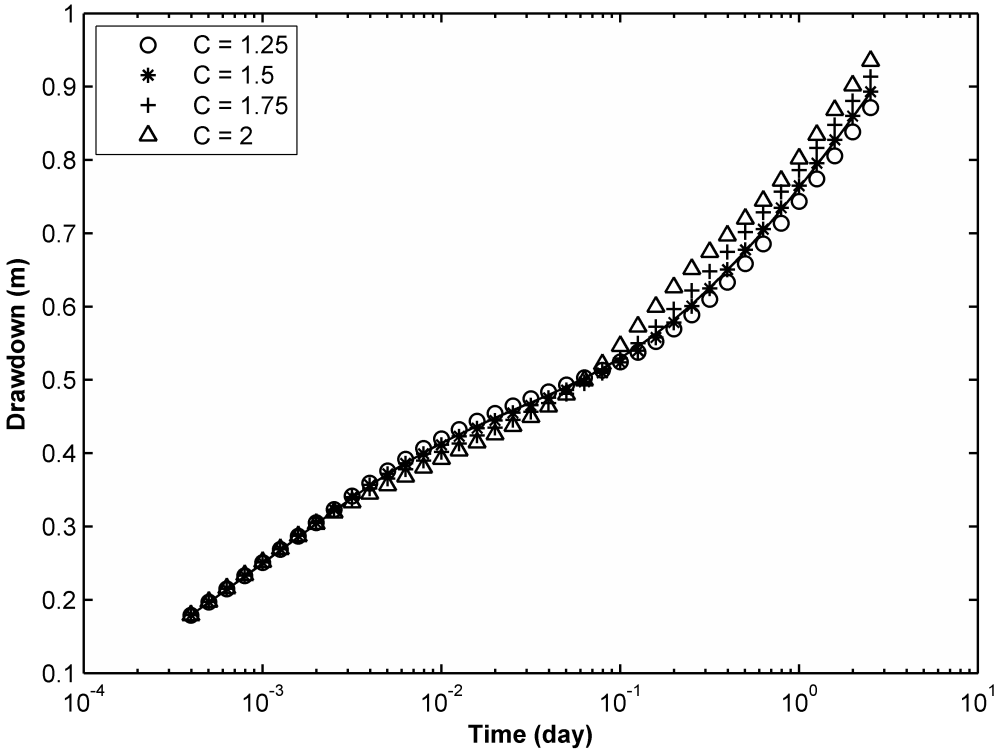

Figure 7.7. Drawdown Estimations for Various C Coefficient Values.

Equation 4.19 was applied to identify the most suitable C value to measure estimation performance. Mean absolute error (MAE), root mean squared error (RMSE) and coefficient of determination (R^2) values for each C are summarized in Table 7.1. Figure 7.7 illustrates the effect of C value on drawdown estimation.

Table 7.1. Statistical Comparison for C Coefficient Factor.

Statistical Criteria	1.25	1.50	1.75	2.00
MAE	0.0080	0.0024	0.0111	0.0219
R^2	0.9992	0.9998	0.9976	0.9929

7.3.3. Analytical Test Case 3: Four Ring System ($N = 4$)

Transient response of a hypothetical confined aquifer with a thickness of 10 m was simulated using an extraction rate of 1 m^3/day. The aquifer model was selected to have the following transmissivity distribution:

$$\begin{aligned} T_1 &= 1 \ \text{m}^2/\text{day}, \ r_w \leq r < R_1 = 10\,\text{m} \\ T_2 &= 2 \ \text{m}^2/\text{day}, \ R_1 \leq r < R_2 = 50\,\text{m} \\ T_3 &= 0.5 \ \text{m}^2/\text{day}, \ R_2 \leq r < R_3 = 100\,\text{m} \\ T_4 &= 5 \ \text{m}^2/\text{day}, \ r_3 \leq r \end{aligned} \tag{7.17}$$

Four monitoring wells were placed at radial distances of 5, 25, 75 and 125 m away pumping well, respectively. Drawdown curves of each monitoring well generated with the analytical formulations are depicted in Figure 7.8.

The radial transmissivity variation using the drawdown data at four different monitoring locations is illustrated in Figure 7.9. Butler (1988) indicated that drawdowns in an aquifer system being stressed is a result of the properties of material surrounding the monitoring well and within the influence zone.

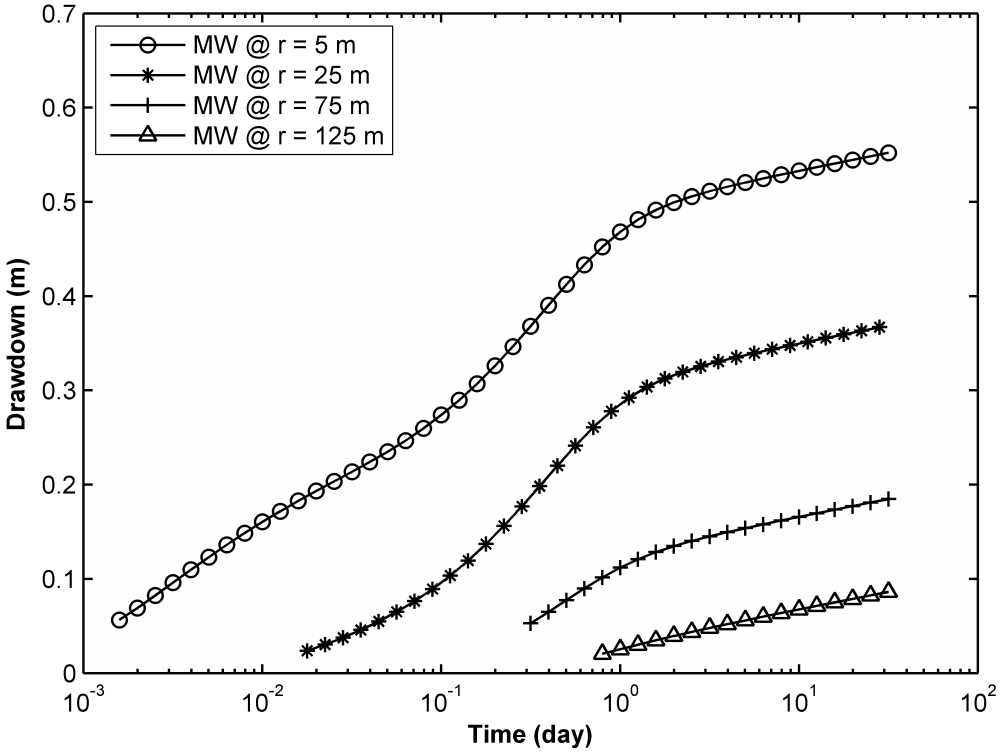

Figure 7.8. Drawdown Curves for Monitoring Points at $r = 5$, 25, 75, and 125 m.

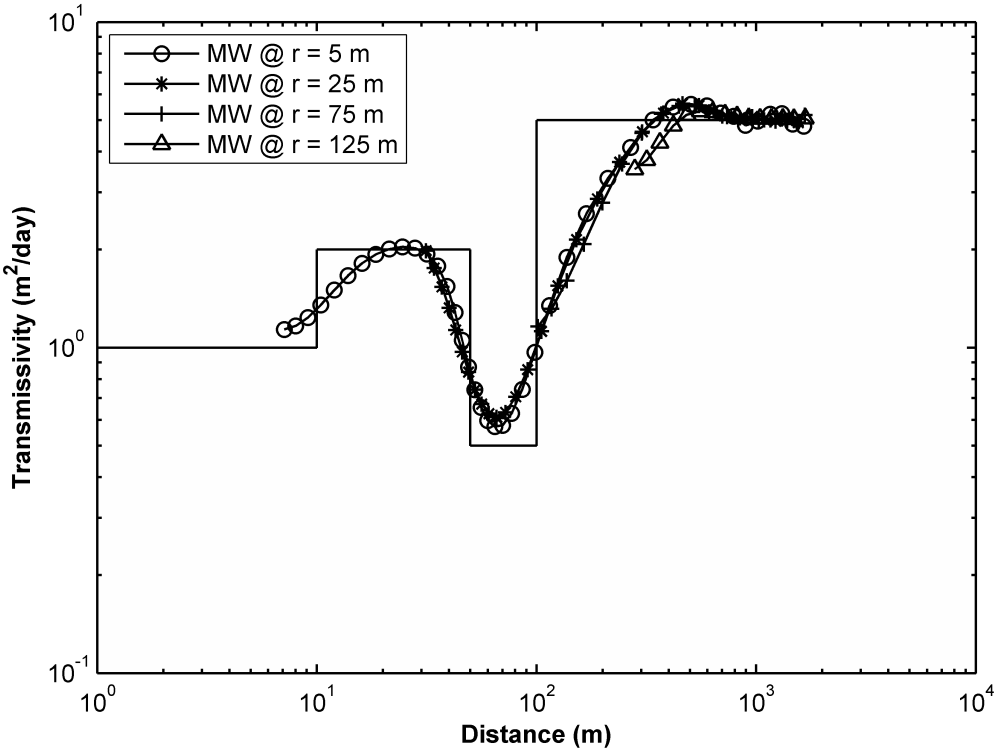

Figure 7.9. ISA Solution $C = 1.5$.

As stated earlier, previous works (Streltsova, 1988; Meier *et al.*, 1998; and Sanchez-Vila *et al.*, 1999) indicated that the estimated transmissivity values varied from an approximate geometric mean of the transmissivity values at early times near to the well location to the effective transmissivity of the heterogeneous system at later stages of pumping period. These works indicated that Cooper and Jacob (1946) solution can be utilized to estimate the effective transmissivity value of heterogeneous media for late time of pumping period to eliminate the uncertainty and nonlinearity effects appeared in early stage of pumping.

The ISA method based transmissivity estimates for all three benchmark assessments show that the groundwater level behavior is indeed influenced by the aquifer characteristics within the cone of depression which expands with time in the aquifer domain. The ISA based predictions show, however, that the Cooper-Jacob (1946) procedure at late times cannot provide an estimation of the overall material within the cone of depression. The slope of the drawdown curves does not represent the transmissivity field within the cone of depression but rather the section under the influence of the weighing function described in the ISA procedure. This is best illustrated in Figure 7.10 where the variation in the distance drawdown and the weighting function location are depicted at two different times.

Figure 7.10 points out that the cone of depression is passing through four different transmissivity zones; the weighting function indicates the weights contributing to the estimation mean. Figure 7.10 also shows that the greatest contributions come from Zone IV while weights of Zone I can be ignored and that it can be concluded that curve matching procedures such as the Cooper-Jacob (1946) method do not estimate the mean transmissivity inside the cone of depression but rather the part toward the end of the cone of depression. The ISA methodology also shows that the transmissivity field predictions are similar for all monitoring well data used independent of the distance from the extraction well. Each well data provides information for the cone of depression ahead of the location of the monitoring well.

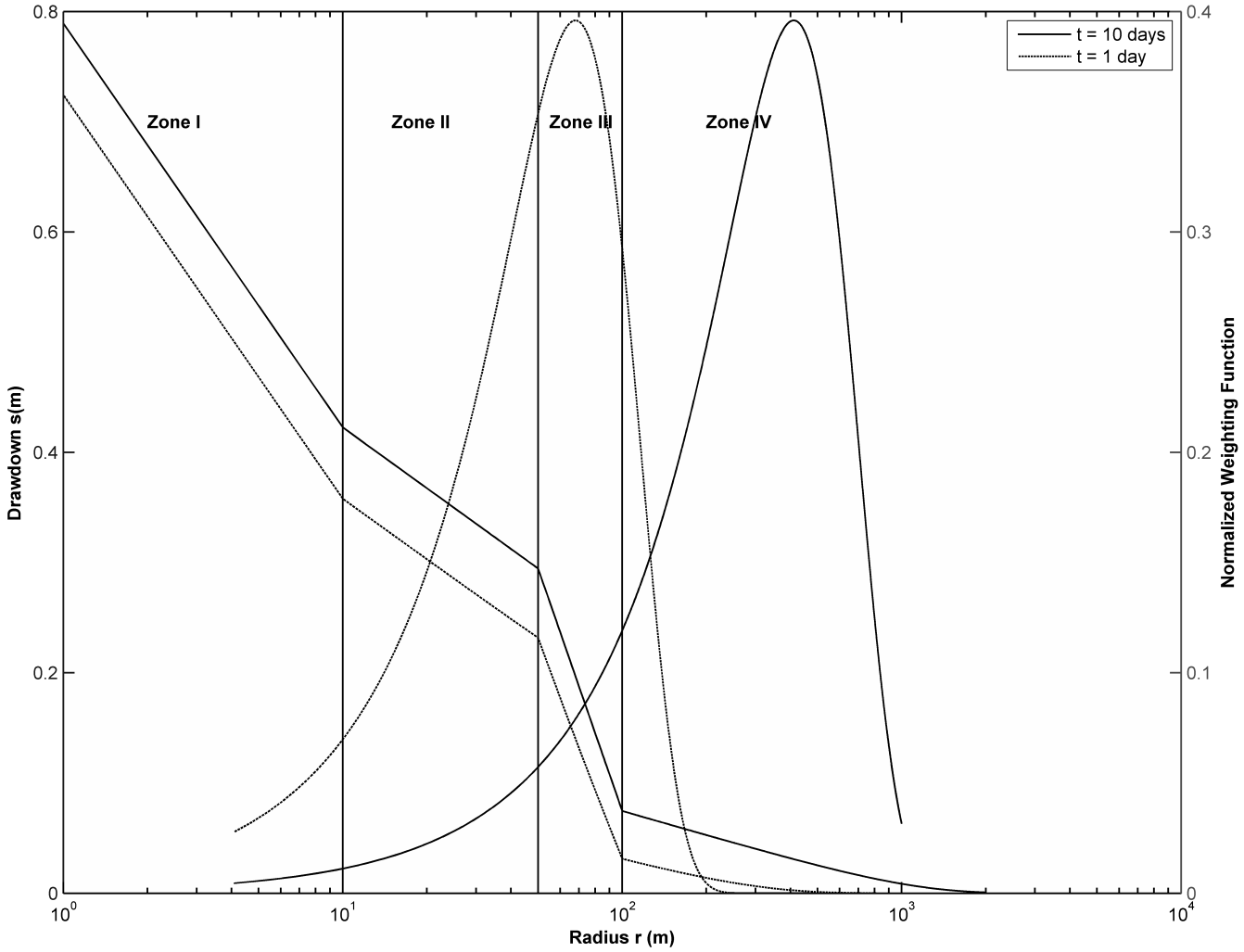

Figure 7.10. Distance Drawdown for $t = 1$ day and $t = 10$ days.

The predicted transmissivity fields based on ISA procedure are noted to accurately predict the increasing and decreasing transmissivity trends within each concentric circle, however the sudden changes in the actual transmissivity field are smoothed by the nature of the ISA. Despite this shortcoming, the proposed algorithm provides a more accurate prediction of the transmissivity field than the techniques that have been developed to date. The existing techniques for predicting radial variation of the transmissivity field consist of the drawdown derivative methods namely Slope Matching Procedure (SMP) (Sen, 1986) and the relatively new method proposed by Copty *et al.* (2011) as well as the drawdown integration within the discrete time such as Incremental Area Method (Avci *et al.*, 2011). These methods were used in the analysis of the four concentric circles example for comparison purposes with the ISA. Figure 7.11 shows the radial transmissivity predictions using the existing methods and compares them with the ISA predictions. The ISA predicted radial transmissivity values are noted to be closer to the actual transmissivity values of the concentric circles that are used to generate the drawdown curves. The existing methods depend mainly on the drawdown slopes and curve shape at the particular point being analyzed rather than assessing the portion of the drawdown curve under the influence of the weighting function used in the ISA. As the cone of depression expands into the final concentric circle transmissivity zone, the drawdown curves are influenced by the transmissivity field of the final concentric circle which in turn allows the slope and integration methods to converge to the transmissivity value of the last concentric circle. However, the inner ring transmissivity predictions of these techniques are less accurate than the ISA.

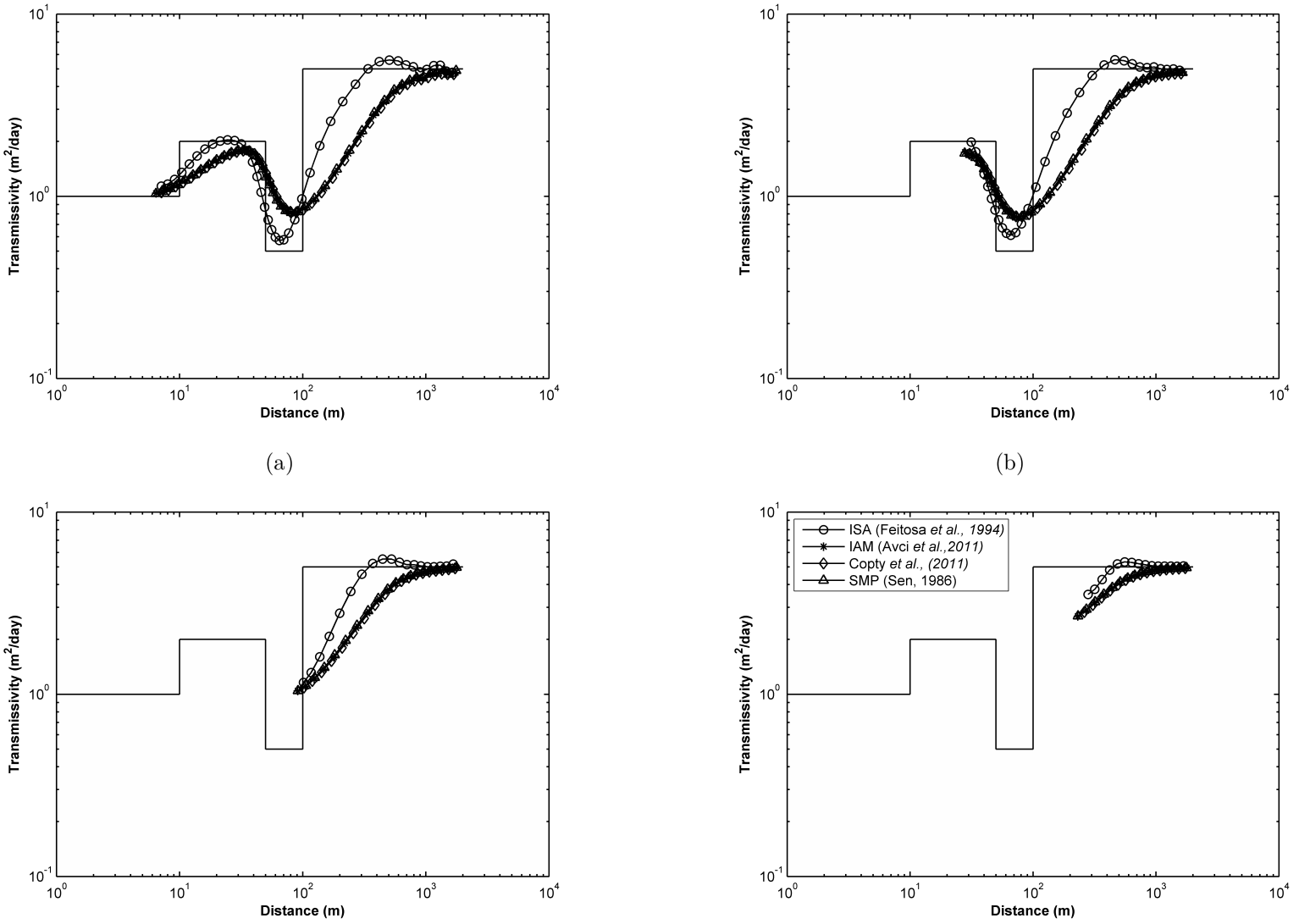

Figure 7.11. Transmissivity Estimation for Monitoring Wells (a) $r = 5$ m (b) $r = 25$ m (c) $r = 50$ m (d) $r = 125$ m.

7.3.4. Numerical Test Case: MODFLOW Simulations for Heterogeneous Aquifers

The ISA methodology can only provide an estimation of a radially varying transmissivity field that can be construed as an integration of the heterogeneous field along concentric circles as given in Equation 4.8. The effectiveness of this assumption was tested by using the ISA methodology on drawdown data generated from pumping tests conducted in heterogeneous aquifers. Confined aquifers with log-normal Gaussian distributed transmissivity settings were selected for establishing numerical benchmark testing conditions. Three transmissivity settings were generated using the Turning Band Algorithm (TBM) (Mantoglou and Wilson, 1982) for small, medium and large heterogeneity with variances of 0.5, 1, and 2, respectively. The integral scale was chosen as 10 m in the generation of the transmissivity field. The aquifer pumping test conditions (100 cases for each setting) were simulated using the MODFLOW computer code (Harbaugh *et al.*, 2000). The aquifer domain was taken as a 500 by 500 m^2 area with a 1 m by 1 m cell size uniform grid spacing. Pumping tests conditions with a constant discharge rate of 2 m^3/day were simulated for all transmissivity fields to obtain drawdown data for 1 day-long pumping period. Eight monitoring well locations were selected at a radial distance of 5 m from the pumping well. Another eight monitoring well locations were selected at a radial distance of 10 m away from pumping well as shown in Figure 7.12.

The storativity was assumed to be uniformly distributed with a value of 2×10^{-4}. A constant head boundary condition was imposed at the outer boundary of the rectangular aquifer domain. The ISA methodology was used to estimate the radial transmissivity variation using the mean drawdowns computed in the monitoring wells located at 5 m and 10 m distance from the pumping well. The t-Test and One-way ANOVA were applied to check that the mean drawdown value of the eight monitoring wells at 5 m and 10 m was not significantly different than each individual well drawdown for each radial distance respectively.

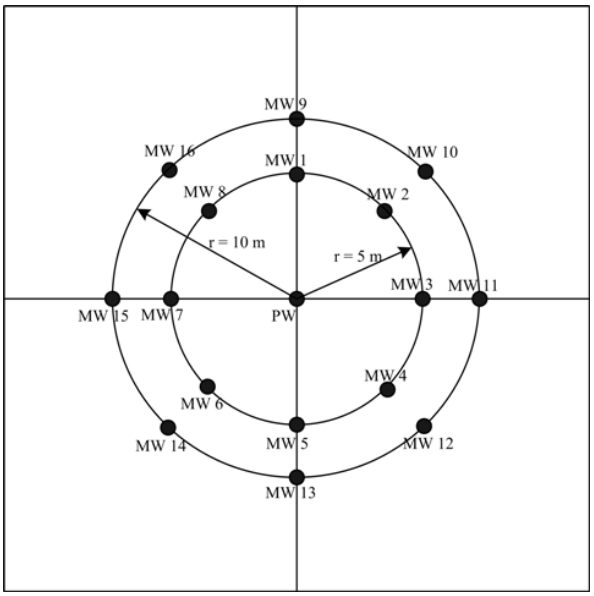

Figure 7.12. Schematic View of Well Configurations.

The integration technique which would provide the most suitable equivalent radially varying transmissivity field for a heterogeneous media along the concentric circles needed to be identified. There different averaging methods given in Equation 7.18 were selected for depicting the radial transmissivity variation of the synthetically generated heterogeneous aquifer settings. These averaging methods were selected as:

$$\begin{aligned} &\text{FEM1 :} T = \sqrt[n]{\prod \mathrm{T_i}} && r \leq r_i \\ &\text{FEM2 :} T = \sqrt[n]{\prod \mathrm{T_i}} && \mathrm{r_i} - 0.5 \leq r \leq \mathrm{r_i} + 0.5 \\ &\text{FEM3 :} T = \sqrt[n]{\prod \mathrm{T_i}} && 0.12 r_w \sqrt{\hat{t}_{D,i}} \leq r \leq 2.34 r_w \sqrt{\hat{t}_{D,i}}_i \end{aligned} \tag{7.18}$$

where n is the number of transmissivity value within given radius limits, r_i is radius obtaining from ISA, $\hat{t}_{D,i}$ is pseudo-time, and r_w is the radius of the pumping well. FEM 1 represents the geometric mean of the transmissivity field inside the cone of depression or investigation radius. According to Butler (1986), FEM 1 is not a reliable averaging method since Theis (1935) based curve matching procedures provide a weighted average of the near well and far field properties. This was also shown to be the case for the analytical benchmark case study investigations discussed in the previous section. FEM 2 represents the geometric mean of the transmissivity field at a distance r from the

pumping well within a 1 m thick concentric ring; FEM 2, therefore, represents a true radially averaged transmissivity term. FEM 3 is based on Oliver (1990) statement that 99% of the contribution of the drawdown behavior at a well comes from the average transmissivity within an annular region between $r_D = 0.12\sqrt{\hat{t}_D}$ and $r_D = 2.34\sqrt{\hat{t}_D}$. The ISA based transmissivity is estimated from the drawdown derivative which is a weighted average of the transmissivity the aquifer domain under the weighting function. The weighting function vanishes for small radial distances and the transmissivity values do not contribute to the slope of the semi-log plot (Ryou, 1995). Furthermore, the weighting function approaches to zero beyond the radius $2.34r_w\sqrt{\hat{t}_{D,i}}$ as illustrated in Figure 4.1 (Oliver, 1990).

The highest coefficient of determination (R^2) value between the predicted transmissivity field obtained from ISA and the integrated transmissivity field was calculated for each heterogeneity condition. The statistical results are summarized in Tables 7.2 through 7.5. Table 7.2 indicates that:

(i) Using FEM 2, 49-53% of the ISA based transmissivity fields estimated from the extraction well data fall in a 0.75-1.0 of R^2 band and 24-28% of those are in a 0.5-0.75 of R^2 band for three different heterogeneity set. This means that ISA based transmissivity field approximation provides between 73-81% agreement within a 0.5-1.0 of R^2 band. The ISA shows a good performance especially in large heterogeneous realization set.

(ii) 20-31% of the ISA based transmissivity fields estimated from the monitoring well located at $r = 5$ m fall in a 0.75-1.0 of R^2 band and 31-33% of those are in a 0.5-0.75 of R^2 band utilizing FEM 2. This means that ISA based transmissivity field approximation provides between 51-61% agreement within a 0.5-1.0 of R^2 band. The monitoring wells should therefore be placed close to the extraction well since the drawdown data reflect local as well as regional characteristics of the transmissivity field. This is based on the R^2 values for all of three sets of heterogeneity characteristics (low, medium and high variation of the transmissivity field).

(iii) FEM 1 which represents a geometric average of the transmissivity within the

cone of depression is not a good approximation to be used for assessing radial transmissivity variations.

(iv) FEM 3 provides the best agreement with ISA based transmissivity fields using the extraction well data. 52-62% of the results fall in a 0.75-1.0 of R^2 band and 22-23% of the results are in a 0.5-0.75 of R^2 band. This means that ISA based transmissivity field approximation provides between 74-85% agreement within a 0.5-1.0 of R^2 values. This is expected since the averaging scheme is based on the ISA approximation.

Through Figure 7.13 to Figure 7.15 show the results of the ISA based transmissivity predictions for large heterogenic character compared with the three averaging methods, namely FEM 1, FEM 2, and FEM 3. The predicted drawdown values using the ISA which provides radially symmetric transmissivity field are also shown in these figures to compare actual drawdown curve.

Table 7.2. The R^2 Comparisons for All Simulations.

Sim. Set	Method	Well Location	Sim. Num.	R^2					
				min.	max.	0-0.25	0.25-0.5	0.5-0.75	0.75-1
Small	ISA	P. Well	65	0.0663	0.9634	12%	22%	21%	45%
	-	r = 5 m	92	0.0011	0.8728	30%	24%	33%	13%
	FEM 1	r = 10 m	31	0.0000	0.7915	48%	36%	15%	1%
	ISA	P. Well	25	0.0860	0.9815	8%	19%	24%	49%
	-	r = 5 m	43	0.0017	0.9552	20%	29%	31%	20%
	FEM 2	r = 10 m	43	0.0001	0.8669	55%	27%	15%	3%
	ISA	P. Well	25	0.1061	0.9909	6%	20%	22%	52%
	-	r = 5 m	43	0.0000	0.9787	19%	26%	30%	25%
	FEM 3	r = 10 m	5	0.0000	0.8776	53%	23%	18%	6%
Medium	ISA	P. Well	65	0.0769	0.9801	9%	22%	21%	48%
	-	r = 5 m	2	0.0101	0.9231	19%	27%	31%	23%
	FEM 1	r = 10 m	31	0.0003	0.8389	45%	28%	23%	4%
	ISA	P. Well	25	0.1172	0.9827	6%	13%	27%	54%
	-	r = 5 m	2	0.0189	0.9678	16%	23%	33%	28%
	FEM 2	r = 10 m	43	0.0000	0.8616	44%	33%	17%	6%
	ISA	P. Well	25	0.2498	0.9935	1%	18%	22%	59%
	-	r = 5 m	5	0.0013	0.9789	12%	19%	34%	35%
	FEM 3	r = 10 m	31	0.0000	0.9626	37%	27%	20%	16%
Large	ISA	P. Well	65	0.0055	0.9853	9%	15%	28%	48%
	-	r = 5 m	65	0.0015	0.9328	19%	25%	26%	30%
	FEM 1	r = 10 m	68	0.0001	0.9146	42%	22%	28%	8%
	ISA	P. Well	85	0.0662	0.9576	5%	14%	28%	53%
	-	r = 5 m	67	0.0140	0.9756	19%	21%	29%	31%
	FEM 2	r = 10 m	31	0.0004	0.9072	48%	25%	17%	10%
	ISA	P. Well	79	0.1174	0.9934	2%	13%	23%	62%
	-	r = 5 m	67	0.0037	0.9841	12%	18%	30%	40%
	FEM 3	r = 10 m	55	0.0000	0.9697	36%	21%	25%	18%

Table 7.3. The Performance of Field Estimation Methods for Small Heterogeneous Set.

Comparison	Well Location	Sim. Number	ISA (m^2/day)		FEM 1 (m^2/day)		FEM 2 (m^2/day)		FEM 3 (m^2/day)		Error Criteria	
			min.	max.	min.	max.	min.	max.	min.	max.	MAE	RMSE
ISA - FEM 1	P. Well	65	0.0669	1.2743	0.1558	1.0986	0.1558	1.2900	0.1581	1.1013	0.1615	0.2278
	r = 5 m	92	0.9126	3.4767	1.0212	2.7597	0.6990	2.6283	1.0193	2.5860	0.1748	0.2271
	r = 10 m	31	1.1669	3.2271	1.3457	2.4653	1.0982	2.2752	1.0983	2.2321	0.1539	0.2369
ISA - FEM 2	P. Well	25	0.1031	1.2544	0.2261	1.0805	0.2260	1.2805	0.2260	1.0844	0.1140	0.1950
	r = 5 m	43	0.9075	3.9831	0.9419	3.4097	0.7554	3.2493	0.9405	3.1139	0.0915	0.1973
	r = 10 m	43	0.9088	3.1615	0.9419	2.7287	0.7520	1.8995	0.9407	1.8319	0.1484	0.2749
ISA - FEM 3	P. Well	25	0.1031	1.2544	0.2261	1.0805	0.2260	1.2805	0.2260	1.0844	0.1112	0.1964
	r = 5 m	43	0.9075	3.9831	0.9419	3.4097	0.7554	3.2493	0.9405	3.1139	0.0874	0.2046
	r = 10 m	5	0.8239	2.6273	0.9144	1.9478	0.6933	1.4583	0.9109	1.3419	0.1161	0.2428

Table 7.4. The Performance of Field Estimation Methods for Medium Heterogeneous Set.

Comparison	Well Location	Sim. Number	ISA (m^2/day)		FEM 1 (m^2/day)		FEM 2 (m^2/day)		FEM 3 (m^2/day)		Error Criteria	
			min.	max.	min.	max.	min.	max.	min.	max.	MAE	RMSE
ISA - FEM 1	P. Well	65	0.0277	1.3658	0.0721	1.1452	0.0721	1.3550	0.0737	1.1314	0.2713	0.3537
	r = 5 m	2	1.0050	4.1016	1.0877	3.5955	0.8646	3.0096	1.0719	2.7077	0.2344	0.2890
	r = 10 m	31	1.1676	3.8825	1.5154	3.3472	1.1706	2.9157	1.0979	3.0008	0.1813	0.2600
ISA - FEM 2	P. Well	25	0.0501	1.3061	0.1222	1.1157	0.1220	1.4187	0.1220	1.1220	0.1981	0.3072
	r = 5 m	2	1.0050	4.1016	1.0877	3.5955	0.8646	3.0096	1.0719	2.7077	0.1378	0.2502
	r = 10 m	43	0.9023	3.8866	0.9205	3.7034	0.6667	2.0517	0.9171	2.0611	0.1826	0.3100
ISA - FEM 3	P. Well	25	0.0501	1.3061	0.1222	1.1157	0.1220	1.4187	0.1220	1.1220	0.1903	0.3107
	r = 5 m	5	0.7826	3.8785	0.8809	3.3072	0.5933	2.8600	0.8774	2.6811	0.1257	0.2562
	r = 10 m	31	1.1676	3.8825	1.5154	3.3472	1.1706	2.9157	1.0979	3.0008	0.1409	0.2615

Table 7.5. The Performance of Field Estimation Methods for Large Heterogeneous Set.

Comparison	Well Location	Sim. Number	ISA (m^2/day)		FEM 1 (m^2/day)		FEM 2 (m^2/day)		FEM 3 (m^2/day)		Error Criteria	
			min.	max.	min.	max.	min.	max.	min.	max.	MAE	RMSE
ISA - FEM 1	P. Well	65	0.0088	1.5262	0.0243	1.2000	0.0243	1.4541	0.0250	1.1861	0.4138	0.5465
	r = 5 m	65	0.0159	1.5591	0.0384	1.2113	0.0624	1.4877	0.0684	1.1833	0.3387	0.4084
	r = 10 m	68	1.1298	4.1462	1.7657	3.9821	1.0650	4.5820	1.0344	3.5818	0.2199	0.2997
ISA - FEM 2	P. Well	85	0.0849	1.2944	0.1893	1.1455	0.1882	1.4879	0.1882	1.1470	0.3480	0.4989
	r = 5 m	67	0.9307	5.3985	0.9169	4.7967	0.5681	3.8743	0.9149	3.8187	0.2299	0.3779
	r = 10 m	31	1.2024	5.4341	1.7392	4.9440	1.2669	4.5224	1.0692	3.7934	0.2424	0.3656
ISA - FEM 3	P. Well	79	0.0425	1.0725	0.1058	0.8707	0.1058	1.1253	0.1064	0.8705	0.3553	0.5203
	r = 5 m	67	0.9307	5.3985	0.9169	4.7967	0.5681	3.8743	0.9149	3.8187	0.1984	0.3666
	r = 10 m	55	1.2012	4.3326	1.6928	3.9819	1.2691	4.5072	1.0857	3.8648	0.1730	0.2888

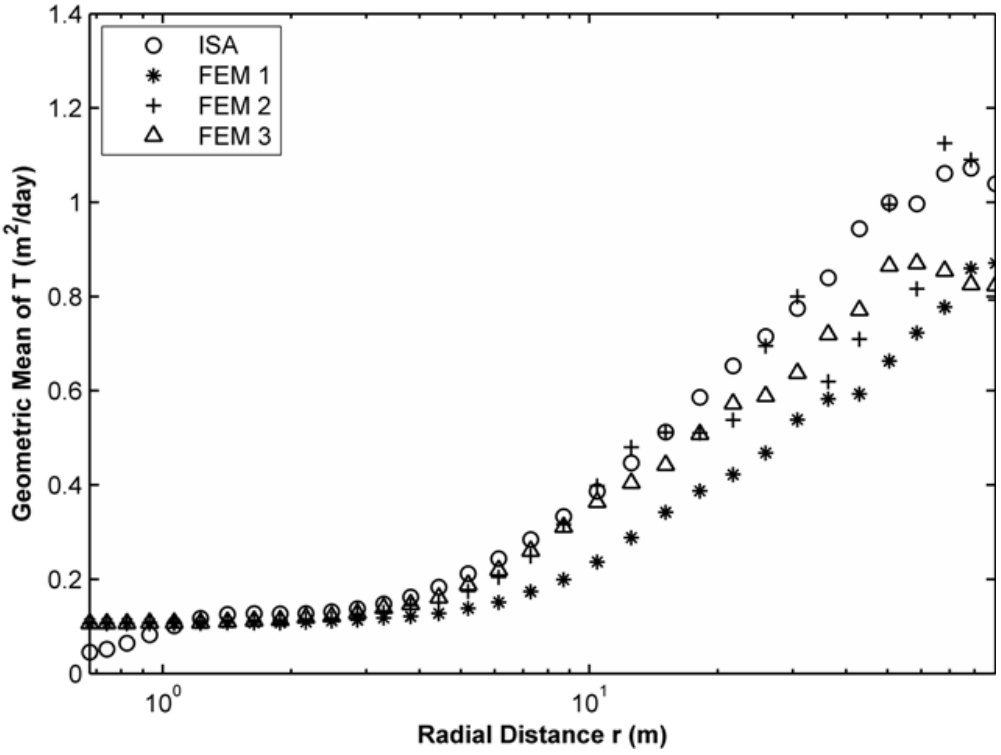

(a)

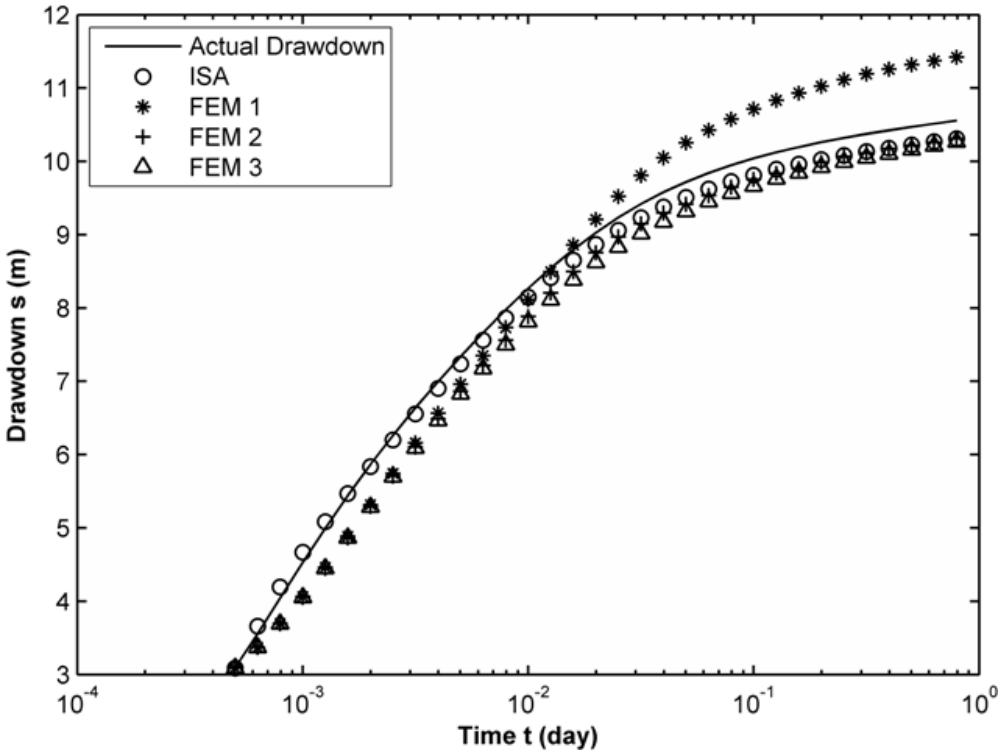

(b)

Figure 7.13. Transmissivity Estimation Results for a Large Heterogeneous Aquifer Setting (a) Transmissivity Estimation Using Extraction Well Data for Simulation # 79 (b) Drawdown Comparison at Extraction Well for Simulation # 79.

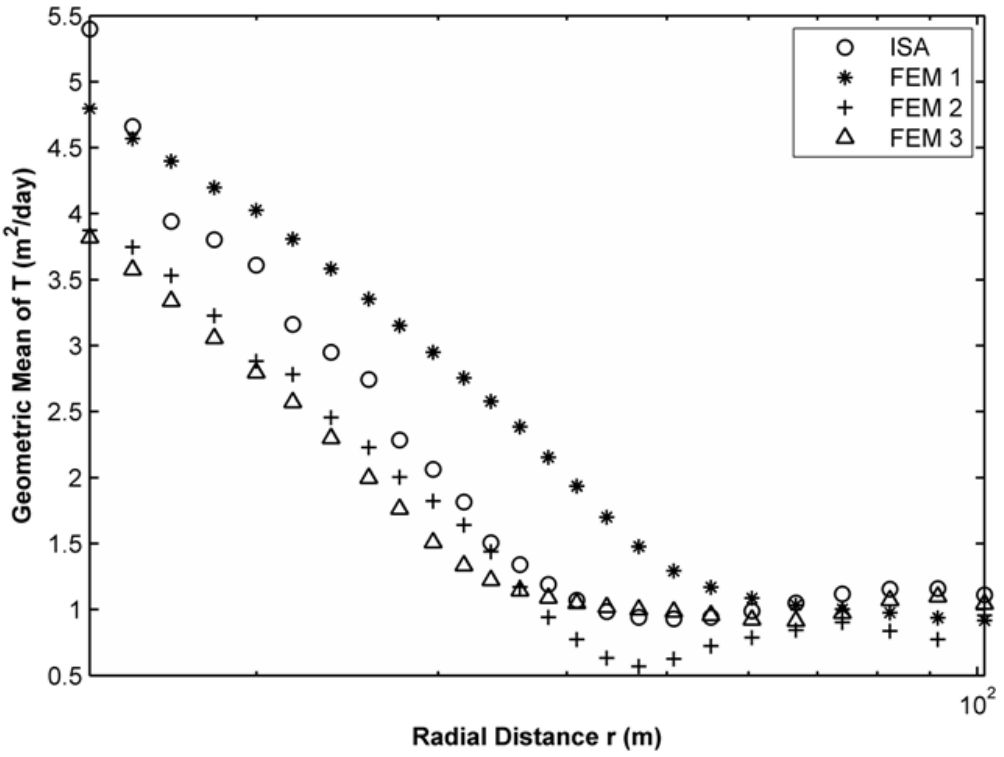

(a)

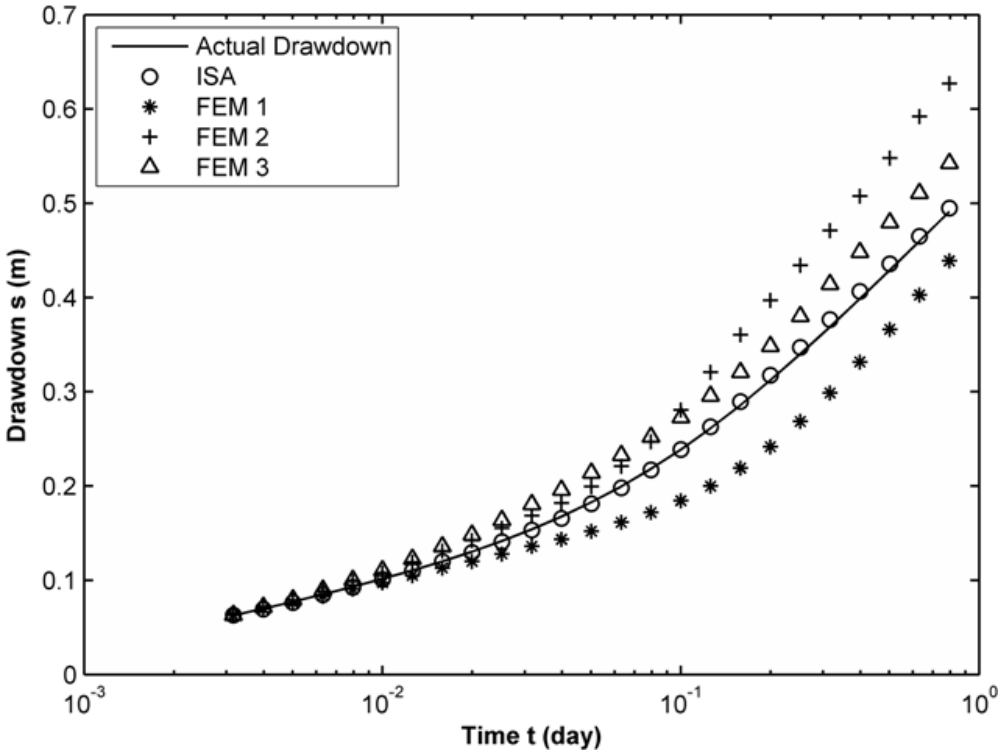

(b)

Figure 7.14. Transmissivity Estimation Results for a Large Heterogeneous Aquifer Setting (a) Transmissivity Estimation Using Monitoring Well Data at $r = 5$ m for Simulation # 67 (b) Drawdown Comparison at Monitoring Well Data at $r = 5$ m for Simulation # 67.

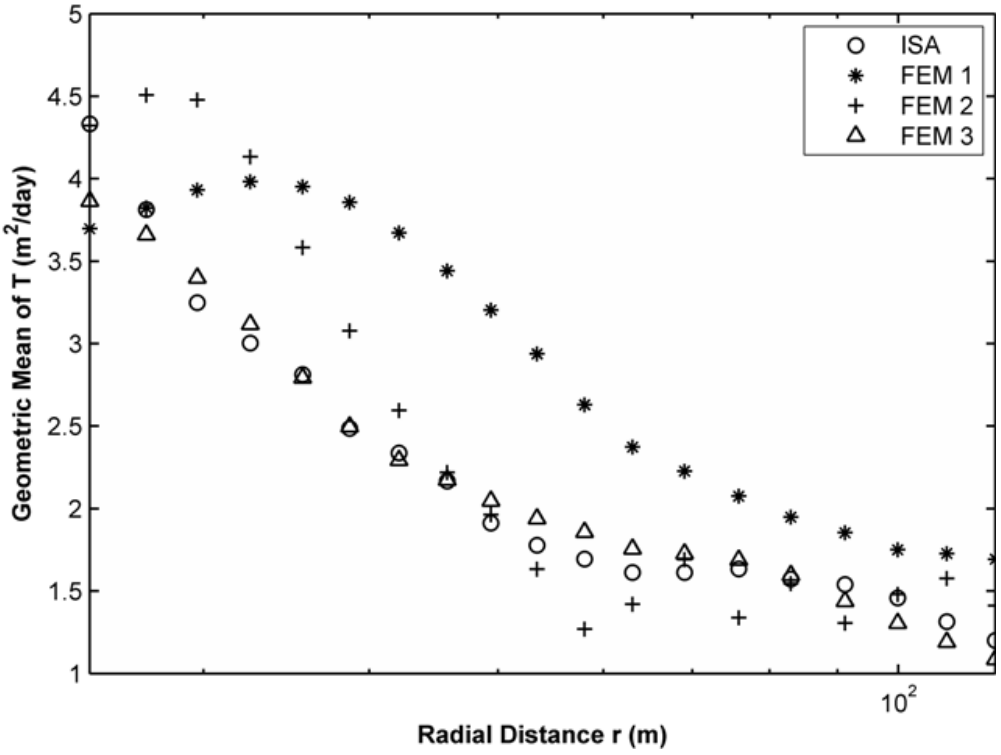

(a)

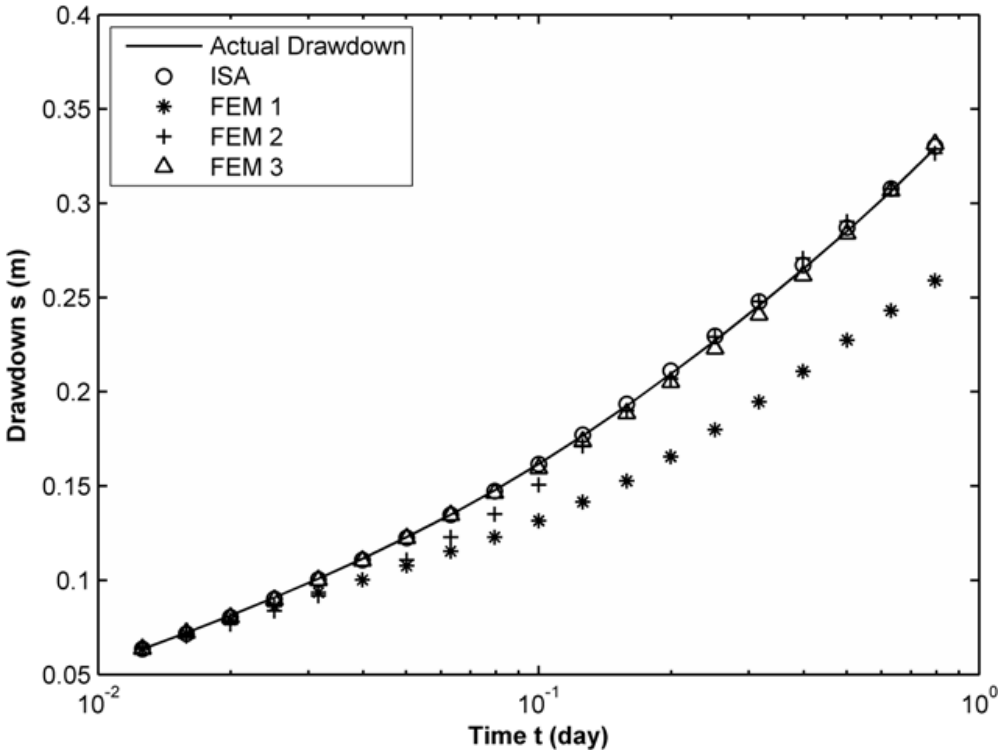

(b)

Figure 7.15. Transmissivity Estimation Results for a Large Heterogeneous Aquifer Setting (a) Transmissivity Estimation Using Monitoring Well Data at $r = 10$ m for Simulation # 55 (b) Drawdown Comparison at Monitoring Well Data at $r = 10$ m for Simulation # 55.

8. CONCLUSION

In the context of this dissertation, a new estimation approach referred as Incremental Area Method (IAM) has been developed to determine aquifer parameters for confined and leaky aquifer systems. The proposed method is based on integrating the logarithmic based drawdown curve values within a discrete time and matching the results with a corresponding time integral of the type curve which governs ideal confined aquifers. These discrete sections of the pumping data from any type of aquifer system and hydrogeologic settings are assessed as an equivalent ideal confined aquifer conditions with corresponding aquifer parameters.

The IAM has been applied to a number of non-ideal aquifer condition cases to test the validity of the proposed approach including synthetically generated drawdown data in ideal, bounded and heterogeneous confined aquifers. The results also showed that the IAM method is suitable to overcome some of the measurement errors and inconsistencies that may be present in the data as random variables. This is mainly due to the fact that the IAM method is based on an integration process which smoothes out potential errors.

The robustness of the method was tested by assessing field data obtained from a mixed aquifer setting that had strong heterogeneous features. The proposed method correctly predicted confined condition present nearby the pumping well as well as the presence of leaky aquifer conditions further from the extraction well location. The contribution of this method was seen to serve as a diagnostic tool as well in identifying the aquifer system being stressed.

For leaky aquifer systems, the applicability of suggested IAM has been tested for various data sets including synthetically generated ideal and heterogeneous aquifer character and real site experiments. The difficulty arisen in leaky aquifer parameter estimation is to match correct leakage factor, and then to predict key parameters. The performance of IAM showed that leakage factor can easily be predicated without much

computation effort with the sufficient estimation accuracy.

One another potential use of IAM is that the IAM can serve as a diagnostic tool for aquifer system identification as well as to supplement the curve matching procedure. The use of derivative plots generated from drawdown data is a common practice in the analysis of aquifer parameters for all types of aquifer settings and pumping test methodology. The IAM based diagnostic plots for ideal aquifer types such as confined, leaky and unconfined aquifers as well as bounded confined aquifer and heterogeneous confined aquifer have been derived and individual features of these plots have been identified.

The key features of IAM which make this method appealing as a diagnostic tool were as follows:

- Combining diagnostic plot shape and transmissivity estimation on the same plot for easier assessment of aquifer properties and aquifer identification.
- Identifying ideal aquifer conditions even in the pre-Cooper Jacob conditions which allow evaluation of early time period of drawdown data. This is a very important feature which allows the confined aquifer conditions to be detected for unconfined as well as leaky aquifer conditions.
- Identifying key signatures of diagnostic plots for aquifer systems.
- Ability to delineate the sections of drawdown data that would be indicative of ideal confined aquifer conditions, leakage conditions, presence of boundaries, or general heterogeneities in non-ideal drawdown data collected from the field.
- Ability to smooth the noise of the field data used in the generation of diagnostic plots.

IAM method properly predicts log-normal transmissivity based heterogeneous behavior of the drawdown data in terms of variability of the aquifer properties as a result of the expansion of the cone of depression with time. The contribution of this method can be seen as an ability to identify the presence of the heterogeneity, as well as to estimate averaged hydraulic parameters inside the cone of depression. However,

IAM does not provide the variation of aquifer parameters with a function of space. For the spatial variation of transmissivity, the inverse solution algorithm (ISA) proposed by Feitosa *et al.* (1994) was formulated for pumping well as well as monitoring well data assessment in groundwater bearing zones.

The ISA methodology was used against analytical benchmark testing conditions which were developed for a radially symmetric non-uniform transmissivity field as well as numerical benchmark testing conditions which were selected for log-normal Gaussian distribution of heterogeneity. The results showed that the predicted transmissivity based on the ISA procedure accurately predicted the increasing and decreasing transmissivity trends and values within each concentric circle for the analytical benchmark cases and provided a more accurate prediction of the transmissivity field than the techniques that have been developed to date. The assessment results also suggested that the transmissivity values obtained from Cooper-Jacob (1946) method based on drawdown behavior for late time period of pumping do not represent the geometric mean of the transmissivity values within the cone of depression. Rather, the section which falls the outer portion of the cone of depression would impact the behavior of the drawdown curves more than initial stage of pumping as the cone depression propagates with time. The ISA showed a good agreement in predicting log-normal based small, medium and large heterogeneous transmissivity field. It was noted that monitoring wells should be placed close to the pumping well location to improve the accuracy of the predictions for radial transmissivity. The ISA predicted much more closely the radial transmissivity field values generated by integrating along concentric circles than ensemble mean of the transmissivity inside the cone of depression. The results of this investigation showed that the ISA, which was first developed in the oil and gas literature, is a powerful technique that can be used for understanding the radial transmissivity characteristics of heterogeneous field conditions in aquifer settings.

This study presents new aspects for groundwater literature as following:

- A new parameter estimation technique called as IAM for confined and leaky aquifer settings has been introduced.

- IAM provides an alternative diagnostic tool for the identification of aquifer characteristic.
- Butler's (1988) solution for two ring system was extended for three and four rings system. A general solution strategy was drawn in the generation of drawdown response of a hypothetical aquifer analytically.
- ISA has been adopted for the groundwater system to elaborate spatial variation of heterogenic transmissivity field.
- A true interpretation of pumping tests in heterogeneous aquifer system has been suggested using both IAM and ISA.

As a conclusion, IAM is a strong alternative to a diagnostic tool for aquifer identification as well as parameter estimation. IAM can identify the aquifer heterogeneity to understand the long term transmissivity variation with time. ISA is recommended to elaborate the radial variation of heterogeneity character for aquifer system being stressed. For further studies, IAM can be extended to estimate the unconfined aquifer parameters or slug tests that needs a curve matching procedure. The link between IAM which provides time variation of transmissivity and ISA which enables radial variation of transmissivity can be investigated to cooperate in the analysis of heterogenic aquifer media. Moreover, a new inversion algorithm similar to the ISA can be established for leaky aquifer system.

REFERENCES

Abramowitz, M., and I. A. Stegun, 1972, *Handbook of Mathematical Functions*, 10th ed., Dover, New York, NY.

Amin, I., 2005, "Determination of the Rate and Volume of Leakage Using the Slopes of Time-Drawdown Data", *Environmental Geology*, Vol. 47, No. 4, pp. 558–564.

Arfken, G., 1985, *Mathematical Methods for Physicists*, 3rd ed., Academic Press, Orlando, FL.

ASTM Standard D4043-96(2010)e1 , 2010, *Guide for Selection of Aquifers – Test Method in Determining Hydraulic Properties by Well Techniques*, ASTM International, West Conshohocken, PA.

Avci, C. B., A. U. Şahin, Çiftci, E., 2011, "Aquifer Parameter Estimation Using an Incremental Integration Method", *Hydrological Processes*, Vol. 25, No. 16, pp. 2584-2596.

Avci, C. B., E. Çiftci, A. U. Şahin, 2010, "Identification of Aquifer and Well Parameters from Step-drawdown Tests", *Hydrogeology Journal*, Vol. 18, No. 7, pp. 1591-1601.

Balkhair, S. K., 2002, "Aquifer Parameters Determination for Large Diameter Wells Using Neural Network Approach", *Journal of Hydrology*, Vol. 265, pp. 118-128.

Batu, V., 1998, *Aquifer Hydraulics: A Comprehensive Guide to Hydrogeologic Data Analysis*, Wiley, New York, NY.

Bear, J., 1979, *Hydraulics of Groundwater*, McGraw-Hill, New York, NY.

Beauheim, R. L., R. M. Roberts, J. D. Avis, 2004, "Well Testing in Fractured Media: Flow Dimensions and Diagnostic Plots", *Journal of Hydraulic Engineering*, Vol. 42, pp. 69-76.

Bibby, R., 1979, *Estimating Sustainable Yield to a Well in Heterogeneous Strata*, `http://www.ags.gov.ab.ca/publications/BUL/PDF/BUL_037.pdf`, accessed at May 2012.

Bohling, G. C., X. Zhan, J. J. Butler, L. Zheng, 2002, "Steady Shape Analysis of Tomographic Pumping Tests for Characterization of Aquifer Heterogeneities", *Water Resources Research*, Vol. 38, No. 12, pp. 1324.

Boulton, N. S., 1963, "Analysis of Data from Non-Equilibrium Pumping Tests Allowing for Delayed Yield from Storage", *ICE Proceedings London*, Vol. 26, No. 3, pp. 469–482.

Boulton, N. S., 1954, "The Drawdown of The Water-Table Under Nonsteady Conditions Near A Pumped Well In An Unconfined Formation", *ICE Proceedings London*, Vol. 3, pp. 564–579.

Bourbiaux, B., J. P. Callot, B. Doligez, M. Fleury, F. Gaumet, M. Guiton, R. Lenormand, J. L. Mari, H. Pourpak, 2007, "Multi-Scale Characterization of a Heterogeneous Aquifer through the Integration of Geological, Geophysical and Flow Data: A Case Study", *Oil & Gas Science and Technology*, Vol. 62, No. 3, pp. 347-373.

Bourdet, D., T. M. Whittle, A. A. Douglas, Y. M. Pirard, 1983, "A New Set of Type Curves Simplifies Well Test Analysis", *World Oil*, May, pp. 95–106.

Bourdet, D., J. A. Ayoub, Y. M. Pirard, 1989, "Use of Pressure Derivative in Well-Test Interpretation", *Society of Petroleum Engineers Formation Evaluation*, Vol. 4, pp. 293–302.

Butler, J. J., 1986, *Pumping Tests in Nonuniform Aquifers: A Deterministic/Stochastic Analysis*, Ph.D. Thesis, Stanford University.

Butler, J. J., 1988, "Pumping Tests in Nonuniform Aquifers—The Radially Symmetric Case", *Journal of Hydrology*, Vol. 101, pp. 15-30.

Butler, J. J., 1990, "The Role of Pumping Tests in Site Characterization: Some Theoretical Considerations", *Ground Water*, Vol. 28, pp. 394–402.

Butler, J. J. and W. Z. Liu, 1991, "Pumping Tests in Non-Uniform Aquifers: The Linear Strip Case", *Journal of Hydrology*, Vol. 128, pp. 69–99.

Butler, J. J. and W. Z. Liu, 1993, "Pumping Tests in Nonuniform Aquifers: The Radially Asymmetric Case", *Water Resources Research*, Vol. 29, No. 2, pp. 259-269.

Butler, J. J., and C. D. McElwee, 1990, "Variable-Rate Pumping Tests for Radially Symmetric Nonuniform Aquifers", *Water Resources Research*, Vol. 26, No. 2, pp. 291–306.

Carrera, J., and S. P. Neuman, 1986a, "Estimation of Aquifer Parameters Under Transient and Steady-State Conditions: 1. Maximum Likelihood Method Incorporating Prior Information", *Water Resources Research*, Vol. 22, No. 2, pp. 199-210.

Carrera, J., and S. P. Neuman, 1986b, "Estimation of aquifer parameters under transient and steady-state conditions: 2. Uniqueness, stability and solution algorithms", *Water Resources Research*, Vol. 22, No. 2, pp. 211-227.

Chiang, W. H., and W. Kinzelbach, 2001, *3D-Groundwater Modeling With PMWIN A Simulation System For Modeling Groundwater Flow And Pollution*, Springer, Berlin, Heidelberg, New York, NY.

Chow, V. T., 1952, "On The Determination of Transmissibility and Storage Coefficients from Pumping Test Data", *Transactions - American Geophysical Union*, Vol. 33, pp. 397–404.

Clifton, P. M., and S. P. Neuman, 1982, "Effects Of Kriging And Inverse Modeling On Conditional Simulation Of The Avra Valley Aquifer In Southern Arizona", *Water Resources Research*, Vol. 18, pp. 1215-1234.

Cooper, H. H. J., and C. E. Jacob, 1946, "A Generalized Graphical Method for Evaluating Formation Constants and Summarizing Well Field History", *Transactions of the American Geophysical Union*, Vol. 27, pp. 526–534.

Cooley, R. L., 1992, *A Modular Finite-Element Model (MODFE) for Areal and Axisymmetric Ground-Water-Flow Problems, Part 2: Derivation of Finite-Element Equations and Comparisons with Analytical Solutions*, `http://pubs.usgs.gov/twri/twri6a4/pdf/TWRI_6-A4.pdf`, accessed at May 2012.

Cheng, J. M., and W. W. G. Yeh, 1992, "A Proposed Quasi-Newton Method for Parameter Identification in a Flow and Transport System", *Advances in Water Resources*, Vol. 15, pp. 239–249.

Copty, N., and A. N. Findikakis, 2004a, "Stochastic Analysis of Pumping Test Drawdown Data in Heterogeneous Geologic Formations", *Journal of Hydraulic Research*, Vol. 42, pp. 59–67.

Copty, N., and A.N. Findikakis, 2004b, "Bayesian Identification of The Local Transmissivity Using Time-Drawdown Data from Pumping Tests", *Water Resources Research*, Vol. 40, pp. 1-11.

Copty N., M. S. Sarioglu, A. N. Findikakis, 2006, "Equivalent transmissivity of heterogeneous leaky aquifers for steady state radial flow", *Water Resources Research*, Vol. 42, No. 4, pp. 1-9.

Copty, N., P. Trinchero, X. Sanchez-Vila, 2011, "Inferring Spatial Distribution of Radially Integrated Transmissivity From Pumping Tests in Heterogeneous Confined Aquifers", *Water Resources Research*, Vol.47, pp. 1-11.

Dagan, G., 1986, "Statistical Theory of Groundwater Flow and Transport: Pore to Laboratory, Laboratory to Formation, and Formation to Regional Scale", *Water Resources Research*, Vol. 22, No. 9, pp. 120-134.

Dagan, G., 1989, *Flow and Transport in Porous Formations*, Springer-Verlag, New York, NY.

Darcy, H. P. G., 1856, *Les Fontaines Publiques de la Ville de Dijon*, V. Dalmont, Paris.

Dawson, K. J., and J. D. Istok, 1991, *Aquifer Testing*, Lewis Publishers, Boca Raton, FL.

de Glee, G. J., 1930, *Over Groundwaterstromingen Bij Teronttrekking Door Middel Van Putten*, Ph.D. Thesis, Delft University.

deMarsily, G., J. P. Delhomme, F. Delay, A. Abuoro, 1999, "40 Years Of Inverse Problems In Hydrogeology", *Earth and Planetary Science*, No. 329, pp. 73–87.

de Fosset, K. L., and T. R. Pratt, 2003, *Results of the St. James Bay Surficial Aquifer Constant Discharge Test Franklin County, Florida*, `http://www.nwfwmd.state.fl.us/rmd/aqtest/st_james_bay_surficial/sjbsurf_final.pdf`, accesed at May 2012.

Delhomme, J. P., 1979, "Spatial Variability and Uncertainty in Groundwater Flow Parameters: A Geostatistical Approach", *Water Resources Research*, Vol. 15, pp. 269-280.

Desbarats, A. J., 1992, "Spatial Averaging of Transmissivity in Heterogeneous Fields with Flow Towards A Well", *Water Resources Research*, Vol. 28, No. 3, pp. 757–767.

Domenico, P. A., and W. Schwartz, 1998, *Physical and Chemical Hydrogeology*, 2nd edition, Wiley, New York, NY.

Ehlig-Economides, C., 1988, "Use of The Pressure Derivative for Diagnosing Pressure-Transient Behavior", *Journal of Petroleum Technology*, Vol. 40, No. 10, pp. 1280-1282.

Feitosa, G. S., L. Chu, L. G. Thompson, A. C. Reynolds, 1994, "Determination of Permeability Distribution From Well Test Pressure Data", *Society of Petroleum Engineers Formation Evaluation*, Vol. 26, pp. 607-615.

Fetter, C. W., 2001, *Applied Hydrogeology*, 4th edition, Prentice Hall, Upper Saddle River, New Jersey.

Firmani, G., A. Fiori, A. Bellin, 2006, "Three-Dimensional Numerical Analysis of Steady State Pumping Tests in Heterogeneous Confined Aquifers", *Water Resources Research*, Vol. 42, pp. 1-10.

Freeze, R .A., 1975, "A Stochastic Conceptual Analysis of One-Dimensional Groundwater Flow in Nonuniform Homogeneous Media", *Water Resources Research*, Vol. 11, pp. 725-741.

Freeze, R. A., and R. A. Cheery, 1979, *Groundwater*, Prentice-Hall, New Jersey.

Gautschi, W., and W. F. Cahill, 1972, "Exponential Integral and Related Functions", In M. Abramowitz and I.A. Stegun, *Handbook of Mathematical Functions*, 10th ed., Dover, New York, NY.

Glover, F., 1993, "A User's Guide to Tabu Search", *Annals of Operations Research*, Vol. 41, pp. 3–28.

Gottlieb, J., and P. Dietrich, 1995, "Identification of The Permeability Distribution in Soil by Hydraulic Tomography", *Inverse Problem*, Vol. 11, pp. 353– 360.

Gringarten, A. C., H. J. Jr. Ramey, R. Raghavan, 1974, "Unsteady-State Pressure Distributions Created by a Well with a Single Infinite-Conductivity Vertical Fracture", *Society of Petroleum Engineers Formation Evaluation*, pp. 347–360.

Hantush, M. S., 1956, "Analysis of Data from Pumping Tests in Leaky Aquifer", *Transactions of the American Geophysical Union*, Vol. 37, pp. 702–714.

Hantush, M. S., 1961, "Drawdown Around Partially Penetrating Well", *Proceedings of the American Society of Civil Engineers*, Vol. 87, pp. 83–98.

Hantush, M. S., 1964, "Hydraulics of Wells", Editor V. T. Chow, *Advances in Hydrosciences*, Academic Press, New York.

Hantush, M. S., and C. E. Jacob, 1955, "Nonsteady Radial Flow In An Infinite Leaky Aquifer", *American Geophysical Union*, Vol. 36, No. 1, pp. 95–100.

Hanush, M. S., 1996a, "Wells in Homogeneous Anisotropic Aquifers", *Water Resource Research*, Vol. 2, No. 2, pp. 273–279.

Hanush, M. S., 1996b, "Analysis of Data from Pumping Tests in Anisotropic Aquifers", *Journal of Geophysical Research*, Vol. 71, No. 2, pp. 421–426.

Harbaugh, A., E. Banta, M. Hill, and M. McDonald, 2000, *Modflow-2000: The US Geological Survey Modular Ground-Water Model-User Guide to Modularization Concepts and The Ground-Water Flow Process*, `http://water.usgs.gov/nrp/gwsoftware/modflow2000/ofr00-92.pdf`, accessed at May 2012.

Hoeksema, R. J., and P. K. Kitanidis, 1985, "Analysis of the Spatial Structure of Properties of Selected Aquifers", *Water Resources Research*, Vol. 21, pp. 563-572.

Huebner, K. H., 1975, *The Finite Element Method for Engineers*, John Wiley and Sons, New York, NY.

Huyakorn P. S., E. P. Springer, V. Guvanasen, and T. D. Wadsworth, 1986, "A Three-Dimensional Finite-Element Model for Simulating Water Flow in Variably Saturated Porous Media", *Water Resources Research*, Vol. 22, pp. 1790-1808.

Illman, W. A., X. Liu, and A. Craig, 2007, "Steady-State Hydraulic Tomography in a Laboratory Aquifer with Deterministic Heterogeneity: Multi-Method and Multiscale Validation of Hydraulic Conductivity Tomograms", *Journal of Hydrology*, Vol 341, pp. 222-234.

Indelman, P., 2003, "Transient Pumping Well Flow in Weakly Heterogeneous Formations", *Water Resources Research*, Vol. 39, No. 10, pp. 1287-1296.

Jiang, Y., and A. D. Woodbury, 2006,"A Full-Bayesian Approach to the Inverse Problem for Steady State Groundwater Flow and Heat Transport", *Geophysical Journal International*, Vol. 167, No. 3, pp. 1501-1512.

Jiang, Y., A. D. Woodbury, S. Painter, 2004, "A Full-Bayesian Inversion of the Edwards Aquifer", *Ground Water*, Vol. 42, No. 5, pp. 724-733.

Karasaki, K., J. Long, P. Witherspoon, 1988., "Analytical Models of Slug Tests", *Water Resource Research*, Vol. 24, No. 1, pp. 115-126.

Kitanidis, P. K., 1986, "Parameter Uncertainty in Estimation of Spatial Functions: Bayesian Analysis", *Water Resources Research*, Vol. 22, No. 4, pp. 499–507.

Kluitenberg, G. J., and A. W. Warrick, 2001, "Improved Evaluation Procedure for Heat-Pulse Soil Water Flux Density Method", *Soil Science Society of America Journal*, Vol. 65, pp. 320–323.

Kruseman, G. P., and N. A. de Ridder, 1992, *Analysis and Evaluation of Pumping Test Data*, 2nd ed., International Institute for Land Reclamation and Improvement, Wageningen, The Netherlands.

Lachassagne, P., E. Ledoux, G. de Marsily, 1989, "Evaluation of Hydrogeological Parameters in Heterogeneous Porous Media", International Association of Scientific Hydrology, *Groundwater Management: Quality and Quantity*, Proceedings of the Benidorm Symposium, October, 1989, IAHS Press, Wallingford, Oxfordshire, UK.

Leap, I. D., 1999, "Geological Occurrence of Groundwater", Edited by Jacques Delleur, *The Handbook of Groundwater Engineering*, CRC Press LLC, New York, NY.

Lee, T. C., 1999, *Applied Mathematics in Hydrogeology*, Lewis Publishers, New York, NY.

Lee, W. J., 1982, *Well Testing*, SPE Textbook Series, Richardson, TX.

Lin, G. F. and G. R. Chen, 2006, "An Improved Neural Network Approach to the Determination Aquifer Parameters", *Journal of Hydrology*, Vol. 316, pp. 281-289.

Liu, X., W. A. Illman, A. J. Craig, J. Zhu, T. C. J. Yeh, 2007, "Laboratory Sandbox Validation of Transient Hydraulic Tomography", *Water Resources Research*, Vol. 43, pp. 1-11.

Mantoglou, A., and J. L. Wilson, 1982, "The Turning Bands Method for Simulation of Random-Fields Using Line Generation by A Spectral Method", *Water Resources Research*, Vol. 18, No. 5, pp. 1379–1394.

McDonald, M. G., and A. W. Harbaugh, 1983, *A Modular Three-Dimensional Finite-Difference Ground-Water Flow Model*, `http://pubs.usgs.gov/twri/twri6a1/pdf/TWRI_6-A1.pdf`, accessed at May 2012.

Mayer, A. S., and C. L. Huang, 1999, "Development and Application of A Coupled-Process Parameter Inversion Model Based on the Maximum Likelihood Estimation Method", *Advances in Water Resources*, Vol. 22, No. 8, pp. 841–853.

McDermott, C. I., M. Sauter, and R. Liedl, 2003, "New Experimental Techniques for Pneumatic Tomographical Determination of the Flow and Transport Parameters of Highly Fractured Porous Rock Samples", *Journal of Hydrology*, Vol. 278, No:4, pp. 51–63.

McKinney, D. C., and M.D. Lin, 1994, "Genetic Algorithm Solution of Groundwater Management Models", *Water Resource Research*, Vol. 30, No. 6, pp. 1897–1906.

McLaughlin, D., and L. R. Townley, 1996, "A Reassessment of the Groundwater Inverse Problem", *Water Resources Research*, Vol. 32, No. 5, pp. 1131–1161.

Meier, P. M., J. Carrera, X. Sanchez-Vila, 1998, "An Evaluation Of Jacob's Method for the Interpretation of Pumping Tests in Heterogeneous Formations", *Water*

Resources Research, Vol. 34, No. 5, pp. 1011–1025.

Meier, P. M., J. Carrera, X. Sanchez-Vila, 1999, "A Numerical Study on the Relationship Between Transmissivity and Specific Capacity in Heterogeneous Aquifers", *Ground Water*, Vol. 37, No. 4, pp. 611–617.

Mejías, M., P. Renard, D. Glenz, 2009, "Hydraulic Testing of Low-Permeability Formations: A Case Study in the Granite of Cadalso De Los Vidrios, Spain", *Engineering Geology*, Vol. 107, pp. 88–97.

Misstear, B. D. R., 2001, "The Value of Simple Equilibrium Approximations for Analyzing Pumping Test Data", *Hydrogeology Journal*, Vol. 9, pp. 125–126.

Moench, A. F., 1997, "Flow to A Well of Finite Diameter in A Homogeneous Anisotropic Water Table Aquifer", *Water Resources Research*, Vol. 33, pp. 1397–1407.

Murakami, H., X. Chen, M. S. Hahn, Y. Liu, M. L. Rockhold, V. R. Vermeul, J. M. Zachara, Y. Rubin, 2010, "Bayesian Approach for Three-Dimensional Aquifer Characterization at the Hanford 300 Area", *Hydrology and Earth System Sciences*, Vol. 7, pp. 2017-2052.

Narasimhan, T. N., and P. A. Witherspoon, 1976, "An Integrated Finite Difference Method for Analyzing Fluid Flow in Porous Media", *Water Resources Research*, Vol. 12, pp.57–64.

Neuman, S. P., 1972, "Theory of Flow in Unconfined Aquifers Considering Delayed Response of the Water Table", *Water Resources Research*, Vol. 8, No. 4, pp. 1031–1045.

Neuman, S. P., 1973, "Supplementary Comments on Theory of Flow in Unconfined Aquifers Considering Delayed Response of the Water Table", *Water Resources Research*, Vol. 9, pp. 1102-1103.

Neuman, S. P., 1974, "Effect of Partial Penetration on Flow in Unconfined Aquifers

Considering Delayed Response of the Water Table", *Water Resources Research*, Vol. 9, pp. 1102-1103.

Neuman, S. P., 1975, "Analysis of Pumping Test Data From Anisotropic Unconfined Aquifers Considering Delayed Gravity Response", *Water Resources Research*, Vol. 11, pp. 329-342.

Neuman, S. P., 1979, "Perspective on Delayed Yield", *Water Resources Research*, Vol. 15, No. 4, pp. 899-908.

Neuman, S. P., A. Blattstein, M. Riva, D. M. Tartakovsky, A. Guadagnini, T. Ptak, 2007, "Type Curve Interpretation of Late-Time Pumping Test Data in Randomly Heterogeneous Aquifers", *Water Resources Research*, Vol. 43, pp. 12-21.

Neuman, S. P., A. Guadagnini, M. Riva, 2004, "Type-Curve Estimation of Statistical Heterogeneity", *Water Resources Research*, Vol. 40, pp. 1-10.

Neuman, S. P., G. R. Water, H. W. Bentley, J. J. Ward, D. D. Gonzalez, 1984, "Determination of Horizontal Anisotropy with Three Wells", *Ground Water*, Vol. 22, No. 1, pp. 66–72.

Oliver, D. S., 1990, "The averaging process in permeability estimation from well-test data", *SPE Formation Evaluation*, Vol. 5, No. 3, 319–324.

Oliver, D. S., 1993, "The Influence of Nonuniform Transmissivity and Storativity on Drawdown", *Water Resources Research*, Vol. 29, No. 1, 169–178.

Osiensky, J. L., R. E. Williams, B. Williams, G. Johnson, 2000, "Evaluation Of Drawdown Curves Derived from Multiple Well Aquifer Tests in Heterogeneous Environments", *Mine Water and the Environment*, Vol. 19, No. 1, pp. 30–55.

Ostrowski, L. P., and M. B. Kloska, 1989, "Use of Pressure Derivatives in Analysis of Slug Test or DST Flow Period Data", *Society of Petroleum Engineers*, No. 18595.

Pan, L., and L. S. Wu, 1998, "A Hybrid Global Optimization Method for Inverse Estimation of Hydraulic Parameters: Annealing-Simplex Method", *Water Resource Research*, Vol. 34, No. 9, pp. 2261–2269.

Papadopulos, I. S., 1965, "Nonsteady Flow to a Well in an Infinite Anisotropic Aquifer", International Association of Scientific Hydrology, *Proceedings of Dubrovnik Symposium on the Hydrology of Fractured Rocks*, Dubrovnik, Yugoslavia, 1965, IASH Press,Wallingford, Oxfordshire, UK.

Papadopulos, I. S., and H. H. Cooper, 1967, "Drawdown in a Well of Large Diameter", *Water Resources Research*, Vol. 3, No. 1, pp. 241–244.

Parks, K. P., and L. Bentley, 1996, "Derivative-Assisted Evaluation of Well Yields in a Heterogeneous Aquifer", *Canadian Geotechnical Journal*, Vol. 33, pp. 458-469.

Peaceman, D. W., 1977, *Fundamentals of Numerical Reservoir Simulation*, Elsevier, Amsterdam.

Peaceman, R. L., 1978, "Interpretation of Well Block Pressure in Numerical Simulation", *SPE Journal*, pp. 183-194.

Pratt, T. R., 1993, *Results of the ECUA OLF4A Constant Discharge Aquifer Test Sand-and-Gravel Aquifer, Escambia County, Florida*, `http://www.nwfwmd.state.fl.us/rmd/aqtest/ecua_olf4a/ecua_olf4a.pdf`, accessed at May 2012.

Prodanoff, J. H. A., W. J. Mansur, and F. C. B. Mascarenhas, 2006, "Numerical Evaluation of Theis and Hantush-Jacob Well Functions", *Journal of Hydrology*, Vol. 318, pp. 173-183.

Raghavan, R., 1993, *Well Test Analysis*, Prentice-Hall, Englewood-Cliffs, New York, NY.

Remson, I., G. M. Hornberger, and F. J. Molz, 1971, *Numerical Methods in Subsurface Hydrology*, Wiley, New York.

Renard, P., 2005a, "Approximate Discharge for Constant Head Test with Recharging Boundary", *Ground Water*, Vol. 43, pp. 439-442.

Renard, P., 2005b, "The Future of Hydraulic Tests", *Hydrogeology Journal*, Vol. 13, No. 1, pp. 259-265.

Renard, P., D. Glenz, M. Mejias, 2009, "Understanding Diagnostic Plots for Well-Test Interpretation", *Hydrogeology Journal*, Vol. 17, pp. 589–600.

Rhode, K. L, J. L. Osiensky, S. M. Miller, 2007, "Numerical Evaluation of Volumetric Weighted Mean Transmissivity Estimates in Laterally Heterogeneous Aquifers", *Journal of Hydrology*, Vol. 347, No. 3-4, pp. 381-390.

Rich, T., 2006, *Results of An Aquifer Test at Vermillion, South Dakota*, `http://www.sdgs.usd.edu/pubs/pdf/UR-91.pdf`, accessed at May 2012.

Riva, M., A. Guadagnini, J. Bodin, F. Delay, 2009, "Characterization of the Hydrogeological Experimental Site of Poitiers (France) by Stochastic Well Testing Analysis", *Journal of Hydrology*, Vol. 369, No. 1-2, pp. 154–164.

Ryou, S., 1995, *Reservoir Permeability Distributions from Well Test Sequences in Heterogeneous Reservoirs*, Ph.D. Dissertation, Texas A&M University.

Sahin, A.U., 2008, *Artificial Neural Network Approach For The Determination of Aquifer Parameters*, M.S. Thesis, Boğaziçi University.

Samani, N., M. G. Moghadam, A. A. Safavi, 2007, "A Simple Neural Network Model for the Determination of Aquifer Parameters", *Journal of Hydrology*, Vol. 340, pp. 1-11.

Sanchez-Vila, X., P. M. Meier, J. Carrera, 1999, "Pumping Tests in Heterogeneous Aquifers: An Analytical Study of What Can Be Obtained from Their Interpretation Using Jacob's Method", *Water Resources Research*, Vol. 35, pp. 943–952.

Schad, H., and G. Teutsch, 1994, "Effects of the Investigation Scale on Pumping Test Results in Heterogeneous Porous Aquifers", *Journal of Hydrology*, Vol. 159, pp. 61–77.

Schwartz, W. F., and H. Zhang, 2003, *Fundamentals of Groundwater*, John Wiley & Sons Inc., New York, NY.

Sen, Z., 1986, "Determination of Aquifer Parameters by the Slope-Matching Method", *Ground Water*, Vol. 24, pp. 217–223.

Sen, Z., 1994, "Hydrogeophysical Concepts in Aquifer Test Analysis", *Nordic Hydrology*, Vol. 25, pp. 183-192.

Sen, Z., and E. Wagdani, 2008, "Aquifer Heterogeneity Determination Through The Slope Method", *Hydrological Process*, Vol. 22, pp. 1788-1795.

Singh, S. K., 2008, "Diagnostic Curve for Confined Aquifer Parameters from Early Drawdowns", *Journal of Irrigation and Drainage Engineering*, Vol. 134, No. 4, pp. 515-520.

Singh, S. K., 2010, "Diagnostic Curves for Identifying Leaky Aquifer Parameters with or without Aquitard Storage", *Journal of Irrigation and Drainage Engineering*, Vol. 136, No. 1, pp. 47-57.

Spane, F. A. Jr., 1993, *Selected Hydraulic Test Analysis Techniques for Constant-Rate Discharge Tests*, Pacific Northwest Laboratory, Richland, W.A.

Spane, F. A. Jr., and S. K. Wurstner, 1992, *DERIV: A Program For Calculating Pressure Derivatives For Hydrologic Test Data*, Pacific Northwest Laboratory, Richland, Washington.

Stallman, R. W., 1965, "Effects of Water Table Conditions on Water Level Changes Near Pumping Wells", *Water Resources Research*, Vol. 1, No. 2, pp. 295-312.

Stehfest, H., 1970, "Numerical Inversion of Laplace Transform", *Communications of the ACM*, Vol.13, No. 1. pp. 1-5.

Straface, S., 2009, "Estimation of Transmissivity and Storage Coefficient by Means of A Derivative Method Using the Early-Time Drawdown", *Hydrogeology Journal*, Vol. 17, pp. 1679–1686.

Straface, S., C. Falico, S. Troisi, E. Rizzo, and A. Revil, 2007, "An Inverse Procedure to Estimate Transmissivities from Heads and SP Signals", *Ground Water*, Vol. 45, No. 4, pp. 420–428.

Streltsova, T. D., 1972a, "Unconfined Aquifer and Slow Drainage", *Journal of Hydrology*, Vol. 16, No. 2, pp. 117-124.

Streltsova, T. D., 1972b, "Unsteady Radial Flow in an Unconfined Aquifer", *Water Resources Research*, Vol. 8, No. 4, pp. 1059-1066.

Streltsova, T. D., 1973, "Flow Near a Pumped Well in an Unconfined Aquifer Under Nonsteady Conditions", *Water Resources Research*, Vol. 9, No. 1, pp. 227-235.

Streltsova, T. D., 1976, "Analysis of Aquifer-Aquitard flow", *Water Resources Research*, Vol. 12, No. 3, pp. 415-422.

Streltsova, T. D., 1988, *Well Testing in Heterogeneous Formations*, Wiley, New York, NY.

Sun, N. Z., and W. W. G. Yeh, 2007, "Development of Objective-Oriented Groundwater Models: 1. Robust Parameter Identification", *Water Resources Research*, Vol. 43, pp. 1-14.

Theis, C. V., 1935, "The Relation Between the Lowering of the Piezometric Surface and Rate and Duration of Discharge of a Well Using Ground Water Storage", *Transactions of the American Geophysical Union*, Vol. 16, pp. 519–524.

Thiem, G., 1906, *Hydrologische Methoden*, Gebhardt, Leipzig, Germany.

Torak, L. J., 1993, *A Modular Finite-element Model (MODFE) for Areal and Axisymmetric Ground-Water-Flow Problems, Part 1: Model Description and User's Manual*, `http://pubs.usgs.gov/twri/twri6a5/pdf/twri_6-A5_c.pdf`, accessed at May 2012.

Tóth, J., 1966, "Mapping and Interpretation of Field Phenomena for Groundwater Reconnaissance in a Prairie Environment, Alberta, Canada", *International Association of Scientific Hydrology Bulletin*, Vol. 16, No. 2, pp. 20–68.

Trinchero, P., X. Sanchez-Vila, N. Copty, A. N. Findikakis, 2008, "A New Method for the Interpretation of Pumping Tests in Leaky Aquifers", *Ground Water*, Vol. 46, No. 1, pp. 133–143.

Tumlinson, L. G., J. L. Osiensky, J. P. Fairley, 2006, "Numerical Evaluation of Pumping Well Transmissivity Estimates in Laterally Heterogeneous Formations", *Hydrogeology Journal*, Vol. 14, No. 1-2, pp. 21-30.

van Poolen, H. K., 1964, "Radius of Drainage and Stabilization Time Equations", *Gas and Oil Journal*, Vol. 1, pp. 138-146.

Voss, C.I., 1984, *SUTRA-Saturated Unsaturated Transport–A Finite-Element Simulation Model for Saturated-Unsaturated Fluid-Density-Dependent Ground-Water Flow With Energy Transport or Chemically-Reactive Single-Species Solute Transport*, `http://pubs.usgs.gov/wri/1984/4369/report.pdf`, accessed at May 2012.

Walton, W. C., 1987, *Groundwater Pumping Tests, Design and Analysis*, Lewis Publishers, Michigan, MI.

Walton, W. C., 1962, *Selected Analytical Methods for Well and Aquifer Evaluation*, Illinois State Water Survey, Illinois, IL.

Wang, H., and Anderson, M. , 1982, *Introduction to Groundwater Modeling - Finite*

Difference and Finite Element Methods, W.H. Freeman, San Francisco.

Warren, J. E., and H. S. Price, 1961, "Flow in Heterogeneous Media", *Society of Petroleum Engineers Journal*, Vol. 1, pp. 153–169.

Woodbury, A. and T. Ulrych, 2000, "A Full-Bayesian Approach to the Groundwater Inverse Problem for Steady State Flow", *Water Resources Research*, Vol. 36, No. 8, pp. 2081-2093.

Wu, C. M., T. C. J. Yeh, J. Zhu, T. H. Lee, N. S. Hsu, C.H. Chen, A.F. Sancho, 2005, "Traditional Analysis of Aquifer Tests: Comparing Apples to Oranges?", *Water Resources Research*, Vol. 41, pp. 1–12.

Yeh, T. C. J., M. H. Jin, S. Hanna, 1996, "An Iterative Stochastic Inverse Method: Conditional Effective Transmissivity and Hydraulic Head Fields", *Water Resource Research*, Vol. 32, No. 1, pp. 85–92.

Yeh, T. C. J., and S. Liu, 2000, "Hydraulic Tomography: Development of A New Aquifer Test Method", *Water Resources Research*, Vol. 36, No. 8, pp. 2095-2105.

Zhang, J. Q., and T. C. J. Yeh, 1997, "An Iterative Geostatistical Inverse Method for Steady Flow in the Vadose Zone", *Water Resources Research*, Vol. 33, No. 1, pp. 63–71.

Zheng, C., and P. Wang, 1999, "An Integrated Global and Local Optimization Approach for Remediation System Design", *Water Resource Research*, Vol. 35, No. 1, pp. 137–148.

Zhu, J., and T. C. J. Yeh, 2006, "Analysis of Hydraulic Tomography Using Temporal Moments of Drawdown Recovery Data", *Water Resources Research*, Vol. 42, pp. 1-11.

Zienkiewicz, O. C., 1971, *The Finite Element Method in Engineering Science*, McGraw-Hill, London.